

University of Salerno

Department of Chemistry and Biology “A. Zambelli”

PhD Doctoral programme in Chemistry

Cycle XXIX

PhD thesis in:

*“Novel macrocyclic systems in
asymmetric phase-transfer catalysis”*

Tutor

Prof. Irene Izzo

PhD student

Rosaria Schettini

Matr.: 8880700207

Co-tutors

Dr. Giorgio Della Sala

Dr. José Alemán Lara

(Universidad Autónoma de Madrid)

Coordinator

Prof. Gaetano Guerra

Academic Year 2015-2016

*“Per quanto difficile possa essere la vita c’è sempre
qualcosa che è possibile fare.
Guardate le stelle invece dei vostri piedi.”*

TABLE OF CONTENTS

List of Schemes	- 5 -
List of Figures	- 5 -
List of Tables	- 5 -
List of Abbreviations	- 10 -
1. INTRODUCTION	- 12 -
1.1 Phase-Transfer Catalysis	- 12 -
1.2 Asymmetric Phase-Transfer Catalysis	- 15 -
1.3 Macrocyclic systems	- 19 -
1.3.1 Macrocyclic systems in PTC: crown ethers	- 21 -
1.3.2 Macrocyclic systems in PTC: calixarenes	- 23 -
1.3.3 Macrocyclic systems in PTC: cyclopeptoids	- 25 -
1.4 Application of macrocyclic systems in asymmetric PTC	- 29 -
1.4.1 Crown ethers in asymmetric PTC	- 30 -
1.4.2 Calixarenes in asymmetric PTC	- 33 -
1.4.3 Cyclopeptoids in asymmetric PTC	- 35 -
1.5 Aims of the work	- 38 -
2. ALKYLATION REACTIONS	- 41 -
2.1 Introduction	- 41 -
2.2 New insights on the asymmetric alkylation reaction of <i>N</i>-(diphenylmethylene)glycine derivatives	- 45 -
2.2.1 Synthesis of Chiral Cyclohexapeptoids	- 46 -
2.2.2 Synthesis of Chiral Cyclotetrapeptoids	- 46 -
2.2.3 Evaluation of complexation ability of cyclotetra and cyclohexapeptoids	- 49 -
2.2.4 Chiral cyclotetrapeptoids in the enantioselective benzylation of <i>N</i>-(diphenylmethylene)glycine <i>t</i>-butyl ester	- 50 -
2.2.5 Further developments in the application of chiral cyclohexapeptoids in the enantioselective alkylation of <i>N</i>-(diphenylmethylene)glycine derivatives: the role of ester functionality	- 51 -
2.2.5 Enantioselective alkylation of <i>N</i>-(diphenylmethylene)glycine cumyl ester	- 53 -
2.4 Calixarenes in asymmetric alkylation	- 56 -
2.5 Asymmetric alkylation of 2-aryl-oxazoline-4-carboxylic acid esters	- 63 -

2.5.1 Synthesis of 2-phenyl-2-oxazoline-4-carboxylic acid esters	- 67 -
2.5.2 Enantioselective alkylation of 2-phenyl-2-oxazoline-4-carboxylic acid esters using cyclopeptoids	- 69 -
2.5.3 Synthesis of 2-aryl-2-oxazoline-4-carboxylic acid esters	- 74 -
2.5.4 Enantioselective alkylation of 2-aryl-2-oxazoline-4-carboxylic acid esters using cyclopeptoids	- 76 -
2.5.5 A new library of chiral hexapeptoids containing different residues	- 78 -
2.6 Conclusions	- 79 -
2.7 Experimental section	- 83 -
2.7.1 General procedures	- 83 -
2.7.2 Mixed monomer/submonomer solid-phase synthesis of tetra linear precursors	- 84 -
2.7.3 Mixed monomer/submonomer solid-phase synthesis of hexa linear precursors	- 85 -
2.7.4 Mixed monomer/submonomer solid-phase synthesis of octa linear precursors	- 86 -
2.7.5 Mixed monomer/submonomer solid-phase synthesis of linear precursor 101	- 87 -
2.7.6 General procedure for high dilution cyclization	- 88 -
2.7.7 Determination of Binding Affinities for Compounds 80 and 94	- 104 -
2.7.8 Computational details	- 105 -
2.7.9 General procedure for enantioselective catalytic alkylation of <i>N</i> -(diphenylmethylene)glycine <i>t</i> -butyl ester under phase-transfer conditions (benzylation) with chiral cyclopeptoids	- 107 -
2.7.10 General procedure for enantioselective catalytic alkylation of <i>N</i> -(diphenylmethylene)glycine cumyl ester under phase-transfer conditions (benzylation) with chiral cyclopeptoids	- 108 -
2.7.11 General procedure for enantioselective catalytic alkylation of <i>N</i> -(diphenylmethylene)glycine <i>t</i> -butyl ester under phase-transfer conditions (benzylation) with chiral calixarenes	- 116 -
2.8 Synthesis of 2-aryl-2-oxazoline-4-carboxylic acid esters	- 117 -
2.8.1 Synthesis of (<i>S</i>)-2-Phenyl-2-oxazoline-4-carboxylic acid cumyl ester (118)	- 117 -
2.8.2 Synthesis of (<i>S</i>)-2-Phenyl-2-oxazoline-4-carboxylic acid benzhydryl ester (119)	- 117 -

2.8.3 Synthesis of 2-(4-Trifluoromethylphenyl)-2-oxazoline-4-carboxylic acid <i>t</i> -butyl ester (129)	- 118 -
2.8.4 Synthesis of (<i>S</i>)-2-(4-Methoxyphenyl)-2-oxazoline-4-carboxylic acid <i>t</i> -butyl ester (130)	- 120 -
2.8.5 General procedure for the Phase-Transfer Enantioselective Catalytic Alkylation of 2-aryl-2 oxazoline-4-carboxylic acid esters	- 120 -
2.8.6 Determination of absolute configuration of alkylated compounds: Synthesis of (<i>S</i>)- α -benzyl serine <i>t</i> -butyl ester (147)	- 121 -
3. DIASTEROSELECTIVE SYNTHESIS OF γ -BUTENOLIDES	- 133 -
3.1 Synthesis of γ -butenolides	- 133 -
3.2 Asymmetric vinylogous synthesis of γ -monosubstituted butenolides by Michael-type addition	- 136 -
3.3 Diastereoselective vinylogous synthesis of γ -monosubstituted butenolides by Michael-type addition	- 140 -
3.4 Novel synthetic strategies for the synthesis of γ - butenolides using a diastereoselective Mukayama-Michael addition	-142-
3.5 Mukayama-Michael addition of <i>trans</i> -chalcone with 2-trimethylsilyloxyfuran catalyzed by TBAF	- 143 -
3.6 Mukayama-Michael addition of trimethylsilyloxyfuran to <i>trans</i> -chalcone catalyzed by dicyclohexane-18-crown-6	- 143 -
3.7 Synthesis of α,β -unsaturated carbonyl compounds	- 148 -
3.8 Mukayama-Michael addition of 2-trimethylsilyloxyfuran to chalcones catalyzed by dicyclohexane-18-crown-6	- 150 -
3.9 Mukayama-Michael addition of 2-trimethylsilyloxyfuran to chalcones catalyzed by benzo-15-crown-5	- 150 -
3.10 KF/crown ether promoted Mukayama-Michael addition of 2-trimethylsilyloxyfuran to different ketones.	- 153 -
3.11 Mechanistic hypothesis of fluoride-promoted Mukayama-Michael addition of 2-trimethylsilyloxyfuran to α,β -unsaturated carbonyl compounds catalyzed by crown ethers	- 156 -
3.12 Conclusions	- 158 -
3.13 Experimental section	- 161 -
3.13.1 Synthesis of chalcone derivatives	- 161 -
3.13.2 Synthesis of <i>trans</i> -1-phenyl-2-octen-1-one (180)	- 161 -
3.13.3 Synthesis of ethyl 3-benzoylacrylate (194)	- 164 -
3.13.4 General procedure for diastereoselective vinylogous Mukayama-Michael addition with KF and 2-trimethylsilyloxyfuan catalyzed by crown ethers	- 165 -

List of Schemes

Scheme 1.1 Reaction of chlorooctane with sodium cyanide.....	- 13 -
Scheme 1.2 Starks extraction mechanism	- 13 -
Scheme 1.3 Makosza interfacial mechanism	- 14 -
Scheme 1.4 Asymmetric synthesis by PTC of indanone derivative	- 16 -
Scheme 1.5 Asymmetric PTC alkylation by O'Donnel and coworkers	- 16 -
Scheme 1.6 Fluorous crown ethers in PTC	- 22 -
Scheme 1.7 Reaction mechanism of phase transfer processes promoted by onium salts or neutral macrocycles	- 30 -
Scheme 1.8 Catalytic oxidation of 1-phenylethanol by peptoids	- 35 -
Scheme 1.9 Benzylation of <i>N</i> -(diphenylmethylene)glycine <i>t</i> -butyl ester	- 36 -
Scheme 1.10 Summary of reactions in every chapter	- 39 -
Scheme 2.1 Asymmetric PTC mechanism of benzofenone imine derivative	- 42 -
Scheme 2.2 Solid phase synthesis of linear hexapeptoids	- 47 -
Scheme 2.3 Head-to-tail cyclization of hexapeptoids	- 47 -
Scheme 2.4 Solid phase synthesis of linear tetrapeptoids	- 48 -
Scheme 2.5 Head-to-tail cyclization of tetrapeptoids	- 48 -
Scheme 2.6 Enantioselective benzylation catalyzed by acyclic peptoid	- 52 -
Scheme 2.7 Enantioselective catalytic alkylation of <i>o</i> -biphenyl-2-oxazoline-4-carboxylic acid <i>t</i> -butyl ester	- 66 -
Scheme 2.8 Synthesis of H-Ser-O- <i>t</i> -butyl ester	- 68 -
Scheme 2.9 Synthesis of 2-aryl-oxazoline-4-carboxylic acid esters	- 68 -
Scheme 2.10 Synthesis 2-phenyl-oxazoline-4-carboxylic acid	- 68 -
Scheme 2.11 Synthesis of 2-phenyl-oxazoline-4-carboxylic acid cumyl ester	- 69 -
Scheme 2.12 Synthesis of 2-phenyl-oxazoline-4-carboxylic acid benzhydryl ester	- 69 -
Scheme 2.13 Solid phase synthesis of linear hexapeptoids with two proline residues	- 71 -
Scheme 2.14 Head-to-tail cyclization of cyclohexapeptoid with C_2 symmetry	- 71 -
Scheme 2.15 Solid phase synthesis of linear octapeptoids	- 71 -
Scheme 2.16 Head-to-tail cyclization of octapeptoid	- 72 -
Scheme 2.17 Synthesis of second generation oxazolines 129-133	- 75 -
Scheme 2.18 Synthesis of (<i>S</i>)- α -benzyl serine <i>t</i> -butyl ester	- 76 -

Scheme 3.1 Possible transformation reactions on γ -butenolide rings	- 134 -
Scheme 3.2 Vinylogous reactions of 2-(5 <i>H</i>)-furanone or 2-silyloxyfuran.....	- 136 -
Scheme 3.3 Organocatalyzed addition of silyloxy furan to α,β -unsaturated aldehydes	- 137 -
Scheme 3.4 Mukayama-Michael reaction of 2-trimethylsilyloxyfuran to (<i>E</i>)-3-crotonyl-1,3-oxazolin-2-one	- 137 -
Scheme 3.5 Direct asymmetric Michael addition of 2-trimethylsilyloxyfuran to nitroalkenes	- 138 -
Scheme 3.6 Direct asymmetric vinylogous Michael addition reactions of γ -butenolides to chalcones	- 139 -
Scheme 3.7 Asymmetric vinylogous Michael addition of γ -butenolides to chalcones derivatives	- 139 -
Scheme 3.8 Organocatalytic direct conjugate addition of γ -Butenolide to chalcones	- 139 -
Scheme 3.9 Organocatalytic asymmetric vinylogous Michael reaction.....	- 140 -
Scheme 3.10 Iodine-catalyzed synthesis of butenolides.....	- 140 -
Scheme 3.11 N-Heterocyclic-Carbene-Catalysed Diastereoselective Vinylogous Mukaiyama/Michael Reaction of 2-(Trimethylsilyloxy)furan and Enones.....	- 141 -
Scheme 3.12 Vinylogous Mukayama-Michael reaction catalyzed with 1,1,3,3-tetrakis(trifluoromethanesulfonyl) propane	- 142 -
Scheme 3.13 Vinylogous Mukayama-Michael reaction promoted by copper catalysts	- 142 -
Scheme 3.14 Synthesis of <i>trans</i> -1-phenyl-2-octen-1-one (174)	- 149 -
Scheme 3.15 Synthesis of ethyl 3-benzoylacrylate (192)	- 156 -
Scheme 3.16 Mechanistic hypothesis of Mukayama-Michael addition of 2-trimethylsilyloxyfuran catalyzed by crown ethers.....	- 157 -
Scheme 3.17 Mukayama-Michael addition of <i>trans</i> -chalcone with 2-(5 <i>H</i>)-furanone catalyzed by DCH-18-crown-6.....	- 158 -
Scheme 3.18 Mukayama-Michael addition of <i>trans</i> -chalcone with 2-(5 <i>H</i>)-furanone catalyzed by benzo-15-crown-5.....	- 158 -

List of Figures

Figure 1.1 Phase transfer catalysts	- 15 -
Figure 1.2 Ion pair intermediate	- 16 -
Figure 1.3 Origin of stereoselectivity in cinchona PTCs	- 18 -
Figure 1.4 Representative chiral phase-transfer catalysts.....	- 19 -

Figure 1.5 Macrocyclization techniques for peptides	- 20 -
Figure 1.6 Measurement to assessing the properties of macrocycles.....	- 21 -
Figure 1.7 Crown ethers and alkali metals complexation.....	- 22 -
Figure 1.8 Calixarene and affinity towards sodium cation.....	- 24 -
Figure 1.9 Effect of PTC on the formation of <i>p</i> -nitrobenzyl butyrate	- 24 -
Figure 1.10 Effect of PTC on the formation of <i>p</i> -nitrobenzyl caprylate.....	- 24 -
Figure 1.11 Peptoid versus α -peptide	- 25 -
Figure 1.12 First cyclopeptoid hetero oligomers	- 26 -
Figure 1.13 <i>N</i> -benzyloxyethyl cyclic α -peptoid and complexation	- 27 -
Figure 1.14 Crystal structure and crystal packing of chiral cyclohexapeptoid	- 28 -
Figure 1.15 Comparison of cyclopeptoids and some commercially available PTC	- 28 -
Figure 1.16 Chiral binaphthyl-modified crown ethers	- 30 -
Figure 1.17 Asymmetric Michael addition with chiral crown ethers	- 31 -
Figure 1.18 Chiral crown ethers tested in asymmetric phase-transfer catalysis.....	- 33 -
Figure 1.19 Calixarene-based chiral phase-transfer catalysts.....	- 34 -
Figure 1.20 Peptoid sequences evaluated for catalysis	- 35 -
Figure 2.1 Blockage of the second alkylation on the benzophenone imine derivative	- 41 -
Figure 2.2 Representative examples of <i>Cinchona</i> Alkaloid Derived Catalysts	- 44 -
Figure 2.3 Maruoka's spirobinaphthyl quaternary ammonium salts.....	- 45 -
Figure 2.4 Representative examples of derived drug candidates	- 45 -
Figure 2.5 General structures of cyclotetrapeptoids and cyclohexapeptoids.....	- 46 -
Figure 2.6 a. X-ray structure for the all-cis cyclo(L-Pro-Sar) ₂ reported by Shimizu; b. predicted lowest energy conformation for the cyclotetrapeptoid 98 by DFT calculations.....	- 49 -
Figure 2.7 Calixarene and affinity towards sodium cation.....	- 58 -
Figure 2.8 Novel chiral calixarenes	- 60 -
Figure 2.9 α -alkyl serines in biologically active natural products	- 65 -
Figure 2.11 Enantioselective benzylation of oxazoline.....	- 66 -
Figure 2.12 Solid-phase synthetic strategy of α -alkylserines	- 66 -
Figure 2.13 First generation of 2-aryl-oxazoline-4-carboxylic acid esters	- 67 -
Figure 2.14 Chiral cyclopeptoids	- 72 -
Figure 2.15 2-aryl-oxazoline-4 carboxylic acid <i>t</i> -butyl ester tested as substrates.....	- 75 -
Figure 2.16 Novel chiral cyclohexapeptoids.....	- 78 -

Figure 2.17 Enantioselective alkylation of <i>N</i> -(diphenyl-methylene)glycine <i>t</i> -butyl esters.....	- 80 -
Figure 2.18 Enantioselective alkylation of <i>N</i> -(diphenylmethylene)-glycine cumyl esters.....	- 80 -
Figure 2.20 Enantioselective alkylation of <i>N</i> -(diphenyl-methylene)glycine <i>t</i> -butyl esters with chiral calixarene.....	- 81 -
Figure 3.1 Representative examples of <i>Securinega</i> alkaloids.....	- 133 -
Figure 3.2 Examples of biologically active γ -butenolides (154-157).....	- 133 -
Figure 3.3 Structures of digitoxin and giganin.....	- 134 -
Figure 3.4 Synthesis of mytomycin C	- 135 -
Figure 3.5 Synthesis of ionomicin.....	- 136 -
Figure 3.6 18-crown-6 and 15-crown-5 derivatives tested in the fluoride promoted Mukaiyama-Michael reaction.....	- 145 -
Figure 3.7 Switchable diastereoselectivity in the vinylogous Mukayama-Michael addition of 2-trimethylsilyloxyfuran by changing reaction conditions.....	- 148 -
Figure 3.8 Structures of aliphatic enone.....	- 153 -
Figure 3.9 General scheme of the developed methodology	- 159 -
Figure 3.10 Best results of Mukayama-Michael reaction of α,β -unsaturated carbonyl compounds catalyzed by crown ethers.....	- 160 -

List of Tables

Table 1.1 S_N2 reaction with cyclopeptoid and common PTC.....	- 29 -
Table 1.2 Asymmetric Michael addition with chiral crown ethers ^a	- 32 -
Table 1.3 Asymmetric epoxidation with the chiral monosaccharide-based crown ether 46	- 32 -
Table 1.4 Asymmetric alkylation of <i>N</i> -(diphenylmethylene)glycine ethyl ester catalyzed by cinchonidine-derived calix[4]arene 50	- 34 -
Table 1.5 Oxidative kinetic resolution reaction with peptoids.....	- 36 -
Table 1.6 Enantioselective benzylation with alkylating agents ^{a,b}	-37 -
Table 2.1 Cram's method with picrate salts and cyclopeptoids	- 50 -
Table 2.2 Enantioselective benzylation with chiral cyclotetrapeptoids 94-98 ^{a,b}	- 51 -
Table 2.3 Screening of ester groups in phase-transfer benzylation of 99 , catalyzed by 80 . ^a	- 52 -
Table 2.4 Screening of catalysts in phase-transfer benzylation of 99c . ^a	- 53 -
Table 2.5 Screening of catalyst loading, solvents and bases promoted by 80 . ^a	- 54 -
Table 2.6 Scope of phase-transfer alkylation of 99c promoted by 80 . ^{a-d}	- 56 -

Table 2.7 Enantioselective benzylation with chiral calixarenes 103-110^a	- 60 -
Table 2.8 Screening of bases in phase-transfer benzylation of 55 promoted by 107^a	- 60 -
Table 2.9 Screening of ester groups in phase-transfer benzylation of 99a-d promoted by 107^a	- 61 -
Table 2.10 Screening of catalyst loading, solvents in the alkylation promoted by 107^a	- 62 -
Table 2.11 Enantioselective alkylation of 55 in presence of catalyst 107 with different alkylating agents ^{a,b}	- 63 -
Table 2.12 Investigation of the role of ester groups and of reaction parameters in phase-transfer benzylation of oxazoline promoted by 80	- 70 -
Table 2.13 Screening of the catalyst 82, 126 and 128	- 73 -
Table 2.14 Screening of the cyclotetrapeptoids 94-98	- 74 -
Table 2.15 Screening of the cyclohexapeptoids in asymmetric benzylation	- 74 -
Table 2.16 Screening of 2-aryl-oxazoline <i>tert</i> -butyl ester substrate promoted by 80	- 77 -
Table 2.17 Scope of phase-transfer alkylation of 129 promoted by 81	- 77 -
Table 2.18 Asymmetric alkylation with new catalysts	- 79 -
Table 3.1 Vinylogous Mukayama-Michael reaction of <i>trans</i> -chalcone catalyzed by TBAF ^{a,b}	- 143 -
Table 3.2 Vinylogous Mukayama-Michael reaction of 2-trimethylsilyloxyfuran and <i>trans</i> -chalcone catalyzed by DCH-18-crown-6 ^a	- 144 -
Table 3.3 Screening of inorganic salts in Mukayama-Michael reaction catalyzed by DCH18-crown-6 ^{a,b}	- 145 -
Table 3.4 Screening of catalysts in Mukayama-Michael reaction of 2-trimethylsilyloxyfuran and <i>trans</i> -chalcone ^a	- 146 -
Table 3.5 Mukayama-Michael reaction catalyzed by 15-crown-5 in halogenated solvents ^{a,b}	- 146 -
Table 3.6 Mukayama-Michael reaction catalyzed by dicyclohexan-18-crown-6 at different temperatures ^{a,b}	- 147 -
Table 3.7 Mukayama-Michael reaction catalyzed by [2,2,2]-cryptand	- 147 -
Table 3.8 Synthesis of <i>trans</i> -chalcone derivatives by aldol condensations ^a	- 149 -
Table 3.9 <i>Syn</i> -diastereoselective vinylogous Mukayama-Michael reaction of α,β -unsaturated carbonyl compounds catalyzed by DCH18-crown-6 ^a	- 151 -
Table 3.10 <i>Anti</i> -diastereoselective vinylogous Mukayama-Michael addition of 2-trimethylsilyloxyfuran to chalcones catalyzed by benzo-15-crown-5 ^a	- 152 -

Table 3.11 Vinylogous Mukayama-Michael reaction of 2-trimethylsilyloxyfuran with <i>trans</i> -1-phenyl-2-octen-1-one catalyzed by crown ethers ^a	- 153 -
Table 3.12 Vinylogous Mukayama-Michael reaction of 2-trimethylsilyloxyfuran with (<i>E</i>)-4-phenyl-3-buten-2-one.....	- 154 -
Table 3.13 Vinylogous Mukayama-Michael reaction of 2-trimethylsilyloxyfuran with (<i>E</i>)-3-octen-2-one.....	- 155 -
Table 3.14 Vinylogous Mukayama-Michael reaction of 2-trimethylsilyloxyfuran with (<i>E</i>)-ethyl 3-benzoylacrylate ^a	- 156 -

List of Abbreviations

ACE: Angiotensin Converting Enzyme

ACN: Acetonitrile

BTEAC: Benzyltriethyl ammonium chloride

DAST: (Diethylamino)sulfur trifluoride

DCE: 1,2-Dichloroethane

DCM: Dichloromethane

DIC: *N,N'*-Diisopropylcarbodiimide

DIPEA: *N,N*-Diisopropylethylamine

DMF: *N,N*-Dimethylformamide

DMSO: Dimethyl sulfoxide

EDC: *N*-(3-Dimethylaminopropyl)-*N'*-ethylcarbodiimide

Fmoc: 9-Fluorenylmethoxycarbonyl

HATU: 1-[Bis(dimethylamino)methylene]-1*H*-1,2,3-triazolo[4,5-*b*]pyridinium 3-oxid hexafluorophosphate

HFIP: 1,1,1,3,3,3-Hexafluoro-2-propanol

HOBt: 1-Hydroxybenzotriazole

PFDMC: perfluoro(1,3-dimethylcyclohexane)

PTC: Phase-transfer catalysis

RP-HPLC: Reverse-phase high-performance liquid chromatography

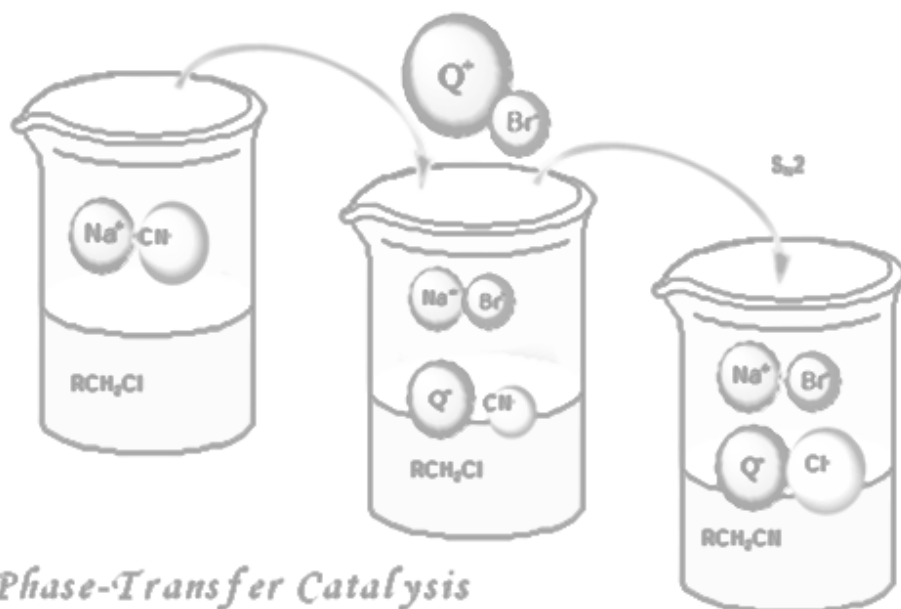
TBAF: Tetrabutylammonium fluoride

TEMPO: (2,2,6,6-tetramethylpiperidine-1-oxyl)

TFA: Trifluoroacetic acid

THF: Tetrahydrofuran

Chapter 1
Introduction



1. INTRODUCTION

1.1 Phase-Transfer Catalysis

In the great realm of organic synthesis, phase-transfer catalysis (PTC) is a well recognized methodology which plays a key role both in industry and academia research. This process involves reactions that take place between reagents which are located in different phases, for example an inorganic water-soluble reagent and a substrate soluble in the organic phase.¹ Different industrial applications in the field of pharmaceuticals, agrochemicals, fragrances, polymers are possible and many reactions can be realized, using this methodology, even for large-scale synthesis (alkylations, epoxidations, nucleophilic additions, oxidations).^{2,3} These reactions generally present numerous advantages: mild conditions and simple operations, high reaction rates and selectivities, the use of inexpensive and environmentally safe reagents and solvents. Most PTC reactions involve displacement of an anionic species from an aqueous phase (liquid-liquid system) or solid phase (solid-liquid system) to an organic phase.⁴ For this reason the main catalysts involved in phase-transfer catalysis are cations, for example ammonium or phosphonium salts, or macrocyclic complexant agents of inorganic cations such as crown ethers and cryptands. The term “phase-transfer catalysis” was introduced by Starks in 1971 to explain the critical role of a catalyst, such as a tetraalkylammonium or phosphonium salt, in the reactions between two substances located in different immiscible phases.⁵ The reaction of 1-chlorooctane with sodium cyanide (scheme 1.1) was accelerated by the presence of a catalytic amount of quaternary phosphonium salt. This salt was able to extract the cyanide from the aqueous phase, making it more reactive. A great number of parameters are known to influence the kinetics of the phase-transfer catalyzed reactions: the nature of the catalyst and its lipophilicity, the stirring rate, the temperature, the interaction between anion and cation in the ion-pair, the number of water

1. F. Montanari, D. Landini, F. Rolla, *Topics in Current Chemistry*, **1982**, 101,147-200.

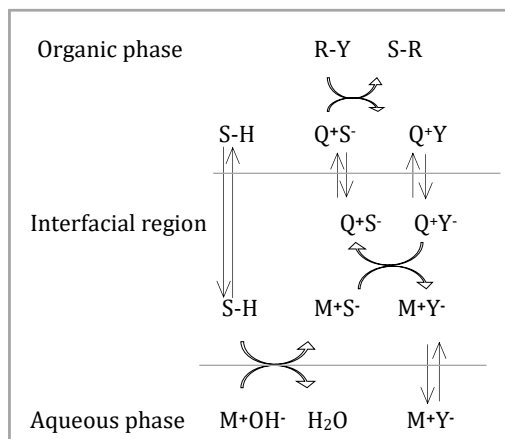
2. J.Tan, N. Yasuda, *Org. Process Res. Dev.*, **2015**, 19, 1731–1746.

3. D. C. M. Albanese, F. Foschi, M. Penso, *Org. Process Res. Dev.*, **2016**, 20, 129–139.

4. M. Fedorynski, M. Jezierska-Zieba, B. Kakol, *Drug Research*, **2008**, 65, 647-654.

5. C. M. Starks, *J. Am. Chem. Soc.*, **1971**, 93, 195-199.

interface by ion-exchange, migrates into the organic phase where it reacts with the substrate. However, the reported mechanisms are not completely general because the catalytically active species, actually involved in the reaction, can be different from those outlined in scheme 1.3.



Scheme 1.3 Makosza interfacial mechanism

As the Coulomb interaction between the anion and the cation decrease, the anion become more reactive. As a result of weak interactions with voluminous counterions, such as a quaternary onium salt or metal cation "trapped" within a neutral ligand, Y⁻ behaves like a "naked" anion. The most used catalysts for this kind of reactions are quaternary onium salts (e.g. **1**, **2**), or neutral ligands such as crown ethers (e.g. **3**, **4**, **5**, **6**), cryptands (e.g. **7**), polydodands (e.g. **8**, **9**) (Figure 1.1). The use of quaternary cations with a long alkyl chain ensures the lipophilicity of the salt, making a very reactive ion pair and accelerating the next reaction. Pedersen's discovery of crown ethers, cyclic polyethers, had led innovation in chemistry in recent years: complexation of a specific metal cation within the macrocycle facilitates the solubility of the salt in a slightly polar solvent and provides very reactive non-solvated anions. Among those most used are 15-crown-5 (**3**), 18-crown-6 (**4**), dicyclohexyl-18-crown-6 (**5**), dibenzo-18-crown-6 (**6**). The advantage of using these catalysts is substantially represented by the favorable partitioning of the crown ethers complexes in the organic phase rather than the aqueous phase and the high complexation constants between the cation and the neutral ligand. The cryptands are the three-dimensional analogues of crown ethers that are

particularly interesting for the anionic activation; in fact, the cation is incorporated within the three-dimensional structure to form an inclusion compound which provides a "naked anion"; therefore the cryptands are neutral ligands that maximize the cation-anion separation. The podands and polypodands, open-chain polyethers, are able to complex alkali and alkaline-earth metal cations, but the complexation constants are generally lower if compared to that of crown ethers, owing to the so-called macrocycle effect; however, they form stable complexes with alkali and alkaline-earth metals when the polyoxyethylene chains are long and with electron-withdrawing substituents.^{7,8}

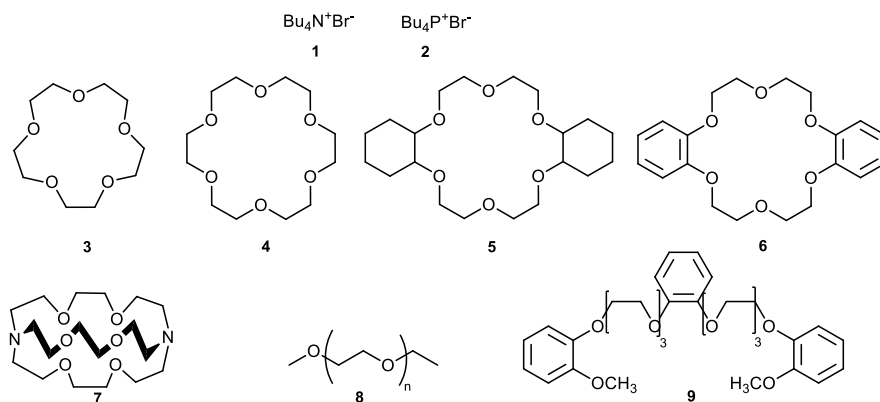


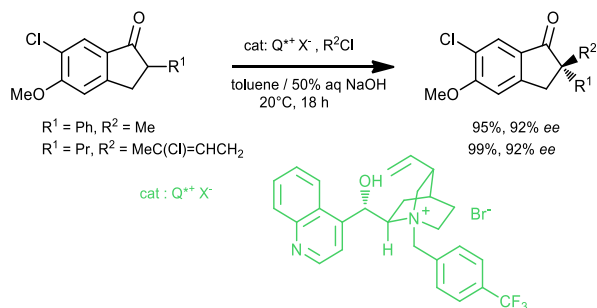
Figure 1.1 Phase transfer catalysts

1.2 Asymmetric Phase-Transfer Catalysis

The growing demand for enantiomerically enriched compounds by industry enforces research towards the development of new synthetic asymmetric methodologies. The asymmetric phase-transfer catalysis involves the use of non-racemic, chiral catalysts, and it is employed in several types of reactions. The pioneering study conducted in 1984 by a research group from Merck is recognized as the first application of asymmetric phase-transfer catalysis (scheme 1.4). A chiral quaternary ammonium salt derived from cinchonine was used as catalyst, for the enantioselective methylation of a 2-phenyl-1-indanone. The asymmetric induction was attributed to the π - π stacking and the hydrogen bond interactions of the resulting enolate with the catalyst (figure 1.2). Subsequently O'Donnell's group

⁸ P.E. Stott, J. S. Bradshaw, W. W. Parish, *J. Am. Chem. Soc.* **1980**, *102*, 4810-4815.

conducted an enantioselective alkylation, using as a substrate a prochiral derivative of protected glycine, providing a valid method for the preparation of both natural and non-natural amino acids (scheme 1.5).



Scheme 1.4 Asymmetric synthesis by PTC of indanone derivative

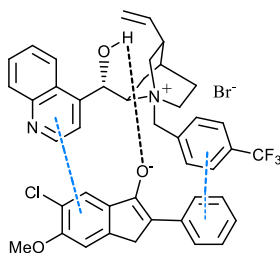
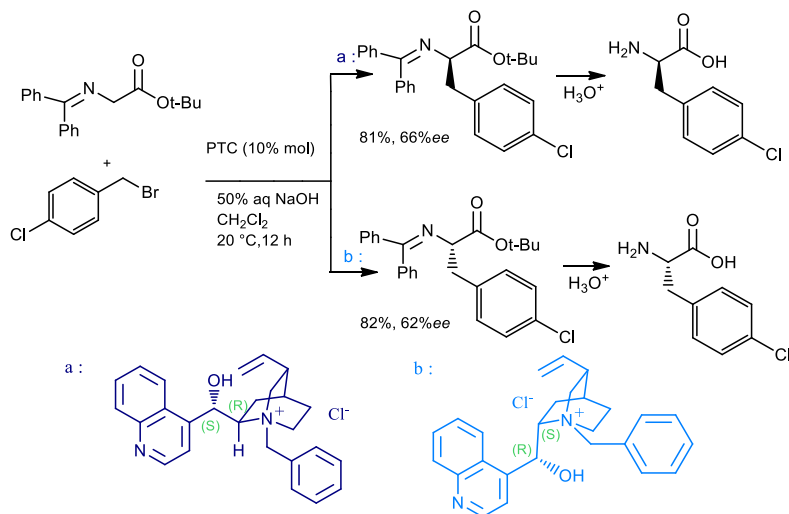


Figure 1.2 Ion pair intermediate



Scheme 1.5 Asymmetric PTC alkylation by O'Donnell and coworkers

In this pioneering study the chiral catalysts used were quaternary ammonium salts derived from *Cinchona* alkaloids. The use of a *Cinchonine*-derived catalyst (**a**), gave

the amino acid (*R*), while using a cinchonidine-derived catalyst (**b**) amino acid with opposite configuration (*S*) was recovered (scheme 1.5). The synthetic scheme primarily envisages an enantioselective alkylation step of *N*-(diphenylmethylene)glycine *t*-butyl ester and the subsequent hydrolysis, which produces the corresponding amino acid with high yields and moderate enantiomeric excesses (scheme 1.5).⁹ The origin of stereoselectivity is ascribed to the different arrangement assumed by the structural elements around the quaternary nitrogen atom in the catalyst: the ammonium ion can be equated to a tetrahedron whose surface is characterized by the four faces F1, F2, F3, and F4 (figure 1.3). The enolate that is generated during the reaction is coordinated to the open face F4 that allows a contact with the positive charge of the cation. The preference for the tetrahedron's F4 face is determined both by conformational effects and steric effects. F1 face is cluttered by the presence of quinuclidinyl moiety and F2 by the presence of -OR group. F3 face is encumbered by the benzyl ring. Therefore, the enolate coordination is prevented on these three faces; face F4 is less hindered and the coordination is stabilized by the attractive interaction between the negative charge on the oxygen atom of the enolate and the positive charge of nitrogen atom of the catalyst.¹⁰ Since their first application in 1989, the *Cinchona* alkaloid-derived quaternary ammonium salts have been received growing attention in the field of asymmetric phase-transfer catalysis and the design of new well-defined chiral catalysts has become a topic of scientific interest. Most of the recent contributions are related to the design and application of ammonium salts catalysts based on *Cinchona* alkaloids or different structural scaffolds.¹¹

In literature, the *Cinchona* quaternary ammonium salts have been largely employed in asymmetric PTC, as derived structure of the pioneering catalysts (*e.g.* **10**, **11**),¹² or as bifunctional PTC in which there are amide or (thio)urea moieties

⁹ M. J. O'Donnell, W. D. Bennett, S. Wu, *J. Am. Chem. Soc.* **1989**, *111*, 2353-2355.

¹⁰ S. Jew, H. Park, *Chem. Comm.* **2009**, 7090-7103.

¹¹ S. Kaneko, Y. Kumatabara, S. Shirakawa, *Org. Biomol. Chem.*, **2016**, *14*, 5367-5376.

¹² For examples see: a) E. J. Corey, F. Xu, M. C. Noe, *J. Am. Chem. Soc.* **1997**, *119*, 12414-12415; b) B. Lygo, B. J. Andrews, J. Crosby, J. A. Peterson, *Tetrahedron Lett.* **2002**, *43*, 8015-8018; c) H. Park, B. Jeong, J. Lee, M. Park, Y. Lee, M. Kim, S. Jew, *Angew. Chem., Int. Ed.* **2002**, *41*, 3036-3038; d) M. Yoo, B. Jeong, J. Lee, H. Park, S. Jew, *Org. Lett.* **2005**, *7*, 1129-1131; e) S. Jew, M. Yoo, B. Jeong, I. Y. Park, H. Park, *Org. Lett.* **2002**, *4*, 4245-4248.

(e.g. **12**, **13**).¹³ More recently biaryl-based quaternary ammonium salts have been introduced by Maruoka and coworkers (**14**, **15**)¹⁴ and used in a wide variety of asymmetric transformations. Recent derivatives of former Maruoka's catalysts are phosphonium salt (**16**)¹⁵ and bifunctional catalyst (**17**).¹⁶ Other onium salts are: tartaric acid derivatives (e.g. **18**, **19** and **20**),¹⁷ C_2 -symmetric chiral cyclic guanidine compounds (e.g. **21**),¹⁸ cyclic ammonium ion (e.g. **22**)¹⁹ (figure 1.4).

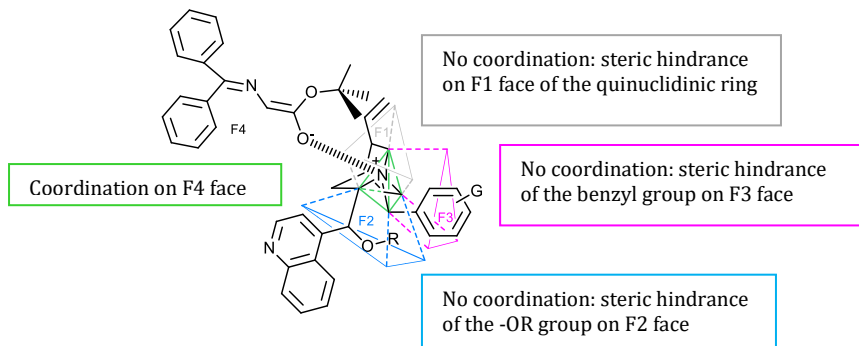


Figure 1.3 Origin of stereoselectivity in cinchona PTCs

¹³. For examples see: a) K. M. Johnson, M. S. Rattley, F. Sladojevich, D. M. Barber, M. G. Nuñez, A. M. Goldys, D. J. Dixon, *Org. Lett.*, **2012**, *14*, 2492–2495; b) P. Bernal, R. Fernández, J. M. Lassaletta, *Chem. Eur. J.*, **2010**, *16*, 7714 – 7718; c) M. Li, P. A. Woods, M. D. Smith, *Chem. Sci.*, **2013**, *4*, 2907–2911.

¹⁴. For examples see: a) T. Ooi, M. Kameda, K. Maruoka, *J. Am. Chem. Soc.*, **1999**, *121*, 6519–6520; b) T. Ooi, Y. Uematsu, M. Kameda, K. Maruoka, *Angew. Chem. Int. Ed.* **2002**, *41*, 1551–1554; c) M. Kitamura, S. Shirakawa, K. Maruoka, *Angew. Chem. Int. Ed.* **2005**, *44*, 1549–1551; d) T. Ooi, M. Takeuchi, M. Kameda, K. Maruoka, *J. Am. Chem. Soc.* **2000**, *122*, 5228–5229; e) T. Ooi, M. Kameda, M. Taniguchi, K. Maruoka, *J. Am. Chem. Soc.* **2004**, *126*, 9685–9694; f) M. Kitamura, Y. Arimura, S. Shirakawa, K. Maruoka, *Tetrahedron Letters*, **2008**, *49*, 2026–2030.

¹⁵. For examples see: a) R. He, X. Wang, T. Hashimoto, K. Maruoka, *Angew. Chem. Int. Ed.* **2008**, *47*, 9466 –9468; b) R. He, C. Ding, K. Maruoka, *Angew. Chem. Int. Ed.* **2009**, *48*, 4559 – 4561; c) C. Zhu, F. Zhang, W. Meng, J. Nie, D. Cahard, J. Ma, *Angew. Chem. Int. Ed.* **2011**, *50*, 5869 –5872.

¹⁶. For examples see: a) T. Ooi, D. Ohara, M. Tamura, K. Maruoka, *J. Am. Chem. Soc.* **2004**, *126*, 6844–6845; b) T. Ooi, D. Ohara, K. Fukumoto, K. Maruoka, *Org. Lett.*, **2005**, *7*, 3195–3197; c) Xisheng Wang, Quan Lan, Seiji Shirakawa and Keiji Maruoka, *Chem. Commun.*, **2013**, *15*, 321–323.

¹⁷. For examples see: a) T. Shibuguchi, Y. Fukuta, Y. Akachi, A. Sekine, T. Ohshima, M. Shibasaki, *Tetrahedron Letters*, **2002**, *43*, 9539–9543; b) T. Ohshima, T. Shibuguchi, Y. Fukuta, M. Shibasaki, *Tetrahedron*, **2004**, *60*, 7743–7754; c) M. Waser, K. Gratzler, R. Herchl, N. Müller, *Org. Biomol. Chem.*, **2010**, *10*, 251–254; d) S. Arai, R. Tsuji, A. Nishida, *Tetrahedron Lett.*, **2002**, *43*, 9535–9537.

¹⁸. T. Kita, A. Georgieva, Y. Hashimoto, T. Nakata, K. Nagasawa, *Angew. Chem. Int. Ed.*, **2002**, *41*, 2832–2834.

¹⁹. S. E. Denmark, N. D. G., L. M. Wolf, *J. Org. Chem.*, **2011**, *76*, 4260–4336.

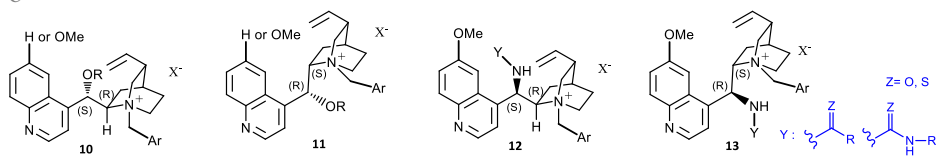
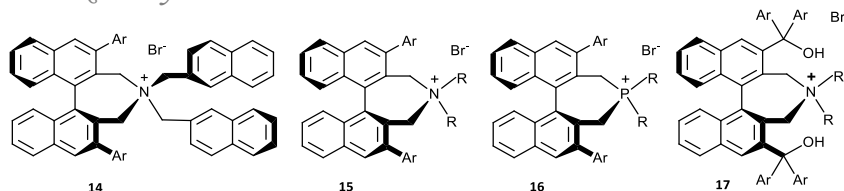
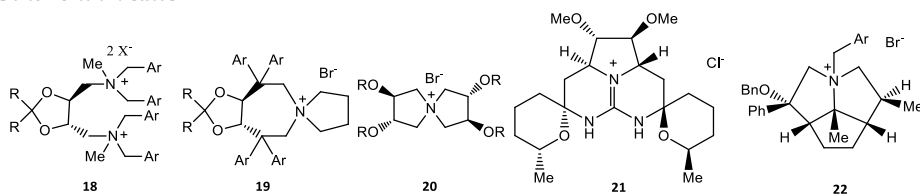
Cinchona derivatives*Maruoka catalysts**Other onium salts*

Figure 1.4 Representative chiral phase-transfer catalysts

1.3 Macroyclic systems

In the early 1960s, at Du Pont, C. J. Pedersen isolated a very small amount of a compound that later was called dibenzo-18-crown-6. The choice to spend efforts to characterize this new, serendipitously discovered, product paved the way to the development of macrocyclic chemistry, one of the most promising research area of chemical science. Since this pioneering work, in the ensuing decades an increasing number of scientists have devoted time and effort to the design, synthesis and characterization of novel macrocyclic chemical structures, getting sometimes inspiration by the amazing macrocyclic compounds, isolated by natural sources.^{20a}

Macrocycles may be applied in a wide range of research fields, including organic and inorganic synthesis, biochemistry, ion transport in membranes, phase-transfer catalysis and structure analysis. Moreover macrocyclic chemistry underpins supramolecular chemistry: in fact the Izatt-Christensen Award is one of the most

^{20.} (a) L. Cascales, D. J. Craik, *Org. Biomol. Chem.* **2010**, *8*, 5035–5047. (b) S. E. Gibson, C. Lecci, *Angew. Chem. Int.Ed.* **2006**, *45*, 1364–1377. (c) L. A.Wessjohann, E.Ruijter, *Top. Curr. Chem.* **2005**, *243*, 137–184.

prestigious in chemistry which recognizes excellence in the developing both fields of macrocyclic and supramolecular chemistry. Three winners, Professor Jean-Pierre Sauvage, Professor Bernard Lucas Feringa and Sir J. Fraser Stoddart were awarded the Nobel Prize in Chemistry very recently.^{20a} In addition the interest in the synthesis of macrocycles is increased with the growing demand of new therapeutic agents, and naturally occurring bioactive macrocycles and their analogues have been synthesized: in fact, generally, cyclization enhances the selective binding, uptake, potency and stability of linear precursors, inducing constraints in a flexible oligomeric system, and preorganizing the structure in a well-defined active conformation. In particular the drug discovery field have received a lot of contributions by the synthesis of cyclic peptides and peptidomimetics.^{20b} Having a well-defined macrocyclic structure is possible to investigate the relationship between structure and function.

From a synthetic point of view the major challenge in macrocycles' synthesis is to minimize the probability of oligomerization or polymerization instead of cyclization. This issue is overcome with high dilution techniques or solid-phase synthesis.²¹

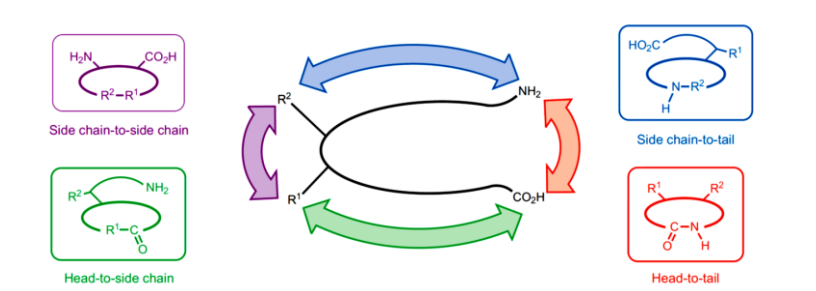


Figure 1.5 Macrocyclization techniques for peptides

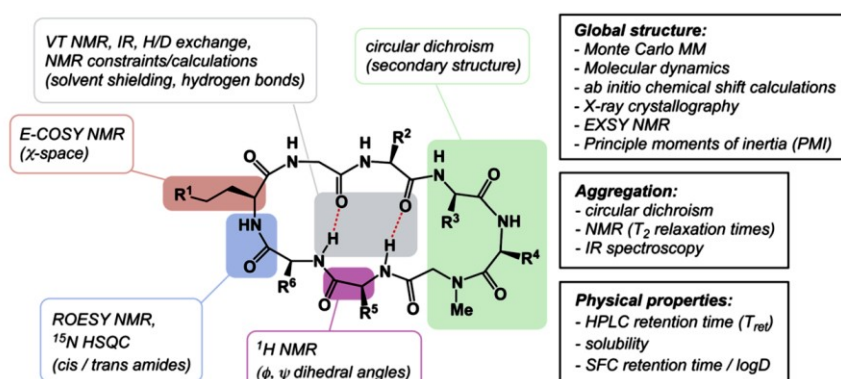
For example in the case of a peptide there are four different strategy: head-to-tail (*C*-terminus to *N*-terminus), head-to-side chain, side chain-to-tail or side-chain-to-side-chain (figure 1.5). Macrocyclization is a way to “freeze” the motifs of linear precursors in order to perform conformational analysis and structure/function relationship studies. There are some powerful techniques employed by chemists to study macrocyclic systems.²² For instance, in the conformational analysis of

²¹. C. J. White, A. K. Yudin, *Nat. Chem.*, **2011**, *3*, 509-524.

²². A. K. Yudin, *Chem. Sci.*, **2015**, *6*, 30-49.

macrocycles leading methods are: X-ray crystallography, Circular Dichroism, indispensable in the comprehension of secondary structure of proteins, and NMR spectroscopic evaluation (figura 1.6). The conformational aspects of macrocycles can influence the reactivity and the knowledge of the three-dimensional structure can direct the design of new scaffolds employed for instance in catalytic processes.²³ The role covered by macrocycles upon interaction with protein target is really crucial in the growing field of drug discovery. The macrocycle is able to adopt different conformations that are responsible of precise interactions which control a wide range of signals inside the cell.²⁴

Figure 1.6 Measurement to assessing the properties of macrocycles



1.3.1 Macrocyclic systems in PTC: crown ethers

Pedersen's discovery of crown ethers,²⁵ represented a big innovation in organic chemistry: thanks to their strong ability to bind metals they have been developed in host-guest chemistry and supramolecular field. Crown ethers act as remarkable host towards alkali and alkaline earth metals based on the molecular organization of the electron-donating oxygen atoms in the macrocycle. They have been investigated in the metal-ion recognition and it is possible to identify a relationship between the cavity of the macrocycle and the cation diameter (figure 1.7).

²³ L. Zheng, A. Marcozzi, J.Y. Gerasimov, A. Herrmann, *Angew. Chem. Int. Ed.*, **2014**, *53*, 7599-7603.

²⁴ J. Gavenonis, B. A. Sheneman, T. R. Siegert, M. R. Eshelman, J. A. Kritzer, *Nat. Chem. Biol.*, **2014**, *10*, 716-722.

²⁵ C. J. Pedersen, *Angew. Chem. Int. Ed. Engl.*, **1988**, *27*, 1021-1027.

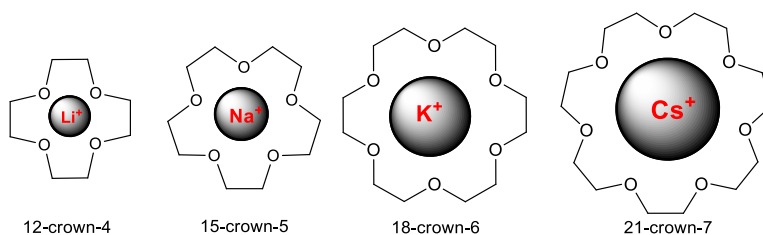
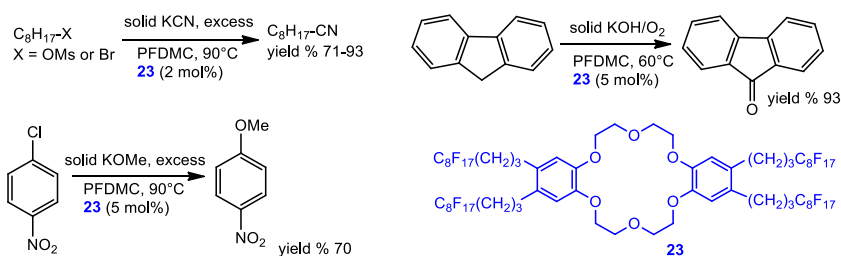


Figure 1.7 Crown ethers and alkali metals complexation

These unique complexation properties have led the crown ethers to be applied in phase-transfer catalysis field. In principles the ammonium salts are able to extract the cation from the aqueous layer while the crown ethers are able to complex the cation with high association constants. The crown ethers in comparison with ammonium salts are more expensive but there are some parameters such as metal-host complexation and lipophilicity of the macrocycle that can radically influence and improve the phase-transfer catalytic process.^{7, 8} From decades to nowadays, crown ethers have been used in PTC especially in solid-liquid processes.²⁶ Macrocyclic polyethers have received importance for applications in PTC reactions taking advantages from their ability to complex metal cations. For example in recent years various fluororous crown ethers derivatives were synthesized.⁶ The interest towards this type of molecules is linked to an easy recycle of the catalytic systems. In particular the catalyst **23** is almost insoluble in common organic solvents but totally soluble in perfluorocarbons; this allows the recovery and reuse of the catalytic species. For instance, these systems find application in PTC nucleophilic substitution and oxidation reactions (scheme 1.6).



Scheme 1.6 Fluororous crown ethers in PTC

²⁶. For examples see: a) A. C. Knipe, *J.Chem.Educ.* **1976**, *53*, 618-622; b) G. W. Gokel, H. D. Durst, *Synthesis*, **1976**, 168-184; c) A. Maia, D. Landini, S. Petricci, *Supramolecular Chemistry*, **2000**, *11*, 289-292; d) L. Xia, Y. Jia, S. Tong, J. Wang, G. Han, *Kinetics and Catalysis*, **2010**, *51*, 69-74.

1.3.2 Macrocyclic systems in PTC: calixarenes

Calixarenes are macrocycles derived from an hydroxyalkylation of a phenol with an aldehyde. Calixarenes are another leading class of macrocycles able to complex metal ions. The ability of the calixarenes in complexing metal ions has been widely investigated. In particular, for example, a calix[4]arene functionalized at the lower rim with ethyl ester groups shows a high affinity towards the sodium cation.²⁷(figure 1.8). Although the ability of calixarenes to complex alkali metals has been well-established, and these macrocycles have been largely employed in metal-based catalysis, applications in phase-transfer catalysis remain elusive.²⁸ In literature is possible to find few examples of reactions in which calixarenes act as phase-transfer catalysts. They have been used in nucleophilic substitution, Darzen condensation, alkylation, esterification, oxidation reactions. It is possible to make a classification of different typologies of calixarenes: “octopus type calixarene”,²⁹ water soluble calixarenes in which the macrocycle act as an inverse phase-transfer catalyst,³⁰ calixarenes with a lower rim functionalization³¹ and calixarenes with an upper rim functionalization.³² For instance, Yilmaz and co-workers reported the design of functionalized calixarenes, bearing alkyl amino groups on their upper rim

²⁷. C. D. Gutsche; *Calixarenes, Monographs in Supramolecular Chemistry*, ed. J. F. Stoddart, *The Royal Society of Chemistry*, UK, **1992**, 158-164.

²⁸. D. M. Homden; C. Redshaw, *Chem. Rev.*, **2008**, *108*, 5086–5130.

²⁹. For examples see: a) E. Nomura, H. Taniguchi, K. Kawaguchi, Y. Otsuji, *Chem. Lett.* **1991**, 2167-2170; b) H. Taniguchi, E. Nomura, *Chem. Lett.* **1988**, 1773–1776; c) H. Taniguchi, Y. Otsuji, E. Nomura, *Bull. Chem. Soc. Jpn.* **1995**, *68*, 3563–3567; d) E. Nomura, H. Taniguchi, K. Kawaguchi, Y. Otsuji, *J. Org. Chem.* **1993**, *58*, 4709–4715; e) E. Nomura, H. Taniguchi, Y. Otsuji, *Bull. Chem. Soc. Jpn.* **1994**, *67*, 792–799; f) E. Nomura, H. Taniguchi, Y. Otsuji, *Bull. Chem. Soc. Jpn.* **1994**, *67*, 309–311; g) Y. Okada, Y. Sugitani, Y. Kasai, J. Nishimura, *Bull. Chem. Soc. Jpn.* **1994**, *67*, 586–588; h) K. Araki, A. Yanagi, S. Shinkai, *Tetrahedron* **1993**, *49*, 6763–6772.

³⁰. For examples see: a) S. Shimizu, K. Kito, Y. Sasaki, C. Hirai, *J. Chem. Soc., Chem. Commun.* **1997**, 1629–1630; b) S. Shimizu, T. Suzuki, S. Shirakawa, Y. Sasaki, C. Hirai, *Adv. Synth. Catal.* **2002**, *344*, 370–378; c) P. Srivastava, R. Srivastava, *Tetrahedron Letters*, **2007**, 4489–4493; d) C. D. Gutsche, I. Alam, *Tetrahedron* **1988**, *44*, 4689–4694; e) S. Shinkai, S. Mori, H. Koreishi, T. Tsubaki, O. Manabe, *J. Am. Chem. Soc.* **1986**, *108*, 2409–2416.

³¹. For examples see: a) F. Yang, Y. Wang, H. Guo, J. Xie, Z. Liu, *Can. J. Chem.* **2010**, *88*, 622–627; b) S. J. Harris, A. M. Kinahan, M. J. Meegan, R. C. Prendergast, *J. Chem. Res.* **1994**, 342–343.

³². E. Akceylan, M. Yilmaz, *Tetrahedron* **2011**, *67*, 6240-6245.

for the esterification reaction of *p*-nitrobenzyl bromide and sodium butyrate or sodium caprylate.³²

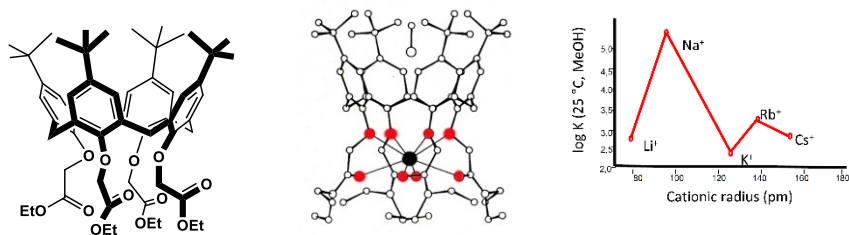


Figure 1.8 Calixarene and affinity towards sodium cation

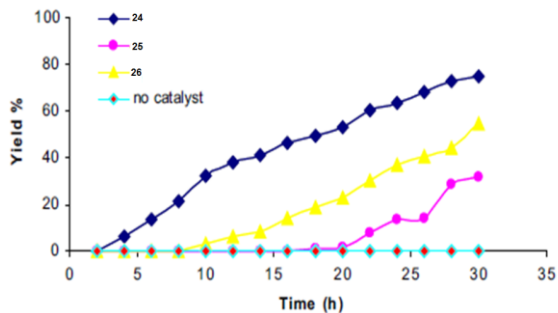
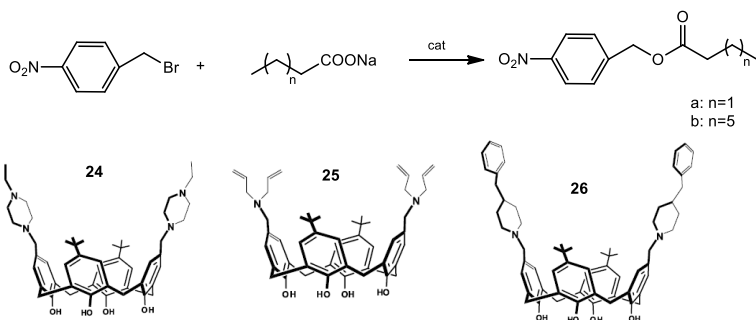


Figure 1.9 Effect of PTC on the formation of *p*-nitrobenzyl butyrate

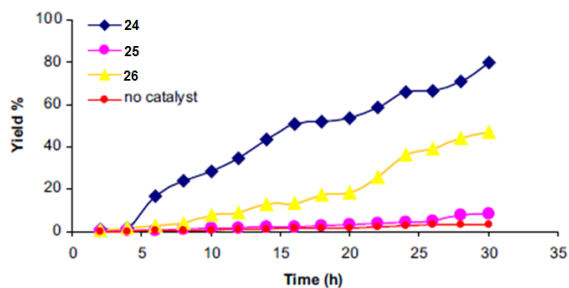


Figure 1.10 Effect of PTC on the formation of *p*-nitrobenzyl caprylate

The catalytic activity of calixarenes **24**, **25**, **26** were examined for the esterification reactions. First of all, the uncatalyzed reaction did not occur indicating that **24**, **25** and **26** serve as catalysts. From this study the calixarene **24** proved to be the best performing catalyst in terms of reaction time, conversion and yield (figure 1.9 and figure 1.10).

1.3.3 Macrocyclic systems in PTC: cyclopeptoids

Cyclopeptoids are macrocycles derived from the cyclization of linear peptoids (figure 1.11). Peptoids are oligomers of *N*-substituted glycines. These compounds are peptidomimetic that could mimic the biological function of peptides. Peptoids can be described as mimics of α -peptides in which the side chain is attached to the backbone amide nitrogen instead of the α -carbon. Peptoids lack conformation rigidity in comparison to α -peptides; in fact amide bonds are tertiary and can isomerize between *trans* and *cis* conformations far more readily than the secondary amides in α -peptides; further without the presence of amide protons, secondary structure can not be stabilized by backbone hydrogen bonds in the same manner as in peptides.³³ These oligomers are an attractive scaffold for a wide range of applications because they can be generated using a modular synthesis, based on solid-phase approach, that allows the incorporation of a wide variety of functionalities. Macrocyclic constrains are often employed to rigidify the conformation of these flexible systems.

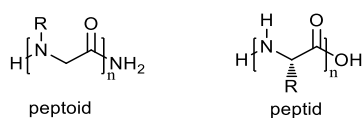


Figure 1.11 Peptoid versus α -peptide

In 2007 Kirshenbaum and co-workers reported the first cyclopeptoid hetero oligomers prepared through an head-to-tail cyclization reaction. It is important to underline that, in the crystal structure, aromatic and alkyl side chains were segregated to opposite faces of the macrocycle. This result in partitioning of hydrophobic and polar side chain groups on either face of the macrocycle.

³³. S. A. Fowler, H. E. Blackwell, *Org. Biomol. Chem.* **2009**, *7*, 1508-1524.

Furthermore analysis of peptoid macrocycle crystal structure revealed a remarkable similarity of the backbone to protein β -turn (figure 1.12).^{34, 35}

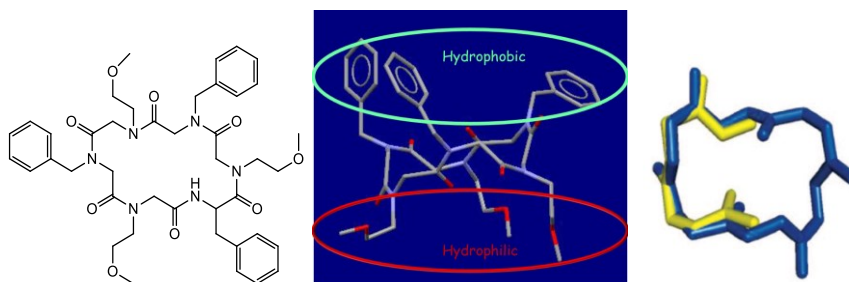


Figure 1.12 First cyclopeptoid hetero oligomers

Subsequently cyclopeptoids proved to have interesting ability in complexing metal ions. For instance, the investigation of *N*-benzyloxyethyl cyclic α -peptoids showed the attitude to complex first group alkali metals and ammonium ion. These complexing properties were revealed with NMR techniques, conformational studies and correlated with Cram's method investigation (figure 1.13).^{36,37} The cyclopeptoid **27** showed a good affinity for the smaller cations, in particular for Na^+ . The use of spectroscopy $^1\text{H-NMR}$ revealed for compound **27** a complex mixture of rotamers which interconvert faster than NMR time scale (figure 1.13, a). Addition of sodium picrate (0.5 eq.) revealed the presence of a new species (figure 1.13, b); interestingly an increasing amount of sodium picrate (1.0 eq.) led to the formation of a predominant species with a high symmetry (figure 1.13, c). A conformational search on this cyclopeptoid as sodium complex suggested the presence of a S_6 -symmetry axis passing through the intracavity sodium cation. Finally a crystal structure was obtained as a 2:3 complex with strontium picrate. The structure showed a unique *all-trans* peptoid bond configuration with the carbonyl groups alternately pointing toward the strontium cations and forcing the *N*-linked side chains to assume an alternate pseudo-equatorial arrangement.

³⁴ S. B. Y. Shin, B. Yoo, L. J. Todaro, K. Kirshenbaum, *J. Am. Chem. Soc.* **2007**, *129*, 3218-3225.

³⁵ B. Yoo, S. Bin, Y. Shin, M. L. Huang, K. Kirshenbaum, *Chem. Eur. J.* **2010**, *16*, 5528-5537.

³⁶ N. Maulucci, I. Izzo, G. Bifulco, A. Aliberti, C. De Cola, D. Comegna, C. Gaeta, A. Napolitano, C. Pizza, C. Tedesco, D. Flot, F. De Riccardis, *Chem. Commun.*, **2008**, 3927-3929.

³⁷ K. E. Koenig, G. M. Lein, P. Stuckler, T. Kaneda, D. J. Cram, *J. Am. Chem. Soc.*, **1979**, *101*, 3553-3566.

In 2013 the design and synthesis of chiral cyclopeptoids has been reported. The choice to introduce L-Proline residues was ascribed to the ability of this natural amino acid to induce conformational features on secondary structures of peptides and protein. Hexameric cyclic peptoids containing L-Proline and *N*-methoxyethyl glycine showed interesting complexation properties towards first group metal cations, and in particular compound **28** showed a unique crystal structure. The arrangement of this cyclic α -peptoid is rather intriguing and intricate. In the solid state structure three cyclopeptoid rings, four Na⁺ ions, and one acetonitrile molecule form a triple-decker salt sandwich metal complex with a crystallographic 3-fold rotation symmetry.³⁸

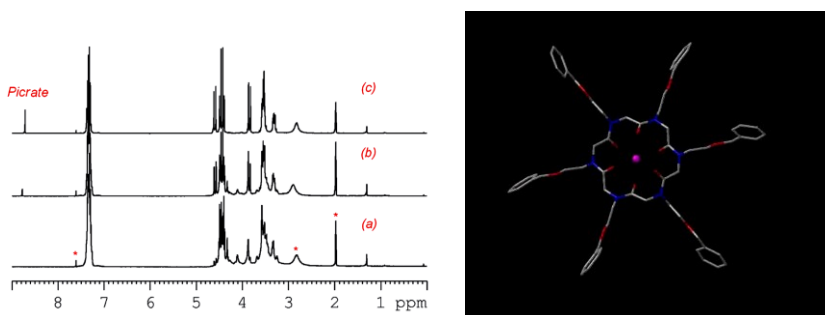
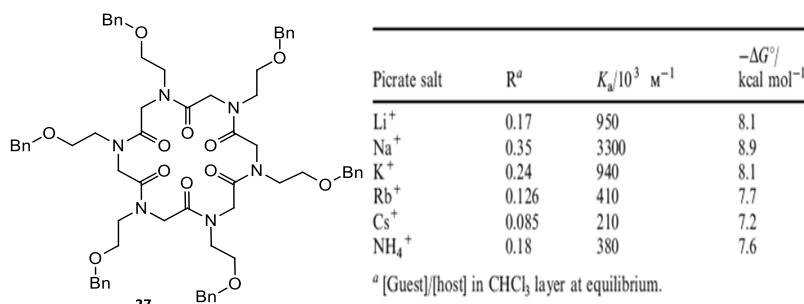


Figure 1.13 *N*-benzyloxyethyl cyclic α -peptoid and complexation

More recently, starting from these well-defined complexation properties, cyclopeptoids have been tested in phase-transfer catalysis.³⁹ In this contribution some differently substituted cyclohexapeptoids were tested in a benchmark phase-transfer reaction, the nucleophilic substitution of *p*-nitrobenzyl bromide with

³⁸. I. Izzo, G. Ianniello, C. De Cola, B. Nardone, L. Erra, G. Vaughan, C. Tedesco, F. De Riccardis, *Organic Letters*. **2013**, 598-601.

³⁹. G. Della Sala, B. Nardone, F. De Riccardis, I. Izzo, *Org. Biomol. Chem.* **2013**, *11*, 726-731.

sodium or potassium thiocyanate. The most active cyclopeptoids **29**, **30** and **31** have showed catalytic activities comparable with those exhibited by crown ethers; furthermore the macrocycle **32**, promoted the reaction with NaSCN, with reaction time and conversion comparable to 2.2.2- cryptand (**7**), one of the best macrocyclic polyether catalyst tested; (table 1.1).

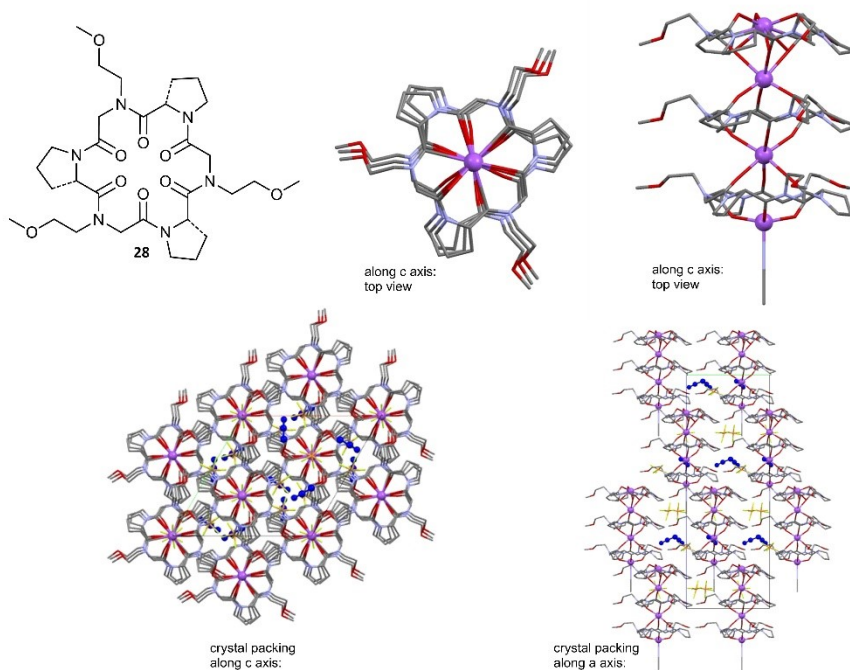


Figure 1.14 Crystal structure and crystal packing of chiral cyclohexapeptoid

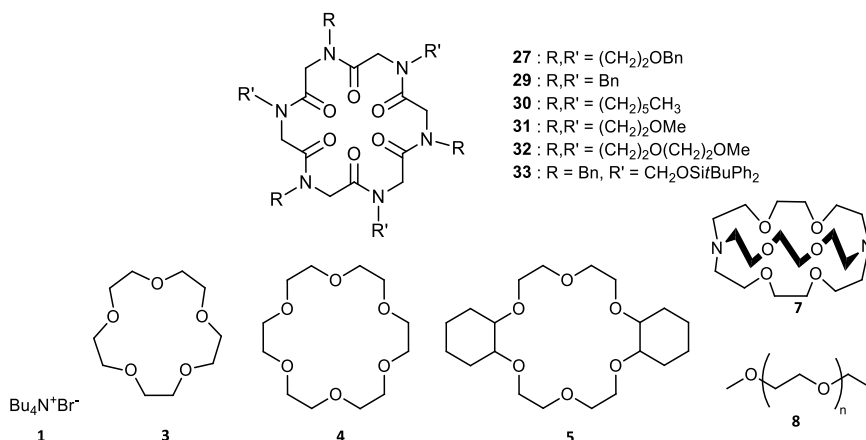
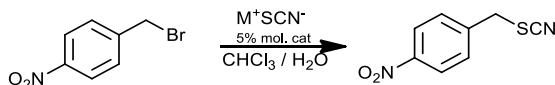


Figure 1.15 Comparison of cyclopeptoids and some commercially available PTC

This contribution represents the first application of cyclopeptoids in phase-transfer catalysis.

Table 1.1 S_N2 reaction catalyzed by cyclopeptoids or some common PTC



	NaSCN		KSCN		
	catalyst	Time (h)	Conversion(%)	Time (h)	Conversion(%)
1	-	24	10	24	5
2	29	24	95	13	>99
3	30	4.5	>99	24	53
4	31	8	>99	24	91
5	32	2.5	>99	7.5	>99
6	33	12	>99	24	71
7	1	4.5	>99	4.5	>99
8	3	8	>99	1	>99
9	4	24	>99	7.5	>99
10	5	6.5	>99	3	>99
11	7	2	>99	1	>99
12	8	24	81	24	85

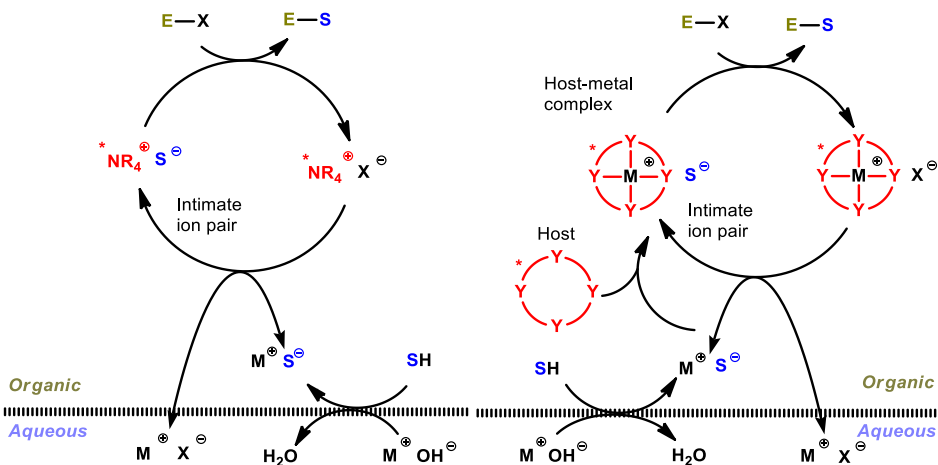
1.4 Application of macrocyclic systems in asymmetric PTC

The continuing search for new chiral catalysts for the synthesis of enantio-enriched molecules, have in some way also exploited the design of novel chiral macrocyclic systems. Compared to the extensively developed above mentioned ammonium salts and Maruoka's catalysts, the macrocyclic systems have been less investigated although they look to be intriguing alternative to the onium salts.^{40, 41} First of all, it must be considered the different reaction mechanism for the two main classes of catalytic systems. The reaction mechanism for onium salts envisages the formation of an intimate ion pair between the quaternary ammonium salt and the anion of the substrate generated by deprotonation (scheme 1.7). On the other hand, the mechanism for neutral macrocyclic systems

⁴⁰. T. Ooi, Keiji Maruoka, *Angew. Chem. Int. Ed.* **2007**, *46*, 4222 – 4266.

⁴¹. S. Shirakawa, K. Maruoka, *Angew. Chem. Int. Ed.* **2013**, *52*, 4312 – 4348.

involves the formation of a metal-macrocycle complex, and then the generation of the intimate ion pair between the host-guest complex and the anion of the substrate (scheme 1.7). The application of different neutral macrocyclic systems will be discussed in the next paragraphs, especially focused on chiral crown ethers and calixarenes.



Scheme 1.7 Reaction mechanism of phase transfer processes promoted by onium salts or neutral macrocycles

1.4.1 Crown ethers in asymmetric PTC

Chiral crown ethers have been used for asymmetric phase-transfer catalysis. The first successful application involved binaphthyl-modified crown ethers (figure 1.16) in Michael reactions between methyl vinyl ketone and 2-methoxycarbonyl-1-indanone or between methyl 2-phenylpropionate and methyl acrylate. The resulting enantioselectivities were good.⁴²

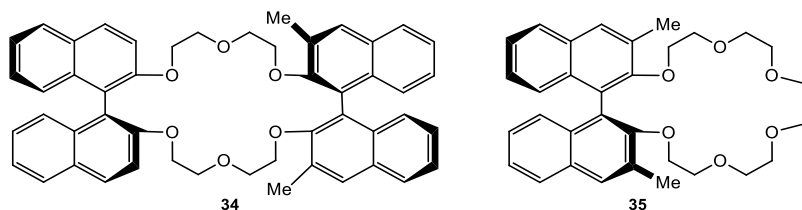


Figure 1.16 Chiral binaphthyl-modified crown ethers

⁴² D. J. Cram, G. D. Y. Sogah, *J. Chem. Soc., Chem. Commun.* **1981**, 625–628.

The addition of methyl phenylacetate to methyl acrylate was also investigated with different chiral crown ethers by other research groups.⁴³ For example, the Michael addition of differently substituted phenylacetates with methyl acrylate was carried out with various chiral crown ethers (**36-44**) (figure 1.17). It has been found that simple chiral C_2 -symmetric chiral crown ethers (**36-42**), in the presence of KOtBu, catalyze the Michael addition with moderate to good enantiomeric excesses (Table 1.2, entries 1-10), while the crown ethers **43** and **44** afforded disappointing results (Table 1.2, entries 11, 12).

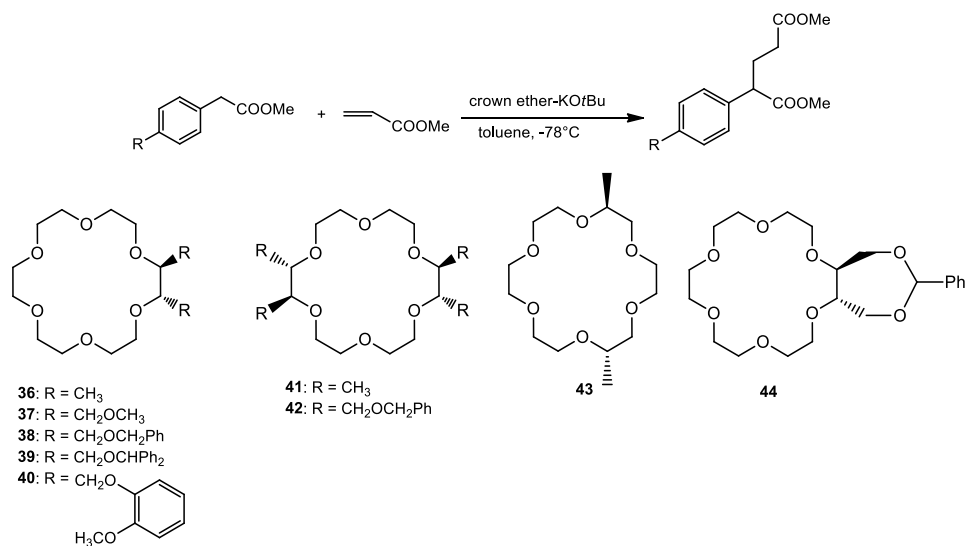


Figure 1.17 Asymmetric Michael addition with chiral crown ethers

Subsequently some chiral azacrown ethers (**45-48**) derived from D-glucose were synthesized and applied in Michael reaction of nitropropane to *trans*-chalcone.⁴⁴ The same catalysts were used also in the Darzens condensation. Moreover, these catalysts (**45**) have been used in asymmetric epoxidation of chalcones. For instance

⁴³. For examples see: a) M. Alonso-López, M. Martín-Lomas, S. Penadés, *Tetrahedron Lett.*, **1986**, 27, 3551–3554; b) S. Aoki, S. Sasaki, K. Koga, *Tetrahedron Lett.*, **1989**, 30, 7229–7230; c) E. Brunet, A. M. Poveda, D. Rabasco, E. Oreja, L. M. Font, M. S. Batra, J. C. Rodríguez-Ubis, *Tetrahedron: Asymmetry*, **1994**, 5, 935–948.; d) L. Töke, P. Bakó, G. M. Keserű, M. Albert, L. Fenichel, *Tetrahedron*, **1998**, 54, 213–222.

⁴⁴. For examples see: a) M. Alonso-López, M. Martín-Lomas, S. Penadés, *Tetrahedron Lett.*, **1986**, 27, 3551–3554; b) S. Aoki, S. Sasaki, K. Koga, *Tetrahedron Lett.*, **1989**, 30, 7229–7230; c) E. Brunet, A. M. Poveda, D. Rabasco, E. Oreja, L. M. Font, M. S. Batra, J. C. Rodríguez-Ubis, *Tetrahedron: Asymmetry*, **1994**, 5, 935–948.; d) L. Töke, P. Bakó, G. M. Keserű, M. Albert, L. Fenichel, *Tetrahedron*, **1998**, 54, 213–222.

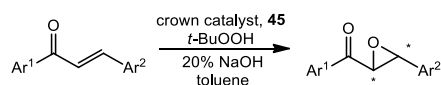
the chiral catalyst **45**, with R = (CH₂)₃OH, is able to catalyze the asymmetric epoxidation of α,β -enones (Table 1.3).^{45b}

Table 1.2 Asymmetric Michael addition with chiral crown ethers^a

Entry	Catalyst	R	Time(h)	Yield(%)	ee ^b (%)
1	36	H	3	95	79 (S)
2	36	OMe	2.5	66	81 - ^b
3 ^a	36	NO ₂	48	73	60 - ^b
4	36	Me	2	80	79 - ^b
5	37	H	3	97	48 (S)
6	38	H	3	98	74 (S)
7	39	H	3	99	70 (S)
8	40	H	1	72	63 (S)
9	41	H	3	89	56 (R)
10	42	H	3	91	56 (R)
11	43	H	3	79	1(R)
12	44	H	3	96	2 (R)

^aCarried out at -45°C. ^bNot yet determined.

Table 1.3 Asymmetric epoxidation with the chiral monosaccharide-based crown ether **46**



Entry	Ar ¹	Ar ²	Time(h)	Yield(%)	ee(%)
1	Ph	Ph	1	82	94
2	CH ₃	Ph	20	-	-
3	<i>t</i> Bu	Ph	16	86	90
4	1-Naphthyl	Ph	10	64	67
5	2-Naphthyl	Ph	3	30	87
6	Ph	CH ₃	6	60	55
7	Ph	<i>t</i> Bu	18	53	34
8	Ph	1-Naphthyl	9	68	83
9	Ph	2-Naphthyl	6	33	66
10	<i>t</i> Bu	1-Naphthyl	12	60	85
11	<i>t</i> Bu	2-Naphthyl	12	52	92

Chiral crown ethers were also employed in the enantioselective oxidation of aromatic ketones,⁴⁵ asymmetric alkylation of glycine derivatives with moderate enantioselectivity,⁴⁶ and conjugated addition of glycine imine with several Michael acceptors (figure 1.18).⁴⁷

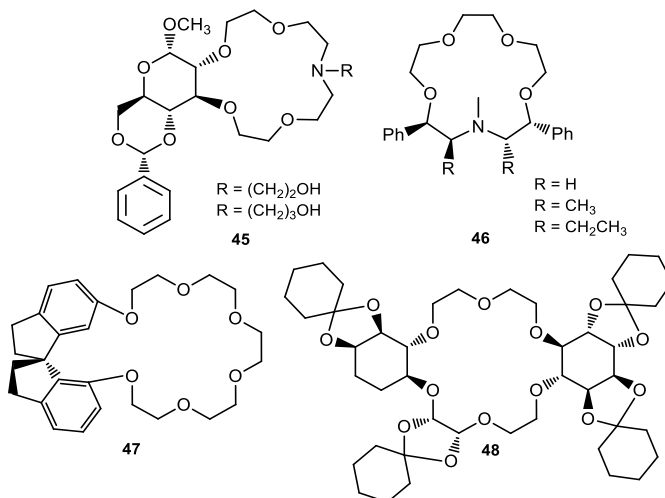


Figure 1.18 Chiral crown ethers tested in asymmetric phase-transfer catalysis

1.4.2 Calixarenes in asymmetric PTC

The use of calixarenes in asymmetric phase transfer catalysis has been rarely investigated and very few examples are reported in literature. To the best of our knowledge there are just two articles in which calixarenes are employed in this field. However, in both examples the calixarene is used as a scaffold to anchor ammonium salts. In the Sirit's group contribution, a cinchonidine-derived chiral calix[4]arene (**49**) has been synthesized and used in the alkylation reaction of the glycine derivatives with moderate enantioselectivity.⁴⁸ The calixarene **49** was used to carry out the asymmetric phase-transfer alkylation of *N*-(diphenylmethylene)glycine ethyl ester with benzyl bromide (Table 1.4).

45. a) E. F.J. de Vries, L. Ploeg, M. Colao, J. Brussee, A. Van der Gen, *Tetrahedron: Asymmetry* **1995**, *6*, 1123–1132; b) T. Bakò, Pèter Bakò, G. Keglevich, P. Bombicz, M. Kubinyi, K. Pál, S. Bodor, A. Makò, L. Tòke, *Tetrahedron: Asymmetry*, **2004**, *15*, 1589–1595.

46. K. Yonezawa, M. L. Patil, S. Takizawa, H. Sasai, *Heterocycles*, **2005**, *66*, 639–644.

47. T. Akiyama, M. Hara, K. Fuchibe, S. Sakamoto, K. Yamaguchi, *Chem. Commun.*, **2003**, *14*, 1734–1735.

48. S. Bozkurt, M. Durmaz, M. Yilmaz, A. Sirit, *Tetrahedron: Asymmetry* **2008**, *19*, 618–623.

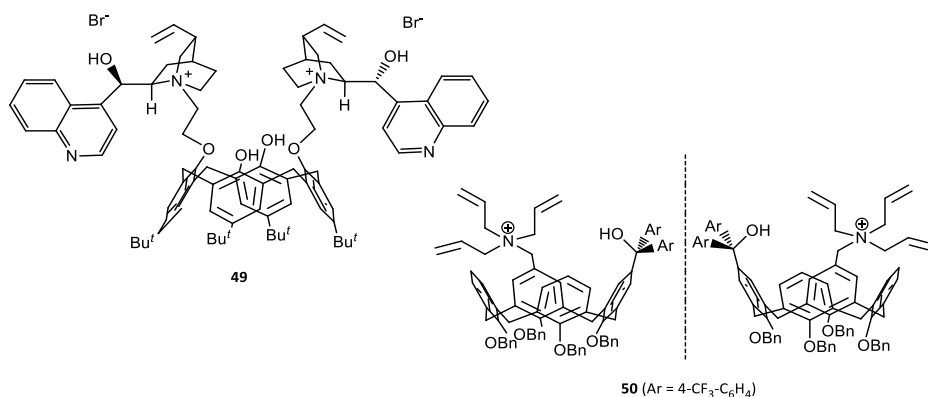
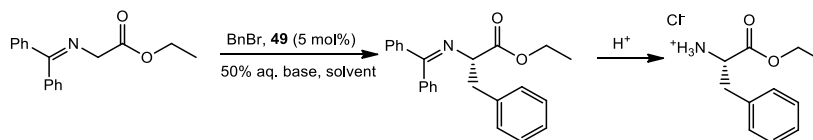


Figure 1.19 Calixarene-based chiral phase-transfer catalysts

Table 1.4 Asymmetric alkylation of *N*-(diphenylmethylene)glycine ethyl ester catalyzed by *cinchonidine*-derived calix[4]arene **49**



Entry	Solvent	T (°C)	Base	Yield ^a (%)	ee ^b (%)
1	Toluene/CHCl ₃ 7/3	-20	KOH	87	25 (S)
2	Toluene/CHCl ₃ 7/3	-20	NaOH	89	46 (S)
3	Toluene/CHCl ₃ 7/3	0	NaOH	95	57 (S)
4	Toluene/CHCl ₃ 7/3	rt	NaOH	92	52 (S)

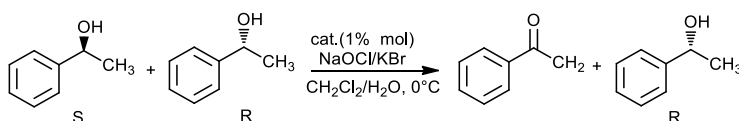
^aIsolated yields. ^bEnantiomeric excess was determined by HPLC analysis using a chiral column (DAICEL Chiralcel OD-H) using hexane/isopropanol (99:1) as an eluent.

The best level of enantioselectivity was accomplished with an aqueous solution of NaOH at 0°C (Table 1.4, entry 3). The enantioselectivity was sensitive to the cation of the base: in fact, with an aqueous solution of KOH, (Table 1.4, entry 1) a low ee was achieved. The temperature also affected the outcome of this reaction with a lower ee value at -20°C (Table 1.4, entries 2,3). In 2010, Shimizu's group reported the synthesis of inherently chiral calix[4]arenes **50** containing a quaternary ammonium moiety, which were applied in the asymmetric alkylation reaction of glycine derivatives. Although the enantioselectivity was very low, this represents the first application of inherently chiral calix[4]arene as a chiral phase-transfer

catalyst.⁴⁹ Although the calixarenes are involved in PTC processes these two contributions did not exploit the ability of macrocycles in complexing metal ions.

1.4.3 Cyclopeptoids in asymmetric PTC

Despite the wide use of peptides and synthetic analogues in asymmetric catalysis, to the best of our knowledge, up to the date, peptoids, peptide analogues, have been scarcely explored for applications in this field: in fact despite the wide use of peptide systems in catalysis, in literature is reported a single example in which a linear peptoidic system is employed as enantioselective catalyst.⁵⁰ The study, reported by Kirshenbaum, focuses on the use of linear peptoidic oligomers in the enantioselective catalysis.⁵¹



Scheme 1.8 Catalytic oxidation of 1-phenylethanol by peptoids

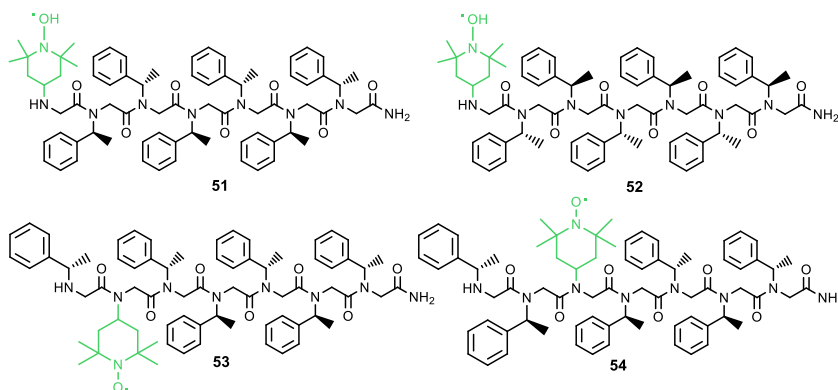


Figure 1.20 Peptoid sequences evaluated for catalysis

The approach involves the synthesis of hexapeptoids containing different TEMPO (2,2,6,6-tetramethylpiperidine-1-oxyl) residues into peptoidic backbone. These catalysts were effectively used for the oxidative kinetic resolution of 1-phenylethanol (scheme 1.8). The peptoid (**51**) is characterized by right-handed

⁴⁹ S. Shirakawa, S. Shimizu, *New J. Chem.* **2010**, *34*, 1217-1222.

⁵⁰ R. P. Megens, G. Roelfes, *Chem. Eur. J.*, **2011**, *17*, 8514-8523.

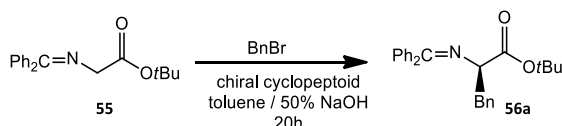
⁵¹ G. Maayan, M. D. Ward, K. Kirshenbaum, *PNAS.*, **2009**, *106*, 13679-13684.

helical configuration and the TEMPO group is covalently attached at the N terminus; this compound was able to perform the kinetic resolution; the same behaviour was revealed by the linear oligomer (**52**) presenting left-handed helical configuration. When the TEMPO was attached on internal positions of the oligomer (**53** or **54**), on the other hand, no enantioselectivity (Table 1.5) was observed.

Table 1.5 Oxidative kinetic resolution reaction with peptoids

Catalyst	Conversion %	Time (min)	ee%
51	84	120	>99(<i>R</i>)
52	85	120	>99(<i>S</i>)
53	26	30	-
54	25	30	-

The challenge of using macrocyclic peptoid in asymmetric phase-transfer catalysis started few years ago in our laboratories where the first application of chiral cyclopeptoids was successfully performed. The efficiency of this novel class of macrocycle catalysts was tested in the benzylation of *N*-(diphenylmethylene)glycine *t*-butyl ester (scheme 1.9).⁵² The investigation was performed with a liquid-liquid biphasic system of toluene and 50% NaOH aqueous solution. All reactions were conducted with a catalyst loading of 5 mol%.



Scheme 1.9 Benzylation of *N*-(diphenylmethylene)glycine *t*-butyl ester

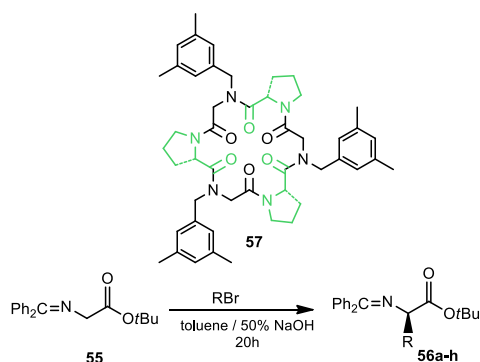
Preliminary studies showed a partial decomposition of the starting material performing the alkylation under aerobic conditions. The degradation process was revealed by the presence of benzophenone, observed by ¹H-NMR. Similar secondary reactions have been reported for imines derivatives of glycine, under phase-transfer catalysis.⁵³ This problem has been overcome, by the Maruoka's group, by conducting the reactions under inert atmosphere. Also in this

⁵² R. Schettini, B. Nardone, F. De Riccardis, G. Della Sala, I. Izzo, *Eur. J. Org. Chem.*, **2014**, 7793–7797.

⁵³ J.-H. Lee, M.-S. Yoo, J.-H. Jung, S.-s. Jew, H.-G. Park, B.-S. Jeong, *Tetrahedron* **2007**, *63*, 7906–7915.

cyclopeptoid catalyzed process, the use of inert atmosphere, after deoxygenation of the two phases, totally suppressed the decomposition of the substrate. This result confirms that the decomposition of the substrate was favored by the presence of oxygen in the reaction medium. After an exhaustive screening of different catalysts and reaction conditions, this investigation showed that the cyclopeptoid **57**, consisting of alternating residues of L-Proline and *N*-benzyl glycine, is able to catalyze the reaction of asymmetric alkylation with 67% ee. The (*R*) absolute configurations of **56a-h** was determined by comparison of the HPLC retention times reported in the literature: *R* enantiomer was obtained.

Table 1.6 Enantioselective benzylation of **55** with alkylating agents, catalyzed by **57**^{a,b}



Entry	RBr	Product	Time (h)	Yield (%)	ee (%) ^{c,d}
1	Benzyl bromide	56a	20	64	67 (<i>R</i>)
2	4-Nitrobenzyl bromide	56b	5	86	57 (<i>R</i>)
3	4-Fluorobenzyl bromide	56c	24	62	60 (<i>R</i>)
4	4-Cyanobenzyl bromide	56d	45	62	45 (<i>R</i>)
5	4-Methylbenzyl bromide	56e	24	66	73 (<i>R</i>)
6	3,5-Dimethylbenzyl bromide	56f	18	60	60 (<i>R</i>)
7	4-(<i>t</i> -Butyl)benzyl bromide	56g	24	53	47 (<i>R</i>)
8 ^e	Allyl bromide	56h	23	55	55 (<i>R</i>)

^aAll reactions were carried out in liquid-liquid system for 20 h, at 0.08 mmol scale using **55** (1.0 eq.), benzyl bromide (1.2 eq.) and catalyst (5 mol%) in toluene (0.8 mL), with 50% aq. NaOH (0.5 mL), unless otherwise stated. ^bAll reactions were performed under an inert atmosphere by deoxygenating the two phases. ^cDetermined by HPLC using a Chiralcel OD-H chiral stationary phase.

^dThe absolute configurations of products **56a-e**, **56g**, and **56h** were determined by comparison of the HPLC retention times and optical rotations with literature values^{12a, 53} and for **56f** by analogy with known products. ^eAllyl bromide (1.5 equiv.).

To expand the scope of the reaction different alkylating agents were tested using catalyst **57** under optimized reaction conditions. As can be seen, in Table 1.6, all the alkylating agents afforded enantioselectivities and yields comparable to those obtained with benzyl bromide. The reaction carried out in presence of 4-methylbenzyl bromide gave the best enantioselectivity (73% ee).

1.5 Aims of the work

Considering the well-defined advantages of asymmetric phase-transfer catalysis as a powerful method for organic synthesis, the aim of this research project is to introduce novel macrocycle systems as new and efficient catalysts in this field.

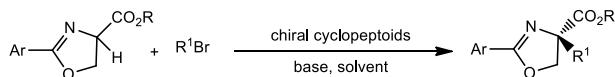
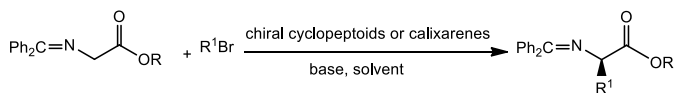
First of all, considering the advantages of the easy synthetic process for the preparation of cyclopeptoids, their well-explored complexation properties and the preliminary study on the application as phase-transfer catalysts,⁵² the idea is to deeply investigate their use in PTC. The advantages of the solid phase synthesis, such as the easy purification of the intermediates and the modular nature of the products, make cyclopeptoids ideal candidates for the discovery of new catalytic systems, as it is possible to incorporate a wide variety of functionalities inside the backbone of the macrocycle in an expeditious way. As a consequence, a library of peptoid-based chiral macrocycles of different size, decorated with alternating residues of L-Proline and different aromatic side chains, will be prepared and used for enantioselective alkylation reactions.

The scope of this project extends also to the investigation of novel chiral calixarenes. However, in this case, the idea is to exploit the ability of calixarenes to form host-guest complexes with alkali cations. The study is also devoted to further explore the potential of crown ethers in new catalytic processes. The second chapter focus first on the synthesis of novel chiral cyclopeptoids and then on their application in asymmetric phase-transfer alkylations, in particular for the enantioselective synthesis of α -amino acids. Afterwards the application of new designed calixarenes for the same alkylation reaction is described. Finally the application of cyclopeptoidic systems in the enantioselective alkylation of 2-aryl-oxazoline-4 carboxylic acid esters is discussed. The third chapter describes the application of crown ethers in phase-transfer processes. For this purpose a

diastereoselective methodology for the synthesis of γ -substituted butenolides by a direct vinylogous Mukayama-Michael reaction has been developed.

The following chapters are summarized in the scheme 1.10.

chapter 2



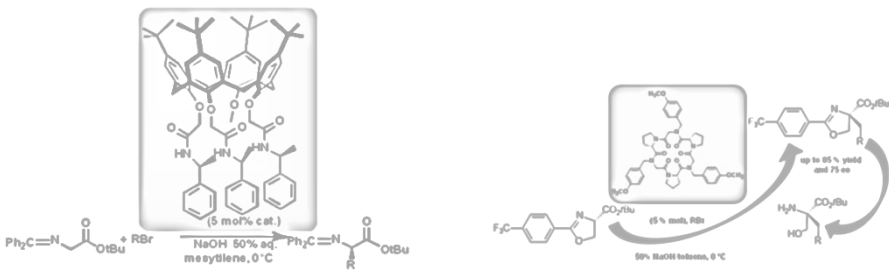
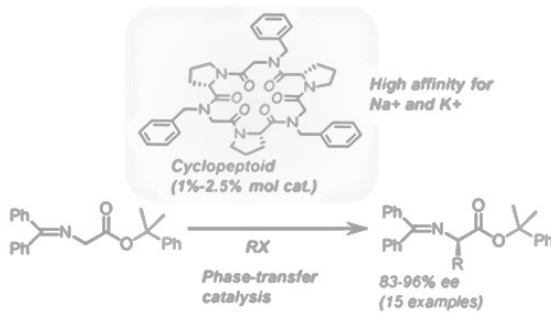
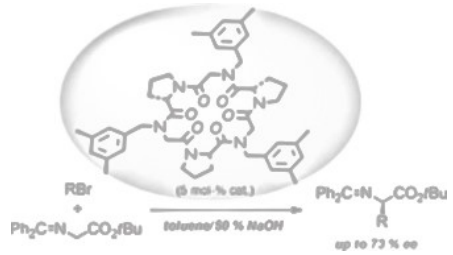
chapter 3



Scheme 1.10 Summary of reactions in every chapter

Chapter 2

Alkylation Reactions



2. ALKYLATION REACTIONS

2.1 Introduction

Since its first application, the asymmetric alkylation of glycine derivatives, introduced by O'Donnell's group, has proved to be a valid method for the preparation of α -amino acids and their analogues with high enantioselectivity. Nowadays the alkylation of *N*-(diphenylmethylene)glycine *t*-butyl ester is generally used as benchmark reaction in order to investigate the performances of new catalytic systems in phase-transfer reactions. An important aspect of the reaction is the selective formation of the mono-alkylated product without the undesired dialkylated byproduct. This result has been attributed to the lower acidity of the α proton in the product compared to the acidity of protons in the reagent. This is crucial for the configurational stability of chiral center generated in the course of the reaction (figure 2.1).^{54, 55}

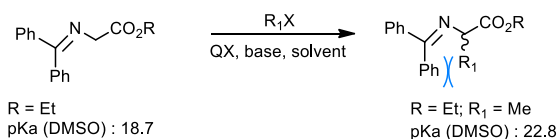
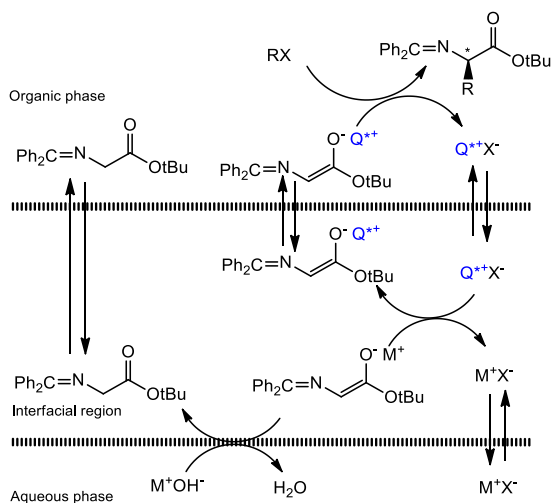


Figure 2.1 Blockage of the second alkylation on the benzophenone imine derivative

The mechanistic aspects of the reaction have been studied. The substrate, soluble in the organic phase, is distributed by diffusion in the interfacial region where, in the presence of a base, is deprotonated in α position, leading to the formation of a metallic enolate; the use of a chiral phase-transfer catalyst enables the exchange of the cationic species and consequently generates a chiral enolate, characterized by two π enantiotopic faces. This enolate is more soluble in the organic phase where it reacts with the alkylating agent (scheme 2.1). It is important to underline that the generation of the chiral enolate must be fast to prevent any stereoselective alkylation reactions; it is also important that the chiral enolate is characterized by an intimate ion pair, so that the chiral species can be actively engaged in the asymmetric induction of the next alkylation reaction.

⁵⁴. M. J. O'Donnell, *Acc. Chem. Res.*, **2004**, *37*, 506-517.

⁵⁵. M. J. O'Donnell, *J. Am. Chem. Soc.*, **1988**, *110*, 8520-8525.



Scheme 2.1 Asymmetric PTC mechanism of benzofenone imine derivative

The increasing development of this enantioselective reaction has led to a large number of new catalysts. In figure 2.2 are reported the most common catalysts, used in this reaction, featuring the most significant structural modifications introduced, thanks to the understanding of different aspects of this reaction. For example Corey's^{12a} and Lygo's groups⁵⁶, developed a modified *Cinchona* alkaloid-derived quaternary ammonium catalysts with a *N*-anthracenylmethyl group. These catalysts showed an increased enantioselectivity in the asymmetric alkylation of a benzophenone-derived glycine-imine. A recent systematic study on structure/activity relationship revealed that the Corey/Lygo catalysts gave the higher values of enantioselectivity because the *N*-anthracenylmethyl group was able to direct the enolate molecular recognition.⁵⁷ The synthesis of dimeric and trimeric quaternary ammonium salts⁵⁸ offers the possibility to investigate different aspects of this reaction such as the counter-anion effect or electronic features. The counter-anion generally affected the final enantioselectivity, for instance, the hexafluorophosphate salt **64** and its analogue tetrafluoroborate salt anions gave

⁵⁶ B. Lygo, P. G. Wainwright, *Tetrahedron*, **1997**, *38*, 8595-8597.

⁵⁷ S. E. Denmark, N. D. Gould, L. M. Wolf, *J. Org. Chem.* **2011**, *76*, 4337-4357.

⁵⁸ a) H. Park, B. Jeong, M. Yoo, J. Lee, B. Park, M. G. Kim, S. Jew, *Tetrahedron Letters* **2003**, *44*, 3497-3500; b) R. Chinchilla, P. Mazón, C. Nájera, F. J. Ortega, *Tetrahedron: Asymmetry* **2004**, *15*, 2603-2607.

higher ee in comparison with chloride or bromide. The increased enantioselectivity was attributed to the formation of a less tight ion pairs between tetrafluoroborate or hexafluorophosphate anions and the quaternary ammonium cation. Moreover, various functional groups with different electronic properties were introduced on the catalyst's structure to improve their performances. In some cases, the presence of fluorine atoms allowed higher enantioselectivity. Another leading class of catalysts successfully used in the same reaction are the Maruoka's catalysts. The first synthesis of Maruoka's spirobinaphthyl quaternary ammonium salts, reported in 1999, was realized starting from commercially available (*S*)- or (*R*)-1,1'-bi-2-naphthol (figure 2.3).^{14a} These new C_2 -symmetric phase-transfer catalysts were successfully applied in the alkylation reaction with high levels of enantioselectivity. In summary *Cinchona* alkaloids and Maruoka's catalysts are extensively involved in this reaction, while catalysts based on different chiral scaffolds are less common. As described in the first chapter there are several efficient binaphthyl-derived quaternary ammonium salts based on Maruoka's scaffold while catalysts based on different chiral scaffold are less common (chapter 1, figure 1.4). The interest in developing new phase-transfer catalysts for this type of reaction also lies in the opportunity to realize the synthesis of biologically active compounds or drugs on large scale preparation. Some examples are: the synthesis of (*S*)-*N*-acetylindoline-2-carboxylic acid *t*-butyl ester (**66**), a key intermediate in the synthesis of the angiotensin converting enzyme (ACE) inhibitor, or L-Dopa *t*-butyl ester (**67**).⁵⁹ This methodology was applied for the first asymmetric synthesis of levobupivacaine (**68**) a long-acting local anaesthetic drug.⁶⁰ The use of *N*-(diphenylmethylene)glycine *t*-butyl ester in the total synthesis of (-)-antofine (**69**) is an important application in the antitumor discovery field.⁶¹ The growing interest towards cancer chemotherapy drives the research of new agents for examples benzamide derivatives are ideal candidates in this area (**70**).⁶²

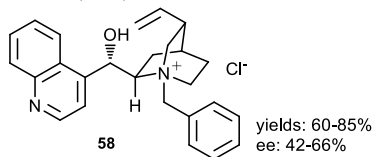
⁵⁹ T. Ooi, M. Kameda, K. Maruoka, *J. Am. Chem. Soc.*, **2003**, *125*, 5139-5151.

⁶⁰ S. Kumar, U. Ramachandran, *Tetrahedron Letters*, **2005**, *46*, 19-21.

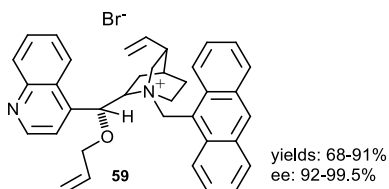
⁶¹ S. Kim, J. Lee, T. Lee, H. Park, D. Kim, *Org. Lett.* **2003**, *5*, 2703-2706.

⁶² R. K. Boeckman, T. J. Clark, B. C. Shook, *Org. Lett.*, **2002**, *4*, 2109-2112.

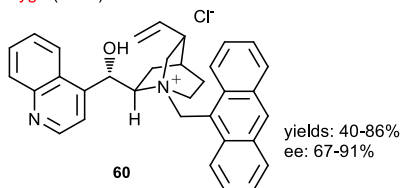
O'Donnell (1989)



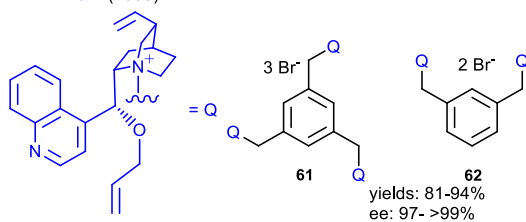
Corey (1997)



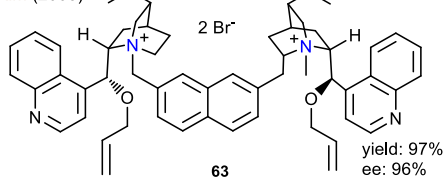
Lygo (1997)



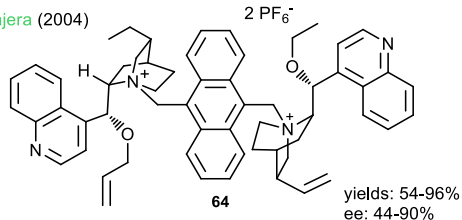
Park (2003)



Kim (2003)



Nájera (2004)

Figure 2.2 Representative examples of *Cinchona* Alkaloid Derived Catalysts

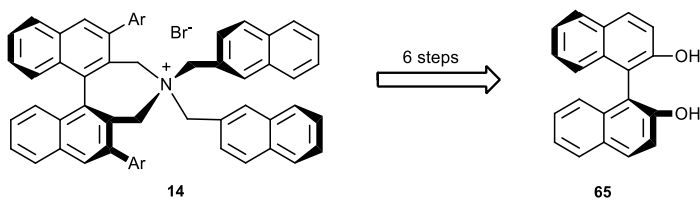


Figure 2.3 Maruoka's spirobinaphthyl quaternary ammonium salts

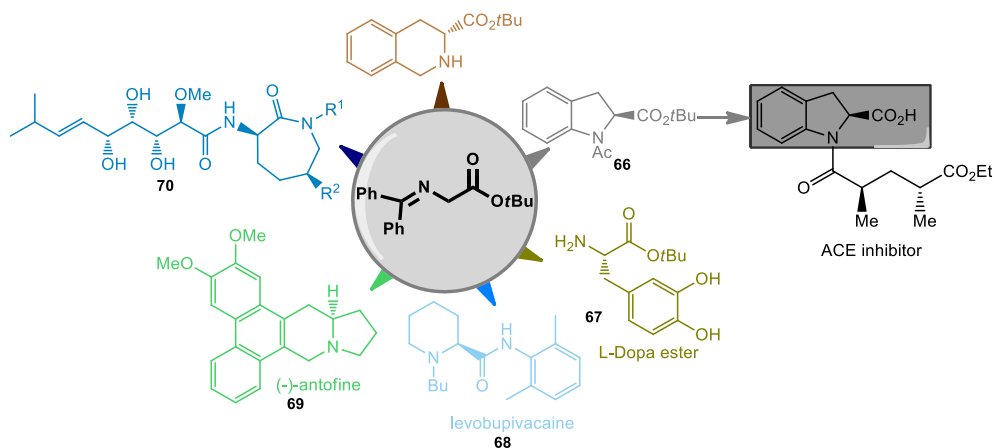


Figure 2.4 Representative examples of *N*-(diphenylmethylene)glycine *t*-butyl ester derived drug candidates

2.2 New insights on the asymmetric alkylation reaction of *N*-(diphenylmethylene)glycine derivatives

The purpose of the research study has been the synthesis and application of new cyclopeptoid scaffolds in phase-transfer catalysis. Considering the complexation abilities, the metal ion affinities, the similarities with the well know crown ethers and the promising results observed with a catalyst decorated with *N*-benzyl groups alternating with residues of L-Proline,⁵² the design and the synthesis of new cyclopeptoids, containing differently substituted aromatic side chains, was planned.

The first target has been the preparation of a library of cyclohexapeptoids and cyclotrapeptoids in order to study not only the influence of the side chain but also of cavity size on the catalytic efficiency (figure 2.5). Moreover, considering the promising results obtained with the first application of the chiral cyclopeptoids

in the alkylation of *N*-(diphenylmethylene)glycine *t*-butyl ester (**55**, figure 2.5)⁵² we decided to investigate more deeply this reaction, considering new parameters, such as the structure of the substrate, in order to improve the enantiomeric excesses and to obtain results comparable to the best catalysts reported in literature.

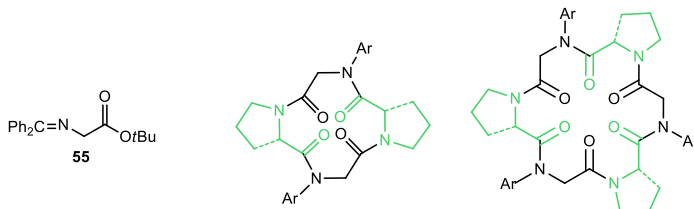


Figure 2.5 General structures of cyclotetrapeptoids and cyclohexapeptoids

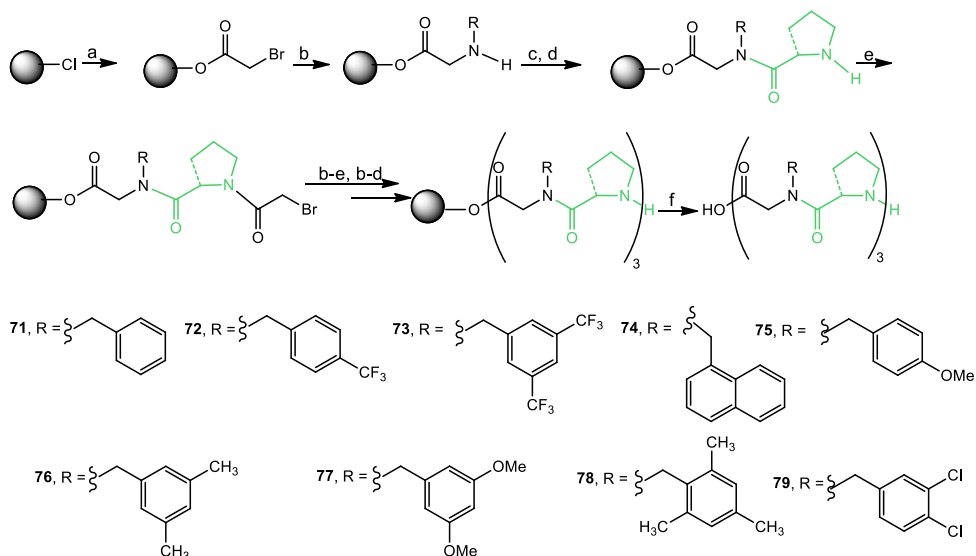
2.2.1 Synthesis of Chiral Cyclohexapeptoids

Taking advantage of a mixed sub-monomeric/monomeric approach, nine chiral C_3 -symmetric cyclohexapeptoids (**80-88**) were prepared, containing alternating residues of *N*-arylmethylglycine and L-Proline. The modular synthesis is based on a solid-phase process, potentially automated, characterized by quick preparation and easy workup/purification. The first step is the loading of bromoacetic acid on a chlorotriptyl resin; this step is followed by a nucleophilic substitution with a primary amine to build the first monomer. Then there is a coupling reaction with a chiral monomer, in this case L-Proline, in presence of a coupling reagent such as HATU followed by a deprotection step. The repetition of the steps described above affords a linear peptoid oligomer, attached on the resin. Cleavage reaction, in mild acidic conditions, affords the free linear hexapeptoid (scheme 2.2). No purification steps are required and by-products are eliminated by easy filtration. The next step is a cyclization reaction that involves an head-to-tail connection in high dilution conditions (scheme 2.3). By this way, compounds **80-88** were prepared in a good yield and purity as confirmed by NMR and HPLC analysis.

2.2.2 Synthesis of Chiral Cyclotetrapeptoids

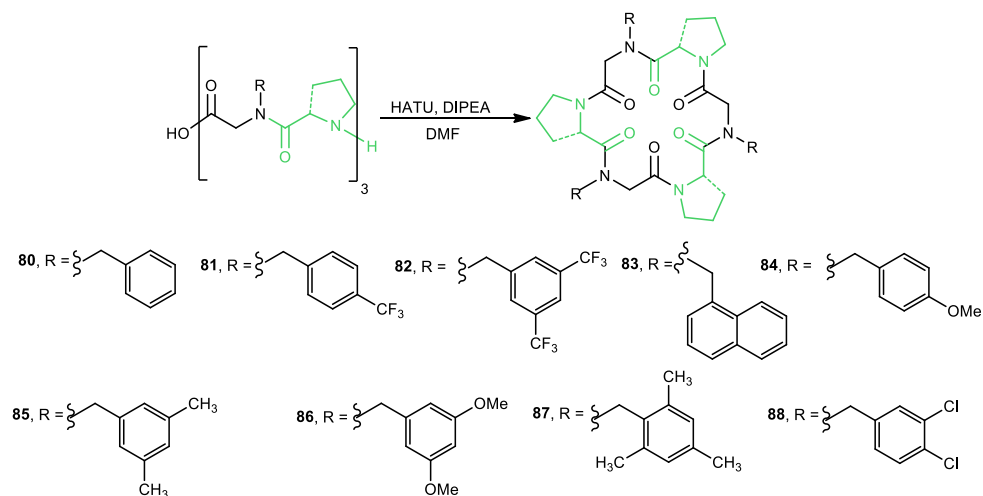
Subsequently, in order to investigate the role of the macrocycle's cavity size in the catalytic process, the synthesis of a small library of cyclotetrapeptoids,

containing aromatic chains, was performed, using the same sub-monomeric/monomeric approach (Scheme 2.4).



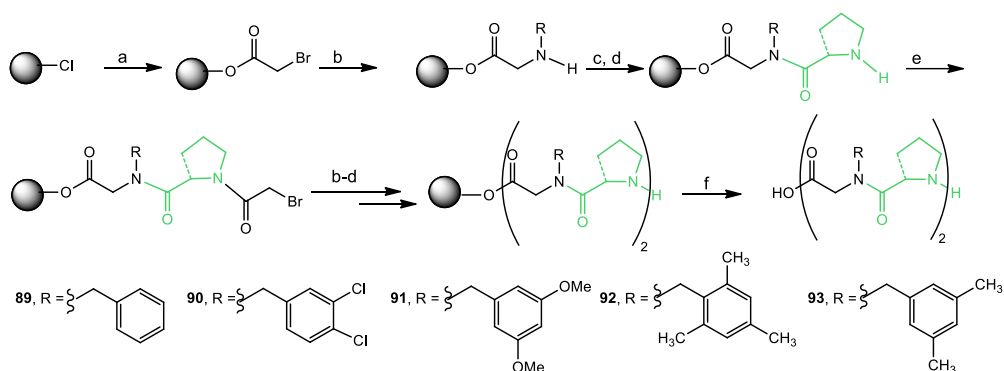
Reagents and conditions: a) bromoacetic acid, DIPEA; b) RNH₂; c) *N*-Fmoc-L-Proline, HATU; d) 20% piperidine/DMF; e) bromoacetic acid, DIC; f) HFIP/CH₂Cl₂ [1:4]. DIPEA = *N,N* diisopropylethylamine; DIC = *N,N'*-diisopropyl carbodiimide. HATU = 1-[Bis(dimethylamino)methylene]-1*H*-1,2,3-triazolo[4,5-*b*]pyridinium 3-oxid hexafluorophosphate.

Scheme 2.2 Solid phase synthesis of linear hexapeptides



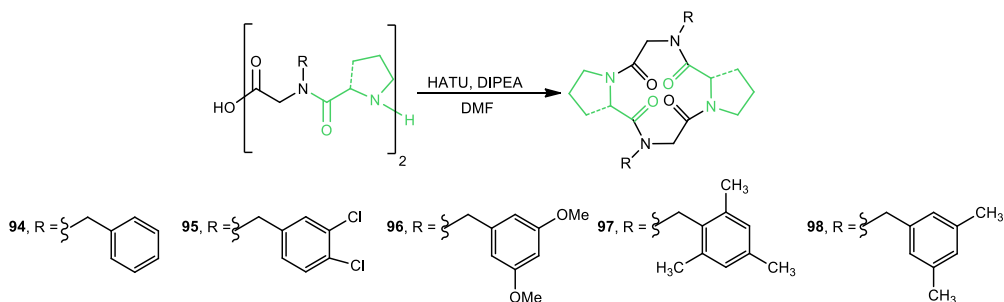
Yields: **80** 49%, **81** 18%, **82** 23%, **83** 22%, **84** 57%, **85** 43%, **86** 20%, **87** 10%, **88** 53%.

Scheme 2.3 Head-to-tail cyclization of hexapeptides



Reagents and conditions: a) bromoacetic acid, DIPEA; b) RNH₂; c) *N*-Fmoc-L-Proline, HATU; d) 20% piperidine/DMF; e) bromoacetic acid, DIC; f) HFIP/CH₂Cl₂ (1:4). DIPEA = *N,N* diisopropylethylamine; DIC = *N,N*-diisopropyl carbodiimide. HATU= 1-[Bis(dimethylamino)methylene]-1*H*-1,2,3-triazolo[4,5-*b*]pyridinium 3-oxid hexafluorophosphate.

Scheme 2.4 Solid phase synthesis of linear tetrapeptides



Yields: **94** 19%, **95** 11% **96** 62%, **97** 13%, **98** 27%.

Scheme 2.5 Head-to-tail cyclization of tetrapeptides

Cyclic tetrapeptides, unlike the cyclohexapeptides, present a rigid conformation and non prolinated cyclotetrapeptides, previously described in literature, adopt a *cis-trans-cis-trans* peptoid sequence.^{36,63,64} To the best of our knowledge only one example of a *bis*-prolinated analogue is reported in literature.^{65,66} The cyclo(L-Pro-Sar)₂, prepared by Shimizu and co-workers, showed a rigid all-*cis* peptoid bond conformation, as revealed by X-ray analysis (figure 2.6, a). In our case this C₂-

63. C. Tedesco, L. Erra, I. Izzo, F. De Riccardis, *CrystEngComm*, **2014**, *16*, 3667–3687.

64. (a) A. S. Culf, M. Čuperlović-Culf, D. A. Léger, A. Decken, *Org. Lett.* **2014**, *16*, 2780–2783. (b) P. Groth, *Acta Chem. Scand.* **1970**, *24*, 780–790. (c) J. Dale, K. Titlestad, *J. Chem. Soc.* **1970**, 1403–1404.

65. T. Shimizu, Y. Tanaka, K. Tsuda, *Biopolymers* **1983**, *22*, 617–632

66. K. Ueno, T. Shimizu, *Biopolymers* **1983**, *22*, 633–641.

symmetric structure was confirmed by a ROESY experiment performed on cyclotetrapeptoid **98**.⁶⁷ The key cross peak between the Pro-H α (d, 5.52 ppm) and the Gly-H (d, 4.67 ppm) corroborated a *cis* peptoid bond junction for the Pro-*N*(alkyl)-Gly sequence (figure 2.6, b). Starting from the X-rays analysis reported in literature by Shimizu a computational study by DFT calculations was performed. This study confirmed the proximity of Pro-H α and Gly-H.

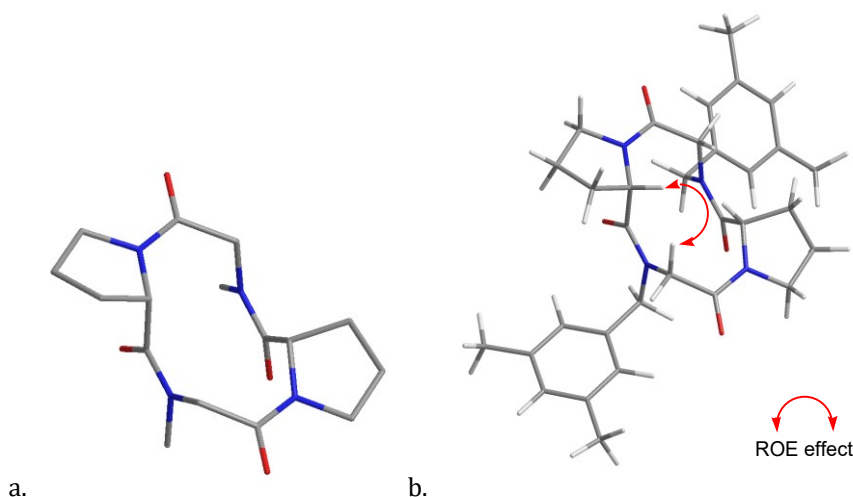


Figure 2.6 a. X-ray structure for the all-*cis* cyclo(L-Pro-Sar)₂ reported by Shimizu; b. predicted lowest energy conformation for the cyclotetrapeptoid **98** by DFT calculations (atom type: C gray, N blue, O red, H white; hydrogen atoms omitted for clarity). The ROE effect is depicted by the red arrow. Gaussian 08 Software Package.

2.2.3 Evaluation of complexation ability of cyclotetra and cyclohexapeptoids

Considering the influence of the complexation ability towards cations on the efficiency of phase-transfer catalysis, the association constants with alkali metal for cyclotetra and cyclohexapeptoids containing L-Proline residues was evaluated for the first time.

For this reason the complexing abilities of the simplest members of the two cyclic peptoid series (the *N*-benzyl- substituted compounds **80** and **94**), the association constants (K_a), $-\Delta G^\circ$ and R_{CHCl_3} ,⁶⁸ in the presence of Na⁺ and K⁺, were calculated

⁶⁷. A. Bax, D. G. Davis, *J. Magn. Reson.* **1985**, 63, 207.

⁶⁸. $R_{\text{CHCl}_3} = \frac{[\text{M}]_{\text{CHCl}_3}}{[\text{Hi}]_{\text{CHCl}_3}} = \frac{[\text{Guest}]}{[\text{Host}]}$ in CHCl₃ layer at equilibrium.

following the Cram's method³⁷ and reported in table 2.1.

To our delight we observed that the association constant between sodium cation and **80** was one order magnitude higher than the association constant determined for the well-known sodium complexing agent 15-crown-5.³⁸ Interestingly the association constant of cyclotetrapeptoid was higher than that determined for the non prolinated cyclohexapeptoids³⁶ which, however, performed as good phase-transfer catalyst too.³⁹

Table 2.1 Cram's method with picrate salts and cyclopeptoids

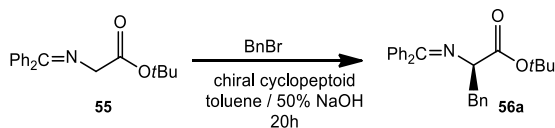
Entry	Complexing agent	M ⁺	R _{CHCl₃} ^a	K _a × 10 ⁻⁴ /M ⁻¹	-ΔG°/Kcal/mol
1	94	Na ⁺	0.38	530	9.1
2		K ⁺	0.34	206	8.5
3	80	Na ⁺	0.73	10000	10.8
4		K ⁺	0.62	2000	9.9

^a[Guest]/[Host] in CHCl₃ layer at equilibrium obtained by direct measurement, or calculated by difference from measurement made on aqueous phase at 25 °C (figures within ±10% in multiple experiments). Guest : host stoichiometry for extractions was assumed as 1 : 1.

2.2.4 Chiral cyclotetrapeptoids in the enantioselective benzylation of *N*-(diphenylmethylene) glycine *t*-butyl ester

Taking into account the complexation ability observed for the prolinated cyclotetrapeptoid, the small library of these macrocyclic compounds was studied in the asymmetric alkylation of *N*-(diphenylmethylene) glycine *t*-butyl ester which was previously investigated only for the larger cyclohexapeptoids.⁵²

Cyclotetrapeptoids proved to be able to catalyze the benzylation reaction (Table 2.2), even though with lower ee values than those with cyclohexapeptoids. Also in this case the macrocycles containing *N*-benzylic and 3,5-dimethylbenzylic side chains (**94** and **98**) proved to be the best, albeit modest, values of enantioselectivity (Table 2.2, entries 1 and 5).

Table 2.2 Enantioselective benzylation with chiral cycloheptapeptoids **94-98**^{a,b}

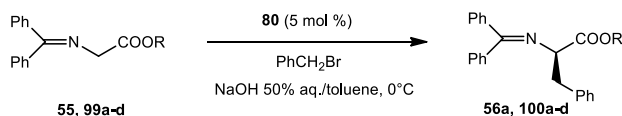
Entry	Catalyst	Yield (%)	ee (%) ^{c,d}
1	94	67	36 (<i>R</i>)
2	95	39	31 (<i>R</i>)
3	96	64	10 (<i>R</i>)
4	97	75	4 (<i>R</i>)
5	98	54	41 (<i>R</i>)

^aAll reactions were carried out in liquid-liquid system for 20 h, at 0.08 mmol scale using **55** (1.0 eq.), benzyl bromide (1.2 eq.) and catalyst (5 mol%) in toluene (0.8 mL), with 50% aq. NaOH (0.5 mL), unless otherwise stated. ^bAll reactions were performed under an inert atmosphere by deoxygenating the two phases. ^cDetermined by HPLC using a Chiralcel OD-H chiral stationary phase. ^dThe absolute configurations of product was determined by comparison of the HPLC retention times and optical rotations with literature values.^{12a,53}

2.2.5 Further developments in the application of chiral cyclohexapeptoids in the enantioselective alkylation of *N*-(diphenylmethylene)glycine derivatives: the role of ester functionality

As told before, the promising results in the enantioselective monoalkylation of *N*-(diphenylmethylene)glycine *t*-butyl ester in the presence of chiral cycloheptapeptoids, prompted us to thoroughly explore different aspects of the enantioselective alkylation in order to improve yields and ee's of the reaction products.⁶⁹ First of all we decided to investigate the influence of the substrate's ester group on the outcome of the alkylation reaction. Therefore the synthesis of different *N*-(diphenylmethylene)glycine esters (table 2.3) was realized and the enantioselective benzylation was tested using catalyst **80** under the best reaction conditions.

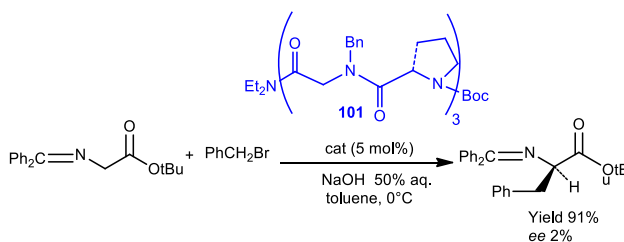
⁶⁹ R. Schettini, F. De Riccardis, G. Della Sala, I. Izzo, *J. Org. Chem.*, **2016**, *81*, 2494–2505.

Table 2.3 Screening of ester groups in phase-transfer benzylation of **99**, catalyzed by **80**^a

Entry	R	Product	Time (h)	Yield (%) ^b	ee (%) ^{c,d}
1	<i>t</i> -Bu (55)	56a	20	91	75
2	Et (99a)	100a	4	88	41
3	Bn (99b)	100b	4	89	49
4	Ph(Me) ₂ C (99c)	100c	20	74	81
5	Ph ₂ CH (99d)	100d	3	70	18

^aAll reactions were performed in a liquid-liquid system with 0.08 mmol of **95**, benzyl bromide (1.2 equiv.), and catalyst **80** (5 mol %) in toluene (0.8 mL) and NaOH 50% aq (0.5 mL). ^bIsolated yields. ^cDetermined by HPLC using a Chiralcel OD-H chiral stationary phase. ^dThe absolute configuration of the products was determined by comparison of the HPLC retention time and optical rotation with literature values^{12a,53,48,56,70}

In order to assess the actual effect of macrocyclic system, the same alkylation reaction was performed using an acyclic peptoid. Although the reaction proceeded with high yields, the enantiomeric excess was low (scheme 2.6). This result confirmed that the conformational restrictions imposed by the macrocycle are crucial for the enantioselective discrimination.

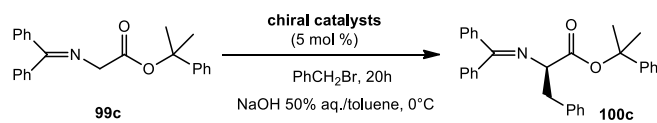
**Scheme 2.6** Enantioselective benzylation catalyzed by acyclic peptoid

The presence of ethyl or benzyl group gave moderate ee in comparison with the *t*-butyl ester residue (Table 2.3, entries 2, 3) while the presence of two aromatic rings, as in benzydryl group, gave a decrease of ee (Table 2.3, entry 5). Finally, to our delight, a significant increase of ee was obtained with cumyl ester **99c** (Table 2.3, entry 4).

2.2.5 Enantioselective alkylation of *N*-(diphenylmethylene)glycine cumyl ester

With the best substrate in our hands, the *N*-(diphenylmethylene)glycine cumyl ester **99c**, the asymmetric benzylation was realized in the presence of different cyclopeptoids as macrocyclic chiral catalysts. The best results were obtained with the cyclohexapeptoid **80** (Table 2.4, entry 1). The presence of substituents in *meta* and *para* positions on the aromatic ring gave a slight decrease in terms of enantioselectivity (Table 2.4, entries 2, 3, 5 and 6). 3,4-Dimethoxybenzyl group (Table 2.4, entry 7) and the α -naphthyl group 3,4-dichloro derivative (Table 2.4, entry 4) afforded moderate ee's and yields. Very low levels of enantioselectivity were observed with *ortho* substitution (Table 2.4, entry 8) and with 3,4-dichloro derivative (Table 2.4, entry 9).

Table 2.4 Screening of catalysts in phase-transfer benzylation of **99c**^a



Entry	Catalyst	Yield (%) ^b	ee (%) ^{c,d}
1	80	74	81
2	81	71	65
3	82	89	77
4	83	61	48
5	84	86	77
6	85	92	77
7	86	54	45
8	87	60	12
9	88	50	5
10	94	55	52
11	95	55	46
12	96	54	46
13	97	54	10
14	98	55	<i>rac</i>

^aAll reactions were performed in a liquid-liquid system with 0.08 mmol of **99c**, benzyl bromide (1.2 equiv.), and catalyst (5 mol %) in toluene (0.8 mL) and NaOH 50% aq (0.5 mL). ^bIsolated yields.

^cDetermined by HPLC using a Chiralcel OD-H chiral stationary phase.

^dThe absolute configuration of **100c** was determined by comparison of the HPLC retention time and optical rotation with literature values.⁷⁰

The previous trend, changing the cavity dimension, was observed during the investigation with cyclotrapeptoids. In fact, although they were able to catalyze the asymmetric alkylation, the catalytic efficiency and the enantioselectivity were lower in comparison with the corresponding cyclohexapeptoids (compare entry 1 and 10, 6 and 14, 7 and 12, 8 and 13, 9 and 11). Subsequently, an extensive study was performed on various parameters of the reaction using the best catalyst **80** and substrate **99c**. First, the screening of solvents revealed that toluene as the best solvent for this process (Table 2.5, entries 1-5).

Table 2.5 Screening of catalyst loading, solvents and bases promoted by **80**^a

Entry	Solvent	Base	Catalyst loading (% mol)	T (°C)	Yield (%) ^b	ee (%) ^{c,d}
1	toluene	NaOH 50% aq.	5	0	74	81
2	Et ₂ O	NaOH 50% aq.	5	0	63	49
3	<i>p</i> -xylene	NaOH 50% aq.	5	0	72	62
4	toluene/CHCl ₃ 9:1	NaOH 50% aq.	5	0	72	17
5	toluene/CH ₂ Cl ₂ 9:1	NaOH 50% aq.	5	0	69	78
6	toluene ^e	NaOH 50% aq.	5	0	73	75
7	toluene	NaOH 50% aq.	10	0	70	73
8	toluene	NaOH 50% aq.	2.5	0	75	86
9	toluene	NaOH 50% aq.	1	0	68	46
10	toluene	NaOH 50% aq.	5	-20	71	82
11	toluene	NaOH 50% aq.	2.5	-20	50	74
12	toluene	KOH 50% aq.	5	0	71	78
13	toluene	KOH 50% aq.	5	-20	70	87
14	toluene	KOH 50% aq.	2.5	-20	75	93
15	toluene	KOH 50% aq.	1	-20	76	92
16	toluene	CsOH 66% aq.	5	0	65	78
17	toluene	CsOH 66% aq.	5	-20	77	18
18	toluene	CsOH·H ₂ O (s) ^f	5	0	69	<i>rac</i>

^aAll reactions were performed in a liquid-liquid system with 0.08 mmol of **93c**, benzyl bromide (1.2 equiv.), and catalyst **80** in the appropriate solvent (0.8 mL) and aqueous base (0.5 mL). ^bIsolated yields. ^cDetermined by HPLC using a Chiralcel OD-H chiral stationary phase. ^dThe absolute configuration of **100c** was determined by comparison of the HPLC retention time and optical rotation with literature values.⁷⁰ ^e1.6 mL of toluene were used. ^f5.0 equiv. of solid base were used.

More diluted condition afforded a small decrease in enantioselectivity (Table 2.5, entry 6). The screening about the catalyst loading showed an important aspect: amazingly, we could appreciate an improvement of ee with a lower amount of catalyst (2.5 mol %, Table 2.5, entry 8). At lower temperature (-20°C) a slight decrease of the enantioselectivity was observed in (Table 2.5, entries 10, 11). Then, we evaluated the effect of the base. With 5 mol % of catalyst and aqueous KOH 50% at 0°C the ee value was comparable to NaOH at 0°C (Table 2.5, entry 12). Interestingly, a lower temperature with aqueous KOH 50% gave the best results: we obtained 87% ee with 5 mol % of catalyst (Table 2.5, entry 13), 93% ee with 2.5 mol % of catalyst (Table 2.5, entry 14), and, with our surprise, 92% ee, a very slight drop, with 1 mol % of catalyst (Table 2.5, entry 15). On the other hand, disappointing results were obtained with CsOH as the base (Table 2.5, entry 16-18).

To summarize, careful studies on the influence of substrate structure, solvent and nature of base allowed us to select the best conditions to obtain enantiomeric excesses comparable with the best reported to date in literature for this type of reaction. The *N*-(diphenylmethylene)glycine cumyl ester proved to be the substrate of choice, in presence of the chiral cyclohexapeptoid **80** as catalyst and employing toluene and an aqueous solution of KOH 50% at -20°C. Notably, only 2.5 mol% of catalyst (Table 2.5, entry 14) was necessary to reach the best ee, but even using a very low catalyst loading (1 mol%) the enantioselectivity was still remarkable (Table 2.5, entry 15). This is a remarkable achievement considering that normally higher loading (10%) are required with the most used chiral ammonium salts.

With the optimized conditions in our hands we decided to extend the scope of reaction with different alkylating agents. Very good yields and ee values with benzyl, allyl, alkyl bromides and iodides (83-96%) were achieved. The presence of an *ortho* methyl group in the alkylating agent allowed an ee up to 96% (Table 2.6, **100c**). The introduction of *para* substituents gave high enantioselectivities (Table 2.6, **102d-i**). Comparable enantioselectivities were achieved with allyl, propargyl, *t*-butoxycarbonylmethyl and ethyl substrates (Table 2.6, **102j-n**).

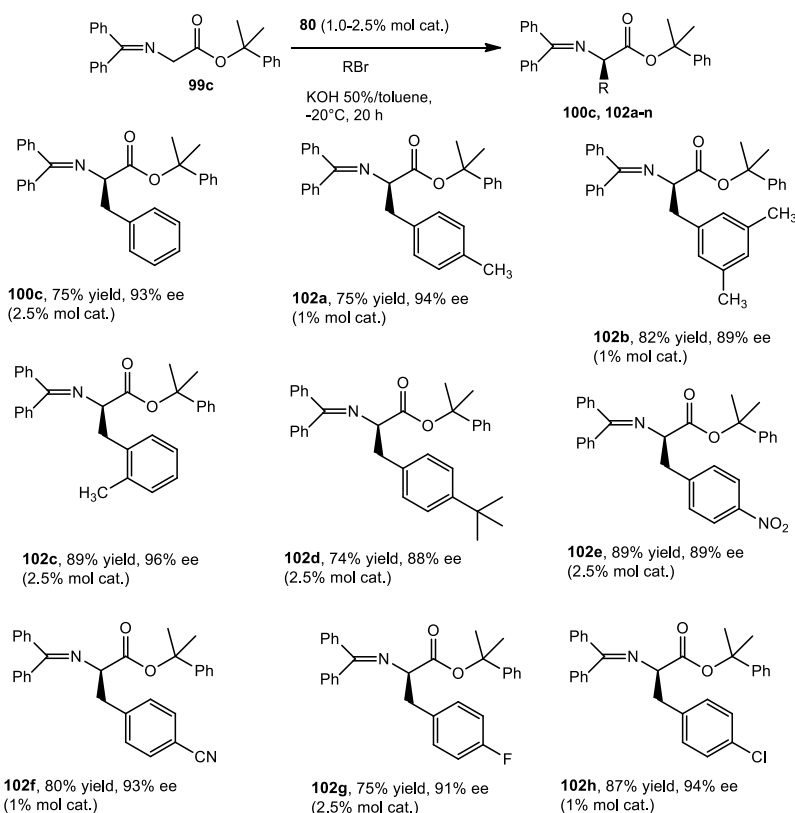
Moreover, to the best of our knowledge only one example of asymmetric alkylation of *N*-(diphenylmethylene)glycine cumyl ester is reported in literature, by

Kodanko's group, which described the phase-transfer process catalyzed by *O*-allyl-*N*-(9-antracenylnmethyl)-cinchonidinium bromide (10 mol% of catalyst loading).⁷⁰ The cumyl ester group is useful in transformation of the glycine derivatives to free amino acids, as can be cleaved by hydrogenolysis without affecting acid-labile groups in the scaffold molecule; for this reason it represents a valide alternative to a *t*-butyl group.

2.4 Calixarenes in asymmetric alkylation

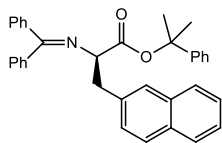
Taking into account our successful results and experience in the enantioselective alkylation of *N*-(diphenylmethylene)glycine derivatives we decided to investigate the potential of new macrocyclic compounds in phase-transfer catalysis.

Table 2.6 Scope of phase-transfer alkylation of **99c** promoted by **80** a-d

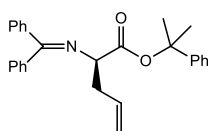


⁷⁰ T. Respondek, E. Cueny, J. J. Kodanko, *Org. Lett.*, **2012**, *14*, 1, 150-153

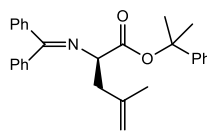
Table 2.6 (Continue)



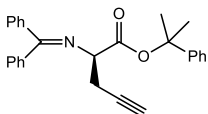
102i, ^e 97% yield, 95% ee
(2.5% mol cat.)



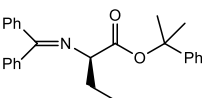
102j, ^e 90% yield, 93% ee
(2.5% mol cat.)



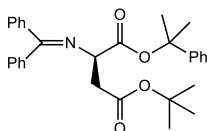
102k, ^e 93% yield, 86% ee
(2.5% mol cat.)



102l, ^e 91% yield, 83% ee
(2.5% mol cat.)



102m, ^{f,g} 86% yield, 86% ee
(1% mol cat.)



102n, 86% yield, 92% ee
(2.5% mol cat.)

^aReactions were performed in a liquid-liquid system on a 0.5 mmol scale by using **99c**, alkyl bromide (1.2 equiv.), and catalyst **80** in toluene (5.0 mL) and KOH 50% aq (3.0 mL), unless otherwise noted. ^bThe yields are referred to the isolated products. ^cThe ee values are determined by HPLC using a Chiralcel OD-H chiral stationary phase. ^dThe absolute configurations of products **102c**, **102j**, **102l** and **102m** were assigned by comparison of the HPLC retention times and optical rotations with literature values.⁷⁰ For the other products the same (*R*) absolute configuration was assumed. ^e1.5 equiv. of alkyl bromide were used. ^f3.0 equiv. of alkyl bromide were used. ^gEthyl iodide was used as alkylating agent.

As previously anticipated, calixarenes have been largely employed in metal-based catalysis but applications in phase-transfer processes remain elusive.²⁸ The few examples of calixarenes applied in PTC reported to date are limited to macrocycles functionalized with chiral quaternary ammonium moieties.^{26a,49} In collaboration with Neri's group at the Department of Chemistry and Biology "A. Zambelli" of the University of Salerno the design and the synthesis of novel chiral calixarenes was performed and their ability as PTC catalysts was tested during this PhD project. The first attempts in the enantioselective benzylation of *N*-(diphenylmethylene)glycine *t*-butyl ester were performed with calixarenes **103** and **104** (figure 2.8), containing free -OH groups at lower rim and chiral residues of α -methyl benzylamine. As described in the first chapter, the ability of the calixarenes in complexing metal ions has been widely investigated. For instance, a calix[4]arene functionalized at the lower rim with ethyl ester groups shows a high affinity towards the sodium cation (figure 2.7).²⁷ Based on these proprieties, initially some calixarene analogues were syntetized with the lower rim decorated with chiral amide groups. The introduction of

chirality was achieved with (*S*)-(-)- α -methyl benzylamine groups. The chiral amine is commercially available. Although these compounds were able to catalyze the alkylation reaction of *N*-(diphenylmethylene)glycine *t*-butyl ester with benzyl bromide in toluene and an aqueous solution of NaOH 50% with high reaction rate (total conversion after 4h was observed) the enantiomeric excesses observed were very low (5% and 7% respectively) (Table 2.6, entries 1, 2). We wondered if the presence of free -OH groups could be detrimental for the catalytic activity and enantioselectivity. For this reason a small library of chiral calixarenes containing methoxy groups instead of free -OH was prepared (**105-107** figure 2.8).

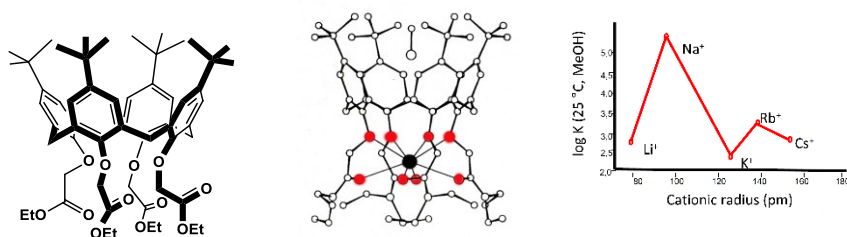


Figure 2.7 Calixarene and affinity towards sodium cation

The novel macrocycles were tested using 5 mol% of catalyst loading and a 50% aqueous NaOH/toluene biphasic system. All compounds were able to catalyze the reaction and in particular compound **107**, containing three chiral side chains at lower rim, afforded the alkylated compound with 26% of ee (Table 2.7, entry 5). Subsequently, with the best catalyst **107** the influence of different bases was investigated (table 2.8). All the basic systems afforded lower enantioselectivities in comparison to 50% aqueous NaOH solution. Interestingly, inversion of configuration was observed with 50% aqueous KOH solution (table 2.8, entry 1). Considering the beneficial effect of an appropriate ester moiety, previously observed using chiral cyclopeptoids, different glycine ester derivatives were examined. The presence of ethyl or benzyl group gave really low ee in comparison with the *t*-butyl ester residue (Table 2.9, entries 2, 3); in presence of two aromatic rings, as with the benzydrilic ester, was observed an inversion of enantioselectivity (Table 2.9, entry 5). With cumyl ester (Table 2.9, entry 4) was obtained an ee value comparable to *t*-butyl group.

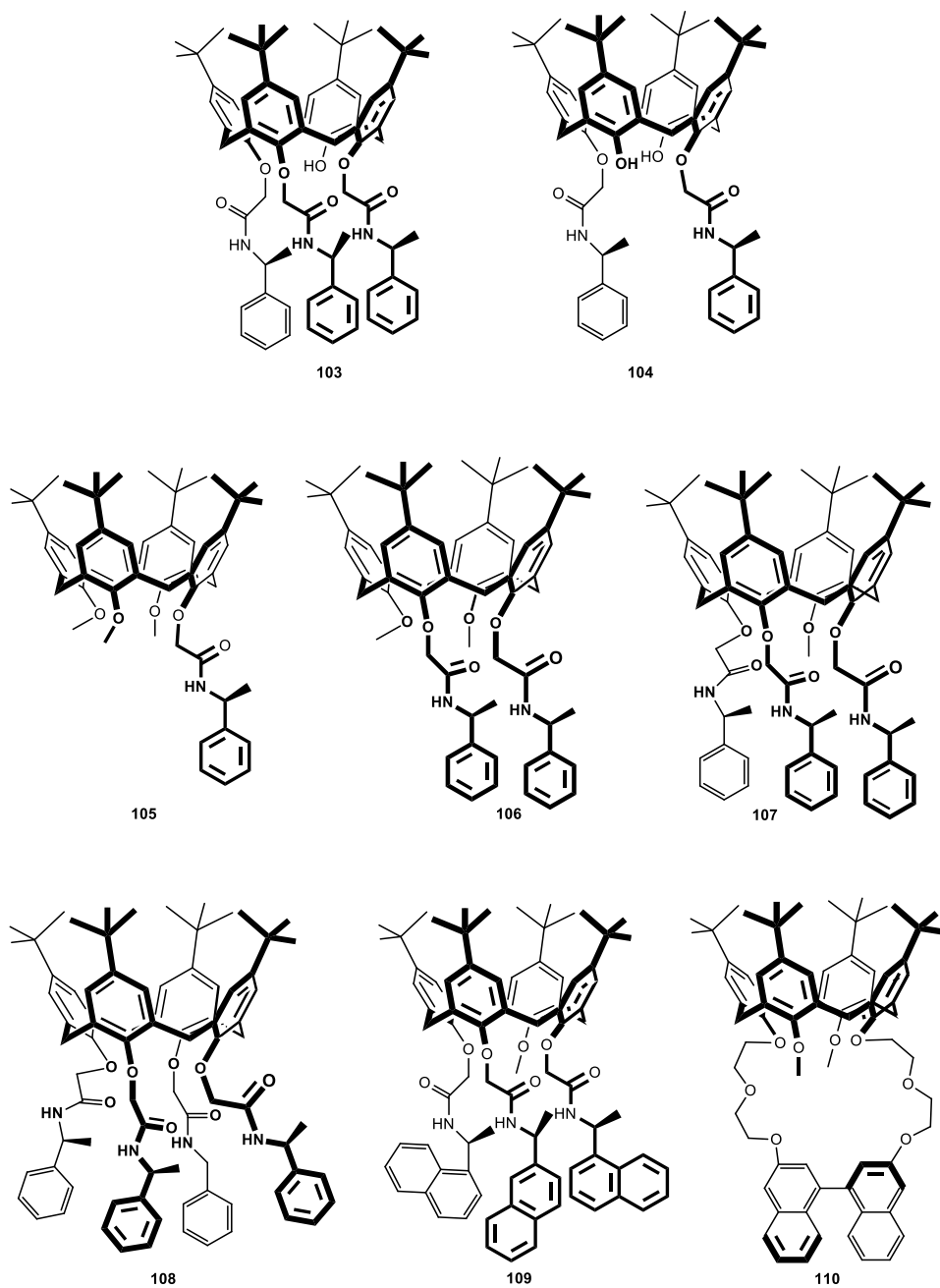
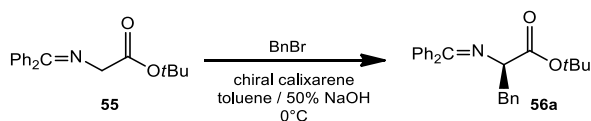
**Figure 2.8** Novel chiral calixarenes

Table 2.7 Enantioselective benzylation with chiral calixarenes **103-110**^a

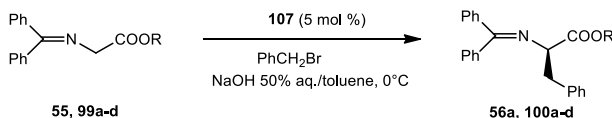
Entry	Catalyst	Time (h)	Yield (%)	ee (%) ^{b,c}
1	103	4	53	5(<i>R</i>)
2	104	4	65	7(<i>R</i>)
3	105	28	48	rac
4 ^d	106	4	92	13(<i>R</i>)
5	107	5	92	26(<i>R</i>)
6	108	21	66	13(<i>R</i>)
7	109	19	97	9(<i>R</i>)
8	110	22	84	rac

^aAll reactions were carried out in liquid-liquid system, at 0.08 mmol scale using **55** (1.0 eq.), benzyl bromide (1.2 eq.) and catalyst (5 mol%) in toluene (0.8 mL), with 50% aq. NaOH (0.5 mL), unless otherwise stated. ^bAll reactions were performed under an inert atmosphere by deoxygenating the two phases. ^cDetermined by HPLC using a Chiralcel OD-H chiral stationary phase. ^dThe absolute configurations of **56a** were determined by comparison of the HPLC retention times and optical rotation with literature values.^{12a,53}

Table 2.8 Screening of bases in phase-transfer benzylation of **55** promoted by **107**^a

Entry	Base	T (°C)	Time (h)	Yield (%)	ee (%) ^{b,c}
1	KOH 50% aq.	0	48	80	5(<i>S</i>)
2 ^d	CsOH 66% aq.	0	72	84	5(<i>R</i>)
3	CsOH·H ₂ O (s)	0	28	72	7(<i>R</i>)
4	NaOH 50% aq.	-20	72	12	14(<i>R</i>)

^aAll reactions were carried out in liquid-liquid system, at 0.08 mmol scale using **55** (1.0 eq.), benzyl bromide (1.2 eq.) and catalyst (5 mol%) in toluene (0.8 mL), with 50% aq. NaOH (0.5 mL), unless otherwise stated. ^bAll reactions were performed under an inert atmosphere by deoxygenating the two phases. ^cDetermined by HPLC using a Chiralcel OD-H chiral stationary phase. ^dThe absolute configurations of **56a** were determined by comparison of the HPLC retention times and optical rotation with literature values.^{12a,53}

Table 2.9 Screening of ester groups in phase-transfer benzylation of **99a-d** promoted by **107**^a

Entry	R	Product	Time (h)	Yield (%) ^b	ee (%) ^{c,d}
1	<i>t</i> -Bu (55)	56a	5	89	28
2	Et (99a)	100a	3	77	4
3	Bn (99b)	100b	7	60	rac
4	Ph(Me) ₂ C (99c)	100c	6	84	24
5	Ph ₂ CH (99d)	100d	5	74	6(S)

^aAll reactions were performed in a liquid-liquid system with 0.08 mmol of **99**, benzyl bromide (1.2 equiv.), and catalyst **107** (5 mol %) in toluene (0.8 mL) and NaOH 50% aq (0.5 mL). ^bIsolated yields. ^cDetermined by HPLC using a Chiralcel OD-H chiral stationary phase. ^dThe absolute configuration of the products was determined by comparison of the HPLC retention time and optical rotation with literature values.

12a,53,48,56,70

Finally the nature of solvent and the catalyst loading were investigated (Table 2.10). Taking into account the ameliorative results obtained using mesitylene (35% ee, Table 2.10, entry 8), the influence of catalyst loading and some different basic system were evaluated using this solvent. 10 mol% of catalyst gave a slight decrease of enantioselectivity (Table 2.10, entry 10) while a dramatic effect was observed with 2.5 mol% (Table 2.10, entry 11). In addition, using a solid-liquid system (NaOH (s)/mesitylene) an inversion of the enantioselectivity (Table 2.10, entry 12) was observed, as previously revealed in presence of 50% aqueous NaOH solution. This results seems to suggest that the catalytic process is sensitive to the cation (Table 2.10, entries 13-15), which may play a key role in the transition state. Finally, to extend the scope of the reaction, we tested different alkylating agents (Table 2.11). The presence of a 4-methyl or *t*-butyl groups in the aromatic ring of the alkylating agent led to 44% ee (Table 2.11, entries 2, 3); the introduction of electron withdrawing groups afforded a decrease of ee (Table 2.11, entries 5, 8, 9). The presence of an ortho methyl group resulted in a decrease of ee (Table 2.11, entry 6). Low enantioselectivities were also observed with allyl, propargyl and *t*-

butoxymethyl bromides. In conclusion this is the first example based on the use of chiral calixarenes in asymmetric phase-transfer catalysis.

Table 2.10 Screening of catalyst loading, solvents in the alkylation promoted by **107**^a

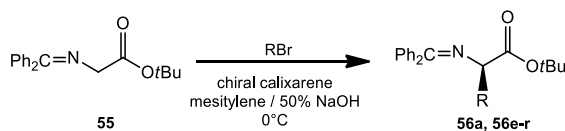
Entry	Solvent	Base	Time (h)	Catalyst loading (% mol)	Yield (%) ^b	ee (%) ^{c,d}
1	toluene	NaOH 50% aq.	5	5	84	24
2	CH ₂ Cl ₂	NaOH 50% aq.	7	5	83	6
3	Et ₂ O	NaOH 50% aq.	5	5	87	4
4	<i>p</i> -xylene	NaOH 50% aq.	7	5	84	rac
5	<i>m</i> -xylene	NaOH 50% aq.	28	5	82	3
6	<i>o</i> -xylene	NaOH 50% aq.	5	5	88	17
7	chlorobenzene	NaOH 50% aq.	5	5	90	rac
8	mesitylene	NaOH 50% aq.	7	5	86	35
9	mesitylene/ CH ₂ Cl ₂ 9/1	NaOH 50% aq.	7	5	89	26
10	mesitylene	NaOH 50% aq.	18	10	73	28
11	mesitylene	NaOH 50% aq.	18	2.5	73	13
12	mesitylene	NaOH (s) ^f	96	5	55	4(<i>S</i>)
13	mesitylene	KOH 50% aq.	96	5	66	10(<i>S</i>)
14	mesitylene	KOH (s) ^f	47	5	69	15(<i>S</i>)
15	toluene	CsOH·H ₂ O (s) ^f	48	5	72	11(<i>S</i>)

^aAll reactions were performed in a liquid-liquid system with 0.08 mmol of **99c**, benzyl bromide (1.2 equiv.), and catalyst **107** in the appropriate solvent (0.8 mL) and aqueous base (0.5 mL) at 0°C. ^bIsolated yields. ^cDetermined by HPLC using a Chiralcel OD-H chiral stationary phase. ^dThe absolute configuration of **100c** was determined by comparison of the HPLC retention time and optical rotation with literature values.⁷⁰ ^e1.6 mL of toluene were used. ^f5.0 equiv. of solid base were used.

In conclusion this is the first example based on the use of chiral calixarenes in asymmetric phase-transfer catalysis, where the complexation ability was exploited. Using the *N*-(diphenylmethylene)glycine *t*-butyl ester as substrate and the 4-methyl or *t*-butylbenzyl bromides as alkylating agents a moderate enantioselectivity (44% ee) was obtained (Table 2.11, entries 2 and 3). Despite the levels of enantioselectivity were moderate or low, these results pave the way to deeper investigations: indeed some interesting insights have emerged. The cation

seems to be crucial in the formation of the specific transition state so that an inversion of the enantioselectivity has been registered. Moreover, the structure substrate also influenced the configuration of the product, suggesting the opportunity to finely tune the enantioselective outcome of the reaction.

Table 2.11 Enantioselective alkylation of **55** in presence of catalyst **107** with different alkylating agents^{a,b}



Entry	RBr	Product	Time (h)	Yield (%)	ee (%) ^{c,d}
1	Benzyl bromide	56a	7	86	35(<i>R</i>)
2	4-Methylbenzyl bromide	56e	7	76	44(<i>R</i>)
3	4-(<i>t</i> -Butyl)benzyl bromide	56g	15	79	44(<i>R</i>)
4 ^e	Allyl bromide	56h	24	67	15(<i>R</i>)
5	4-Chlorobenzyl bromide	56i	7	75	rac
6	2-Methylbenzyl bromide	56l	7	72	15(<i>R</i>)
7	2-(bromomethyl)naphtalene	56m	7	76	3(<i>R</i>)
8	4-Fluorobenzyl bromide	56n	20	72	11(<i>R</i>)
9	4-Nitrobenzyl bromide	56o	3	69	7(<i>R</i>)
10	3,5-Dimethylbenzyl bromide	56p	20	75	rac
11 ^e	Propargyl bromide	56q	5	88	4(<i>R</i>)
12 ^e	<i>t</i> -Butylbromoacetate	56r	5	78	9(<i>R</i>)

^aAll reactions were carried out in liquid-liquid system for 20 h, at 0.08 mmol scale using **55** (1.0 eq.), benzyl bromide (1.2 eq.) and catalyst (5 mol%) in toluene (0.8 mL), with 50% aq. NaOH (0.5 mL), unless otherwise stated. ^bAll reactions were performed under an inert atmosphere by deoxygenating the two phases. ^cDetermined by HPLC using a Chiralcel OD-H chiral stationary phase. ^dThe absolute configurations of products **56a–e**, **56g** and **56h** were determined by comparison of the HPLC retention times and optical rotations with literature values ^{12a,53} and for **56f** by analogy with known products. ^eAllyl bromide (1.5 equiv.).

2.5 Asymmetric alkylation of 2-aryl-oxazoline-4-carboxylic acid esters

The efficient formation of quaternary stereocenters is a fundamental task

in organic synthesis.⁷¹ In this context the catalytic asymmetric preparation of C^α-tetrasubstituted α-amino acids has gained considerable attention in the recent years, because these building blocks are widely present in drugs and biologically and pharmaceutically active compounds. Since the pioneering work of O'Donnell in 1992,⁷² phase transfer catalysis proved to be an efficient methodology for the preparation of non proteogenic, chiral α,α-dialkyl-α-amino acid, through asymmetric alkylation of Schiff bases derivatives of α-amino acids. The construction of C^α-tetrasubstituted α-amino acids represents a challenge in organic synthesis and various phase-transfer catalysts have been designed for this purpose. The most common catalysts are *Cinchona* alkaloids-derived and binaphthyl-derived quaternary ammonium salts and very few examples are based on different alternative chiral scaffolds.^{17,73} In particular macrocyclic systems are scarcely investigated.^{46,74} Generally, chiral crown ethers afford moderate enantioselectivities in this process.

α-Alkyl serines or, more generally, β-hydroxy-α-amino acids, are widespread in peptidomimetics and bioactive natural products: some examples are conagenin,⁷⁵ myriocin⁷⁶, mycestericins⁷⁷ (figure 2.9). The conagenin is a low molecular weight immunomodulator produced by *Streptomyces roseosporus*. Myriocin possesses a more potent immunosuppressant activity than ciclosporin. Mycestericins are a family of potent immunosuppressants as well.

⁷¹ (a) H. Vogt, S. Bräse, *Org. Biomol. Chem.*, **2007**, *5*, 406-430. (b) S. Cabrera, E. Reyes, J. Alemán, A. Milelli, S. Kobbelgaard, K. A. Jørgensen, *J. Am. Chem. Soc.* **2008**, *130*, 12031-12037. (c) J. Zhou, *Organic Chem. Curr. Res.* **2014**, *3*, e136. (d) L. Yiyang, H. Seo-Jung, L. Wen-Bo, B. M. Stoltz, *Acc. Chem. Res.* **2015**, *48*, 740-751.

⁷² M. J. O'Donnell, S. Wu, *Tetrahedron: Asymmetry* **1992**, *3*, 591-594.

⁷³ a) Y. N. Belokon, K. A. Kochetkov, T. D. Churkina, N. S. Ikonnikov, A. A. Chesnokov, O. V. Larionov, I. Singh, V. S. Parmar, S. Vyskocil, H. B. Kagan, *J. Org. Chem.* **2000**, *65*, 7041-7048; (b) Y. N. Belokon, T. D. North, T. D. Churkina, N. S. Ikonnikov, V. I. Maleev, *Tetrahedron* **2001**, *57*, 2491-2498. (c) B. Lygo, U. Butt, M. Cormack, *Org. Biomol. Chem.* **2012**, *10*, 4968-4976.

⁷⁴ T. Itoh, S. Shirakami, *Heterocycles* **2001**, *55*, 37-43.

⁷⁵ T. Yamashita, M. Iijima, H. Nakamura, K. Issiki, H. Naganawa, S. Hattori, M. Hamada, M. Ishizuka, T. Takeuchi, Y. Itaka, *J. Antibiot.* **1991**, *44*, 557-559.

⁷⁶ (a) T. Fujita, K. Inoue, S. Yamamoto, T. Ikumoto, S. Sasaki, R. Toyama, K. Chiba, Y. Hoshino, T. Okumoto, *J. Antibiot.* **1994**, *47*, 216-224. (b) T. Fujita, K. Inoue, S. Yamamoto, T. Ikumoto, S. Sasaki, R. Toyama, K. Chiba, Y. Hoshino, T. Okumoto, *J. Antibiot.* **1994**, *47*, 208-215. (c) C. R. Strader, C. J. Pearce, N. H. Oberlies, *J. Nat. Prod.* **2011**, *74*, 900-907.

⁷⁷ (a) S. Sasaki, R. Hashimoto, M. Kiuchi, K. Inoue, T. Ikumoto, R. Hirose, K. Chiba, Y. Hoshino, T. Okumoto, T. Fujita, *J. Antibiot.* **1994**, *47*, 420-433. (b) T. Fujita, N. Hamamichi, M. Kiuchi, T. Matsuzaki, Y. Kitao, K. Inoue, R. Hirose, M. Yoneta, S. Sasaki, K. Chiba, *J. Antibiot.* **1996**, *49*, 846-853.

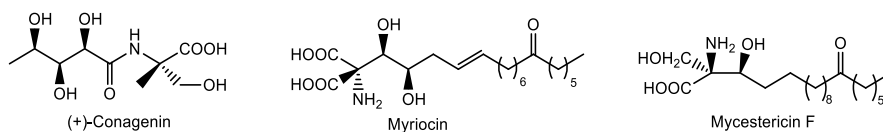


Figure 2.9 α -alkyl serines in biologically active natural products

Moreover chirality of α -alkyl serines proved to be relevant for the binding affinity to biological targets.⁷⁸ The first application of phase-transfer catalysis for the asymmetric synthesis of α -alkyl serines was reported in 2004 by Jew and Park,⁷⁹ exploiting the alkylation of a carboxyl-activated oxazoline ring. The oxazoline moiety enhances the acidity of the α -proton of the ester and acts as a protecting group for the amino- and hydroxy- functionalities of the serine. Here too, *Cinchona* alkaloids and Maruoka's catalysts (figure 2.10) have been applied. In that case starting point was the asymmetric alkylatoin of the 2-phenyl-oxazoline-4-carboxylic acid *t*-butyl ester (figure 2.11). The following acid hydrolysis affords the unprotected α -alkyl serines. In the first report the enantioselective phase-transfer catalytic benzylation was performed in the presence of different catalysts (**111–114**). The commercially available (*S*)-binaphthol-derived catalyst **111**, disclosed by the Maruoka group, afforded the alkylated product with very high enantioselectivity (>99% ee).

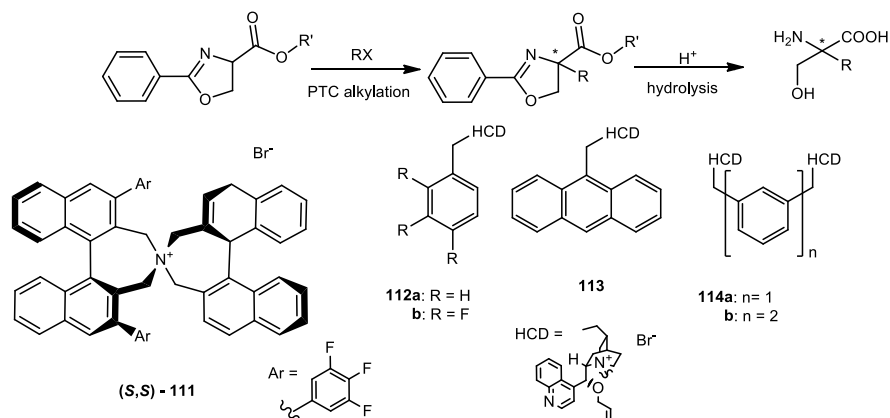


Figure 2.10 Phase-transfer catalysts for asymmetric alkylation of oxazoline-carboxylic esters

78. O. Frączczak, A. Lasota, Leśniak, A. W. Lipkowski, A. Olma, *Chem. Biol. Drug Des.* **2014**, *84*, 199–206.

79. (a) S. Jew, Y. J. Lee, J. Lee, M. J. Kang, B. S. Jeong, J. H. Lee, M. S. Yoo, M. Kim, S. Choi, J. M. Ku, H. Park, *Angew. Chem. Int. Ed.* **2004**, *43*, 2382–2385; (b) H. Park, J. Lee, M. J. Kang, Y. Lee, B. Jeong, J. Lee, M. Yoo, M. Kim, S. Choi, S. Jew, *Tetrahedron* **2004**, *60*, 4243–4249.

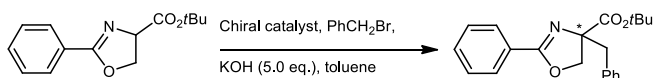


Figure 2.11 Enantioselective benzylation of oxazoline-carboxylic esters

Subsequently Maruoka exploited this method for the preparation of α -methyl serines.⁸⁰ Later on a solid-phase synthetic strategy to obtain α -alkyl serines⁸¹ was proposed by Park and coworkers: Merrifield resin-supported 2-phenyl-2-oxazoline-4-carboxylate was exposed to alkylation conditions, showing moderate enantioselectivity for the products (figure 2.12). More recently Park and Jew investigated the role of 2-aryl oxazoline substituent in the asymmetric alkylation. Reaction of *o*-biphenyl-2-oxazoline-4-carboxylic acid *t*-butyl ester in presence of *Cinchona* alkaloids-derived catalysts afforded very high enantioselectivity (scheme 2.7).⁸²

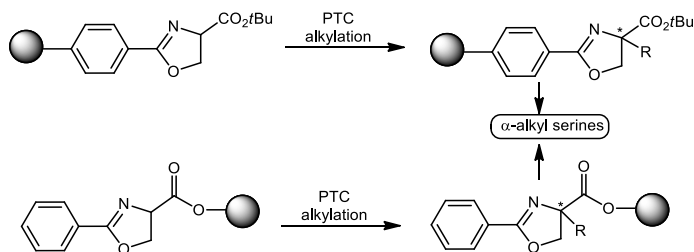
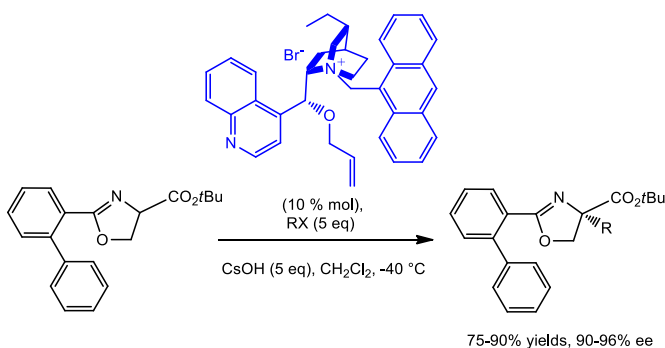


Figure 2.12 Solid-phase synthetic strategy of α -alkylserines



Scheme 2.7 Enantioselective catalytic alkylation of *o*-biphenyl-2-oxazoline-4-carboxylic acid *t*-butyl ester

⁸⁰ K. Nakayama, K. Maruoka, *Tetrahedron Letters* **2008**, 49, 5461–5463.

⁸¹ J. Lee, M. W. Ha, T. Kim, M. Kim, J. Ku, S. Jewa, H. Park, B. Jeong, *Tetrahedron*, **2009**, 65, 8839–8843.

⁸² Y. Lee, J. Lee, M. Kim, T. Kim, H. Park, S. Jew, *Organic Letters*, **2009**, 7, 1557–1560.

Considering that neutral chiral macrocycles have never been investigated in this synthetically useful enantioselective process, we decided to prove the catalytic ability of chiral cyclopeptoids in the asymmetric alkylation of 2-aryl-oxazoline-4-carboxylic acid esters.

2.5.1 Synthesis of 2-phenyl-2-oxazoline-4-carboxylic acid esters.

In order to evaluate the ability of cyclopeptoids as phase-transfer catalysts in the alkylation of 2-aryl-2-oxazoline-4-carboxylic acid esters, the first step was the synthesis of the substrates. We began our study investigating the role of ester moiety in the oxazoline derivatives, so the synthesis of different 2-phenyl-2-oxazoline-4-carboxylic acid esters (figure 2.13) was planned and realized. Subsequently the role of aryl moiety was investigated and a second set of substrates, containing different aryl groups was prepared.

The synthetic strategy used for the 2-phenyl-2-oxazoline-4-carboxylic acid esters was based on the described approach for the known oxazoline **115**.⁸¹ This route required the preparation of the desired serine esters. While the ethyl and benzyl esters of serine are commercially available, the *t*-butyl ester was prepared by reacting Z-Ser-OH (Z = Cbz = carbobenzyloxy) with *t*-butyl bromide in presence of potassium carbonate and benzyltriethyl ammonium chloride (BTEAC),⁸³ followed by Pd/C catalyzed hydrogenolysis⁸⁴ (scheme 2.8).

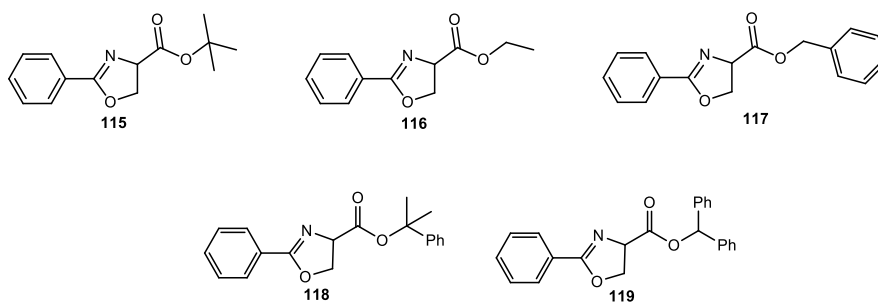
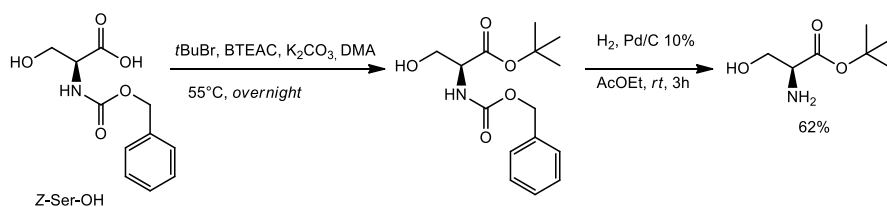


Figure 2.13 First generation of 2-aryl-oxazoline-4-carboxylic acid esters

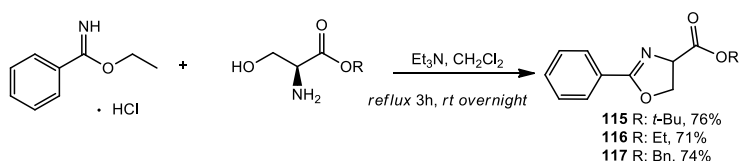
⁸³. P. Chevallet, P. Garrouste, B. Malawska, J. Martinez, *Tetrahedron Lett.*, **1994**, 34, 46, 7409-7412.

⁸⁴. L. Le Corre, C. Gravier-Pelletier, Y. Merrer, *Eur. J. Org. Chem.*, **2007**, 5386-5394.



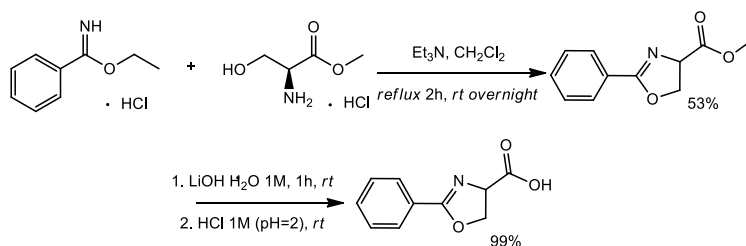
Scheme 2.8 Synthesis of H-Ser-O-*t*-butyl ester

Then the synthesis of oxazoline **115-117** was accomplished through the coupling reaction between serine esters and ethyl benzimidate hydrochloride with trimethylamine (scheme 2.9).



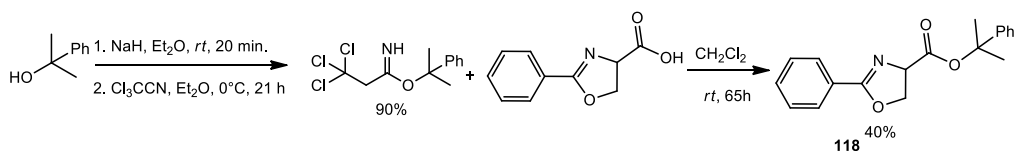
Scheme 2.9 Synthesis of 2-aryl-oxazoline-4-carboxylic acid esters

On the other hand, the synthesis of oxazolines **118** and **119** started with the preparation of 2-phenyl-2-oxazoline-4-carboxylic acid. The coupling reaction between ethyl benzimidate hydrochloride and the commercially available H-Ser-O-methyl ester afforded the corresponding oxazoline methyl ester. The saponification with LiOH·H₂O⁸³ gave the desired carboxylic acid (scheme 2.10). The preparation of the oxazoline **118** required the synthesis of the intermediate 1-methyl-1-phenylethyl 2,2,2-trichloro acetimidate, starting from cumyl alcohol (scheme 2.11).⁷² The synthesis of **119** was instead accomplished through a radical reaction between 2-phenyl-oxazoline-4-carboxylic acid and benzophenone hydrazone in presence of iodine and diacetoxyiodobenzene (scheme 2.12).⁸⁵

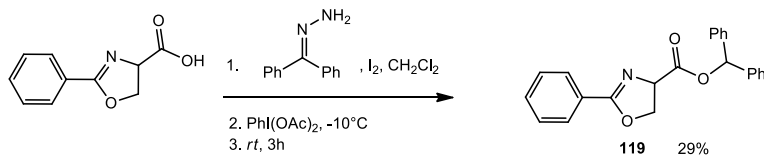


Scheme 2.10 Synthesis 2-phenyl-2-oxazoline-4-carboxylic acid

⁸⁵ P. Elsner, L. Bernardi, G. Della Sala, J. Overgaard, K. A. Jørgensen, *J. Am. Chem. Soc.*, **2008**, *130*, 4897-4905.



Scheme 2.11 Synthesis of 2-phenyl-2-oxazoline-4-carboxylic acid cumyl ester

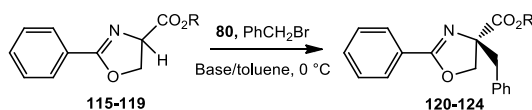


Scheme 2.12 Synthesis of 2-phenyl-2-oxazoline-4-carboxylic acid benzhydryl ester

2.5.2 Enantioselective alkylation of 2-phenyl-2-oxazoline-4-carboxylic acid esters using cyclopeptoids.

With various substrates in our hands the enantioselective alkylation was investigated. The starting point chosen to begin our screening involved the same reaction conditions previously described in the enantioselective alkylation of glycine ester (using toluene/NaOH 50% at 0°C with 5 mol% of catalyst loading in a liquid-liquid biphasic system with the chiral cyclopeptoid **80**).

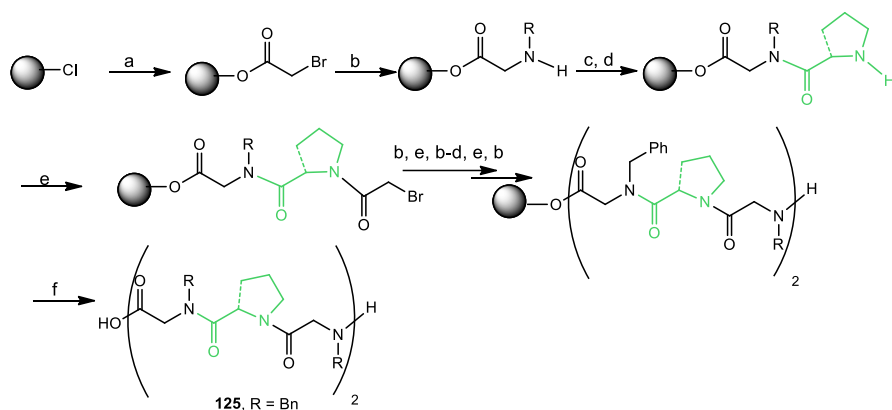
The use of bulky *t*-butyl and benzhydryl esters (Table 2.12, entries 1 and 5) appeared to be beneficial for the enantiomeric excesses, while benzyl, cumyl and the smaller ethyl group led gave from moderate to very low ee (Table 2.12, entries 2-4). However the best yield was observed again with the *t*-butyl ester and therefore further optimization or reaction conditions (base, catalyst loading, solvent, concentration) were performed on compound **115** (Table 2.12). Only with solid KOH better enantiomeric excess was obtained albeit with a lower yield (Table 2.12, entry 10). A reduction in the catalyst loading resulted in a lost of enantioselectivity both for NaOH and for KOH (Table 2.12, entries 6,9). More diluted conditions did not affect yield and ee (Table 2.12, entry 14). Performing the reaction at -20°C caused a turbidity of the NaOH aqueous phase and, consequently, a worse catalytic performance (Table 2.12, entry 13). Finally, the use of different solvents did not improve the results obtained with toluene (Table 2.12, entries 15-17).

Table 2.12 Investigation of the role of ester groups and of reaction parameters in phase-transfer benzylation of oxazoline promoted by **80**

Entry	R	Base	Cat (%)	Time (h)	Solvent	Product	Yield ^a (%)	ee ^b (%)
1	<i>t</i> Bu (115)	NaOH 50% aq	5	20	toluene	120	76	62
2	Et (116)	NaOH 50% aq	5	21	toluene	121	61	18
3	Bn (117)	NaOH 50% aq	5	1.5	toluene	122	50	47
4	Ph(Me) ₂ C (118)	NaOH 50% aq	5	23	toluene	123	68	45
5	Ph ₂ CH (119)	NaOH 50% aq	5	3	toluene	124	50	61
6	<i>t</i> Bu (115)	NaOH 50% aq	2.5	72	toluene	120	74	23
7	<i>t</i> Bu (115)	NaOH(s)	5	144	toluene	120	29 ^c	22
8	<i>t</i> Bu (115)	KOH 50% aq	5	46	toluene	120	32 ^c	62
9	<i>t</i> Bu (115)	KOH 50% aq	2.5	72	toluene	120	46 ^c	54
10	<i>t</i> Bu (115)	KOH(s)	5	20	toluene	120	47	61
11	<i>t</i> Bu (115)	CsOH(s)	5	46	toluene	120	40 ^c	34
12	<i>t</i> Bu (115)	LiOH(s)	5	144	toluene	120	-	-
13	<i>t</i> Bu (115)	NaOH 50% aq	5	96	toluene	120	16 ^c	54
14	<i>t</i> Bu (115)	NaOH 50% aq	5	22	toluene ^e	120	74	62
15	<i>t</i> Bu (115)	NaOH 50% aq	5	22	Et ₂ O	120	74	57
16	<i>t</i> Bu (115)	NaOH 50% aq	5	5	<i>p</i> -xylene	120	75	50
17	<i>t</i> Bu (115)	NaOH 50% aq	5	6	toluene/ DCM (9/1)	120	60	61

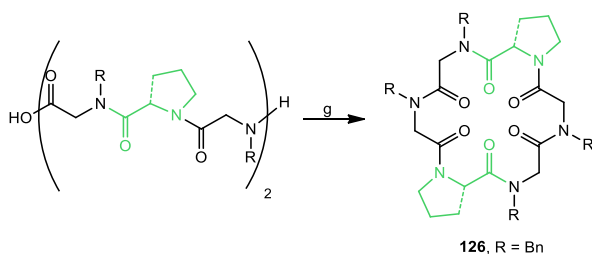
^aIsolated yields: yields refer to complete conversion, unless otherwise stated. ^bDetermined by chiral HPLC. The absolute configuration was determined by comparison of the HPLC retention times and optical rotation with literature values. ^{79a} ^cConversions were incomplete and reactions were stopped at the times reported. ^dThe reaction was performed at -20°C. ^eToluene (1.6 mL) was used.

Also in this case the role of macrocycle cavity size in the asymmetric induction was investigated and, for this purpose, the synthesis of a new chiral cyclooctapeptoid was performed on solid-phase system (scheme 2.15, 2.16). Moreover the synthesis of a cyclohexapeptoid containing two proline residues was done (scheme 2.13, 2.14) to study the influence of catalyst's symmetry.



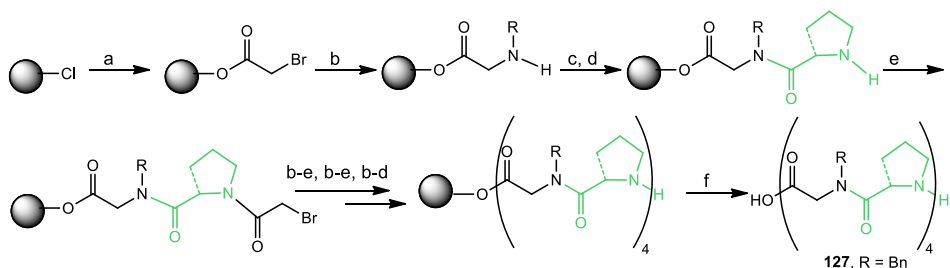
Reagents and conditions: a) bromoacetic acid, DIPEA; b) RNH₂; c) *N*-Fmoc-L-Proline, HATU; d) 20% piperidine/DMF; e) bromoacetic acid, DIC; f) HFIP/CH₂Cl₂ (1:4). DIPEA = *N,N* diisopropylethylamine; DIC = *N,N'*-diisopropyl carbodiimide.

Scheme 2.13 Solid phase synthesis of linear hexapeptoids with two proline residues



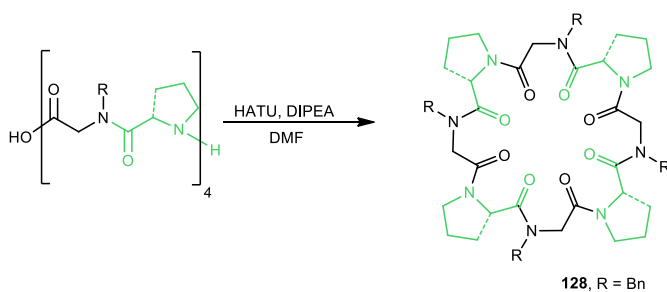
126: 46% yield.

Scheme 2.14 Head-to-tail cyclization generating cyclohexapeptoid with C₂ symmetry



Reagents and conditions: a) bromoacetic acid, DIPEA; b) RNH₂; c) *N*-Fmoc-L-Proline, HATU; d) 20% piperidine/DMF; e) bromoacetic acid, DIC; f) HFIP/CH₂Cl₂ (1:4). DIPEA = *N,N* diisopropylethylamine; DIC = *N,N'*-diisopropyl carbodiimide.

Scheme 2.15 Solid phase synthesis of linear octapeptoids



128: 41% yield.

Scheme 2.16 Head-to-tail cyclization generating octapeptoid

The screening was performed testing the cyclotetra, cyclohexa and cyclooctapeptoids with benzyl side chains, under the previously developed best conditions. In the figure below, are summarized all the cyclopeptoids previously synthesized and described, used in this investigation (figure 2.14).

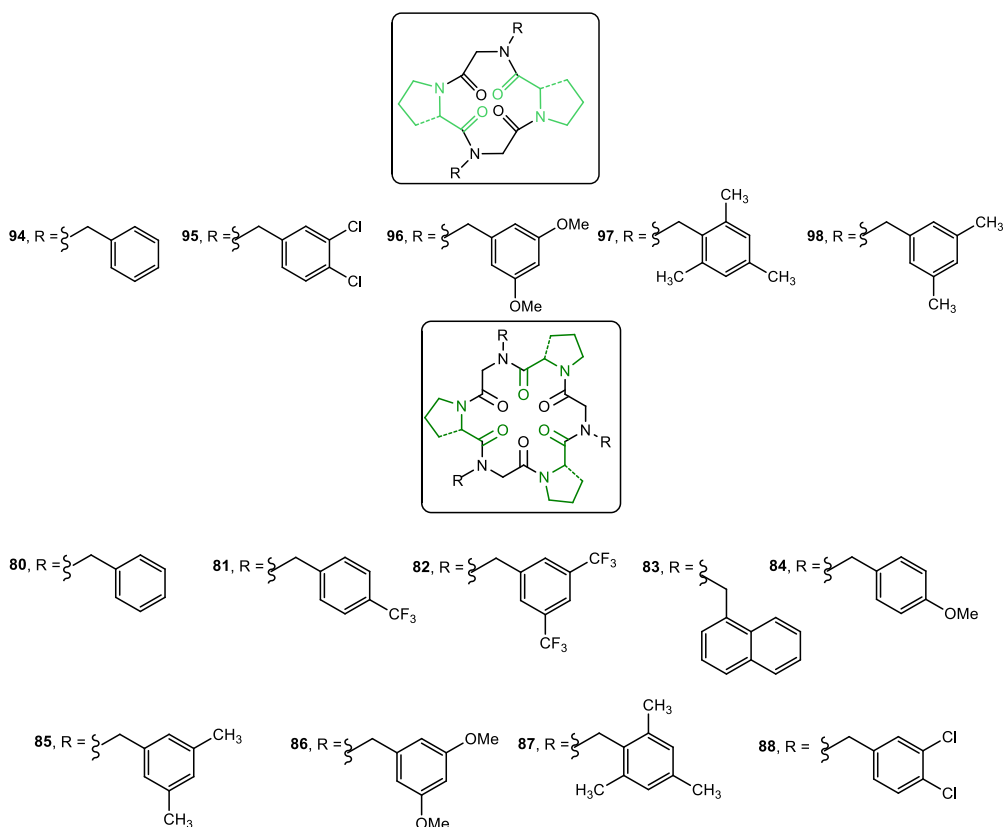
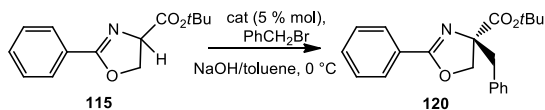


Figure 2.14 Chiral cyclopeptoids

Table 2.13 Screening of the catalyst **82**, **126** and **128**

Entry	catalyst	Time (h)	Yield ^a (%)	ee ^{b,c} (%)
1	94	24	83	44
2	126	21	88	47
3	128	23	67	19
4 ^d	128	24	30 ^e	62

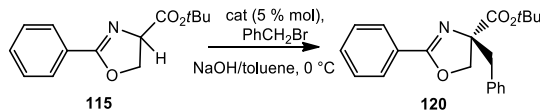
^aIsolated yields. ^bDetermined by chiral HPLC. ^cThe absolute configuration was determined by comparison of the HPLC retention time and optical rotation with literature values.^{79a} ^dThe reaction was performed in presence of solid KOH/toluene, 0°. ^eConversion was incomplete and the reaction was stopped at the time reported.

Reduction or increase in the macrocyclic cavity size caused a lowering in the enantioselectivity (Table 2.13, entries 1,3). The bis-prolinated C₂ symmetric cyclopeptoids showed a good catalytic activity, but the enantioselectivity was lower than the usual C₃ symmetric analogue (Table 2.13, entry 2). Cyclooctapeptoid **126** was further tested in a biphasic system (solid KOH/toluene), considering its presumed ability in complexing larger K⁺ cation. Enantioselectivity was comparable with that exhibited by **80** (Table 2.12, entry 1) but the yield was very low. Moreover the catalytic activity of cyclotetrapeptoids, containing different aromatic side chains were tested and compared to the results obtained with the related cyclohexapeptoids. As previously observed cyclotetra-compounds catalyzed efficiently the reaction but affording lower ee (Table 2.14), so we decided to continue our investigation on the influence of substituents in the benzylic side chains of cyclohexapeptoids.

The presence of *p*-substituents on the aromatic side chain of cyclohexapeptoids (OMe and CF₃) gave comparable values of ee (Table 2.15, entries 2,5), while more substituted or more hindered benzyl side groups, as in **86**, **87**, **82** and **83**, resulted in drop of the ee values (Table 2.15, entries 3, 4, 6 and 7). However, a slight

improvement of the enantioselectivity was observed with *p*-CF₃-benzylated cyclopeptoid **84**, this was the catalyst employed with other substrates.

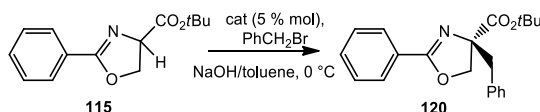
Table 2.14 Screening of the cyclohexapeptoids **94-98**



Entry	catalyst	Time (h)	Yield ^a (%)	ee ^{b,c} (%)
1	94	24	83	44
2	95	20	64	33
3	96	20	79	7
3	97	18	87	10
4	98	18	62	3

^aIsolated yields. ^bDetermined by chiral HPLC. ^cThe absolute configuration was determined by comparison of the HPLC retention time and optical rotation with literature values.^{76a}

Table 2.15 Screening of the cyclohexapeptoids in asymmetric benzylation



Entry	catalyst	Time (h)	Yield ^a (%)	ee ^{b,c} (%)
1	80	20	76	62
2	81	18	90	65
3	82	20	69	47
4	83	20	74	57
5	84	18	67	66
6	86	24	88	56
7	87	20	69	56

^aIsolated yields. ^bDetermined by chiral HPLC. ^cThe absolute configuration was determined by comparison of the HPLC retention time and optical rotation with literature values.^{79a}

2.5.3 Synthesis of 2-aryl-2-oxazoline-4-carboxylic acid esters

With the purpose to investigate the steric and electronic effects of the phenyl ring in the oxazoline moiety, a small library of 2-aryl-2-oxazoline-4-carboxylic acid *t*-

butyl ester was synthesized **129-133** (figure 2.15).

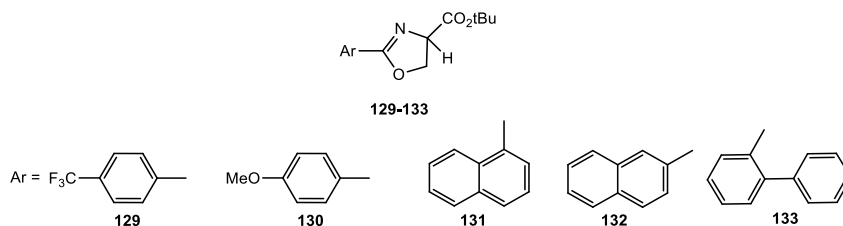
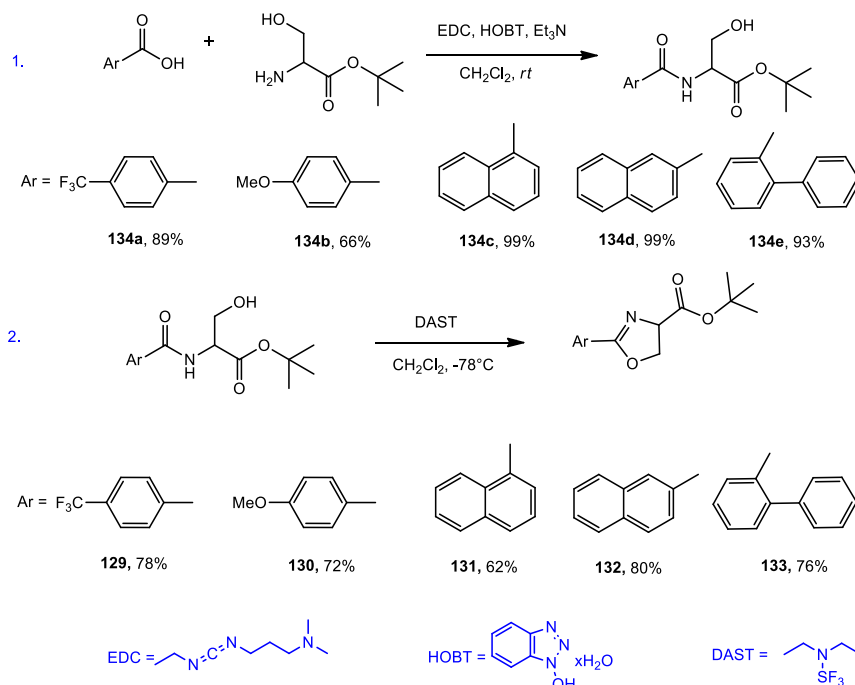


Figure 2.15 2-aryl-2-oxazoline-4-carboxylic acid *t*-butyl esters tested as substrates

The synthesis was realized in two steps: a reaction between HO-Ser-OtBu with aryl carboxylic acid, mediated by 1-ethyl-3-(3-dimethylaminopropyl)carbodiimide (EDC) in presence of hydroxybenzotriazole (HOBT), followed by a cyclization reaction with (diethylamino)sulfur trifluoride (DAST) (scheme 2.17).

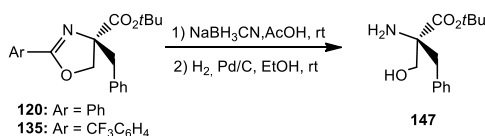


Scheme 2.17 Synthesis of 2-aryl-2-oxazolines **129-133**

2.5.4 Enantioselective alkylation of 2-aryl-2-oxazoline-4-carboxylic acid esters using cyclopeptoids.

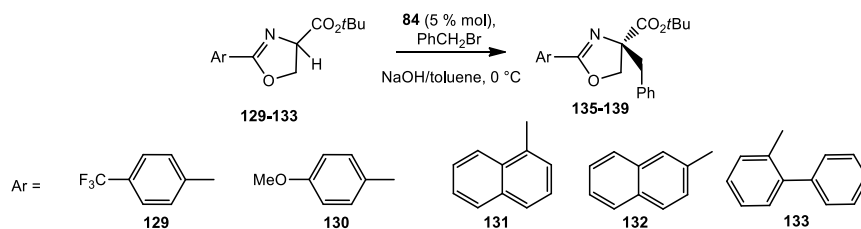
Once prepared, the different oxazoline *t*-butyl esters (**129-133**) were submitted to enantioselective alkylation catalyzed by **84** under the previously optimized reaction conditions. The best ee value was achieved with *o*-biphenyl-2-oxazoline-4-carboxylic acid *t*-butyl ester like as in the Park's work⁸⁴ albeit the yield was lower (Table 2.16, entry 5) than those obtained with other substrates. It is interesting to observe that the presence of electron withdrawing group on the phenyl ring allowed to substantially reach the best ee value obtained with **133**, ensuring a better yield (Table 2.16, entry 1). Subsequently, with the best substrate **129** and catalyst **84** we decided to expand the scope of this reaction with different alkylating agents. The introduction of methyl groups in *ortho* or *para* position furnished comparable ee values (Table 2.17, entries 1, 2). The steric hindrance of a *t*-butyl or naphthyl group gave better ee values (Table 2.17, entries 3, 6). The presence of electron withdrawing group such as fluoride or chloride groups did not affect the enantioselectivities (Table 2.17, entries 4, 5). Lower level of ee was instead achieved with allyl bromide (Table 2.17, entry 7).

α -Alkyl serines can be easily generated through the procedure described by Zervosen and coworkers.⁸⁶ Using this methodology, which envisage the NaBH₃CN reduction followed by hydrogenolysis of the benzyl amine residue (Scheme 2.19), we were able to confirm that **135** had the same (*S*) absolute configuration of the previously reported **120** (determined by comparison of the HPLC retention time and optical rotation with literature values): ^{81a} both oxazolines afforded (*S*)- α -benzyl serine *t*-butyl ester **147**.



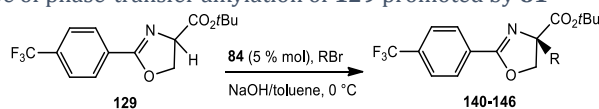
Scheme 2.18 Synthesis of (*S*)- α -benzyl serine *t*-butyl ester

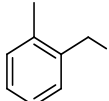
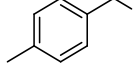
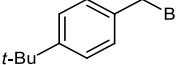
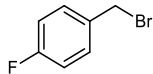
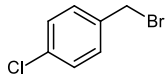
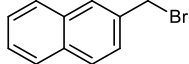
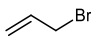
⁸⁶. (a) T. Denoël, A. Zervosen, C. Lemaire, B. Joris, M. Hervé, D. Blanot, G. Zaragoza, A. Luxena, *Org. Biomol. Chem.* **2014**, *12*, 9853. (b) T. Denoël, A. Zervosen, C. Lemaire, A. Plenevaux, Luxena, *Tetrahedron* **2014**, *70*, 4526.

Table 2.16 Screening of 2-aryl-oxazoline *t*-butyl ester substrate promoted by **80**

Entry	oxazoline	Time (h)	product	Yield ^a (%)	ee ^{b,c} (%)
1	129	20	135	75	72
2	130	21	136	67	62
3	131	21	137	52	46
4	132	21	138	64	62
5	133	96	139	44	73

^aIsolated yields. ^bDetermined by chiral HPLC.

Table 2.17 Scope of phase-transfer alkylation of **129** promoted by **81**

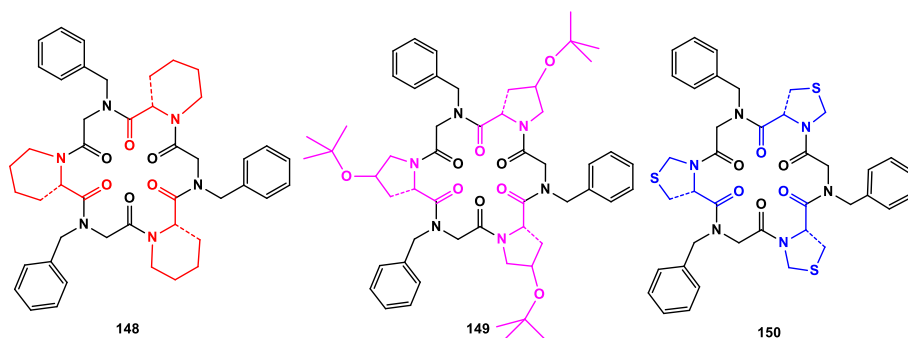
Entry	RBr	Product	Time (h)	Yield ^a (%)	ee ^{b,c} (%)
1		140	20	73	67
2		141	20	61	68
3		142	23	58	74
4		143	23	83	70
5		144	24	74	62
6		145	23	74	75
7		146	19	55	48

^aIsolated yields. ^bDetermined by chiral HPLC.

In conclusion, this work represents the first application of nonionic macrocycles systems in the efficient phase-transfer alkylation of oxazoline carboxylic esters. The enantiomeric excesses were moderate to good (67-75%). Anyway, since the previous results could be improved, this process can be considered as a new benchmark for the design and the application of different cyclopeptoidic phase-transfer catalysts.⁸⁷

2.5.5 A new library of chiral hexapeptoids containing different chiral residues.

With the aim of further expand the diversity of this original macrocyclic catalysts, a small library of new chiral hexacyclopeptoids, containing different chiral proline analogs, was designed (figure 2.16). L-Pipecolic acid (**148**), L-*t*-butyl-hydroxyproline (**149**), and L-thiazolidine-2-carboxylic acid (**150**), were used as monomers in place of L-Proline. The synthesis was realized following the previously described “sub-monomer/monomer solid phase approach” for the linear oligomer (scheme 2.2), followed by cyclization in high dilution conditions (scheme 2.3). The solid phase synthesis of **148**, **149** and **150** was made using Fmoc-protected monomers.



Yield: **148** 3%, **149** 27%, **150** 21%.

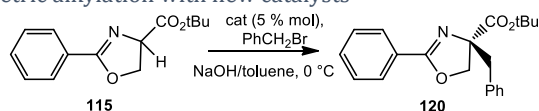
Figure 2.16 Novel chiral cyclohexapeptoids

Preliminary results on their potential catalytic activity have been obtained in the enantioselective benzylation of 2-phenyl-2-oxazoline-4-carboxylic acid *t*-butyl

⁸⁷ R. Schettini, A. D’Amato, F. De Riccardis, G. Della Sala, I. Izzo, *Synthesis*, 2016, eFirst, DOI: 10.1055/s-0036-1588102.

ester (**115**). The reaction carried out with the catalyst **148** gave a racemic mixture (Table 2.18, entry 1). More interesting was the catalyst **149**, with with *L*-*t*-butyl-hydroxyproline, which gave an ee comparable to the value achieved with the catalyst **80** (Table 2.18, entry 2). Finally, the presence of a sulfur atom in the five-member ring, as in **150**, had a drastic effect in the enantioselectivity of this reaction (Table 2.18, entry 3); in this case an inversion of configuration was observed. This preliminar screening indicated compound **149** as the most promising macrocycle. This structure, among other things, offer the possibility of different structural modification by deprotection of the *L*-*t*-butyl- hydroxyproline residues and subsequent functionalization, paving the way to the synthesis of new catalysts.

Table 2.18 Asymmetric alkylation with new catalysts



entry	catalyst	Time (h)	Yield ^a (%)	ee ^{b,c} (%)
1	148	24	20	rac
2	149	5	39	63
3	150	5	68	17(<i>R</i>)

^aIsolated yields. ^bDetermined by chiral HPLC. ^cThe absolute configuration was determined by comparison of the HPLC retention time and optical rotation with literature values.^{79a}

2.6 Conclusions

In conclusion, the starting point of this PhD project was the first evidence that chiral cyclopeptoids are good phase-transfer catalysts in the alkylation reaction of glycine derivatives (figure 2.17).

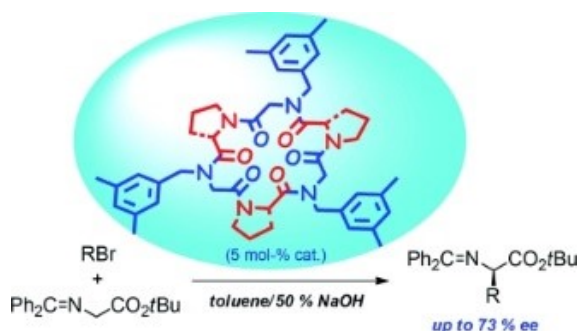


Figure 2.17 Enantioselective alkylation of *N*-(diphenyl-methylene)glycine *t*-butyl esters

Further studies in the alkylation reaction allowed to reach higher levels of enantioselectivity using *N*-(diphenylmethylene)glycine cumyl ester as the substrate (83-96% ee) and low catalyst loading. This work represents the first example of efficient macrocyclic neutral catalysts used in phase-transfer reactions. This result becomes all the more relevant if we take into account that cyclopeptoids can be prepared with a very convenient solid-phase synthesis in a modular approach which offers the opportunity to prepare differently decorated compounds in a very expeditious way.

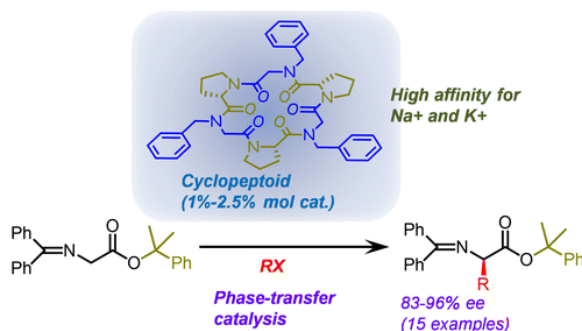


Figure 2.18 Enantioselective alkylation of *N*-(diphenylmethylene)-glycine cumyl ester

Good enantioselectivity were also obtained in the asymmetric alkylation of 2-aryl-2-oxazoline-4-carboxylic esters, affording synthetic precursors of α -alkyl serines (figure 2.19). This additional application confirms the potential of this type of compounds in asymmetric phase-transfer catalysis and suggests further uses in asymmetric organic synthesis.

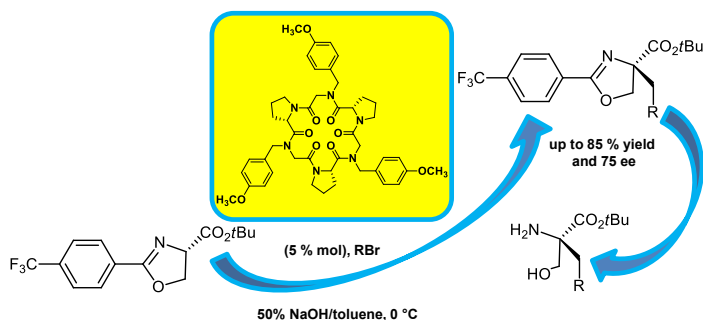


Figure 2.19 Enantioselective alkylation of 2-aryl-2-oxazolin-4-carboxylic esters

Moreover different macrocycles, based on the calixarene scaffold, were also investigated. In collaboration with Neri's group, the asymmetric alkylation of *N*-(diphenyl-methylene)glycine *t*-butyl esters with chiral calixarenes (figure 2.20) was evaluated. Even if the enantiomeric excesses obtained were moderate, this is the first example employing metal-complexing calixarenes as asymmetric phase-transfer catalysts.

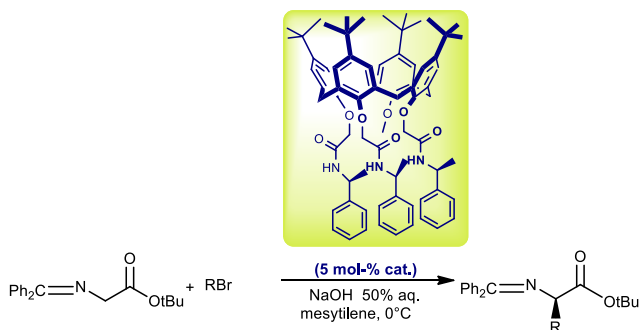


Figure 2.20 Enantioselective alkylation of *N*-(diphenyl-methylene)glycine *t*-butyl esters with chiral calixarene

In summary, during this period, 19 novel chiral cyclopeptoids were synthesized and totally characterized with monodimensional and bidimensional spectroscopy.

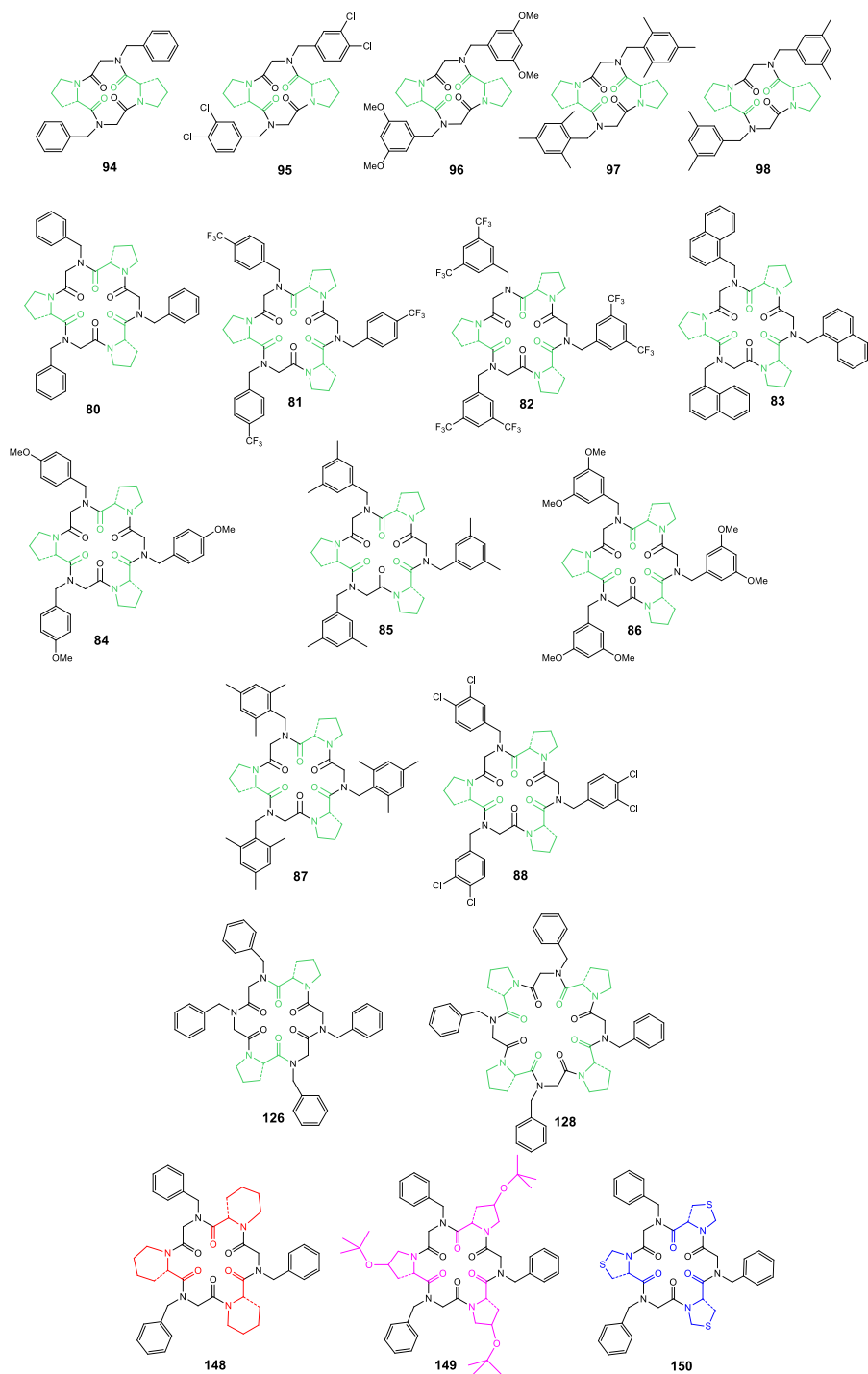


Figure 2.21 Novel chiral cyclopeptoids

2.7 Experimental section

2.7.1 General procedures

Starting materials and reagents purchased from commercial suppliers were generally used without purification unless otherwise mentioned. Reaction temperatures were measured externally; reactions were monitored by analytical thin layer chromatography (TLC) on precoated silica gel plates (0.25 mm) and visualized by UV light. Flash chromatography was performed on silica gel 60 (particle size: 0.040–0.063 mm) and the solvents employed were of analytical grade. Cyclopeptoids **94-98**, **80-88**, **126**, **128**, **148-150** were purified by reversed-phase chromatography on C18 bonded silica (particle size 0.040–0.063 mm) and the purity grade were checked by HPLC analysis using a C18 reversed-phase analytical column (Bondapak, 10 μm , 125 \AA , 3.9 mm \times 300 mm) run with linear gradients of ACN (0.1% TFA) into H₂O (0.1% TFA) over 30 min, at a flow rate of 1.0 mL/min, with an UV detector set at 220 nm. Enantiomeric excesses of products **56a-r**, **100c**, **102a-n**, **140-146** were determined by chiral HPLC using Chiralcel OD-H columns with an UV detector set at 260 nm. All ultraviolet (UV) measurements were made at 24–26 $^{\circ}\text{C}$, using spectrophotometric grade solvents. Low-resolution ESI-MS analysis in positive ion mode were performed using a Bio-Q triple quadrupole mass spectrometer equipped with an electrospray ion source. High resolution mass spectra (HRMS) in positive ion mode were recorded on a Fourier transform ion cyclotron resonance mass spectrometer (FTICR-MS) using electrospray ionization (ESI). Optical rotation values were measured at $\lambda = 589$ nm, corresponding to the sodium D line, at the temperatures indicated. ^1H NMR and ^{13}C spectra were recorded on a 600 MHz, 400 and 300 MHz instruments. Chemical shifts (δ) are reported in ppm relative to the residual solvent peak (CHCl_3 , $\delta = 7.26$; $^{13}\text{CDCl}_3$, $\delta = 77.0$; $^1\text{H-DMSO-}d_6$, $\delta = 2.50$; $^{13}\text{C-DMSO-}d_6$, $\delta = 39.5$) and the multiplicity of each signal is designated by the following abbreviations: s, singlet; d, doublet; t, triplet; m, multiplet; bs, broad singlet; bd, broad doublet. Coupling constants (J) are quoted in Hertz. COSY and ROESY spectra of compound **98** were measured on a 600 MHz instrument.

2.7.2 Mixed monomer/submonomer solid-phase synthesis of tetra linear precursors

Linear peptoids **89-93** were synthesized by alternating submonomer solid-phase method using standard manual Fmoc solid-phase peptide synthesis protocols. Typically 0.40 g of 2-chlorotrityl chloride resin (2, α -dichlorobenzhydryl-polystyrene cross-linked with 1% DVB; 100–200 mesh; 1.20 mmol/g) was swelled in dry DCM (4 mL) for 45 min and washed twice in dry DCM (3 mL). Bromoacetic acid (107 mg, 0.77 mmol) and DIPEA (310 mg, 2.4 mmol) in dry DCM (4 mL) were added to the resin and the vessel was stirred on a shaker platform for 40 min at room temperature, and then washed with dry DCM (3 \times 4 mL) and then with DMF (3 \times 4 mL). Then the arylmethylamine (4.80 mmol) in dry DMF (4 mL) was added to the bromoacetylated resin. The mixture was left on a shaker platform for 40 min at room temperature, then the resin was washed with DMF (3 \times 4 mL). The resin was incubated with a solution of *N*-Fmoc-L-Proline (486 mg, 1.44 mmol), HATU (529 mg, 1.39 mmol) and DIPEA (248 mg, 1.92 mmol) in dry DMF (4 mL) on a shaker platform for 1 h, followed by extensive washes with DMF (3 \times 4 mL), DCM (3 \times 4 mL) and DMF (3 \times 4 mL). Chloranil test was performed and once the coupling was complete the Fmoc group was deprotected by sequential additions of two aliquots of 20% piperidine/DMF (v/v, 3 mL), stirring on a shaker platform for 3 and 7 min respectively, followed by extensive washes with DMF (3 \times 3 mL), DCM (3 \times 3 mL) and DMF (3 \times 3 mL). Subsequent bromoacetylation reactions were accomplished by reacting the oligomer with a solution of bromoacetic acid (690 mg, 4.8 mmol) and DIC (666 mg, 5.28 mmol) in DMF (4 mL), stirring on a shaker platform for 40 min at room temperature. Then, reaction with arylmethylamine, with *N*-Fmoc-L-Proline, Fmoc deprotection and bromoacetylation steps were repeated as described above. Generally, addition of the proline at the fourth position required longer reaction time (3 h). The synthesis was stopped for the tetramer. The oligomer-resin was cleaved by treatment with three aliquots of a solution of 20% HFIP in DCM (v/v; 3 \times 4 mL), with stirring each time on a shaker platform for 30 min at room temperature, and filtering the resin away after each treatment. The combined filtrates were concentrated in vacuo. The final product

was analyzed by ESI mass spectrometry and RP-HPLC and used for the cyclization step without further purification.

2.7.3 Mixed monomer/submonomer solid-phase synthesis of hexa linear precursors

Linear peptoids **71-79** were synthesized by alternating submonomer solid-phase method using standard manual Fmoc solid-phase peptide synthesis protocols as described in section 2.8.1. The synthesis proceeded until the desired hexaoligomer was obtained before the cleavage treatment.

The synthesis of the linear hexapeptoid **125** required a different solid-phase scheme. Linear peptoid was synthesized by alternating submonomer solid-phase method using standard manual Fmoc solid-phase peptide synthesis protocols. 0.20 g of 2-chlorotrityl chloride resin (Novabiochem; 2,α-dichlorobenzhydryl-polystyrene crosslinked with 1% DVB; 100-200 mesh; 1.63 mmol/g) was swelled in dry DCM (2 mL) for 45 min and washed twice in dry DCM (2 mL). Bromoacetic acid (72 mg, 0.52 mmol) and DIPEA (207 mg, 1.6 mmol) in dry DCM (2 mL) were added to the resin and the vessel was stirred on a shaker platform for 40 min at room temperature, and then washed with dry DCM (3 × 4 mL) and then with DMF (3 × 4 mL). Then the benzylamine (349 mg, 3.26 mmol) in dry DMF (2 mL) was added to the bromoacetylated resin. The mixture was left on a shaker platform for 40 min at room temperature, then the resin was washed with DMF (3 × 2 mL), DCM (3 × 2 mL) and then with DMF (3 × 2 mL). The resin was incubated with a solution of *N*-Fmoc-L-Proline (330 mg, 0.98 mmol), HATU (361 mg, 0.95 mmol) and DIPEA (168 mg, 1.30 mmol) in dry DMF (2 mL) on a shaker platform for 1 h, followed by extensive washes with DMF (3 × 2 mL), DCM (3 × 2 mL) and DMF (3 × 2 mL). Chloranil test was performed and once the coupling was complete the Fmoc group was deprotected by sequential additions of two aliquots of 20% piperidine/DMF (v/v, 2 mL), stirring on a shaker platform for 3 and 7 min respectively, followed by extensive washes with DMF (3 × 2 mL), DCM (3 × 2 mL) and DMF (3 × 2 mL). Subsequent bromoacetylation reactions were accomplished by reacting the oligomer with a solution of bromoacetic acid (453 mg, 3.26 mmol) and DIC (453 mg, 3.59 mmol) in DMF (2 mL), stirring on a shaker platform for 40 min at room temperature. Then, reaction with benzylamine, bromoacetylation step

and again reaction with benzylamine were repeated, followed by the reaction with *N*-Fmoc-L-Proline and Fmoc deprotection. The addition of this proline residue required longer reaction time (3 h). Then bromoacetylation step and reaction with benzylamine were repeated as described above. The oligomer-resin was cleaved by treatment with three aliquots of a solution of 20% HFIP in DCM (v/v; 3 × 2 mL), with stirring each time on a shaker platform for 30 min at room temperature, and filtering the resin away after each treatment. The combined filtrates were concentrated in vacuo. The final product was analyzed by ESI mass spectrometry and RP-HPLC and used for the cyclization step without further purification.

2.7.4 Mixed monomer/submonomer solid-phase synthesis of octa linear precursors

Linear peptoid **127** was synthesized by alternating submonomer solid-phase method using standard manual Fmoc solid-phase peptide synthesis protocols. 0.20 g of 2-chlorotrityl chloride resin (Novabiochem; 2,α-dichlorobenzhydryl-polystyrene crosslinked with 1% DVB; 100-200 mesh; 1.63 mmol/g) was swelled in dry DCM (2 mL) for 45 min and washed twice in dry DCM (2 mL). Bromoacetic acid (72 mg, 0.52 mmol) and DIPEA (207 mg, 1.6 mmol) in dry DCM (2 mL) were added to the resin and the vessel was stirred on a shaker platform for 40 min at room temperature, and then washed with dry DCM (3 × 4 mL) and then with DMF (3 × 4 mL). Then benzylamine (349 mg, 3.26 mmol) in dry DMF (2 mL) was added to the bromoacetylated resin. The mixture was left on a shaker platform for 40 min at room temperature, then the resin was washed with DMF (3 × 2 mL), DCM (3 × 2 mL) and then with DMF (3 × 2 mL). The resin was incubated with a solution of *N*-Fmoc-L-Proline (330 mg, 0.98 mmol), HATU (361 mg, 0.95 mmol) and DIPEA (168 mg, 1.30 mmol) in dry DMF (2 mL) on a shaker platform for 1 h, followed by extensive washes with DMF (3 × 2 mL), DCM (3 × 2 mL) and DMF (3 × 2 mL). Chloranil test was performed and once the coupling was complete the Fmoc group was deprotected by sequential additions of two aliquots of 20% piperidine/DMF (v/v, 2 mL), stirring on a shaker platform for 3 and 7 min respectively, followed by extensive washes with DMF (3 × 2 mL), DCM (3 × 2 mL) and DMF (3 × 2 mL). Subsequent bromoacetylation reactions were accomplished by reacting the

oligomer with a solution of bromoacetic acid (453 mg, 3.26 mmol) and DIC (453 mg, 3.59 mmol) in DMF (2 mL), stirring on a shaker platform for 40 min at room temperature. Then, reaction with benzylamine, with *N*-Fmoc-L-Proline, Fmoc deprotection and bromoacetylation steps were repeated twice as described above. Subsequently, a further sequence consisting of reaction with benzylamine, with *N*-Fmoc-L-Proline and Fmoc deprotection was effected. The addition of the proline at the fourth, sixth and eighth positions required longer reaction time (3 h). The oligomer-resin was finally cleaved by treatment with three aliquots of a solution of 20% HFIP in DCM (v/v; 3 × 2 mL), with stirring each time on a shaker platform for 30 min at room temperature, and filtering the resin away after each treatment. The combined filtrates were concentrated in vacuo. The final product was analyzed by ESI mass spectrometry and RP-HPLC and used for the cyclization step without further purification.

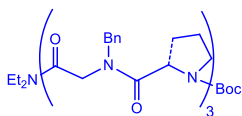
2.7.5 Mixed monomer/submonomer solid-phase synthesis of linear precursor 101

0.40 g of 2-chlorotriethyl chloride resin (Fluka; 2, α -dichlorobenzhydryl-polystyrene cross-linked with 1% DVB; 100–200 mesh; 1.20 mmol/g) was swelled in dry DCM (4 mL) for 45 min and washed twice in dry DCM (3 mL). Bromoacetic acid (107 mg, 0.77 mmol) and DIPEA (310 mg, 2.4 mmol) in dry DCM (4 mL) were added to the resin and the vessel was stirred on a shaker platform for 40 min at room temperature, and then washed with dry DCM (3 × 4 mL) and then with DMF (3 × 4 mL). Then benzylamine (514 mg, 4.80 mmol) in dry DMF (4 mL) was added to the bromoacetylated resin. The mixture was left on a shaker platform for 40 min at room temperature, then the resin was washed with DMF (3 × 4 mL). The resin was incubated with a solution of *N*-Fmoc-L-Proline (485 mg, 1.44 mmol), HATU (529 mg, 1.39 mmol), DIPEA (248 mg, 1.92 mmol) in dry DMF (4 mL) on a shaker platform for 1 h, followed by extensive washes with DMF (3 × 4 mL), DCM (3 × 4 mL) and DMF (3 × 4 mL). Chloranil test was performed and once the coupling was complete the Fmoc group was deprotected by sequential additions of two aliquots of 20% piperidine/DMF (v/v, 3 mL), stirring on a shaker platform for 3 and 7 min respectively, followed by extensive washes with DMF (3 × 3 mL), DCM (3 × 3 mL)

and DMF (3 × 3 mL). Subsequent bromoacetylation reaction was accomplished by reacting the oligomer with a solution of bromoacetic acid (690 mg, 4.8 mmol) and DIC (666 mg, 5.28 mmol) in DMF (4 mL), stirring on a shaker platform for 40 min at room temperature. Then, reaction with benzylamine, with *N*-Fmoc-L-Proline, Fmoc deprotection and bromoacetylation steps were repeated as described above. Addition of the proline at the fourth position required longer reaction time (3 h). A solution of *N*-Boc-L-Proline (310 mg, 1.44 mmol), HATU (529 mg, 1.39 mmol) and DIPEA (248 mg, 1.92 mmol) in dry DMF (4 mL) was added, stirring on a shaker platform for 3 h, followed by extensive washes with DMF (3 × 4 mL), DCM (3 × 4 mL) and DMF (3 × 4 mL). The oligomer-resin was cleaved by treatment with three aliquots of a solution of 20% HFIP in DCM (v/v; 3 × 4 mL), with stirring each time on a shaker platform for 30 min at room temperature, and filtering the resin away after each treatment. The combined filtrates were concentrated in vacuo. The residue (25.3 mg, 0.030 mmol) was dissolved in in DCM (0.9 mL), then EDC (11.5 mg, 0.060 mmol), HOBT (8.0 mg, 0.060 mmol), DIPEA (7.8 mg, 0.060 mmol) and diethylamine (4.4 mg, 0.060 mmol) were added, and the solution was stirred overnight. The reaction mixture was diluted with DCM (2 × 4 mL) and water (2 mL), and the combined organic layers were washed with HCl 1 M (2 mL), dried over Na₂SO₄, filtered, and concentrated in vacuo. The crude residue was purified by HPLC semipreparative column (Waters, Bondapak, 10 μm, 125 Å, 7.8 × 300 mm) affording peptoid **101**.

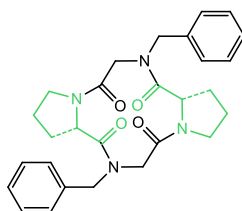
2.7.6 General procedure for high dilution cyclization

To a stirred solution of HATU (178 mg, 0.47 mmol), DIPEA (93.0 mg, 0.72 mmol) in dry DMF (30 mL) at room temperature, a solution of linear precursors (0.12 mmol) in dry DMF (10 mL) was added by syringe pump during 6 h. After 18 h the resulting mixture was concentrated in vacuo, diluted with DCM (20 mL) and washed with 1M HCl (3 × 7 mL). The mixture was extracted with DCM (2 × 10 mL) and the combined organic phases were washed three times with water (10 mL), dried (MgSO₄) and concentrated in vacuo. The crude residues were purified by reversedphase chromatography on C18 bonded silica.

Linear acyclic peptoid 101

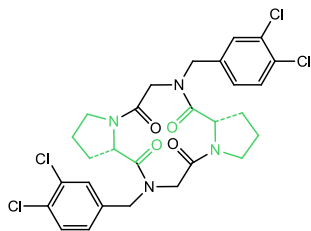
13.5 mg, 67% yield, white amorphous solid; $[\alpha]_{\text{D}}^{19} -6.0$ ($c = 0.8$, CHCl_3);

RP-HPLC analysis: Bondapak, 5% B in A \rightarrow 100% B in 30 min (A: 0.1% TFA in water, B: 0.1% TFA in acetonitrile), 1.0 mL/min, 220 nm, tr 15.1 min.; ^1H NMR (400 MHz, CDCl_3 , mixture of rotamers) δ 7.46–7.27 (m, 15H), 5.45–3.07 (m, 28H), 2.40–1.68 (m, 9H), 1.45 (s, 9H), 1.09 (m, 6H); ^{13}C NMR (150 MHz, CDCl_3 , mixture of rotamers, broad signals) δ 174.0, 173.4, 172.3, 169.8, 166.9, 166.7, 160.4, 160.2, 159.9, 154.6, 154.3, 153.6, 136.8, 136.6, 135.7, 135.4, 129.2, 128.9, 128.8, 128.6, 127.9, 127.8, 127.4, 116.5, 114.6, 80.1, 79.8, 79.5, 58.2, 57.5, 57.0, 55.9, 51.9, 50.8, 49.2, 48.1, 47.4, 46.7, 46.1, 41.3, 40.7, 31.6, 31.2, 30.8, 30.4, 29.8, 29.4, 28.5, 28.4, 25.1, 24.6, 13.9, 12.9; MS (ESI) $[\text{M} + \text{Na}]^+$ 929.0; HRMS (FTICR) $[\text{M} + \text{H}]^+$ calcd for $\text{C}_{51}\text{H}_{68}\text{N}_7\text{O}_8$ 906.5124, found 906.5144.

Cyclotetrapeptoid 94

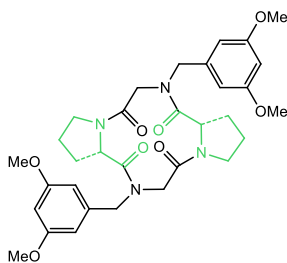
10.2 mg, 19% yield, white amorphous solid; $[\alpha]_{\text{D}}^{25} -113.5$ ($c = 1.0$, CHCl_3);

RP-HPLC analysis: Bondapak, 5% B in A \rightarrow 100% B in 30 min (A: 0.1% TFA in water, B: 0.1% TFA in acetonitrile), 1.0 mL/min, 220 nm, tr 10.3 min.; ^1H NMR (400 MHz, CDCl_3) δ 7.29 (m, 10H), 5.36 (d, $J = 15.0$ Hz, 2H), 5.06 (d, $J = 7.9$ Hz, 2H), 4.36 (d, $J = 14.6$ Hz, 2H), 3.87 (m, 2H), 3.76 (d, $J = 14.6$ Hz, 2H), 3.74 (m, 2H), 3.51 (d, $J = 15.0$ Hz, 2H), 2.23–1.81 (m, 8H); ^{13}C NMR (100 MHz, CDCl_3) δ 169.1 ($\times 2$), 165.9 ($\times 2$), 136.0 ($\times 2$), 128.9 ($\times 4$), 128.7 ($\times 4$), 127.6 ($\times 2$), 57.1 ($\times 2$), 50.7 ($\times 2$), 47.9 ($\times 2$), 47.5 ($\times 2$), 30.8 ($\times 2$), 21.7 ($\times 2$); MS (ESI) $[\text{M} + \text{H}]^+$ 489.6; HRMS (FTICR) $[\text{M} + \text{H}]^+$ calcd for $\text{C}_{28}\text{H}_{33}\text{N}_4\text{O}_4$ 489.2496, found 489.2501.

Cyclotetrapeptoid 95

8.2 mg, 11% yield, white amorphous solid; $[\alpha]_{\text{D}}^{20} -211.5$ ($c = 0.9$, CHCl_3);

RP-HPLC analysis: Bondapak, 5% B in A \rightarrow 100% B in 30 min (A: 0.1% TFA in water, B: 0.1% TFA in acetonitrile), 1.0 mL/min, 220 nm, tr 14.3 min.; ^1H NMR (400 MHz, CDCl_3) δ 7.39 (m, 4H), 7.16 (m, 2H), 5.22 (d, $J = 15.0$ Hz, 2H), 4.97 (d, $J = 8.2$ Hz, 2H), 4.32 (d, $J = 15.0$ Hz, 2H), 3.85 (m, 2H), 3.72 (m, 2H), 3.71 (d, $J = 15.0$ Hz, 2H), 3.46 (d, $J = 15.0$ Hz, 2H), 2.24 (m, 6H), 1.78 (m, 2H); ^{13}C NMR (100 MHz, CDCl_3) δ 169.2 ($\times 2$), 165.1 ($\times 2$), 136.0 ($\times 2$), 132.7 ($\times 2$), 132.0 ($\times 2$), 130.8 ($\times 2$), 130.7 ($\times 2$), 128.5 ($\times 2$), 57.1 ($\times 2$), 50.8 ($\times 2$), 47.8 ($\times 2$), 46.4 ($\times 2$), 30.9 ($\times 2$), 21.7 ($\times 2$); MS (ESI) $[\text{M} + \text{Na}]^+$ 647.4; HRMS (FTICR) $[\text{M} + \text{H}]^+$ calcd for $\text{C}_{28}\text{H}_{29}\text{Cl}_4\text{N}_4\text{O}_4$ 625.0937, found 625.0942.

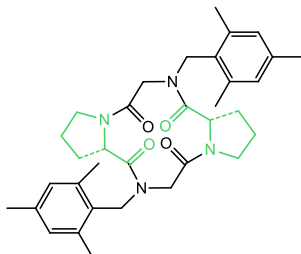
Cyclotetrapeptoid 96

45.3 mg, 62% yield, white amorphous solid; $[\alpha]_{\text{D}}^{25} -149.2$ ($c = 1.0$, CHCl_3);

RP-HPLC analysis: Bondapak, 5% B in A \rightarrow 100% B in 30 min (A: 0.1% TFA in water, B: 0.1% TFA in acetonitrile), 1.0 mL/min, 220 nm, tr 11.8 min.; ^1H NMR (300 MHz, CDCl_3) δ 6.44 (m, 4H), 6.34 (m, 2H), 5.27 (d, $J = 14.9$ Hz, 2H), 5.12 (d, $J = 8.2$ Hz, 2H), 4.42 (d, $J = 14.8$ Hz, 2H), 3.92–3.60 (m, 6H), 3.73 (m, 12H), 3.42 (d, $J = 14.9$ Hz, 2H), 2.26–1.75 (m, 8H); ^{13}C NMR (75 MHz, CDCl_3) δ 169.5 ($\times 2$), 165.9 ($\times 2$), 160.8 ($\times 4$), 138.4 ($\times 2$), 106.2 ($\times 4$), 99.9 ($\times 2$), 57.1 ($\times 2$), 55.2 ($\times 12$), 50.7 ($\times 2$).

$\times 2$), 47.8 ($\times 2$), 47.5 ($\times 2$), 30.7 ($\times 2$), 21.6 ($\times 2$); MS (ESI) $[M + H]^+$ 609.3; HRMS (FTICR) $[M + H]^+$ calcd for $C_{32}H_{41}N_4O_8$ 609.2919, found 609.2899.

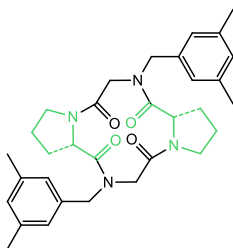
Cyclotetrapeptoid 97



8.9 mg, 13% yield, white amorphous solid; $[\alpha]_D^{20} -3.1$ ($c = 0.5$, $CHCl_3$);

RP-HPLC analysis: Bondapak, 5% B in A \rightarrow 100% B in 30 min (A: 0.1% TFA in water, B: 0.1% TFA in acetonitrile), 1.0 mL/min, 220 nm, tr 14.8 min.; 1H NMR (600 MHz, DMSO- d_6) δ 6.79 (s, 4H), 5.48 (d, $J = 9.0$ Hz, 2H), 5.20 (d, $J = 15.6$ Hz, 2H), 4.50 (d, $J = 15.6$ Hz, 2H), 3.96 (d, $J = 15.6$ Hz, 2H), 3.55 (m, 4H), 3.45 (m, 2H), 3.17 (d, $J = 15.6$ Hz, 2H), 2.21 (s, 18H), 1.89 (m, 4H), 1.78 (m, 2H); ^{13}C NMR (100 MHz, DMSO- d_6) δ 169.2 ($\times 2$), 166.4 ($\times 2$), 137.6 ($\times 4$), 136.1 ($\times 2$), 128.9 ($\times 4$), 128.3 ($\times 2$), 57.1 ($\times 2$), 49.9 ($\times 2$), 47.8 ($\times 2$), 30.9 ($\times 2$), 21.8 ($\times 2$), 20.5 ($\times 2$), 19.5 ($\times 6$); MS (ESI) $[M + H]^+$ 573.7; HRMS (FTICR) $[M + H]^+$ calcd for $C_{34}H_{45}N_4O_4$ 573.3435, found 573.3425.

Cyclotetrapeptoid 98

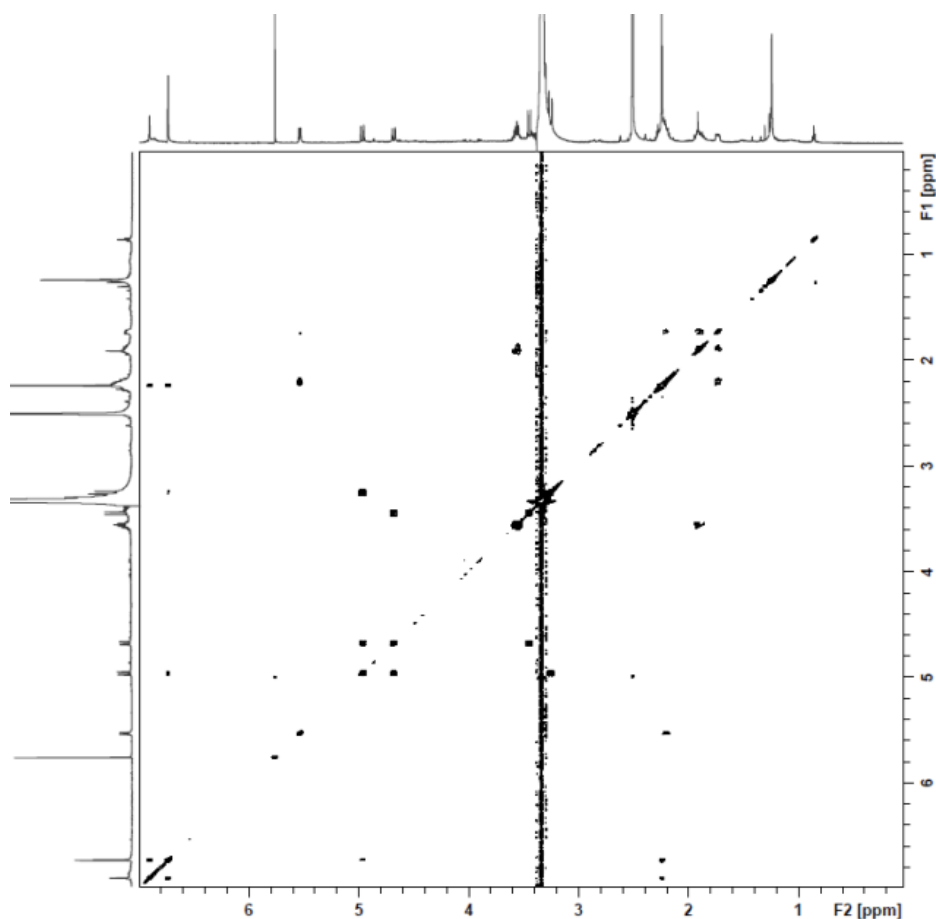


17.9 mg, 27% yield, white amorphous solid; $[\alpha]_D^{25} -108.6$ ($c = 1.0$, $CHCl_3$);

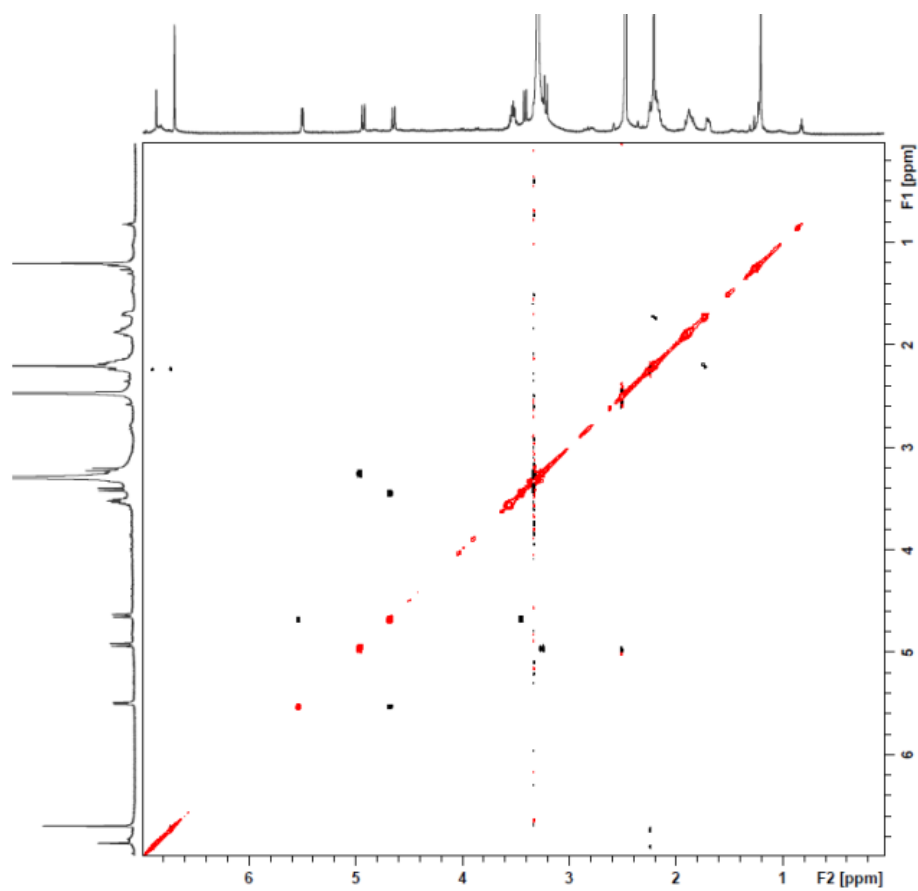
RP-HPLC analysis: Bondapak, 5% B in A \rightarrow 100% B in 30 min (A: 0.1% TFA in water, B: 0.1% TFA in acetonitrile), 1.0 mL/min, 220 nm, tr 12.8 min.; 1H NMR (600 MHz, DMSO- d_6) δ : 6.88 (s, 2H), 6.73 (s, 4H), 5.53 (d, $J = 9.0$ Hz, 2H), 4.96 (d, $J = 15.3$

Hz, 2H), 4.68 (d, $J = 15.0$ Hz, 2H), 3.56 (m, 4H), 3.45 (d, $J = 15.0$ Hz, 2H), 3.25 (d, $J = 15.3$ Hz, 2H), 2.25 (m, 14H), 1.92 (m, 4H), 1.73 (m, 2H); ^{13}C NMR (150 MHz, $\text{DMSO-}d_6$) δ 170.1 ($\times 2$), 165.7 ($\times 2$), 137.5 ($\times 2$), 128.0 ($\times 2$), 127.8 ($\times 2$), 127.6 ($\times 2$), 125.4 ($\times 4$), 56.2 ($\times 2$), 50.8 ($\times 2$), 47.3 ($\times 2$), 46.3 ($\times 2$), 30.4 ($\times 2$), 21.4 ($\times 2$), 20.9 ($\times 4$); MS (ESI) $[\text{M} + \text{H}]^+ 545.7$, $[\text{M} + \text{Na}]^+ 567.7$; HRMS (FTICR) $[\text{M} + \text{H}]^+$ calcd for $\text{C}_{32}\text{H}_{41}\text{N}_4\text{O}_4$ 545.3122, found 545.3134.

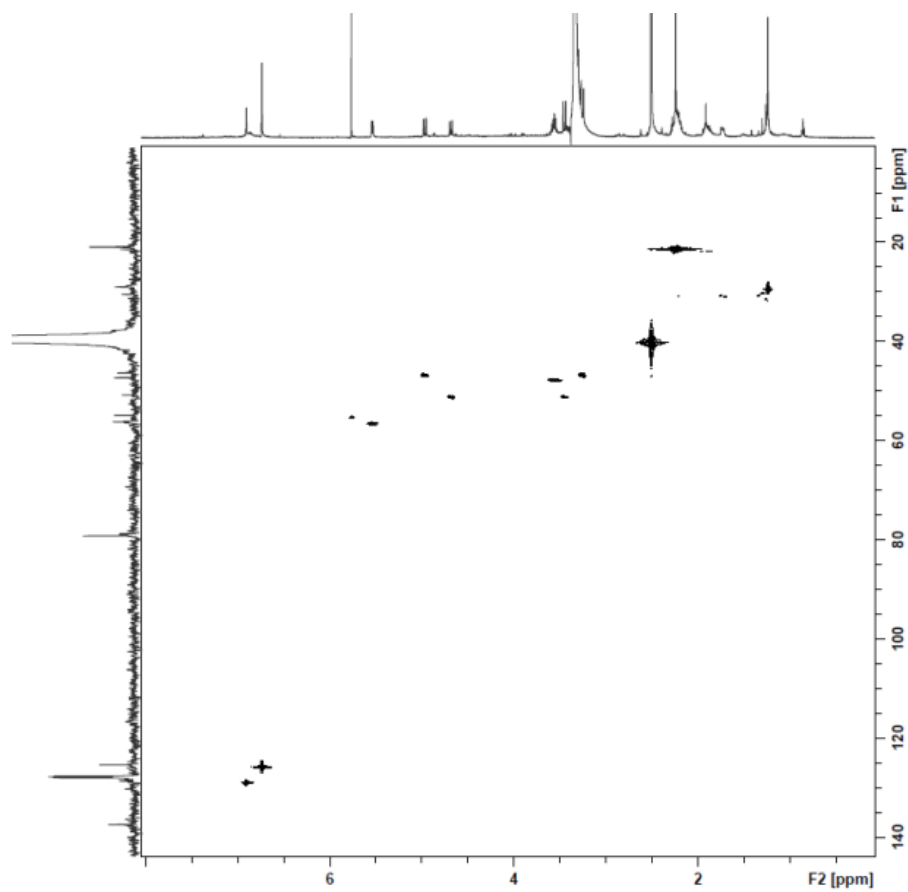
^1H - ^1H COSY NMR of compound **98** (600 MHz, $\text{DMSO-}d_6$)

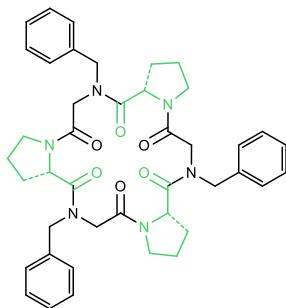


^1H - ^1H ROESY NMR of compound **98** (600 MHz, $\text{DMSO-}d_6$)



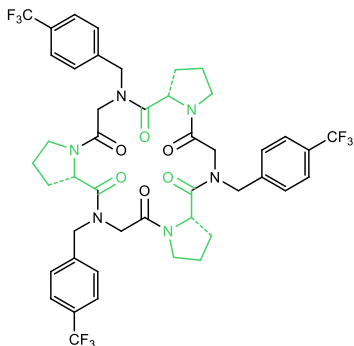
^1H - ^{13}C HMQC NMR of compound **98** (600 MHz, $\text{DMSO-}d_6$)



Cyclohexapeptoid 80

43.0 mg, 49% yield, white amorphous solid; $[\alpha]_D^{25} + 25.5$ ($c = 1.0$, CHCl_3);

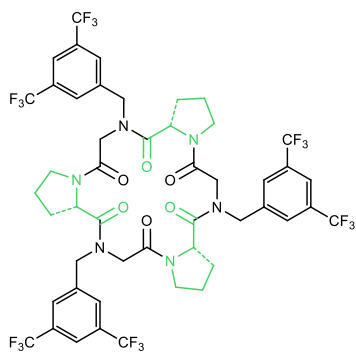
RP-HPLC analysis: Bondapak, 5% B in A \rightarrow 100% B in 30 min (A: 0.1% TFA in water, B: 0.1% TFA in acetonitrile), 1.0 mL/min, 220 nm, tr 14.8 min.; ^1H NMR (400 MHz, CDCl_3 , mixture of rotamers) δ 7.69–6.85 (m, 15H), 5.98–3.04 (m, 21H), 2.59–1.26 (m, 12H); ^{13}C NMR (100 MHz, CDCl_3 , mixture of rotamers, broad signals) δ 174.0, 173.8, 173.2, 172.7, 172.6, 172.2, 171.9, 170.9, 169.9, 168.9, 168.4, 168.1, 167.9, 167.7, 167.3, 167.1, 166.8, 166.7, 165.4, 137.0, 136.7, 136.6, 136.5, 136.4, 136.2, 136.1, 135.7, 129.3, 129.0, 128.7, 128.5, 128.4, 128.3, 128.2, 128.0, 127.8, 127.7, 127.6, 127.5, 127.3, 127.1, 126.9, 126.7, 126.6, 126.4, 126.2, 58.9, 58.8, 57.9, 57.8, 57.3, 56.7, 56.5, 56.1, 53.6, 53.3, 53.1, 53.0, 52.3, 51.7, 51.4, 50.8, 50.1, 50.0, 49.9, 49.8, 49.4, 49.1, 48.8, 48.4, 48.1, 47.8, 47.7, 47.6, 47.4, 47.1, 46.9, 46.8, 46.4, 46.3, 46.2, 32.2, 32.0, 31.9, 31.4, 31.3, 29.9, 29.6, 29.4, 29.2, 28.9, 28.6, 28.2, 25.9, 25.4, 25.2, 25.0, 24.8, 24.6, 22.7, 22.6, 22.0, 21.6; MS (ESI) $[\text{M} + \text{Na}]^+$ 755.2; HRMS (FTICR) $[\text{M} + \text{Na}]^+$ calcd for $\text{C}_{42}\text{H}_{48}\text{N}_6\text{NaO}_6$ 755.3528, found 755.3510.

Cyclohexapeptoid 81

20.2 mg, 18% yield, white amorphous solid; $[\alpha]_D^{25} + 28.6$ ($c = 1.0$, CHCl_3);

RP-HPLC analysis: Bondapak, 5% B in A → 100% B in 30 min (A: 0.1% TFA in water, B: 0.1% TFA in acetonitrile), 1.0 mL/min, 220 nm, tr 17.5 min.; ^1H NMR (400 MHz, CDCl_3 , mixture of rotamers) δ 7.78–7.26 (m, 12H), 5.90–2.85 (m, 21H), 2.35–1.00 (m, 12H); ^{13}C NMR (150 MHz, CDCl_3 , mixture of rotamers, broad signals) δ 174.4, 173.9, 173.8, 173.6, 173.5, 172.9, 172.4, 172.1, 171.9, 171.5, 171.0, 169.9, 169.8, 169.7, 169.2, 168.8, 168.5, 168.2, 167.7, 167.0, 166.8, 166.6, 166.3, 165.9, 165.6, 165.3, 141.5, 141.3, 141.1, 140.9, 140.5, 140.1, 139.8, 139.6, 139.1, 130.8, 130.3, 130.0, 129.7, 129.4, 129.2, 128.5, 128.3, 127.9, 127.7, 127.4, 127.1, 126.9, 126.7, 126.5, 126.0, 125.6, 125.5, 125.3, 122.5, 59.5, 58.9, 57.7, 57.5, 57.3, 56.6, 56.5, 56.2, 53.3, 53.2, 52.7, 52.3, 51.8, 51.7, 51.5, 51.0, 50.7, 50.5, 50.6, 50.4, 49.8, 49.6, 49.3, 49.0, 48.8, 48.4, 48.3, 48.1, 47.8, 47.6, 47.4, 47.2, 46.9, 46.6, 46.5, 46.3, 37.4, 32.7, 32.1, 31.9, 31.6, 31.4, 30.3, 30.0, 29.3, 28.9, 28.7, 28.3, 27.8, 27.3, 27.1, 26.3, 25.9, 25.6, 25.4, 25.2, 25.0, 24.8, 23.0, 22.9, 22.6, 22.1, 21.6, 21.1, 19.7; MS (ESI) $[\text{M} + \text{K}]^+$ 975.0; HRMS (FTICR) $[\text{M} + \text{H}]^+$ calcd for $\text{C}_{45}\text{H}_{46}\text{F}_9\text{N}_6\text{O}_6$ 937.3329, found 937.3337.

Cyclohexapeptoid **82**

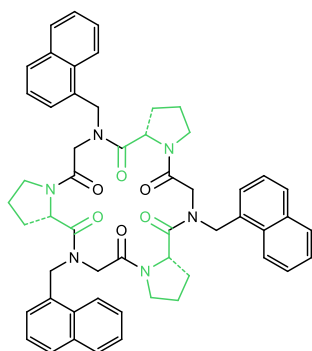


31.4 mg, 23% yield, white amorphous solid; $[\alpha]_{\text{D}}^{25} + 22.9$ ($c = 1.0$, CHCl_3);

RP-HPLC analysis: Bondapak, 5% B in A → 100% B in 30 min (A: 0.1% TFA in water, B: 0.1% TFA in acetonitrile), 1.0 mL/min, 220 nm, tr 19.0 min.; ^1H NMR (400 MHz, CDCl_3 , mixture of rotamers) δ 8.17–7.56 (m, 9H), 5.73–2.79 (m, 21H), 2.34–1.03 (m, 12H); ^{13}C NMR (150 MHz, CDCl_3 , mixture of rotamers, broad signals) δ 174.4, 173.7, 172.8, 172.4, 169.9, 169.7, 168.4, 168.2, 167.4, 168.2, 167.4, 166.3, 166.1, 139.6, 139.1, 138.3, 133.0, 132.7, 132.4, 132.1, 131.8, 131.5, 128.5, 128.3,

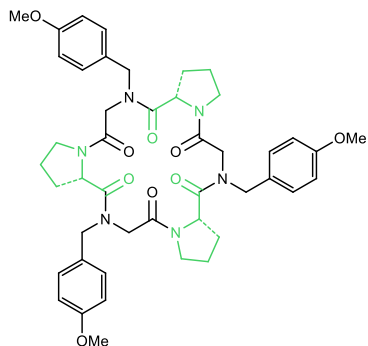
127.5, 127.2, 127.0, 126.5, 124.6, 124.5, 124.3, 122.2, 121.9, 121.6, 121.4, 119.2, 118.9, 116.6, 113.7, 59.6, 58.0, 57.8, 57.8, 56.6, 56.3, 53.4, 53.1, 52.4, 52.0, 51.9, 50.7, 50.4, 49.8, 49.2, 48.8, 48.5, 47.6, 46.9, 46.8, 46.6, 37.4, 37.1, 32.7, 31.9, 31.6, 31.3, 30.0, 29.5, 29.3, 28.5, 27.8, 27.6, 27.3, 27.0, 25.5, 25.4, 25.1, 24.4, 22.8, 22.7, 20.8, 19.7; MS (ESI) $[M + H]^+$ 1141.0; HRMS (FTICR) $[M + H]^+$ calcd for $C_{48}H_{43}F_{18}N_6O_6$ 1141.2951, found 1141.2972.

Cyclohexapeptoid **83**

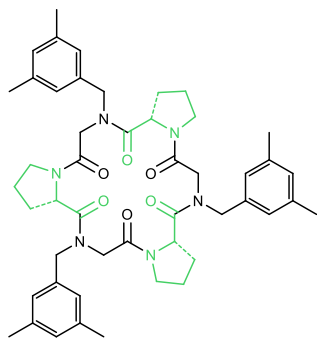


23.3 mg, 22% yield, white amorphous solid; $[\alpha]_D^{25} +8.3$ ($c = 0.9$, $CHCl_3$);

RP-HPLC analysis: Bondapak, 5% B in A \rightarrow 100% B in 30 min (A: 0.1% TFA in water, B: 0.1% TFA in acetonitrile), 1.0 mL/min, 220 nm, tr 17.4 min.; 1H NMR (400 MHz, $CDCl_3$, mixture of rotamers) δ 8.30–6.96 (m, 21H), 6.10–3.10 (m, 21H), 2.74–1.26 (m, 12H); ^{13}C NMR (100 MHz, $CDCl_3$, mixture of rotamers, broad signals) δ 175.5, 174.4, 173.7, 173.4, 173.2, 173.0, 172.2, 172.1, 171.8, 171.4, 169.9, 169.8, 169.1, 168.9, 168.5, 168.3, 168.0, 167.6, 166.9, 166.1, 166.0, 165.8, 133.8, 133.7, 133.0, 132.6, 132.5, 132.3, 132.1, 131.9, 131.7, 131.5, 131.3, 131.2, 131.0, 130.9, 130.8, 130.6, 130.3, 129.2, 129.0, 128.7, 128.4, 128.3, 128.2, 127.8, 127.6, 127.0, 126.8, 126.6, 126.3, 125.9, 125.6, 125.4, 125.3, 125.2, 124.4, 123.6, 123.5, 123.1, 122.9, 122.6, 122.5, 122.3, 121.7, 59.0, 58.9, 58.6, 57.9, 57.8, 57.4, 57.3, 56.9, 56.7, 56.6, 56.1, 55.8, 51.6, 51.5, 51.1, 50.7, 50.5, 50.1, 50.0, 49.3, 48.9, 48.7, 48.5, 47.9, 47.6, 47.5, 47.3, 47.2, 46.8, 46.6, 46.4, 46.2, 45.6, 32.0, 31.9, 31.6, 31.3, 31.2, 31.1, 30.0, 29.3, 29.1, 28.7, 28.3, 27.5, 27.3, 27.1, 25.8, 25.4, 25.2, 25.1, 24.8, 23.2, 23.0, 22.6, 22.1, 21.4, 20.6, 20.1, 19.7; MS (ESI) $[M + Na]^+$ 905.4; HRMS (FTICR) $[M + H]^+$ calcd for $C_{54}H_{55}N_6O_6$ 883.4178, found 883.4152.

Cyclohexapeptoid 84

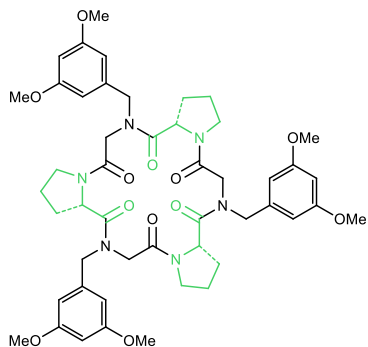
60.4 mg, 57% yield, white amorphous solid; $[\alpha]_D^{25} + 30.8$ ($c = 1.0$, CHCl_3); RP-HPLC analysis: Bondapak, 5% B in A \rightarrow 100% B in 30 min (A: 0.1% TFA in water, B: 0.1% TFA in acetonitrile), 1.0 mL/min, 220 nm, tr 14.1 min.; $^1\text{H NMR}$ (300 MHz, CDCl_3 , mixture of rotamers) δ 7.53–6.59 (m, 12H), 5.26–3.16 (m, 30H), 2.52–1.21 (m, 12H); $^{13}\text{C NMR}$ (100 MHz, CDCl_3 , mixture of rotamers, broad signals) δ 173.3, 173.2, 172.5, 171.9, 171.8, 171.6, 171.0, 169.8, 168.5, 168.3, 168.0, 167.3, 167.1, 166.9, 166.8, 165.6, 159.4, 159.2, 159.0, 158.7, 129.9, 129.5, 129.2, 129.0, 128.9, 128.7, 128.4, 128.3, 128.1, 127.9, 127.7, 114.4, 114.3, 114.2, 114.1, 113.9, 113.7, 58.7, 58.5, 58.2, 57.8, 57.6, 57.3, 57.0, 56.7, 56.2, 56.1, 55.7, 55.3, 55.1, 53.0, 52.6, 52.5, 52.3, 51.2, 50.8, 50.4, 50.3, 49.5, 49.2, 48.7, 48.4, 47.9, 47.7, 47.5, 47.4, 47.2, 46.7, 46.5, 46.4, 46.2, 37.4, 37.0, 36.8, 32.7, 32.0, 31.9, 31.6, 31.5, 31.4, 31.2, 30.2, 30.0, 29.3, 29.2, 28.9, 28.2, 27.7, 27.5, 27.3, 27.0, 25.7, 25.4, 24.9, 24.8, 24.4, 22.9, 22.6, 22.1, 21.7, 21.3, 21.1, 20.5, 20.3, 19.7; MS (ESI) $[\text{M} + \text{H}]^+$ 823.4, $[\text{M} + \text{Na}]^+$ 845.5; HRMS (FTICR) $[\text{M} + \text{H}]^+$ calcd for $\text{C}_{45}\text{H}_{46}\text{F}_9\text{N}_6\text{O}_6$ 823.4025, found 823.3998.

Cyclohexapeptoid 85

42.1 mg, 43% yield, white amorphous solid; $[\alpha]_D^{25} + 9.9$ ($c = 0.3$, CHCl_3);

RP-HPLC analysis: Bondapak, 5% B in A \rightarrow 100% B in 30 min (A: 0.1% TFA in water, B: 0.1% TFA in acetonitrile), 1.0 mL/min, 220 nm, tr 17.2 min.; ^1H NMR (400 MHz, CDCl_3 , mixture of rotamers) δ 7.20–6.72 (m, 9H), 5.75–3.22 (m, 21H), 2.66–0.94 (m, 30H); ^{13}C NMR (100 MHz, CDCl_3 , mixture of rotamers, broad signals) δ 173.9, 173.4, 172.6, 171.9, 171.6, 171.5, 168.5, 168.3, 167.6, 167.4, 166.1, 165.8, 138.8, 138.7, 138.6, 138.3, 138.1, 137.8, 136.9, 136.8, 135.9, 129.5, 129.3, 129.1, 128.6, 126.3, 125.9, 125.5, 125.0, 124.5, 124.4, 124.2, 58.4, 58.1, 57.5, 56.8, 56.1, 53.6, 53.0, 52.8, 52.0, 51.3, 50.5, 50.1, 48.8, 48.1, 47.9, 47.6, 47.1, 46.7, 46.4, 46.2, 37.4, 37.1, 32.8, 32.2, 31.9, 31.4, 30.0, 29.7, 29.4, 29.2, 28.3, 27.4, 25.0, 24.9, 24.8, 23.0, 22.7, 22.0, 21.7, 21.4, 20.9, 19.7, 18.3; MS (ESI) $[\text{M} + \text{H}]^+$ 817.0; HRMS (FTICR) $[\text{M} + \text{H}]^+$ calcd for $\text{C}_{48}\text{H}_{61}\text{N}_6\text{O}_6$ 817.4647, found 817.4634.

Cyclohexapeptoid **86**

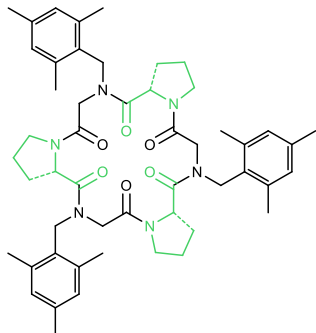


21.9 mg, 20% yield, white amorphous solid; $[\alpha]_D^{25} + 6.5$ ($c = 1.0$, CHCl_3);

RP-HPLC analysis: Bondapak, 5% B in A \rightarrow 100% B in 30 min (A: 0.1% TFA in water, B: 0.1% TFA in acetonitrile), 1.0 mL/min, 220 nm, tr 13.5 min.; ^1H NMR (300 MHz, CDCl_3 , mixture of rotamers) δ 6.75–6.10 (m, 9H), 5.31–3.94 (m, 9H), 3.63 (bs, 18H), 3.70–3.20 (m, 12H), 2.01–1.65 (m, 12H); ^{13}C NMR (100 MHz, CDCl_3 , mixture of rotamers, broad signals) δ 173.4, 172.3, 171.9, 171.3, 169.8, 168.4, 167.9, 166.9, 161.2, 160.9, 160.7, 139.1, 138.8, 106.2, 105.9, 105.4, 105.0, 104.5, 104.2, 103.5, 100.2, 100.0, 99.6, 99.3, 58.6, 57.6, 56.7, 55.3, 55.1, 54.9, 53.2, 52.8, 52.4, 52.1, 51.4, 50.7, 50.5, 49.1, 47.8, 47.5, 46.9, 46.4, 46.1, 40.4, 40.2, 39.9, 39.7, 32.3, 31.8, 31.4, 29.9, 29.6, 29.3, 28.6, 27.4, 25.8, 25.2, 24.8, 23.0, 22.6, 22.2, 21.8, 19.7; MS (ESI) $[\text{M}$

+ H]⁺ 913.7, [M + Na]⁺ 935.8; HRMS (FTICR) [M + H]⁺ calcd for C₄₈H₆₁N₆O₁₂ 913.4342, found 913.4328.

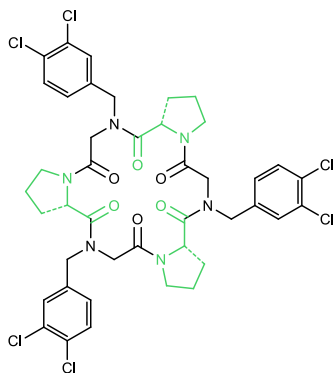
Cyclohexapeptoid **87**



10.3 mg, 10% yield, white amorphous solid; $[\alpha]_D^{25} + 9.9$ ($c = 0.3$, CHCl₃);

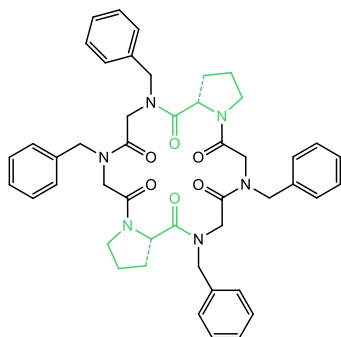
RP-HPLC analysis: Bondapak, 5% B in A → 100% B in 30 min (A: 0.1% TFA in water, B: 0.1% TFA in acetonitrile), 1.0 mL/min, 220 nm, *tr* 17.1 min.; ¹H NMR (400 MHz, CDCl₃, mixture of rotamers) δ 6.89–6.81 (m, 6H), 5.28–4.53 (m, 9H), 3.98–3.17 (m, 12H), 2.31–1.90 (m, 39H); ¹³C NMR (150 MHz, CDCl₃, mixture of rotamers, broad signals) δ 178.4, 172.9, 172.2, 171.6, 170.4, 169.9, 168.2, 140.1, 139.9, 139.4, 138.3, 138.1, 137.8, 136.9, 130.8, 130.5, 130.4, 130.0, 129.4, 59.3, 57.9, 48.6, 48.3, 47.7, 47.0, 46.7, 46.2, 45.6, 45.5, 44.8, 32.9, 32.3, 30.7, 29.3, 28.0, 26.8, 23.6, 23.5, 21.9, 21.0, 20.5; MS (ESI) (M + H)⁺ 859.6; HRMS (FTICR) (M + H)⁺ calcd for C₅₁H₆₇N₆O₆ 859.5116, found 859.5142.

Cyclohexapeptoid **88**



59.5 mg, 53% yield, white amorphous solid; $[\alpha]_D^{20}$ -2.5 ($c = 0.5$, CHCl_3); RP-HPLC analysis: Bondapak, 5% B in A \rightarrow 100% B in 30 min (A: 0.1% TFA in water, B: 0.1% TFA in acetonitrile), 1.0 mL/min, 220 nm, tr 15.5 min.; ^1H NMR (600 MHz, CDCl_3 , mixture of rotamers) δ 7.72–6.97 (m, 9H), 5.66–2.88 (m, 21H), 2.40–1.00 (m, 12H); ^{13}C NMR (150 MHz, CDCl_3 , mixture of rotamers, broad signals) δ 173.0, 172.4, 172.1, 171.9, 171.3, 171.2, 171.05, 170.0, 169.5, 168.7, 168.4, 167.9, 167.5, 166.8, 166.6, 166.5, 165.3, 165.1, 137.6, 137.5, 137.2, 136.7, 136.4, 136.1, 134.8, 133.7, 133.5, 133.3, 132.9, 132.7, 132.6, 132.4, 132.2, 132.1, 132.0, 131.5, 131.4, 131.2, 130.8, 130.7, 130.5, 130.3, 130.0, 129.9, 129.7, 129.6, 129.0, 128.6, 128.4, 127.8, 127.3, 127.2, 127.0, 126.9, 126.7, 62.7, 59.7, 58.8, 58.2, 57.9, 57.5, 56.5, 56.2, 51.0, 50.5, 50.2, 49.7, 49.1, 48.9, 48.2, 47.3, 46.6, 31.7, 29.3, 28.7, 27.7, 25.6, 25.2, 24.8, 23.0, 22.6, 21.9, 21.1; MS (ESI) $[\text{M} + \text{Na}]^+$ 959.1; HRMS (FTICR) $[\text{M} + \text{H}]^+$ calcd for $\text{C}_{42}\text{H}_{43}\text{Cl}_6\text{N}_6\text{O}_6$ 937.1370, found 937.1402.

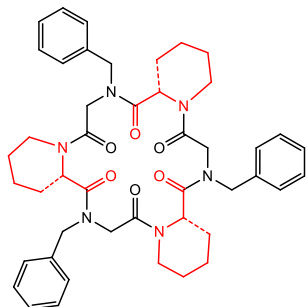
Cyclohexapeptoid **126**



117.0 mg, 46% yield, white amorphous solid; $[\alpha]_D^{28}$ $+3.4$ ($c = 1.0$, CHCl_3); RP-HPLC analysis: Bondapak, 5% B in A \rightarrow 100% B in 30 min (A: 0.1% TFA in water, B: 0.1% TFA in acetonitrile), 1.0 mL/min, 220 nm, tr 12.4 min.; ^1H NMR (400 MHz, CDCl_3 , mixture of rotamers) δ 7.39–7.10 (m, 20H), 5.43–3.07 (m, 22H), 2.29–1.93 (m, 8H); ^{13}C NMR (100 MHz, CDCl_3 , mixture of rotamers, broad signals) δ 175.2, 172.3, 171.0, 169.9, 167.8, 165.5, 160.3, 160.0, 136.8, 136.6, 136.5, 129.2, 129.0, 128.7, 128.7, 128.6, 128.6, 128.4, 128.3; 128.0, 127.9, 127.8, 127.6, 127.3, 127.2, 126.9, 126.6, 119.9, 117.0, 114.1, 58.6, 57.8, 57.6, 57.3, 57.0, 54.7, 53.6, 52.3, 51.4, 50.0, 49.6, 48.4, 48.0, 47.6, 47.3, 46.7, 46.0, 43.4, 31.9, 31.8, 31.7, 30.2, 30.1,

30.0, 29.7, 29.3, 29.1, 28.9, 28.6, 28.3, 27.3, 25.7, 24.3, 22.7, 20.6, 19.6; HRMS (MALDI) m/z $[M + H]^+$ 783.3865 calcd for $C_{46}H_{51}N_6O_6^+$; found 783.3870.

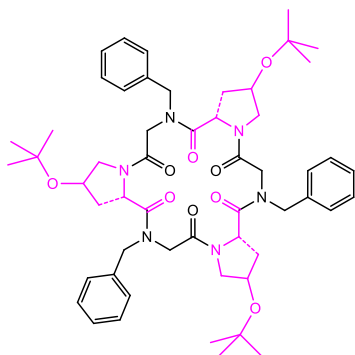
Cyclohexapeptoid **148**



19 mg, 3% yield, amorphous solid;

RP-HPLC analysis: Bondapak, 5% B in A → 100% B in 30 min (A: 0.1% TFA v/v in water, B: 0.1% TFA v/v in acetonitrile), 1.0 mL/min, 220 nm, tr 13.3 min; ¹H NMR (400 MHz, CDCl₃, mixture of rotamers) δ 7.36–7.20 (m, 15H), 5.08–2.90 (m, 21H), 2.34–0.83 (m, 18H); ¹³C NMR (100 MHz, CDCl₃, mixture of rotamers, broad signals) δ 176.8, 172.9, 171.7, 170.6, 169.9, 166.4, 165.7, 161.2, 160.9, 137.0, 136.8, 136.0, 134.8, 130.0, 129.7, 129.5, 129.0, 128.8, 128.0, 127.7, 127.5, 127.2, 126.5, 126.3, 125.8, 124.4, 124.0, 119.0, 117.0, 115.1, 113.2, 111.2, 103.1, 70.5, 62.7, 58.0, 54.7, 53.4, 53.0, 51.9, 51.5, 51.3, 50.0, 49.3, 47.2, 46.8, 46.3, 46.0, 45.5, 45.1, 44.8, 43.8, 43.0, 42.7, 41.2, 40.2, 39.4, 37.4, 37.0; MS (ESI) m/z $[M + Na]^+$ 796.8, $[M + H]^+$ 774.8.

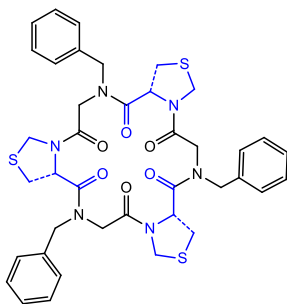
Cyclohexapeptoid **149**



95 mg, 27% yield, amorphous yellow solid; $[\alpha]_{\text{D}}^{26} + 15.3$ ($c = 1.0$, CHCl_3);

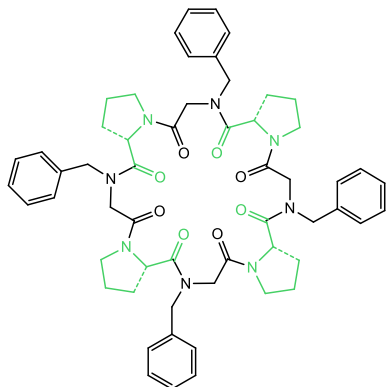
RP-HPLC analysis: Bondapak, 5% B in A \rightarrow 100% B in 30 min (A: 0.1% TFA v/v in water, B: 0.1% TFA v/v in acetonitrile), 1.0 mL/min, 220 nm, t_{r} 13.2 min.; ^1H NMR (400 MHz, CDCl_3 , mixture of rotamers) δ 7.63–6.98 (m, 15H), 5.38–3.10 (m, 24H), 2.32–1.60 (m, 6H), 1.21–1.08 (m, 27H); ^{13}C NMR (100 MHz, CDCl_3 , mixture of rotamers, broad signals) δ 174.0, 173.2, 172.8, 172.5, 172.3, 172.1, 168.7, 168.3, 168.0, 167.2, 166.1, 165.9, 137.0, 136.6, 136.4, 135.5, 129.1, 128.9, 128.7, 128.6, 128.5, 128.0, 127.8, 127.7, 127.3, 127.0, 126.7, 126.6, 126.5, 75.2, 74.6, 74.3, 74.1, 70.8, 70.2, 70.0, 69.7, 68.4, 68.1, 67.6, 57.5, 56.8, 56.4, 55.7, 55.3, 54.8, 54.6, 53.9, 53.7, 53.3, 52.2, 51.6, 50.7, 49.2, 48.7, 48.6, 48.2, 47.3, 39.1, 37.5, 37.2, 36.5, 28.2, 28.0; MS (ESI) m/z $[\text{M} + \text{Na}]^+$ 971.1, $[\text{M}]^+$ 949.1.

Cyclohexapeptoid 150



61 mg, 21% yield, amorphous solid; $[\alpha]_{\text{D}}^{27} - 34.1$ ($c = 1.0$, CHCl_3);

RP-HPLC analysis: Bondapak, 5% B in A \rightarrow 100% B in 30 min (A: 0.1% TFA v/v in water, B: 0.1% TFA v/v in acetonitrile), 1.0 mL/min, 220 nm, t_{r} 11.0 min.; ^1H NMR (400 MHz, CDCl_3 , mixture of rotamers) δ 7.63–7.20 (m, 15H), 5.34–2.81 (m, 21H), 1.56–0.83 (m, 6H); ^{13}C NMR (100 MHz, CDCl_3 , mixture of rotamers, broad signals) δ 171.9, 170.8, 170.0, 166.8, 165.8, 164.7, 160.6, 136.8, 136.5, 136.3, 135.1, 129.4, 129.2, 129.0, 128.3, 128.1, 128.0, 127.9, 127.7, 127.6, 126.8, 126.5, 126.4, 126.0, 125.8, 114.9, 60.2, 59.8, 59.3, 58.6, 53.8, 53.6, 52.9, 52.4, 51.8, 51.4, 51.2, 50.8, 50.5, 50.2, 49.2, 48.6, 48.4, 47.8, 37.4, 35.4, 33.3, 32.5, 31.8, 30.0, 29.7, 29.3, 27.2, 23.4, 22.6, 20.6, 20.3; MS (ESI) m/z $[\text{M} + \text{Na}]^+$ 971.1, $[\text{M}]^+$ 948.1.

Cyclooctapeptoid 128

58.0 mg, 41% yield, white amorphous solid; $[\alpha]_{\text{D}}^{30}$: -48.1 ($c = 0.7$, CHCl_3);

RP-HPLC analysis: Bondapak, 5% B in A \rightarrow 100% B in 30 min (A: 0.1% TFA in water, B: 0.1% TFA in acetonitrile), 1.0 mL/min, 220 nm, t_{r} 12.9 min; $^1\text{H NMR}$ (400 MHz, CDCl_3 , mixture of rotamers) δ 7.37-7.13 (m, 20H), 5.62-3.28 (m, 28H), 2.26-1.42 (m, 16H); $^{13}\text{C NMR}$ (100 MHz, CDCl_3 , mixture of rotamers, broad signals) δ 173.7, 171.8, 168.2, 165.8, 165.1, 136.6, 129.0, 128.8, 128.4, 128.3, 127.8, 127.6, 126.9, 126.8, 57.2, 57.0, 51.5, 50.7, 50.2, 49.7, 47.7, 47.4, 47.1, 46.8, 31.6, 29.8, 28.7, 27.2, 25.1, 24.6, 22.7, 22.2; HRMS (MALDI) m/z $[\text{M} + \text{H}]^+$ 977.4920 calcd for $\text{C}_{56}\text{H}_{65}\text{N}_8\text{O}_8^+$; found 977.4911.

2.7.7 Determination of Binding Affinities for Compounds 80 and 94.

Association constants K_a were calculated from the equation $K_a = K_e / K_d$, according to methodology reported by Cram and co-workers.³⁷ K_d values, which represent the distribution constants of the picrate salts between water and CHCl_3 , were previously determined by Cram,³⁷ while K_e values were calculated following the "ultraviolet method" reported by Cram and co-workers.³⁷ All ultraviolet (UV) measurements were made at 380 nm at 24–26 °C, using spectrophotometric grade solvents. The picrate salts were prepared according to literature procedures,^{86,88} and dried under high vacuum before use. 0.0150 M aqueous solutions (250 μL) of sodium or potassium picrates were mixed thoroughly with 0.0150 M solution of the host in CHCl_3 (250 μL) into an Eppendorf vial, using a Vortex mixer, for 5 min

⁸⁸. Bhatnagar, M.; Awasthy, A.; Sharma, U. *Main Group Met. Chem.* **2004**, *27*, 163–168.

and then centrifuged (14000 rpm). An aliquot of 50 μL of the aqueous phase was diluted with CH_3CN up to 5.0 mL. Successively 200 μL of this solution was diluted with CH_3CN up to 5.0 mL. Successively 200 μL of the latter solution was diluted with CH_3CN up to 1.0 mL. The absorbance of each sample was then measured against the appropriate blank solution at 380 nm at 25 $^\circ\text{C}$. R , K_e , K_a and ΔG° were thus calculated in the proper way.³⁷

2.7.8 Computational details for compound 98

Density functional calculations were performed on all the systems with the Gaussian09 set of programs.⁸⁹ BP86 was used as a functional and gradient corrections were taken from the works of Becke^{88,90} and Perdew.^{89,91} The electronic configuration of the molecular systems was described by the split-valence basis set with polarization functions of Ahlrichs and co-worker (standard SVP basis set in Gaussian09), for H, C, N, and O.^{90,92} Minimum free-energy structures were characterized by the presence of zero imaginary frequency.

Cartesian coordinates of the cycloptoid 98 structure

80

O	2.673041	-3.187140	-1.264518
O	-0.867981	-1.805740	0.718647
O	-2.672681	3.187240	-1.263528
O	0.867747	1.805730	0.718424
N	1.749164	-0.057603	-0.286051
N	-0.478008	2.652486	-1.525094

⁸⁹ M. J. Frisch, G. W. Trucks, H. B. Schlegel, G. E. Scuseria, M. A. Robb, J. R. Cheeseman, G. Scalmani, V. Barone, B. Mennucci, G. A. Petersson, H. Nakatsuji, M. Caricato, X. Li, H. P. Hratchian, A. F. Izmaylov, J. Bloino, G. Zheng, J. L. Sonnenberg, M. Hada, M. Ehara, K. Toyota, R. Fukuda, J. Hasegawa, M. Ishida, T. Nakajima, Y. Honda, O. Kitao, H. Nakai, T. Vreven, J. A. Montgomery J. E. Peralta, F. Ogliaro, M. Bearpark, J. J. Heyd, E. N. Brothers, K. Kudin, V. N. Staroverov, R. Kobayashi, J. Normand, K. Raghavachari, A. Rendell, J. C. Burant, S. S. Iyengar, J. Tomasi, M. Cossi, N. Rega, J. M. Millam, M. Klene, J. E. Knox, J. B. Cross, V. Bakken, C. Adamo, J. Jaramillo, R. Gomperts, R. E. Stratmann, O. Yazyev, A. J. Austin, R. Cammi, C. Pomelli, J. W. Ochterski, R. L. Martin, K. Morokuma, V. G. Zakrzewski, G. A. Voth, P. Salvador, J. J. Dannenberg, S. Dapprich, A. D. Daniels, Ó Farkas, J. B. Foresman, J. V. Ortiz, J. Cioslowski, D. J. Fox, Gaussian 09, Revision A.02, Gaussian, Inc., Wallingford, CT, 2009.

⁹⁰ Becke, A. *Phys. Rev. A* **1988**, *38*, 3098–3100.

⁹¹ J. P. Perdew, *Phys. Rev. B* **1986**, *33*, 8822–8824.

⁹² A. Schaefer, H. Horn, R. Ahlrichs, *J. Chem. Phys.* **1992**, *97*, 2571–2577.

N	-1.749160	0.057660	-0.285887
N	0.478201	-2.652385	-1.524640
C	1.801574	-2.321720	-1.399981
C	2.184235	-0.821100	-1.455439
H	3.293316	-0.814996	-1.526116
H	1.792887	-0.360053	-2.381564
C	2.242416	-0.550781	1.022940
H	2.039131	-1.639099	1.072477
H	1.625493	-0.049859	1.790689
C	3.718556	-0.262636	1.243666
C	4.694440	-1.222245	0.913595
H	4.375995	-2.192650	0.494848
C	6.070856	-0.952661	1.095924
C	6.444252	0.302245	1.613299
H	7.516065	0.523492	1.759596
C	5.487094	1.286014	1.953657
C	4.124972	0.988464	1.760896
H	3.355886	1.735741	2.017726
C	7.106348	-2.002462	0.755116
H	8.135018	-1.590589	0.786188
H	6.935458	-2.428628	-0.255739
H	7.064356	-2.853346	1.469653
C	5.926253	2.617731	2.524042
H	5.069081	3.307279	2.657529
H	6.668012	3.118206	1.865430
H	6.413459	2.491997	3.515391
C	1.090544	1.154860	-0.307138
C	0.658645	1.742757	-1.681917
H	0.404089	0.948761	-2.411196
C	1.764143	2.682220	-2.236305
H	1.637058	2.786418	-3.335291
H	2.786414	2.297018	-2.047012
C	1.468793	4.013290	-1.517683
H	1.882314	3.983343	-0.490240
H	1.905231	4.887447	-2.040499
C	-0.067735	4.068340	-1.459559
H	-0.458471	4.537709	-0.534059
H	-0.513236	4.620629	-2.316957
C	-1.801318	2.321826	-1.399685
C	-2.184044	0.821227	-1.455314
H	-3.293118	0.815155	-1.526125
H	-1.792566	0.360192	-2.381387
C	-2.242587	0.550779	1.023066
H	-2.039387	1.639105	1.072636
H	-1.625720	0.049874	1.790870
C	-3.718740	0.262575	1.243616
C	-4.694588	1.222223	0.913528
H	-4.376068	2.192648	0.494894

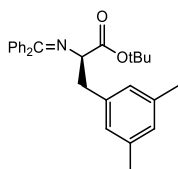
C	-6.071018	0.952645	1.095722
C	-6.444472	-0.302300	1.612969
H	-7.516300	-0.523539	1.759166
C	-5.487357	-1.286108	1.953322
C	-4.125210	-0.988561	1.760711
H	-3.356153	-1.735859	2.017556
C	-7.106476	2.002467	0.754888
H	-6.935740	2.428407	-0.256097
H	-7.064269	2.853508	1.469225
H	-8.135180	1.590698	0.786225
C	-5.926588	-2.617882	2.523525
H	-5.069393	-3.307339	2.657318
H	-6.668040	-3.118424	1.864615
H	-6.414194	-2.492222	3.514687
C	-1.090589	-1.154822	-0.306933
C	-0.658496	-1.742727	-1.681641
H	-0.403912	-0.948759	-2.410937
C	-1.763883	-2.682275	-2.236129
H	-2.786197	-2.297148	-2.046906
H	-1.636706	-2.786444	-3.335107
C	-1.468482	-4.013334	-1.517516
H	-1.904851	-4.887519	-2.040341
H	-1.882015	-3.983404	-0.490078
C	0.068042	-4.068281	-1.459371
H	0.458785	-4.537795	-0.533946
H	0.513611	-4.620379	-2.316856

2.7.9 General procedure for enantioselective catalytic alkylation of *N*-(diphenylmethylene)glycine *t*-butyl ester under phase-transfer conditions (benzylation) with chiral cyclopeptoids.

To a solution of *N*-(diphenylmethylene)glycine *t*-butyl ester **55** (23.6 mg, 0.08 mmol) and chiral catalyst **80** (3.3 mg, 0.004 mmol) in toluene (0.8 mL) under inert atmosphere, benzyl bromide (11.4 μ L, 0.096 mmol) was added. The mixture was degassed under vacuo at low temperature (-78° C) and then left at 0° C. Then degassed 50% aqueous NaOH (0.5 mL) was added. The reaction mixture was stirred at 0° C until disappearance of the starting material was observed by TLC. The suspension was diluted with DCM (4 mL) and water (2.5 mL), and the organic layer was taken. The aqueous layer was extracted other two times with DCM (4 mL \times 2) and the combined organic phases were dried over Na₂SO₄, filtered, and

concentrated in vacuo. Purification of the residue by flash column chromatography on silica gel (petroleum ether–EtOAc: 98:2 → 9:1) afforded the desired product **56a** (17.0 mg, 54% yield) as a colorless oil.

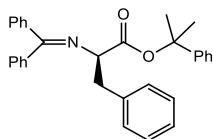
***t*-Butyl (*R*)-*N*-(Diphenylmethylene)-3,5-dimethylphenylalaninate (**56f**)**



20.2 mg, yield 60%, colorless oil; ee 73%, $[\alpha]_{\text{D}}^{30}$: 20.2 ($c = 1.0$, CHCl_3 , 73% ee); $^1\text{H NMR}$ (400 MHz, CDCl_3) δ : 7.55 (d, $J = 7.9$ Hz, 2 H), 7.39-7.23 (m, 6 H), 6.78 (s, 1 H), 6.69- 6.54 (m, 4 H), 4.09 (dd, $J = 9.3, 4.3$ Hz, 1 H), 3.15 (dd, $J = 13.3, 4.3$ Hz, 1 H), 3.07 (dd, $J = 13.3, 9.3$ Hz, 1 H), 2.18 (s, 6 H), 1.45 (s, 9 H); $^{13}\text{C NMR}$ (100 MHz, CDCl_3) δ : 171.0, 170.2, 139.7, 138.1, 137.4, 136.5, 130.0, 128.7, 128.2, 127.9, 127.8, 127.8, 127.7, 127.6, 81.0, 67.9, 39.4, 28.1, 21.1.

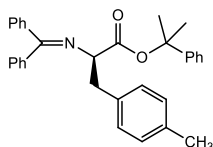
2.7.10 General procedure for enantioselective catalytic alkylation of *N*-(diphenylmethylene)glycine cumyl ester under phase-transfer conditions (benzylation) with chiral cyclopeptoids.

To a solution of *N*-(diphenylmethylene)glycine 1-methyl-1-phenylethyl ester **99c** (178 mg, 0.50 mmol) and cyclopeptoid **80** (9.2 mg, 0.012 mmol) in toluene (5.0 mL) under nitrogen, the alkyl bromide (1.2–3.0 equiv) was added. The mixture was degassed and then cooled to -20 °C. Degassed 50% aqueous KOH (3.0 mL) was then added. The reaction mixture was stirred at -20 °C for 20 h. Then the suspension was diluted with CH_2Cl_2 (25 mL) and H_2O (15 mL), and the organic layer was taken. The aqueous layer was extracted twice with CH_2Cl_2 (25 mL \times 2) and the combined organic phases were dried over Na_2SO_4 , filtered, and concentrated in vacuo. Purification of the residue by flash column chromatography on silica gel (petroleum ether–ethyl acetate: 98:2 to 90:10) afforded the pure alkylated products.

(R)-2-Phenylpropan-2-yl-2-((diphenylmethylene)amino)-3-phenylpropanoate (100c)

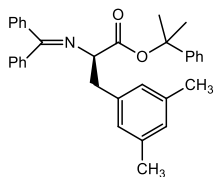
168 mg, yield 75%, colorless oil; ee 93%; the spectroscopic data were in good agreement with the literature.⁷¹ $[\alpha]^{22}_D + 13.4$ ($c = 1.0$, CHCl_3 , 93% ee);

HPLC analysis: Chiralcel OD-H, i-PrOH/hexane = 1/99, 0.5 mL/min, 260 nm, tr (major) = 19.8 min, tr (minor) = 24.7 min; ^1H NMR (400 MHz, CDCl_3) δ 7.61 (m, 2H), 7.46–7.13 (m, 14H), 7.07 (m, 2H), 6.60 (bd, $J = 6.6$ Hz, 2H), 4.20 (dd, $J = 9.3, 4.2$ Hz, 1H), 3.28 (dd, $J = 13.4, 4.2$ Hz, 1H), 3.18 (dd, $J = 13.4, 9.3$ Hz, 1H), 2.30 (s, 3H), 1.80 (s, 3H), 1.75 (s, 3H); ^{13}C NMR (100 MHz, CDCl_3) δ 170.4, 170.0, 145.6, 139.4, 138.3, 136.2, 130.2, 129.9, 128.7, 128.2, 128.2, 128.1, 128.1, 128.0, 127.6, 126.9, 126.2, 124.3, 82.4, 67.9, 39.3, 28.9, 28.3; MS (ESI) $[\text{M} + \text{H}]^+ 462.3$, $[\text{M} + \text{Na}]^+ 484.2$; HRMS (FTICR) $[\text{M} + \text{H}]^+$ calcd for $\text{C}_{31}\text{H}_{30}\text{NO}_2$ 448.2277, found 448.2268.

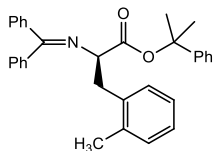
(R)-2-Phenylpropan-2-yl 2-((diphenylmethylene)amino)-3-(4-methylphenyl)propanoate (102a).

173 mg, yield 75%, yellow oil; ee 94%; $[\alpha]^{25}_D + 101.5$ ($c = 1.0$, CHCl_3 , 94% ee);

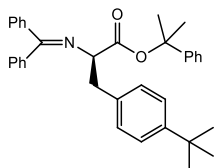
HPLC analysis: Chiralcel OD-H, i-PrOH/hexane = 1/99, 0.5 mL/min, 260 nm, tr (minor) = 13.9 min, tr (major) = 17.0 min; ^1H NMR (400 MHz, CDCl_3) δ 7.61 (m, 2H), 7.44–7.17 (m, 11H), 7.01 (d, $J = 7.9$, 2H), 6.94 (d, $J = 7.9$ Hz, 2H), 6.63 (bd, $J = 6.8$ Hz, 2H), 4.18 (dd, $J = 9.2, 4.3$ Hz, 1H), 3.24 (dd, $J = 13.4, 4.3$ Hz, 1H), 3.13 (dd, $J = 13.4, 9.2$ Hz, 1H), 2.30 (s, 3H), 1.80 (s, 3H), 1.74 (s, 3H); ^{13}C NMR (100 MHz, CDCl_3) δ 170.2, 170.0, 145.7, 139.5, 136.3, 135.6, 135.1, 130.1, 129.7, 128.7, 128.7, 128.2, 128.2, 128.1, 127.9, 127.7, 126.9, 124.3, 82.3, 68.0, 38.9, 28.9, 28.3, 21.0; MS (ESI) $[\text{M} + \text{H}]^+ 462.3$, $[\text{M} + \text{Na}]^+ 484.2$; HRMS (FTICR) $[\text{M} + \text{H}]^+$ calcd for $\text{C}_{32}\text{H}_{32}\text{NO}_2$ 462.2433, found 462.2440.

(R)-2-Phenylpropan-2-yl 2-((diphenylmethylene)amino)-3-(3,5-dimethylphenyl)propanoate (102b).

195 mg, yield 82%, colorless oil; ee 89%; $[\alpha]^{20}_D + 97.9$ ($c = 0.9$, CHCl_3 , 89% ee); HPLC analysis: Chiralcel OD-H, $i\text{-PrOH/hexane} = 1/99$, 0.5 mL/min, 260 nm, tr (minor) = 14.2 min, tr (major) = 19.5 min; $^1\text{H NMR}$ (400 MHz, CDCl_3) δ 7.59 (m, 2H), 7.42–7.14 (m, 11H), 6.80 (s, 1H), 6.66 (s, 2H), 6.61 (bd, $J = 6.8$ Hz, 2H), 4.18 (dd, $J = 9.2, 4.2$ Hz, 1H), 3.21 (dd, $J = 13.3, 4.2$ Hz, 1H), 3.09 (dd, $J = 13.3, 9.2$ Hz, 1H), 2.19 (s, 6H), 1.80 (s, 3H), 1.76 (s, 3H); $^{13}\text{C NMR}$ (100 MHz, CDCl_3) δ 170.3, 170.1, 145.7, 139.6, 137.9, 137.4, 136.3, 130.0, 128.7, 128.2, 128.2, 127.9, 127.9, 127.8, 127.7, 127.7, 126.9, 124.3, 82.3, 67.8, 39.1, 28.9, 28.3, 21.1; MS (ESI) $[\text{M} + \text{H}]^+$ 476.4; HRMS (FTICR) $[\text{M} + \text{H}]^+$ calcd for $\text{C}_{33}\text{H}_{34}\text{NO}_2$ 476.2590, found 476.2580.

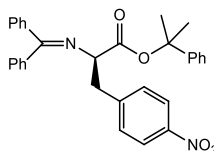
(R)-2-Phenylpropan-2-yl 2-((diphenylmethylene)amino)-3-(2-methylphenyl)propanoate (102c).

205 mg, yield 89%, yellow oil; ee 96%; $[\alpha]^{22}_D + 111.4$ ($c = 1.0$, CHCl_3 , 96% ee); HPLC analysis: Chiralcel OD-H, $i\text{-PrOH/hexane} = 1/99$, 0.5 mL/min, 260 nm, tr (major) = 20.8 min, tr (minor) = 24.1 min; $^1\text{H NMR}$ (400 MHz, CDCl_3) δ 7.63 (m, 2H), 7.43–7.19 (m, 11H), 7.14–6.98 (m, 4H), 6.49 (m, 2H), 4.23 (m, 1H), 3.32 (m, 1H), 3.20 (m, 1H), 2.08 (s, 3H), 1.83 (s, 3H), 1.77 (s, 3H); $^{13}\text{C NMR}$ (100 MHz, CDCl_3) δ 170.2, 170.2, 145.7, 139.2, 136.9, 136.3, 136.1, 131.0, 130.1, 130.0, 128.7, 128.2, 128.1, 128.0, 127.9, 127.7, 127.0, 126.4, 125.6, 124.3, 82.4, 66.5, 36.4, 29.0, 28.3, 19.3; MS (ESI) $[\text{M} + \text{H}]^+$ 462.1, $[\text{M} + \text{Na}]^+$ 484.1; HRMS (FTICR) $[\text{M} + \text{H}]^+$ calcd for $\text{C}_{32}\text{H}_{32}\text{NO}_2$ 462.2433, found 462.2431.

(R)-2-Phenylpropan-2-yl 2-((diphenylmethylene)amino)-3-(4-*t*-butylphenyl)propanoate (102d).

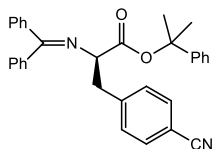
86 mg, yield 74%, yellow oil; $[\alpha]^{22}_D + 38.2$ ($c = 1.0$, CHCl_3 , 88% ee);

HPLC analysis: Chiralcel OD-H, *i*-PrOH/hexane = 1/99, 0.5 mL/min, 260 nm, tr (minor) = 11.3 min, tr (major) = 14.1 min; $^1\text{H NMR}$ (400 MHz, CDCl_3) δ 7.63 (m, 2H), 7.44–7.17 (m, 13H), 6.98 (d, $J = 8.1$ Hz, 2H), 6.52 (m, 2H), 4.16 (dd, $J = 9.3, 4.0$ Hz, 1H), 3.25 (dd, $J = 13.4, 4.0$ Hz, 1H), 3.13 (dd, $J = 13.4, 9.3$ Hz, 1H), 1.80 (s, 3H), 1.75 (s, 3H), 1.31 (s, 9H); $^{13}\text{C NMR}$ (100 MHz, CDCl_3) δ 170.2, 170.1, 149.1, 145.7, 139.5, 136.2, 135.2, 130.1, 129.5, 128.7, 128.2, 128.2, 128.0, 128.0, 127.6, 126.9, 125.0, 124.3, 82.3, 68.1, 38.7, 34.4, 31.4, 28.9, 28.3; MS (ESI) $[\text{M} + \text{H}]^+ 504.2$, $[\text{M} + \text{Na}]^+ 526.2$; HRMS (FTICR) $[\text{M} + \text{H}]^+$ calcd for $\text{C}_{35}\text{H}_{38}\text{NO}_2$ 504.2903, found 504.2910.

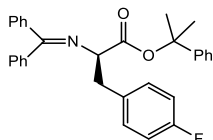
(R)-2-Phenylpropan-2-yl 2-((diphenylmethylene)amino)-3-(4-nitrophenyl)propanoate (102e).

219 mg, yield 89%, yellow oil; ee 89%; $[\alpha]^{25}_D + 170.7$ ($c = 1.0$, CHCl_3 , 89% ee);

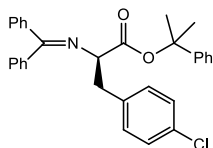
HPLC analysis: Chiralcel OD-H, *i*-PrOH/hexane = 1/99, 1.0 mL/min, 260 nm, tr (minor) = 16.6 min, tr (major) = 35.4 min; $^1\text{H NMR}$ (400 MHz, CDCl_3) δ 8.07 (m, 2H), 7.61 (m, 2H), 7.45–7.21 (m, 13H), 6.70 (bd, $J = 7.0$ Hz, 2H), 4.26 (dd, $J = 8.7, 4.5$ Hz, 1H), 3.35 (dd, $J = 13.4, 4.5$ Hz, 1H), 3.29 (dd, $J = 13.4, 8.7$ Hz, 1H), 1.80 (s, 3H), 1.76 (s, 3H); $^{13}\text{C NMR}$ (100 MHz, CDCl_3) δ 171.0, 169.2, 146.6, 146.3, 145.2, 138.9, 135.8, 130.6, 130.5, 128.6, 128.6, 128.3, 128.2, 128.1, 127.4, 127.1, 124.2, 123.2, 82.8, 66.9, 39.1, 28.8, 28.2; MS (ESI) $[\text{M} + \text{H}]^+ 493.1$, $[\text{M} + \text{Na}]^+ 515.0$; HRMS (FTICR) $[\text{M} + \text{H}]^+$ calcd for $\text{C}_{31}\text{H}_{29}\text{N}_2\text{O}_4$ 493.2127, found 493.2138.

(R)-2-Phenylpropan-2-yl 2-((diphenylmethylene)amino)-3-(4-cyanophenyl)propanoate (102f).

189 mg, yield 80%, yellow oil; ee 93%; $[\alpha]^{20}_{\text{D}} + 50.8$ ($c = 0.9$, CHCl_3 , 93% ee); HPLC analysis: Chiralcel OD-H, *i*-PrOH/hexane = 1/99, 1.0 mL/min, 260 nm, tr (minor) = 18.4 min, tr (major) = 30.7 min; $^1\text{H NMR}$ (400 MHz, CDCl_3) δ 7.60 (m, 2H), 7.49 (m, 2H), 7.45–7.21 (m, 11H), 7.18 (m, 2H), 6.66 (bd, $J = 6.8$ Hz, 2H), 4.21 (dd, $J = 8.9, 4.4$ Hz, 1H), 3.30 (dd, $J = 13.4, 4.4$ Hz, 1H), 3.23 (dd, $J = 13.4, 8.9$ Hz, 1H), 1.79 (s, 3H), 1.75 (s, 3H); $^{13}\text{C NMR}$ (100 MHz, CDCl_3) δ 170.9, 169.3, 145.3, 144.2, 139.0, 135.9, 131.8, 130.7, 130.5, 128.7, 128.6, 128.3, 128.2, 128.1, 127.5, 127.1, 124.2, 119.0, 110.1, 82.8, 67.0, 39.3, 28.8, 28.2; MS (ESI) $[\text{M} + \text{H}]^+$ 473.2, $[\text{M} + \text{Na}]^+$ 495.2; HRMS (FTICR) $[\text{M} + \text{H}]^+$ calcd for $\text{C}_{32}\text{H}_{29}\text{N}_2\text{O}_2$ 473.2229, found 473.2240.

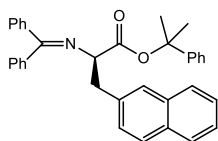
(R)-2-Phenylpropan-2-yl 2-((diphenylmethylene)amino)-3-(4-fluorophenyl)propanoate (102g).

175 mg, yield 75%, yellow oil; ee 91%; $[\alpha]^{25}_{\text{D}} + 170.9$ ($c = 0.8$, CHCl_3 , 91% ee); HPLC analysis: Chiralcel OD-H, *i*-PrOH/hexane = 1/99, 0.5 mL/min, 260 nm, tr (minor) = 13.9 min, tr (major) = 20.5 min; $^1\text{H NMR}$ (400 MHz, CDCl_3) δ 7.61 (m, 2H), 7.43–7.19 (m, 11H), 7.02 (m, 2H), 6.89 (m, 2H), 6.65 (bd, $J = 6.6$ Hz, 2H), 4.17 (dd, $J = 9.2, 4.2$ Hz, 1H), 3.24 (dd, $J = 13.5, 4.2$ Hz, 1H), 3.15 (dd, $J = 13.5, 9.2$ Hz, 1H), 1.79 (s, 3H), 1.75 (s, 3H); $^{13}\text{C NMR}$ (100 MHz, CDCl_3) δ 170.5, 170.0, 161.5 (d, $J = 244$ Hz), 145.5, 139.3, 136.1, 134.0 (d, $J = 2$ Hz), 131.3 (d, $J = 8$ Hz), 130.3, 128.7, 128.3, 128.2, 128.2, 128.0, 127.6, 127.0, 124.3, 114.8 (d, $J = 21$ Hz), 82.5, 67.8, 38.4, 28.8, 28.3; MS (ESI) $[\text{M} + \text{H}]^+$ 466.2, $[\text{M} + \text{Na}]^+$ 488.2; HRMS (FTICR) $[\text{M} + \text{H}]^+$ calcd for $\text{C}_{31}\text{H}_{29}\text{FO}_2$ 466.2182, found 466.2174.

(R)-2-Phenylpropan-2-yl 2-((diphenylmethylene)amino)-3-(4-chlorophenyl)propanoate (102h).

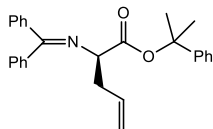
210 mg, yield 87%, yellow oil; ee 94%; $[\alpha]^{22}_{\text{D}} + 109.2$ ($c = 1.0$, CHCl_3 , 94% ee);

HPLC analysis: Chiralcel OD-H, $i\text{-PrOH/hexane} = 1/99$, 0.5 mL/min, 260 nm, tr (minor) = 14.8 min, tr (major) = 23.6 min; $^1\text{H NMR}$ (400 MHz, CDCl_3) δ 7.62 (m, 2H), 7.44–7.21 (m, 11H), 7.18 (d, $J = 8.3$ Hz, 2H), 7.01 (d, $J = 8.3$ Hz, 2H), 6.67 (bd, $J = 6.5$ Hz, 2H), 4.19 (dd, $J = 9.2, 4.2$ Hz, 1H), 3.24 (dd, $J = 13.4, 4.2$ Hz, 1H), 3.15 (dd, $J = 13.4, 9.2$ Hz, 1H), 1.80 (s, 3H), 1.76 (s, 3H); $^{13}\text{C NMR}$ (100 MHz, CDCl_3) δ 170.6, 169.7, 145.5, 139.2, 136.8, 136.1, 132.0, 131.2, 130.3, 128.7, 128.4, 128.2, 128.2, 128.2, 128.0, 127.6, 127.0, 124.3, 82.5, 67.6, 38.6, 28.9, 28.3; MS (ESI) $[\text{M} + \text{Na}]^+$ 504.1; HRMS (FTICR) $[\text{M} + \text{H}]^+$ calcd for $\text{C}_{31}\text{H}_{29}\text{ClNO}_2$ 482.1887, found 482.1878.

(R)-2-Phenylpropan-2-yl 2-((diphenylmethylene)amino)-3-(2-naphthyl)propanoate (102i).

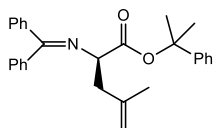
241 mg, yield 97%, colorless oil; ee 95%; $[\alpha]^{22}_{\text{D}} + 50.7$ ($c = 1.0$, CHCl_3 , 95% ee);

HPLC analysis: Chiralcel OD-H, $i\text{-PrOH/hexane} = 1/99$, 0.5 mL/min, 260 nm, tr (minor) = 20.1 min, tr (major) = 29.8 min; $^1\text{H NMR}$ (400 MHz, CDCl_3) δ 7.78 (m, 1H), 7.67 (m, 2H), 7.59 (m, 2H), 7.52 (s, 1H), 7.46–7.12 (m, 14H), 6.53 (m, 2H), 4.33 (dd, $J = 9.2, 4.3$ Hz, 1H), 3.45 (dd, $J = 13.5, 4.3$ Hz, 1H), 3.33 (dd, $J = 13.5, 9.2$ Hz, 1H), 1.80 (s, 3H), 1.76 (s, 3H); $^{13}\text{C NMR}$ (100 MHz, CDCl_3) δ 170.5, 170.0, 145.6, 139.4, 136.1, 135.8, 133.4, 132.1, 130.1, 128.7, 128.3, 128.2, 128.2, 128.0, 127.9, 127.6, 127.5, 127.5, 126.9, 125.8, 125.2, 124.3, 82.4, 67.8, 39.4, 28.9, 28.3; MS (ESI) $[\text{M} + \text{H}]^+$ 498.2; HRMS (FTICR) $[\text{M} + \text{H}]^+$ calcd for $\text{C}_{35}\text{H}_{32}\text{NO}_2$ 498.2433, found 498.2423.

(R)-2-Phenylpropan-2-yl-2-((diphenylmethylene)amino)pent-4-enoate**(102j).**

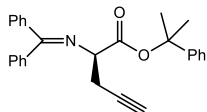
179 mg, yield 90%, yellow oil; ee 93%; the spectroscopic data were in good agreement with the literature.⁶⁷ $[\alpha]^{22}_D + 5.7$ ($c = 0.9$, CHCl_3 , 93% ee);

HPLC analysis: Chiralcel OD-H, *i*-PrOH/hexane = 1/99, 0.5 mL/min, 260 nm, tr (minor) = 11.1 min, tr (major) = 12.7 min; ^1H NMR (400 MHz, CDCl_3) δ 7.67 (m, 2H), 7.48–7.20 (m, 11H), 7.16 (m, 2H), 5.74 (m, 1H), 5.09 (m, 1H), 5.04 (m, 1H), 4.10 (dd, $J = 7.8, 5.1$ Hz, 1H), 2.78–2.60 (m, 2H), 1.80 (s, 3H), 1.75 (s, 3H); ^{13}C NMR (100 MHz, CDCl_3) δ 170.2, 170.0, 145.7, 139.6, 136.5, 134.6, 130.2, 128.8, 128.5, 128.4, 128.2, 128.0, 127.9, 126.9, 124.3, 117.4, 82.3, 65.8, 37.8, 28.9, 28.3; MS (ESI) $[\text{M} + \text{H}]^+ 398.5$; HRMS (FTICR) $[\text{M} + \text{H}]^+$ calcd for $\text{C}_{27}\text{H}_{28}\text{NO}_2$ 398.2120, found 398.2115.

(R)-2-Phenylpropan-2-yl-2-((diphenylmethylene)amino)-4-methyl-pent-4-enoate (102k).

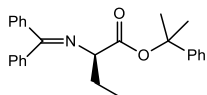
191 mg, yield 93%, colorless oil; ee 86%; $[\alpha]^{22}_D + 66.9$ ($c = 1.0$, CHCl_3 , 86% ee);

HPLC analysis: Chiralcel OD-H, *i*-PrOH/hexane = 1/99, 0.5 mL/min, 260 nm, tr (minor) = 10.2 min, tr (major) = 14.2 min; ^1H NMR (400 MHz, CDCl_3) δ 7.67 (m, 2H), 7.48–7.20 (m, 11H), 7.16 (m, 2H), 4.77 (m, 1H), 4.74 (m, 1H), 4.18 (dd, $J = 8.5, 4.9$ Hz, 1H), 2.70 (dd, $J = 13.5, 4.9$ Hz, 1H), 2.62 (dd, $J = 13.5, 8.5$ Hz, 1H), 1.81 (s, 3H), 1.77 (s, 3H), 1.54 (s, 3H); ^{13}C NMR (100 MHz, CDCl_3) δ 170.3, 170.0, 145.7, 141.8, 139.7, 136.3, 130.2, 128.8, 128.5, 128.3, 128.2, 128.1, 128.0, 126.9, 124.3, 113.4, 82.3, 64.8, 41.5, 28.9, 28.3, 22.7; MS (ESI) $[\text{M} + \text{Na}]^+ 434.3$; HRMS (FTICR) $[\text{M} + \text{H}]^+$ calcd for $\text{C}_{28}\text{H}_{30}\text{NO}_2$ 412.2277, found 412.2288.

(R)-2-Phenylpropan-2-yl-2-((diphenylmethylene)amino)pent-4-ynoate**(102l).**

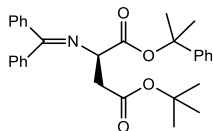
180 mg, yield 91%, colorless oil; ee 83%; the spectroscopic data were in good agreement with the literature.⁶⁷ $[\alpha]^{22}_D + 25.4$ ($c = 1.0$, CHCl_3 , 83% ee);

HPLC analysis: Chiralcel OD-H, *i*-PrOH/hexane = 1/99, 0.5 mL/min, 260 nm, tr (minor) = 17.3 min, tr (major) = 18.6 min; $^1\text{H NMR}$ (400 MHz, CDCl_3) δ 7.69 (m, 2H), 7.48–7.19 (m, 13H), 4.27 (dd, $J = 8.1, 5.1$ Hz, 1H), 2.90–2.72 (m, 2H), 1.97 (t, $J = 2.4$ Hz, 1H), 1.79 (s, 3H), 1.75 (s, 3H); $^{13}\text{C NMR}$ (100 MHz, CDCl_3) δ : 171.6, 168.8, 145.4, 139.5, 136.1, 130.4, 128.9, 128.7, 128.4, 128.2, 128.2, 128.0, 127.0, 124.3, 82.8, 81.2, 70.2, 64.7, 28.8, 28.2, 23.2; MS (ESI) $[\text{M} + \text{Na}]^+$ 418.3; HRMS (FTICR) $[\text{M} + \text{H}]^+$ calcd for $\text{C}_{27}\text{H}_{26}\text{NO}_2$ 396.1964, found 396.1955.

(R)-2-Phenylpropan-2-yl-2-((diphenylmethylene)amino)-butanoate (102m).

166 mg, yield 86%, colorless oil; ee 86%; the spectroscopic data were in good agreement with the literature.⁷¹ $[\alpha]^{22}_D + 33.1$ ($c = 1.0$, CHCl_3 , 86% ee);

HPLC analysis: Chiralcel OD-H, *i*-PrOH/hexane = 1/99, 0.5 mL/min, 260 nm, tr (minor) = 11.5 min, tr (major) = 12.9 min; $^1\text{H NMR}$ (400 MHz, CDCl_3) δ 7.67 (m, 2H), 7.47–7.19 (m, 11H), 7.15 (m, 2H), 3.94 (dd, $J = 7.9, 5.0$ Hz, 1H), 2.03–1.86 (m, 2H), 1.79 (s, 3H), 1.75 (s, 3H), 0.87 (t, $J = 7.5$ Hz, 3H); $^{13}\text{C NMR}$ (100 MHz, CDCl_3) δ 170.9, 170.3, 146.1, 139.9, 136.9, 130.4, 129.0, 128.7, 128.7, 128.4, 128.3, 128.2, 127.2, 124.6, 82.3, 67.6, 29.1, 28.6, 26.9, 10.9; MS (ESI) $[\text{M} + \text{H}]^+$ 386.3; HRMS (FTICR) $[\text{M} + \text{H}]^+$ calcd for $\text{C}_{26}\text{H}_{28}\text{NO}_2$ 386.2120, found 386.2114.

(R)-2-Phenylpropan-2-yl 3-(carbo-*t*-butoxy) - 2 - ((diphenylmethylene)amino)propanoate (102n).

196 mg, yield 86%, colorless oil; ee 92%; $[\alpha]_{\text{D}}^{19} + 40.4$ ($c = 1.0$, CHCl_3 , 92% ee); HPLC analysis: Chiralcel OD-H, *i*-PrOH/hexane = 1/99, 0.5 mL/min, 260 nm, t_{r} (minor) = 18.7 min, t_{r} (major) = 21.9 min; $^1\text{H NMR}$ (600 MHz, CDCl_3) δ 7.63 (m, 2H), 7.48–7.12 (m, 13H), 4.47 (dd, $J = 7.7, 5.8$ Hz, 1H), 2.98 (dd, $J = 15.8, 5.8$ Hz, 1H), 2.78 (dd, $J = 15.8, 7.7$ Hz, 1H), 1.78 (s, 3H), 1.72 (s, 3H), 1.39 (s, 9H); $^{13}\text{C NMR}$ (150 MHz, CDCl_3) δ 171.3, 170.3, 169.3, 145.5, 139.6, 136.2, 130.3, 128.8, 128.7, 128.3, 128.2, 128.0, 127.9, 126.9, 124.3, 82.6, 80.6, 62.8, 39.4, 28.9, 28.1, 28.0; MS (ESI) $[\text{M} + \text{Na}]^+$ 494.5; HRMS (FTICR) $[\text{M} + \text{H}]^+$ calcd for $\text{C}_{26}\text{H}_{28}\text{NO}_2$ 472.2482, found 472.2501.

2.7.11 General procedure for enantioselective catalytic alkylation of *N*-(diphenylmethylene)glycine *t*-butyl ester under phase-transfer conditions (benzylation) with chiral calixarenes.

To a solution of *N*-(diphenylmethylene)glycine *t*-butyl ester (**55**) (23.6 mg, 0.08 mmol) and chiral catalyst (**107**) (4.6 mg, 0.004 mmol) in mesitylene (0.8 mL) under inert atmosphere, benzyl bromide (11.4 μL , 0.096 mmol) was added. The mixture was degassed under vacuo at low temperature (-78°C) and then left at 0°C . Then degassed 50% aqueous NaOH (0.5 mL) was added. The reaction mixture was stirred at 0°C until disappearance of the starting material was observed by TLC. The suspension was diluted with DCM (4 mL) and water (2.5 mL), and the organic layer was taken. The aqueous layer was extracted other two time with DCM (4 mL \times 2) and the combined organic phases were dried over Na_2SO_4 , filtered, and concentrated *in vacuo*. Purification of the residue by flash column chromatography on silica gel (petroleum ether–EtOAc: 98:2 \rightarrow 9:1) afforded the desired product (**56a**) (26.4 mg, 86% yield) as a colorless oil.

2.8 Synthesis of 2-aryl-2-oxazoline-4-carboxylic acid esters

2-Aryl-2-oxazoline-4-carboxylic acid esters **115**,^{81a} **116**,⁹³ **117**,⁹⁴ **131**,⁸⁴ **132**,⁸⁴ and **133**⁸⁴ were synthesized as described in literature. Previously undescribed substrates **118**, **119**, **129** and **130** were prepared as described below.

2.8.1 Synthesis of (S)-2-Phenyl-2-oxazoline-4-carboxylic acid cumyl ester (**118**)

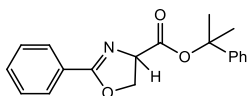
To a solution of (S)-2-phenyl-2-oxazoline-4-carboxylic acid (112 mg, 0.59 mmol) in dry DCM (2.5 mL) under nitrogen atmosphere 1-methyl-1-phenylethyl 2,2,2-trichloroacetimidate (0.17 mg, 0.59 mmol) was added. The reaction mixture was stirred for 65 h, diluted with DCM (2 mL), and centrifuged for two times. The recovered organic phase was concentrated in vacuo. The residue was purified by column chromatography (silica gel, petroleum ether–ethyl acetate: 100:0 to 98:2); to afford **118**.

2.8.2 Synthesis of (S)-2-Phenyl-2-oxazoline-4-carboxylic acid benzhydryl ester (**119**)

To a solution of (S)-2-Phenyl-2-oxazoline-4-carboxylic acid (212 mg, 1.11 mmol) and benzophenone hydrazone (327 mg, 1.67 mmol) in DCM (3.4 mL) a solution of iodine in DCM [0.15 mL, 1% (w/v)] was added. The mixture was cooled to -10 °C and $\text{PhI}(\text{OAc})_2$ (536 mg, 1.66 mmol) was added portionwise over a period of 30 min. Then the reaction mixture was warmed to room temperature and stirred for 22 h. The solvent was evaporated under reduced pressure and the residue was dissolved in EtOAc (20 mL). The organic phase was washed with H_2O (1 x 10 mL), 5% NaHCO_3 -solution (3 x 10 mL), H_2O (1 x 20 mL) and brine (1 x 10 mL), dried over Na_2SO_4 and concentrated in vacuo. The residue was purified by column chromatography (silica gel, petroleum ether–ethyl acetate: 98:2 to 80:20); to afford **119**.

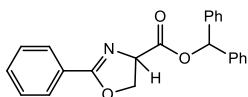
⁹³. A. Laaziri, J. Uziel, S. Jugé, *Tetrahedron: Asymmetry* **1998**, 9, 437.

⁹⁴. F. Meyer, A. Laaziri, A. M. Papini, J. Uziel, S. Jugé, *Tetrahedron: Asymmetry* **2003**, 14, 2229.

(S)-2-Phenyl-2-oxazoline-4-carboxylic acid cumyl ester (118)

66 mg, 40% yield, white solid: mp = 117-120 °C. R_f = 0.41 (petroleum ether–ethyl acetate: 8:2); $[\alpha]_D^{25}$: +8.7 (c = 1.0, CHCl₃);

¹H-NMR (400 MHz, CDCl₃) δ : 8.00 (m, 2H, PhH), 7.50 (m, 1H, PhH), 7.42-7.40 (m, 4H, PhH), 7.32 (m, 2H, PhH), 7.25-7.23 (m, 1H, PhH), 4.92 (dd, J = 10.4, 7.7 Hz, 1H, CHN), 4.63 (br t, J = 8.0 Hz, 1H, CHHO), 4.55 (dd, J = 10.4, 9.1 Hz, 1H, CHHO), 1.85 (s, 3H, OC(CH₃)₂Ph), 1.84 (s, 3H, OC(CH₃)₂Ph); ¹³C NMR (100 MHz, CDCl₃) δ : 169.5, 166.1, 145.2, 131.7, 128.6 (\times 2), 128.3 (\times 4), 127.2, 127.1, 124.3 (\times 2), 83.2, 69.5, 69.3, 28.7, 28.5; HRMS (MALDI) m/z [M + H]⁺ 310.1438 calcd for C₁₉H₂₀NO₃⁺; found 310.1435.

(S)-2-Phenyl-2-oxazoline-4-carboxylic acid benzhydryl ester (119)

113 mg, 29% yield, yellow solid: mp = 124-126 °C. R_f = 0.32 (petroleum ether–ethyl acetate: 9:1); $[\alpha]_D^{25}$: +43.8 (c=1.0, CHCl₃).

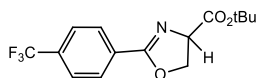
¹H-NMR (400 MHz, CDCl₃) δ : 8.00 (m, 2H, PhH), 7.51 (m, 1H, PhH), 7.45-7.26 (m, 12H, PhH), 6.98 (s, 1H, OCHPh₂), 5.06 (dd, J = 10.4, 7.7 Hz, 1H, CHCO), 4.67 (br t, J = 8.6 Hz, 1H, CHHO), 4.60 (dd, J = 10.4, 8.6 Hz, 1H, CHHO); ¹³C-NMR (100 MHz, CDCl₃) δ : 170.1, 166.4, 139.6 (\times 2), 131.8 (\times 2), 128.6 (\times 4), 128.5 (\times 2), 128.3 (\times 2), 128.1, 127.9, 127.3 (\times 2), 126.9 (\times 2), 77.9, 69.5, 68.8; HRMS (MALDI) m/z [M + Na]⁺ calcd for C₂₃H₁₉NNaO₃⁺ 380.1257; found 380.1256.

2.8.3 Synthesis of 2-(4-Trifluoromethylphenyl)-2-oxazoline-4-carboxylic acid *t*-butyl ester (129)

To a solution of 4-(trifluoromethyl)benzoic acid (200 mg, 1.01 mmol) in DCM (7 mL) serine-*t*-butyl ester hydrochloride (200 mg 1.01 mmol), EDC (232 mg, 1.21

mmol), HOBT (163 mg, 1.21 mmol) and triethylamine (307 mg, 3.04 mmol) were added. The mixture was stirred at room temperature overnight, then diluted with DCM (20 mL) and washed with water (10 mL X 2). The organic layer was dried over MgSO_4 filtered and concentrated in vacuo to afford 2-((4-trifluoromethyl)benzoyl)-amino)-3-hydroxypropionic acid *t*-butyl ester (793.5 mg, 89% yield) as a yellow amorphous solid; $R_f = 0.44$ petroleum ether–ethyl acetate: 7:3). This compound was used without further purification. The 2-((4-trifluoromethyl)benzoyl)-amino)-3-hydroxypropionic acid *t*-butyl ester (286 mg, 0.85 mmol) was dissolved in dry DCM (4 mL), and cooled to -78°C . DAST (208 mg, 1.28 mmol) was added and the solution was stirred overnight. The reaction mixture was diluted with 20 mL of DCM, poured into 5 mL of saturated NaHCO_3 aqueous solution and the resulting mixture was stirred at room temperature for 0.5 h. The organic layer was recovered and washed with water (10 mL), dried over MgSO_4 , filtered and concentrated in vacuo. The residue was purified by column chromatography (silica gel, petroleum ether–ethyl acetate: 95:5 to 80:20); to afford **129**.

2-(4-Trifluoromethylphenyl)-2-oxazoline-4-carboxylic acid *t*-butyl ester (129)

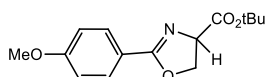


210.6 mg, 78% yield in two steps; white solid; mp= 80-81 $^\circ\text{C}$; $R_f = 0.57$ (petroleum ether–ethyl acetate: 8:2); $[\alpha]_D^{26}$: +70.7 ($c = 1.0$, CHCl_3); $^1\text{H-NMR}$ (400 MHz, CDCl_3) δ : 8.06 (d, $J = 8.2$ Hz, 2H, ArH), 7.63 (d, $J = 8.2$ Hz, 2H, ArH), 4.83 (dd, $J = 10.4, 8.0$ Hz, 1H, CHCO), 4.58 (m, 2H, CH_2O), 1.47 (s, 9H, $\text{COOC}(\text{CH}_2)_3$); $^{13}\text{C-NMR}$ (100 MHz, CDCl_3) δ : 170.0, 164.7, 133.2 (q, $J = 32.3$ Hz), 130.4, 128.9 ($\times 2$), 125.2, 125.1, 123.6 (q, $J = 270.7$ Hz), 82.3, 70.0, 69.4, 27.8 ($\times 3$); HRMS (MALDI): m/z $[\text{M} + \text{H}]^+$ calcd for $\text{C}_{15}\text{H}_{17}\text{F}_3\text{NO}_3^+$ 316.1155; found 316.1154.

2.8.4 Synthesis of (S)-2-(4-Methoxyphenyl)-2-oxazoline-4-carboxylic acid *t*-butyl ester (**130**)

The synthetic strategy was the same described for compound **129**, starting from a solution of 4-methoxybenzoic acid to afford (S)-2-((4-methoxybenzoyl)-amino))-3-hydroxypropionic acid *t*-butyl ester (198.5 mg, 66% yield) as a yellow oil. This compound was used without further purification as described above, affording **130**.

(S)-2-(4-Methoxyphenyl)-2-oxazoline-4-carboxylic acid *t*-butyl ester (**130**)



134 mg, 72% yield, white solid; mp= 70-71 °C. $R_f = 0.35$ (petroleum ether–ethyl acetate: 8:2); $[\alpha]_D^{26}$: +82.3 ($c = 1.0$, CHCl_3).

$^1\text{H-NMR}$ (400 MHz, CDCl_3) δ : 7.91 (d, $J = 8.8$ Hz, 2H, ArH), 6.89 (d, $J = 8.8$ Hz, 2H, ArH), 4.78 (dd, $J = 10.0, 8.2$ Hz, 1H, CHCO), 4.53 (m, 2H, CH_2O), 3.82 (s, 3H, ArOCH_3), 1.49 (s, 9H, $\text{COOC}(\text{CH}_3)_3$); $^{13}\text{C-NMR}$ (100 MHz, CDCl_3) δ : 170.6, 165.8, 162.3, 130.3 (x 2), 119.6, 113.6 (x 2), 82.0, 69.6, 63.3, 55.3, 27.9 (x 3); HRMS (MALDI) m/z $[\text{M} + \text{H}]^+$ calcd for $\text{C}_{15}\text{H}_{20}\text{NO}_4^+$ 278.1387; found 278.1386.

2.8.5 General procedure for the Phase-Transfer Enantioselective Catalytic Alkylation of 2-aryl-2-oxazoline-4-carboxylic acid esters

To a solution of 2-(4-Trifluoromethylphenyl)-2-oxazoline-4-carboxylic acid *t*-butyl ester (**129**) (158 mg, 0.50 mmol) and cyclopeptoid (**84**) (20.6 mg, 0.025 mmol) in toluene (5.0 mL) the benzyl bromide (103 mg, 0.60 mmol) was added. The reaction mixture was stirred at 0 °C and then the 50% aqueous NaOH (3.0 mL) was added. After completion, the reaction mixture was diluted with water (15 mL), washed with DCM (2 x 25 mL), dried over Na_2SO_4 , filtered, and concentrated in vacuo. Purification of the residue by flash column chromatography on silica gel

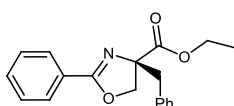
(petroleum ether–ethyl acetate: 98:2 to 90:10) for **135**, **140-145** or (DCM 100%) for **146** afforded the pure alkylated products.

2.8.6 Determination of absolute configuration of alkylated compounds:

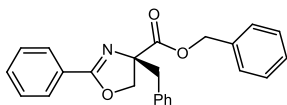
Synthesis of (S)- α -Benzyl serine *t*-butyl ester (**147**).

To a solution of NaBH₃CN (19.9 mg, 0.06 mmol) in AcOH (0.35 mL) at 0°C oxazoline **135** or **120** was added. The mixture was stirred at room temperature for 17h; after this time the solvent was removed and the residue was partitioned between AcOEt (3mL) and a saturated solution of Na₂CO₃ (5mL). The organic layer was treated with 10% NaOH until pH>12 and then recovered. The aqueous layer was washed with AcOEt (2 x 10mL). The combined organic layers were dried with Na₂SO₄ and concentrated in vacuo. The crude, used in the next step without purification, was dissolved in EtOH (1.5 mL) and 10% Pd/C (21.1 mg) was added. The mixture was stirred at rt for 24h under hydrogen atmosphere. The suspension was filtered through Celite, washed with EtOH and concentrated in vacuo. Purification by silica gel chromatography (DCM : MeOH + 0.1% NH₄OH = 95 : 5) afforded **147**.

(S)-2-Phenyl-4-benzyl-2-oxazoline-4-carboxylic acid ethyl ester (**121**)

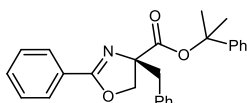


2.6 mg, 11% yield, white solid, mp= 96-97 °C; ee 18%; [α]_D²¹: +0.4 (c = 0.9, CHCl₃).
 HPLC analysis: Chiralcel OD-H, i-PrOH/hexane = 1/99, 1.0 mL/min, 260 nm, t_R (minor) = 22.2 min, t_R (major) = 14.0 min; ¹H-NMR (400 MHz, CDCl₃) δ : 7.93 (m, 2H, Ph_H), 7.48 (m, 1H, Ph_H), 7.39 (m, 3H, Ph_H), 7.22-7.17 (m, 4H, Ph_H), 4.72 (d, J = 8.9 Hz, 1H, CHHO), 4.36 (d, J = 8.9 Hz, 1H, CHHO), 4.27 (m, 2H, OCH₂CH₃), 3.27 (br s, 2H, CH₂Ph), 1.28 (m, 3H, OCH₂CH₃); ¹³C-NMR (100 MHz, CDCl₃) δ : 172.5, 164.8, 135.5, 131.7, 130.3 (x 2), 128.6 (x 3), 128.2 (x 4), 127.0, 78.5, 72.6, 61.8, 43.5, 14.2; HRMS (MALDI) *m/z* [M + H]⁺ calcd for C₁₉H₂₀NO₃⁺ 310.1438, found 310.1437.

(S)-2-Phenyl-4-benzyl-2-oxazoline-4-carboxylic acid benzyl ester (122)

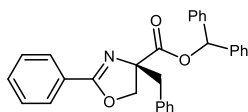
15.0 mg, 50% yield, white solid, mp= 99-100 °C; ee 47%; $[\alpha]_{\text{D}}^{21}$: +1.4 (c = 0.6, CHCl₃).

HPLC analysis: Chiralcel OD-H, i-PrOH/hexane = 1/99, 0.5 mL/min, 260 nm, t_{R} (minor) = 42.1 min, t_{R} (major) = 24.8 min; ¹H-NMR (400 MHz, CDCl₃) δ : 7.93 (m, 2H, Ph \underline{H}), 7.48 (m, 1H, Ph \underline{H}), 7.39-7.33 (m, 7H, Ph \underline{H}), 7.19-7.14 (m, 5H, Ph \underline{H}), 5.28 (d, J = 12.2 Hz, 1H, OCH \underline{H} Ph), 5.21 (d, J = 12.2 Hz, 1H, OCH \underline{H} Ph), 4.71 (d, J = 9.0 Hz, 1H, CH \underline{H} O), 4.35 (d, J = 9.0 Hz, 1H, CH \underline{H} O), 3.30 (d, J = 13.8 Hz, CH \underline{H} Ph), 3.26 (d, J = 13.8 Hz, CH \underline{H} Ph); ¹³C-NMR (100 MHz, CDCl₃) δ : 172.2, 165.0, 135.4, 135.0, 131.7, 130.3 (x 2), 128.5 (x 4), 128.4 (x 3), 128.3 (x 4), 127.1, 127.0, 78.6, 72.5, 67.3, 43.4; HRMS (MALDI) m/z [M + H]⁺ calcd for C₂₄H₂₂NO₃⁺ 372.1594, found 372.1593.

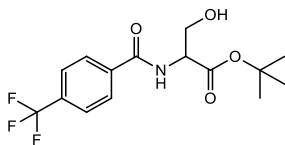
(S)-2-Phenyl-4-benzyl-2-oxazoline-4-carboxylic acid cumyl ester (123)

21.6 mg, 68% yield, colorless liquid; ee 45%; $[\alpha]_{\text{D}}^{20}$: -1.1 (c = 1.0, CHCl₃).

HPLC analysis: Chiralcel OD-H, i-PrOH/hexane = 1/99, 1.0 mL/min, 260 nm, t_{R} (minor) = 24.4 min, t_{R} (major) = 34.4 min; ¹H NMR (400 MHz, CDCl₃) δ : 7.96 (m, 2H, Ph \underline{H}), 7.50 (m, 1H, Ph \underline{H}), 7.42 (m, 2H, Ph \underline{H}), 7.35 (m, 2H, Ph \underline{H}), 7.28-7.22 (m, 8H, Ph \underline{H}), 4.72 (d, J = 8.9 Hz, 1H, CH \underline{H} O), 4.29 (d, J = 8.9 Hz, 1H, CH \underline{H} O), 3.37 (d, J = 13.9 Hz, 1H, CH \underline{H} Ph), 3.30 (d, J = 13.9 Hz, 1H, CH \underline{H} Ph), 1.82 (s, 3H, O(CH \underline{C} ₃)₂Ph), 1.79 (s, 3H, O(CH \underline{C} ₃)₂Ph); ¹³C NMR (100 MHz, CDCl₃) δ : 170.6, 164.8, 145.3, 135.6, 131.6, 130.3 (x 2), 128.5 (x 2), 128.2 (x 6), 127.3, 127.1, 126.8, 124.2 (x 2), 83.2, 78.8, 72.6, 42.8, 28.9, 27.9; HRMS (MALDI) m/z [M + H]⁺ calcd for C₂₆H₂₆NO₃⁺ 400.1907, found 400.1905.

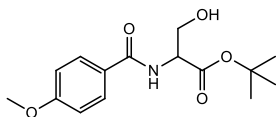
(S)-2-Phenyl-4-benzyl-2-oxazoline-4-carboxylic acid benzhydryl ester (124)

17.8 mg, 50% yield, white solid, mp= 124-127 °C; ee 61%; $[\alpha]_D^{20}$: +9.7 ($c = 0.8$, CHCl_3). HPLC analysis: Chiralcel OD-H, $i\text{-PrOH/hexane} = 1/99$, 0.5 mL/min, 260 nm, t_R (minor) = 29.5 min, t_R (major) = 24.7 min; $^1\text{H NMR}$ (400 MHz, CDCl_3) δ : 7.93 (m, 2H, Ph_H), 7.40-7.10 (m, 18H, Ph_H), 6.96 (s, 1H, OCHPh_2), 4.73 (d, $J = 9.0$ Hz, 1H, CHHO), 4.33 (d, $J = 9.0$ Hz, 1H, CH_O), 3.37 (d, $J = 13.9$ Hz, 1H, CHHPh), 3.27 (d, $J = 13.9$ Hz, 1H, CH_HPh); $^{13}\text{C NMR}$ (100 MHz, CDCl_3) δ : 171.2, 165.0, 143.8 (x 2), 139.7, 135.1, 131.7, 130.3 (x 2), 128.5 (x 4), 128.3, 128.1 (x 2), 127.9, 127.6, 127.4, 127.2, 126.9 (x 2), 126.5 (x 4), 78.7, 77.9, 72.5, 42.9; HRMS (MALDI) m/z $[\text{M} + \text{H}]^+$ calcd for $\text{C}_{30}\text{H}_{26}\text{NO}_3^+$ 448.1907, found 448.1906.

2-((4-Trifluoromethyl)benzoyl)-amino)-3-hydroxypropionic acid *t*-butyl ester (134a)

794 mg, 89% yield; yellow amorphous solid;

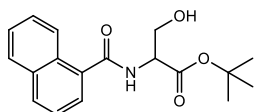
$^1\text{H-NMR}$ (300 MHz, CDCl_3) δ : 7.95 (d, $J = 8.1$ Hz, 2H, Ar_H), 7.71 (d, $J = 8.2$ Hz, 2H, Ar_H), 7.19 (br d, $J = 6.5$ Hz, 1H, NH), 4.74 (m, 1H, CHCO), 4.07 (m, 2H, CH_2OH), 1.52 (s, 9H, $\text{COOC}(\text{CH}_3)_3$).

2-((4-Methoxy)benzoyl)-amino)-3-hydroxypropionic acid *t*-butyl ester (134b)

199 mg, 66% yield; yellow amorphous solid;

$^1\text{H-NMR}$ (300 MHz, CDCl_3) δ : 7.80 (*m*, 2H, ArH), 7.04 (*br d*, $J = 6.5$ Hz, 1H, NH), 6.93 (*d*, $J = 8.8$ Hz, 2H, ArH), 4.72 (*m*, 1H, CHCO), 4.07 (*dd*, $J = 11.2, 3.4$ Hz, 2H, CHHOH), 3.98 (*dd*, $J = 11.2, 4.6$ Hz, 2H, CHHOH), 3.86 (*s*, 3H, ArOCH₃), 1.52 (*s*, 9H, COOC(CH₃)₃).

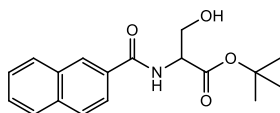
2-[(1-Naphthyl-2-carbonyl)-amino]-3-hydroxy-propionic acid *t*-butyl ester (134c)



316 mg, 99% yield; yellow amorphous solid;

$^1\text{H-NMR}$ (400 MHz, CDCl_3) δ : 8.39 (*d*, $J = 8.2$ Hz, 1H, ArH), 7.95 (*d*, $J = 8.2$ Hz, 1H, ArH), 7.88 (*d*, $J = 7.5$ Hz, 1H, ArH), 7.72 (*d*, $J = 7.1$ Hz, 1H, ArH), 7.59-7.46 (*m*, 2H, ArH), 6.93 (*br s*, 1H, NH), 4.88 (*m*, 1H, CHCO), 4.11 (*br s*, 2H, CH₂OH), 2.60 (*br s*, 1H, CH₂OH), 1.54 (*s*, 9H, COOC(CH₃)₃).

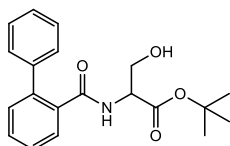
2-[(2-Naphthyl-2-carbonyl)-amino]-3-hydroxy-propionic acid *t*-butyl ester (134d)



322 mg, 99% yield; yellow amorphous solid;

$^1\text{H-NMR}$ (400 MHz, CDCl_3) δ : 8.37 (*br s*, 1H, ArH), 7.92-7.88 (*m*, 3H, ArH), 7.57 (*m*, 2H, ArH), 4.80 (*m*, 1H, CHCO), 4.14 (*dd*, $J = 11.0, 3.0$ Hz, 1H, CHHOH), 4.06 (*dd*, $J = 11.0, 4.2$ Hz, 1H, CHHOH), 2.59 (*br s*, 1H, CH₂OH), 1.54 (*s*, 9H, COOC(CH₃)₃).

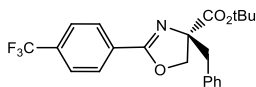
2-[(Biphenyl-2-carbonyl)-amino]-3-hydroxy-propionic acid *t*-butyl ester (134e)



1373 mg, 93% yield; yellow amorphous solid;

$^1\text{H-NMR}$ (300 MHz, CDCl_3) δ : 7.67 (*m*, 1H, ArH), 7.46-7.40 (*m*, 8H, ArH), 6.14 (*br d*, $J = 5.7$ Hz, 1H, NH), 4.48 (*m*, 1H, CHCO), 3.67 (*br s*, 2H, CH_2OH), 2.62 (*br s*, 1H, CH_2OH), 1.40 (*s*, 9H, $\text{COOC}(\text{CH}_3)_3$).

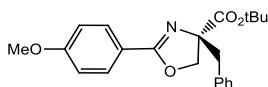
(S)-2-(4-Trifluoromethylphenyl)-4-benzyl-2-oxazoline-4-carboxylic acid *t*-butyl ester (135)



151 mg, 75% yield; white solid; mp= 89-91 °C; ee 72%; $R_f = 0.71$ (petroleum ether–ethyl acetate: 8:2); ee 72%; $[\alpha]_{\text{D}}^{30}$: +89.0 ($c = 1.0$, CHCl_3 , 72% ee);

HPLC analysis: Chiralcel OD-H, *i*-PrOH/hexane = 1/99, 1.0 mL/min, 260 nm, t_R (minor) = 9.5 min, t_R (major) = 6.4 min; $^1\text{H-NMR}$ (400 MHz, CDCl_3) δ : 8.04 (*d*, $J = 8.2$ Hz, 2H, ArH), 7.65 (*d*, $J = 8.2$ Hz, 2H, ArH), 7.26-7.21 (*m*, 5H, PhH), 4.68 (*d*, $J = 9.0$ Hz, 1H, CHHO), 4.34 (*d*, $J = 9.0$ Hz, 1H, CHHO), 3.24 (*br s*, 2H, CH_2Ph), 1.48 (*s*, 9H, $\text{COOC}(\text{CH}_3)_3$); $^{13}\text{C-NMR}$ (100 MHz, CDCl_3) δ : 171.2, 163.4, 135.4, 133.0 (*q*, $J = 32.3$ Hz), 130.7, 130.4 ($\times 2$), 128.9 ($\times 2$), 128.2 ($\times 2$), 127.0, 125.2 ($\times 2$), 123.6 (*q*, $J = 271.9$ Hz), 82.4, 79.0, 73.1, 43.1, 27.9 ($\times 3$); HRMS (MALDI): m/z $[\text{M} + \text{H}]^+$ calcd for $\text{C}_{22}\text{H}_{23}\text{F}_3\text{NO}_3^+$ 406.1625; found: 406.1623.

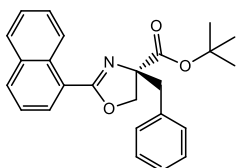
(S)-2-(4-Methoxyphenyl)-4-benzyl-2-oxazoline-4-carboxylic acid *t*-butyl ester (136)



19.6 mg, 67% yield, white solid, mp= 75-77 °C; ee 62%; $[\alpha]_{\text{D}}^{30}$: +69.4 ($c = 1.0$, CHCl_3 , 62% ee); HPLC analysis: Chiralcel OD-H, *i*-PrOH/hexane = 1/99, 0.5 mL/min, 260 nm, t_R (minor) = 24.8 min, t_R (major) = 12.2 min. $^1\text{H NMR}$ (400 MHz, CDCl_3) δ : 7.88 (*d*, $J = 8.9$ Hz, 2H, ArH), 7.25-7.18 (*m*, 5H, PhH), 6.88 (*d*, $J = 8.9$ Hz, 2H, ArH), 4.62 (*d*, $J = 8.8$ Hz, 1H, CHHO), 4.28 (*d*, $J = 8.8$ Hz, 1H, CHHO), 3.84 (*s*, 3H, OCH_3), 3.26 (*d*, $J = 13.8$ Hz, 2H, CHHPh), 3.20 (*d*, $J = 13.8$ Hz, 2H, CHHPh), 1.46 (*s*, 9H, $\text{COOC}(\text{CH}_3)_3$); $^{13}\text{C NMR}$ (100 MHz, CDCl_3) δ : 171.6, 164.4, 162.2, 135.8, 130.4 (\times

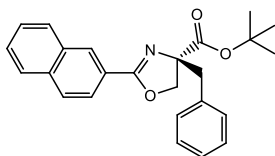
2), 130.3 (x 2), 128.1 (x 2), 126.8, 119.8, 113.6 (x 2), 82.1, 78.8, 72.8, 55.3, 43.3, 28.0 (x 3); HRMS (MALDI) m/z $[M + H]^+$ calcd for $C_{22}H_{26}NO_4^+$ 368.1856, found 368.1854.

2-(1-Naphthyl)-2-oxazoline-4-carboxylic acid *t*-butyl ester (137)

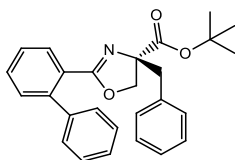


16 mg, 52% yield, white amorphous solid; ee 46%; HPLC analysis: Chiralcel OD-H, *i*-PrOH/hexane = 1/99, 0.5 mL/min, 260 nm, t_R (minor) = 11.8 min, t_R (major) = 10.3 min. 1H -NMR (400 MHz, $CDCl_3$) δ : 8.84 (*d*, J = 8.3 Hz, 1H, ArH), 7.94 (*d*, J = 8.2 Hz, 1H, ArH), 7.90-7.85 (*m*, 2H, ArH), 7.56-7.45 (*m*, 4H, ArH), 7.32-7.22 (*m*, 4H, PhH), 4.72 (*d*, J = 8.8 Hz, 1H, CHHO), 4.37 (*d*, J = 8.8 Hz, 1H, CHHO), 3.34 (*m*, 2H, CH₂Ph), 1.53 (*s*, 9H, COOC(CH₃)₃);

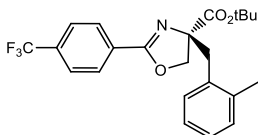
2-(2-Naphthyl)-2-oxazoline-4-carboxylic acid *t*-butyl ester (138)



19.7 mg, 64% yield, white amorphous solid; ee 62%; HPLC analysis: Chiralcel OD-H, *i*-PrOH/hexane = 1/99, 0.5 mL/min, 260 nm, t_R (minor) = 68.4 min, t_R (major) = 30.8 min. 1H -NMR (400 MHz, $CDCl_3$) δ : 8.42 (*s*, 1H, ArH), 8.05 (*d*, J = 8.4 Hz, 1H, ArH), 7.90-7.84 (*m*, 3H, ArH), 7.53 (*m*, 2H, ArH), 7.30-7.18 (*m*, 5H, PhH), 4.72 (*d*, J = 8.8 Hz, 1H, CHHO), 4.38 (*d*, J = 8.8 Hz, 1H, CHHO), 3.30-3.29 (*m*, 2H, CH₂Ph), 1.49 (*s*, 9H, COOC(CH₃)₃);

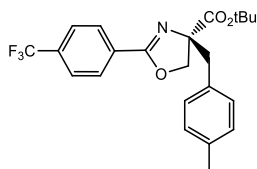
(S)-2-(4-*o*-Biphenyl)-2-oxazoline-4-carboxylic acid *t*-butyl ester (139)

20.6 mg, 62% yield, white amorphous solid; ee 73%; HPLC analysis: Chiralcel OD-H, *i*-PrOH/hexane = 1/99, 0.5 mL/min, 260 nm, t_R (minor) = 26.3 min, t_R (major) = 12.1 min. $^1\text{H-NMR}$ (400 MHz, CDCl_3) δ : 7.74 (*d*, J = 7.6 Hz, 1H, ArH), 7.49 (*m*, 1H, ArH), 7.37-7.21 (*m*, 12H, ArH + PhH), 4.37 (*d*, J = 8.9 Hz, 1H, CHHO), 3.99 (*d*, J = 8.9 Hz, 1H, CHHO), 3.31 (*d*, J = 13.9 Hz, 1H, CHHPh), 3.12 (*d*, J = 13.9 Hz, 1H, CHHPh), 1.48 (*s*, 9H, COOC(CH₃)₃);

(S)-2-(4-Trifluoromethylphenyl)-4-*o*-tolyl-2-oxazoline-4-carboxylic acid *t*-butyl ester (140)

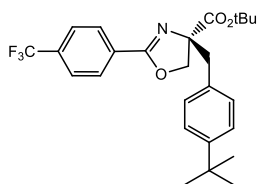
152 mg, 73% yield; colorless liquid; ee 67%; R_f = 0.54 (petroleum ether–ethyl acetate: 9:1); $[\alpha]_{\text{D}}^{28}$: +61.7 (c = 0.7, CHCl_3 67% ee);

HPLC analysis: Chiralcel AD-H, *i*-PrOH/hexane = 1/99, 0.5 mL/min, 260 nm, t_R (minor) = 13.6 min, t_R (major) = 15.8 min; $^1\text{H-NMR}$ (400 MHz, CDCl_3) δ : 8.05 (*d*, J = 8.5 Hz, 2H, ArH), 7.65 (*d*, J = 8.2 Hz, 2H, ArH), 7.19-7.04 (*m*, 4H, ArH + PhH), 4.77 (*d*, J = 8.9 Hz, 1H, CHHO), 4.29 (*d*, J = 8.9 Hz, 1H, CHHO), 3.34-3.27 (*br s*, 2H, CH₂Ar), 2.35 (*s*, 3H, CH₃Ph), 1.46 (*s*, 9H, COOC(CH₃)₃); $^{13}\text{C-NMR}$ (100 MHz, CDCl_3) δ : 171.5, 163.2, 137.3, 134.1, 133.1 (*q*, J = 32.4 Hz), 130.7, 130.4, 130.0, 128.9 (\times 2), 126.9, 125.7, 125.2 (\times 2), 123.5 (*q*, J = 270.9 Hz), 82.4, 79.2, 73.5, 39.4, 27.9 (\times 3), 20.3; HRMS (MALDI): m/z [M + H]⁺ calcd for C₂₃H₂₅F₃NO₃⁺ 420.1781; found: 420.1789.

(S)-2-(4-Trifluoromethylphenyl)-4-*p*-tolyl-2-oxazoline-4-carboxylic acid *t*-butyl ester (141)

129 mg, 61% yield; white solid; mp= 121-123 °C; ee 68%; R_f = 0.78 (petroleum ether–ethyl acetate: 8:2); $[\alpha]_D^{28}$: +62.8 (c = 1.0, CHCl_3 , 68% ee);

HPLC analysis: Chiralcel AD-H, i-PrOH/hexane = 1/99, 0.5 mL/min, 260 nm, t_R (minor) = 17.1 min, t_R (major) = 26.3 min; $^1\text{H-NMR}$ (400 MHz, CDCl_3) δ : 8.05 (d, J = 7.6 Hz, 2H, ArH), 7.65 (d, J = 7.6 Hz, 2H, ArH), 7.12 (d, J = 7.2 Hz, 2H, ArH), 7.04 (d, J = 7.2 Hz, 2H, ArH), 4.68 (d, J = 8.9 Hz, 1H, CHHO), 4.33 (d, J = 8.9 Hz, 1H, CHHO), 3.21 (br s, 2H, CH₂Ph), 2.28 (s, 3H, CH₃Ph), 1.49 (s, 9H, COOC(CH₃)₃); $^{13}\text{C-NMR}$ (100 MHz, CDCl_3) δ : 171.2, 163.3, 136.5, 133.1 (q, J = 32.4 Hz), 132.9, 132.2, 130.8, 130.2 (\times 2), 128.9 (\times 3), 125.2 (\times 2), 123.6 (q, J = 270.4 Hz), 82.4, 79.1, 73.1, 42.7, 27.9 (\times 3), 21.0; HRMS (MALDI): m/z [M + H]⁺ calcd for C₂₃H₂₅F₃NO₃⁺ 420.1781; found: 420.1778.

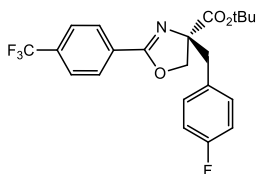
(S)-2-(4-Trifluoromethylphenyl)-4-*t*-butyl-phenyl-2-oxazoline-4-carboxylic acid *t*-butyl ester (142)

135 mg, 58% yield; white solid; mp= 105-107 °C; ee 74%; R_f = 0.88 (petroleum ether–ethyl acetate: 9:1); $[\alpha]_D^{30}$: +53.2 (c = 1.0, CHCl_3 , 74% ee);

HPLC analysis: Chiralcel AD-H, i-PrOH/hexane = 1/99, 0.5 mL/min, 260 nm, t_R (minor) = 12.7 min, t_R (major) = 13.9 min; $^1\text{H-NMR}$ (400 MHz, CDCl_3) δ : 8.05 (d, J = 8.2 Hz, 2H, ArH), 7.65 (d, J = 8.2 Hz, 2H, ArH), 7.25 (d, J = 8.2 Hz, 2H, ArH), 7.17 (d, J = 8.2 Hz, 1H, ArH), 4.70 (d, J = 8.9 Hz, 1H, CHHO), 4.35 (d, J = 8.9 Hz, 1H, CHHO), 3.26 (d, J = 13.9 Hz, 1H, CHHAr), 3.18 (d, J = 13.9 Hz, 1H, CHHAr), 1.47 (s, 9H,

COOC(CH₃)₃, 1.26 (s, 9H, PhC(CH₃)₃); ¹³C-NMR (100 MHz, CDCl₃) δ: 171.2, 163.3, 149.8, 133.1 (q, *J* = 32.8 Hz), 132.3, 130.8, 130.0 (× 2), 128.9 (× 2), 125.2 (× 2), 125.1 (× 2), 123.5 (q, *J* = 270.4 Hz), 82.4, 79.1, 73.3, 42.8, 34.4, 31.3 (× 3), 27.9 (× 3); HRMS (MALDI): *m/z* [M + H]⁺ calcd for C₂₆H₃₁F₃NO₃⁺ 462.2251; found: 462.2246.

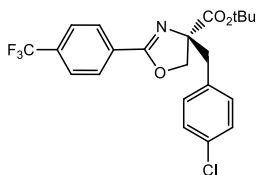
(S)-2-(4-Trifluoromethylphenyl)-4-fluoro-phenyl-2-oxazoline-4-carboxylic acid *t*-butyl ester (143)



175 mg, 83% yield; white solid; mp= 99-100 °C; ee 70%; *R_f* = 0.89 (petroleum ether–ethyl acetate: 7:3); [α]_D²⁷: +76.4 (*c* = 1.0, CHCl₃, 70% ee);

HPLC analysis: Chiralcel OD-H, *i*-PrOH/hexane = 1/99, 1.0 mL/min, 260 nm, *t_R* (minor) = 6.5 min, *t_R* (major) = 5.6 min; ¹H-NMR (400 MHz, CDCl₃) δ: 8.04 (d, *J* = 8.2 Hz, 2H, ArH), 7.66 (d, *J* = 8.2 Hz, 2H, ArH), 7.22 (m, 2H, ArH), 6.92 (m, 2H, ArH), 4.67 (d, *J* = 9.0 Hz, 1H, CHHO), 4.31 (d, *J* = 9.0 Hz, 1H, CHHO), 3.25 (d, *J* = 13.9 Hz, 1H, CH₂Ar), 3.15 (d, *J* = 13.9 Hz, 1H, CH₂Ar), 1.47 (s, 9H, COOC(CH₃)₃); ¹³C-NMR (100 MHz, CDCl₃) δ: 171.1, 163.5, 162.0 (d, *J* = 250.0 Hz), 133.2 (q, *J* = 32.4 Hz), 131.9 (d, *J* = 7.8 Hz) (× 2), 131.1, 130.6, 128.8 (× 2), 125.2 (× 2), 123.6 (q, *J* = 272.5 Hz), 115.0 (d, *J* = 21.1 Hz) (× 2), 82.5, 78.9, 73.2, 42.3, 27.9 (× 3); HRMS (MALDI): *m/z* [M + H]⁺ calcd for C₂₂H₂₂F₄NO₃⁺ 424.1530; found: 424.1529.

(S)-2-(4-Trifluoromethylphenyl)-4-chloro-phenyl-2-oxazoline-4-carboxylic acid *t*-butyl ester (144)

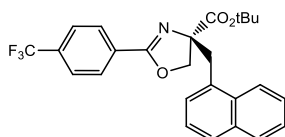


163 mg, 74% yield; white solid; mp= 110-111 °C ; ee 62%; *R_f* = 0.74 (petroleum

ether-ethyl acetate: 7:3); $[\alpha]_D^{27}$: +66.7 ($c = 1.0$, CHCl_3 , 62% ee);

HPLC analysis: Chiralcel OD-H, i-PrOH/hexane = 1/99, 1.0 mL/min, 260 nm, t_R (minor) = 6.6 min, t_R (major) = 5.6 min; $^1\text{H-NMR}$ (400 MHz, CDCl_3) δ : 8.04 (d, $J = 7.6$ Hz, 2H, ArH), 7.66 (d, $J = 7.6$ Hz, 2H, ArH), 7.20 (m, 4H, PhH), 4.67 (d, $J = 8.9$, 1.7 Hz, 1H, CHHO), 4.29 (d, $J = 8.9$, 1.7 Hz, 1H, CHHO), .25 (d, $J = 13.9$ Hz, 1H, CH₂Ar), 3.15 (d, $J = 13.9$ Hz, 1H, CH₂Ar), 1.47 (s, 9H, $\text{COOC}(\text{CH}_3)_3$); $^{13}\text{C-NMR}$ (100 MHz, CDCl_3) δ : 171.0, 163.5, 133.9, 133.2 (q, $J = 32.4$ Hz), 132.8, 131.7 ($\times 2$), 130.5, 128.9 ($\times 2$), 128.3 ($\times 2$), 125.3 ($\times 2$), 123.6 (q, $J = 271.8$ Hz), 82.6, 78.8, 73.3, 42.2, 27.9 ($\times 3$); HRMS (MALDI): m/z $[\text{M} + \text{H}]^+$ calcd for $\text{C}_{22}\text{H}_{22}\text{ClF}_3\text{NO}_3^+$ 440.1235; found: 440.1236.

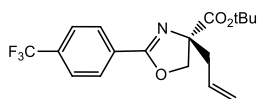
(S)-2-(4-Trifluoromethylphenyl)-4-(2-naphthylmethyl)-2-oxazoline-4-carboxylic acid *t*-butyl ester (145)



167 mg, 74% yield; white solid; mp= 126-128 °C; ee 75%; $R_f = 0.82$ (petroleum ether-ethyl acetate: 9:1); $[\alpha]_D^{30}$: +79.8 ($c = 1.0$, CHCl_3 , 75% ee);

HPLC analysis: Chiralcel OD-H, i-PrOH/hexane = 1/99, 0.5 mL/min, 260 nm, t_R (minor) = 18.8 min, t_R (major) = 24.8 min; $^1\text{H-NMR}$ (400 MHz, CDCl_3) δ : 8.04 (d, $J = 8.0$ Hz, 2H, ArH), 7.78-7.64 (m, 6H, ArH + NpH), 7.42 (m, 3H, NpH), 4.72 (d, $J = 8.9$ Hz, 1H, CHHO), 4.41 (d, $J = 8.9$ Hz, 1H, CHHO), 3.43 (bs, 2H, CH₂O), 1.49 (s, 9H, $\text{COOC}(\text{CH}_3)_3$); $^{13}\text{C-NMR}$ (100 MHz, CDCl_3) δ : 171.2, 163.5, 133.2, 133.1 (q, $J = 32.3$ Hz), 133.0, 132.4, 130.7, 129.1, 128.9 ($\times 2$), 128.6, 127.7, 127.6 ($\times 2$), 126.0, 125.7, 125.2 ($\times 2$), 123.6 (q, $J = 270.2$ Hz), 82.5, 79.2, 73.1, 43.2, 27.3 ($\times 3$); HRMS (MALDI): m/z $[\text{M} + \text{H}]^+$ calcd for $\text{C}_{26}\text{H}_{25}\text{F}_3\text{NO}_3^+$ 456.1781; found: 456.1777.

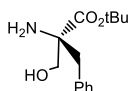
(S)-2-(4-Trifluoromethylphenyl)-4-allyl)-2-oxazoline-4-carboxylic acid *t*-butyl ester (146)



97 mg, 55% yield; colorless liquid; ee 48%; $R_f = 0.87$ (petroleum ether–ethyl acetate: 9:1); $[\alpha]_D^{27}$: +8.9 ($c = 1.0$, CHCl_3 , 48% ee);

HPLC analysis: Chiralcel AS-H, i-PrOH/hexane = 1/99, 0.5 mL/min, 260 nm, t_R (minor) = 7.6 min, t_R (major) = 8.2 min; $^1\text{H-NMR}$ (400 MHz, CDCl_3) δ : 8.09 (d, $J = 8.0$ Hz, 2H, ArH), 7.67 (d, $J = 8.0$ Hz, 2H, ArH), 5.70 (m, 1H, $\text{CCH}_2\text{CHCH}_2$), 5.17 (m, 2H, $\text{CCH}_2\text{CHCH}_2$), 4.73 (d, $J = 8.9$ Hz, CHHO), 4.29 (d, $J = 8.9$ Hz, CHHO), 2.74–2.61 (m, 2H, $\text{CCH}_2\text{CHCH}_2$), 1.50 (s, 9H, $\text{COOC}(\text{CH}_3)_3$); $^{13}\text{C-NMR}$ (100 MHz, CDCl_3) δ : 171.0, 163.4, 133.3 (q, $J = 32.4$ Hz), 131.7, 129.0 ($\times 3$), 125.2 ($\times 2$), 123.5 (q, $J = 270.4$ Hz), 119.7, 82.3, 78.1, 73.4, 42.1, 28.0 ($\times 3$); HRMS (MALDI): m/z $[\text{M} + \text{H}]^+$ calcd for $\text{C}_{18}\text{H}_{21}\text{F}_3\text{NO}_3^+$ 356.1468; found: 356.1464.

(S)- α -Benzyl serine *t*-butyl ester (147)



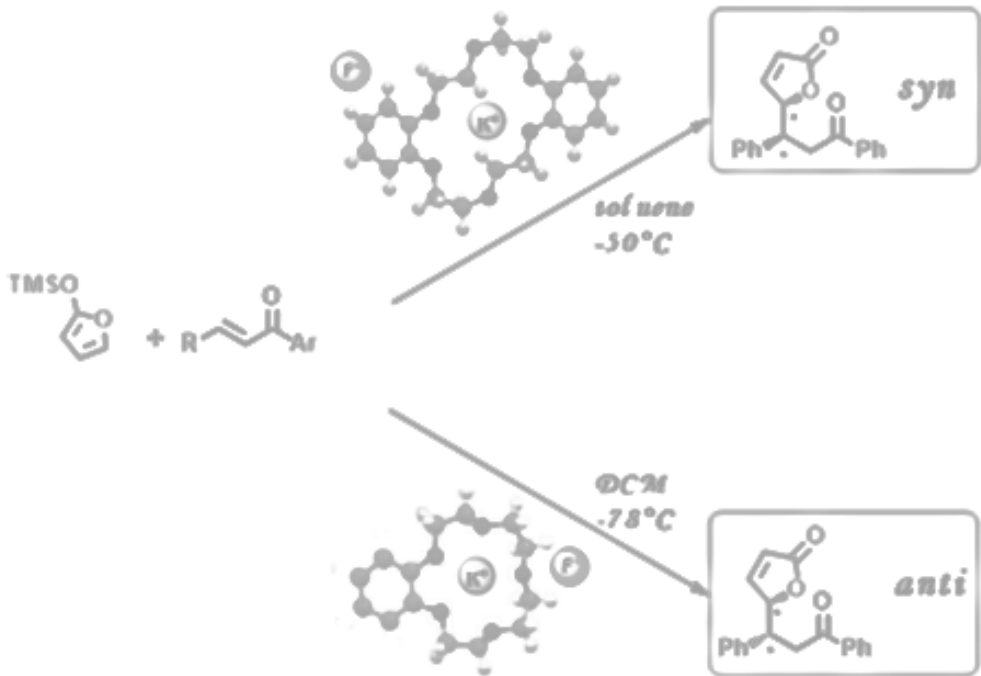
Starting from **135**: 11.5 mg, 70% yield; colorless liquid; $[\alpha]_D^{27}$: +1.3 ($c = 0.9$, CHCl_3).

Starting from **120**: 9.8 mg, 80% yield; colorless liquid; $[\alpha]_D^{27}$: +1.4 ($c = 0.8$, CHCl_3).

$^1\text{H NMR}$ (400 MHz, CDCl_3) δ : 7.37–7.33 (m, 3H, PhH), 7.27 (m, 2H, PhH), 3.83 (d, $J = 10.6$ Hz, 1H, CHHOH), 3.62 (d, $J = 10.6$ Hz, 1H, CHHOH), 3.16 (d, $J = 13.5$ Hz, 1H, CHHPh), 2.89 (d, $J = 13.5$ Hz, 1H, CHHPh), 2.06 (br s, 3H, NH_2 , OH), 1.54 (s, 9H, $\text{O}(\text{CH}_3)_3$); $^{13}\text{C NMR}$ (100 MHz, CDCl_3) δ : 174.2, 135.7, 130.1 ($\times 2$), 128.4 ($\times 2$), 127.0, 82.0, 68.1, 63.1, 41.7, 28.0 ($\times 3$); HRMS (MALDI): m/z $[\text{M} + \text{H}]^+$ calcd for $\text{C}_{14}\text{H}_{22}\text{NO}_3^+$ 252.1594; found: 252.1590.

Chapter 3

Diastereoselective synthesis of γ -butenolides



3. DIASTEROSELECTIVE SYNTHESIS OF γ -BUTENOLIDES

3.1 Synthesis of γ -butenolides

Butenolides are unsaturated γ -lactones, widely diffused as natural biologically active compounds, present in terrestrial, marine and microbial sources. For example, butenolide frameworks are incorporated in naturally occurring steroids from plants and microorganisms.⁹⁵ Other representative examples of butenolide-containing natural products are the *Securinega* alkaloids such as securinine (**151**), phyllanthidine (**152**), and norsecurinine (**153**) (figure 3.1).

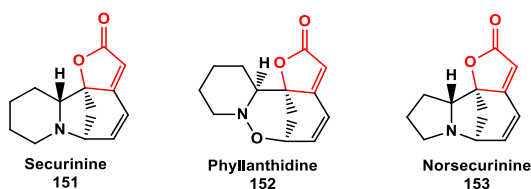


Figure 3.1 Representative examples of *Securinega* alkaloids

The family of *Securinega* alkaloids is composed of 60 different metabolites and the the most abundant is securinine (**151**) that is able to induce apoptosis of several cancer cell lines.⁹⁶

Construction of γ -butenolides received considerable attention in total synthesis of natural products. Some examples of biologically active γ -butenolides are indicated in figure 3.2. These compounds showed unique biologically features such as anti-malarian (**155**) or anti-tumor (**157**) activities.⁹⁷

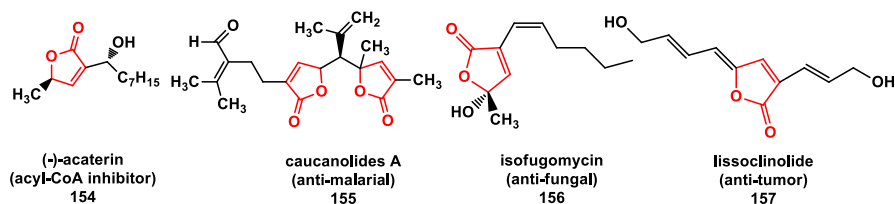


Figure 3.2 Examples of biologically active γ -butenolides (**154-157**)

⁹⁵ Y. S. Rao, *Chem. Rev.*, **1964**, 353-388.

⁹⁶ E. Chirkin, S. Michel, F. H. Porée, *J. Org. Chem.*, **2015**, *80*, 6525-6528.

⁹⁷ L. Vasamsetty, F. A. Khan, G. Mehta, *Tetrahedro Lett.*, **2015**, *71*, 3209-3215.

The presence of a lactone moiety characterized the family of cardenolides which contain a five-membered unsaturated butyrolactone ring. Cardenolides are cardiac glycosides also able to inhibit the growth of cancer cell lines. One of the cardiac glycosides, digitoxin (**158**), has been used for treatment of heart diseases.⁹⁸ Another important bioactive compound is giganin (**159**),⁹⁹ a member of the annonaceous acetogenins, characterized by a long aliphatic chain with a terminal methyl-substituted α,β -unsaturated γ -lactone.

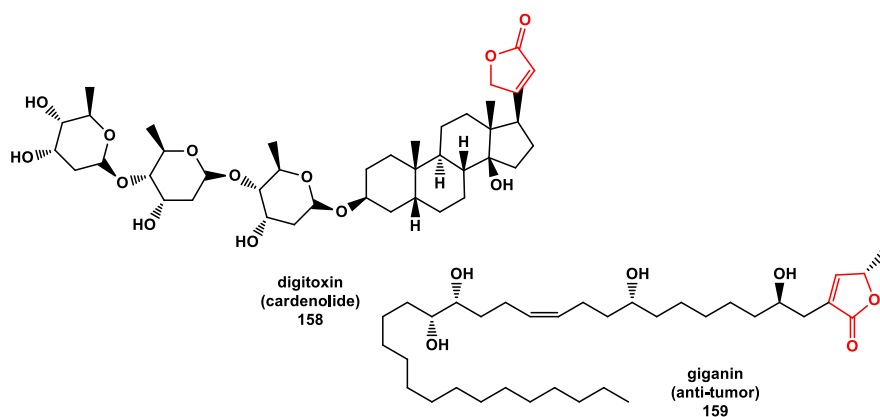
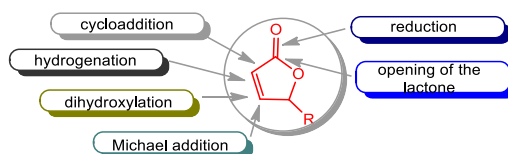


Figure 3.3 Structures of digitoxin and giganin

Furthermore, γ -butenolides are versatile chiral building blocks or intermediates, useful in synthetic strategies for the construction of natural products, that can be subjected to various transformations involving the carbon-carbon double bond or the ester group (scheme 3.1).



Scheme 3.1 Possible transformation of γ -butenolide rings

⁹⁸ I. Prassas, E. P. Diamandis, *Nature Reviews Drug Discovery*, **2008**, 7, 926-935.

⁹⁹ C. J. Fletcher, K. M. P. Wheelhouse, V. K. Aggarwal, *Angew. Chem. Int. Ed.*, **2013**, 52, 2503-2506.

Hydrogenation reactions are widely used for the generation of saturated lactones, synthetic intermediates in the synthesis of natural products such as alkaloids and terpenoids,¹⁰⁰ or biologically active compounds such as anti-tumor, anti-depressants and antiviral compounds.¹⁰¹ Interesting derivatives are also obtained by cycloaddition reactions, dihydroxylations or reduction of the ester group. For example the cycloaddition reactions have been used by Fukuyama in order to obtain mitomycins (figure 3.4) potent anti-tumor agents.¹⁰² Examples of reactions involving the 1,4-addition to the double bond and opening of the lactone have been reported by Hanessian for the synthesis of ionomicine (figure 3.5).¹⁰³ The prominent attention towards butenolides as target molecules or key synthetic intermediates has led to the development of new stereoselective methods of synthesis based on the vinylogous reactivity of γ -butenolides. The idea is to generate a new tertiary stereocenter in the γ -position of butenolide, by reaction of a 2-(5*H*)-furanone derivative (direct vinylogous reaction) with an electrophilic species. Alternatively, a 2-silyloxyfuran, an activated form of 2-(5*H*)-furanone, can be employed (Mukaiyama-type vinylogous reaction).

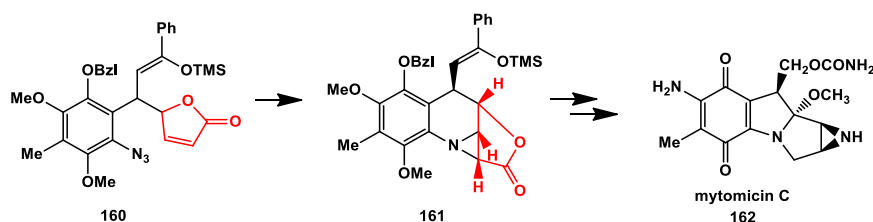


Figure 3.4 Synthesis of mytomicin C

¹⁰⁰. For examples see: a) M. T. Davis-Coleman, D. E. A. Rivett, *Prog. Chem. Nat. Prod.*, **1989**, 55, 1–35; b) C. W. Jefford, D. Jaggi, A. W. Sledeski, Boukouvalas, *J. In Studies in Natural Products Chemistry*, **1989**, 3, 157-171; c) L. A. Paquette, T. Z. Wang, E. Pinard, *J. Am. Chem. Soc.*, **1995**, 117, 1455–1456; d) H. Nemoto, T. Tanabe, K. Fukumoto, *J. Org. Chem.*, **1995**, 60, 6785–6790.

¹⁰¹. For examples see: a) H. Fukui, Y. Tsuchiya, K. Fujita, T. Nakagawa, H. Koshino, T. Nakata, *Bioorg. Med. Chem. Lett.*, **1997**, 7, 2081–2086; b) J. W. Hilborn, Z. H. Lu, A. R. Jurgens, Q. K. Fang, P. Byers, S. A. Wald, C. H. Senanayake, *Tetrahedron Lett.*, **2001**, 42, 8919–8921.

¹⁰². For examples see: a) T. Fukuyama, L. Yang, *Tetrahedron Lett.*, **1986**, 27, 6299-6300; b) T. Fukuyama, L. Yang, *J. Am. Chem. Soc.*, **1987**, 109, 7881-7882; c) T. Fukuyama, L. Yang, *J. Am. Chem. Soc.*, **1989**, 111, 8303-8304.

¹⁰³. For examples see: a) S. Hanessian, P. J. Murray, *Can. J. Chem.*, **1986**, 64, 2231-2234; b) S. Hanessian, N. G. Cooke, B. DeHoff, Y. Sakito, *J. Am. Chem. Soc.*, **1990**, 112, 5276-5290.

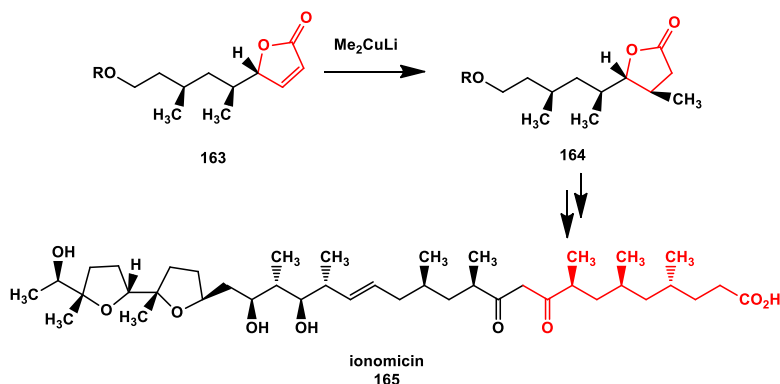
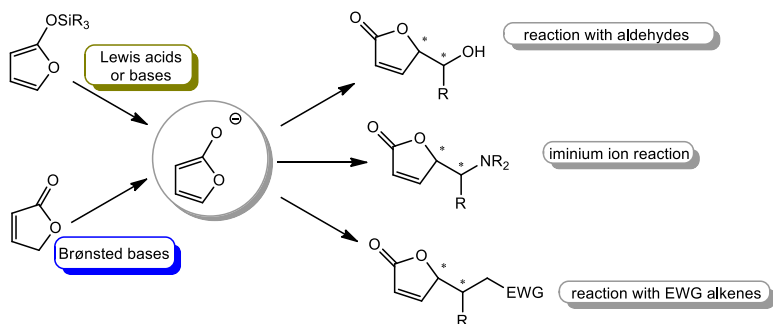


Figure 3.5 Synthesis of ionomicin

Reactions are possible with aldehydes, imines and electron-poor alkenes, to give aldol reactions, Mannich reactions or Michael reactions respectively (scheme 3.2). The following is a brief overview of the stereoselective synthesis of γ -butenolides by vinylogous Michael addition, which is the focus of our study described in this thesis.

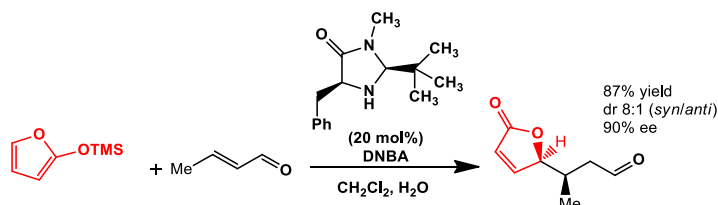


Scheme 3.2 Vinylogous reactions of 2-(5H)-furanone or 2-silyloxyfuran

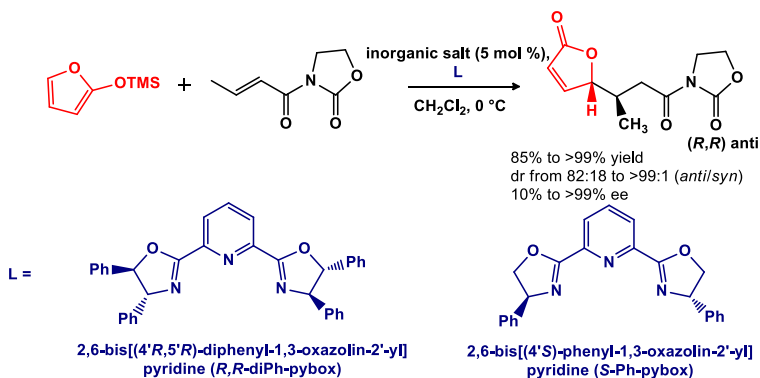
3.2 Asymmetric vinylogous synthesis of γ -monosubstituted butenolides by Michael-type addition.

The enantioselective Michael-type addition of 2-furanones and 2-silyloxyfurans to electron-poor alkenes is a much studied and widely used process. In this section it will be discussed only the protocols for the synthesis of γ -monosubstituted γ -butenolides, starting from 5-unsubstituted substrates, that are most relevant to

our work. In 2003 it was reported the first example of asymmetric addition of 2-silyloxyfuran with various α,β -unsaturated aldehydes by MacMillan and co-workers (scheme 3.3). The catalytic system used, a chiral imidazolidinone, activates the electrophile with an iminium ion mechanism. The reaction takes place with complete regioselectivity towards the 1,4-addition while the steric constraints imposed by the catalyst prevent the 1,2-addition.¹⁰⁴ An investigation on the Mukaiyama-Michael reaction between (*E*)-3-crotonyl-1,3-oxazolidin-2-one and 2-trimethylsilyloxyfuran was conducted by Desimoni and collaborators (scheme 3.4).^{105,106} In particular, lanthanide salts in the presence of pyridine-2,6-bis(oxazoline) ligands was able to promote the highly stereoselective synthesis formation of the product with the *anti* configuration (*R,R*).



Scheme 3.3 Organocatalyzed addition of silyloxy furan to α,β -unsaturated aldehydes



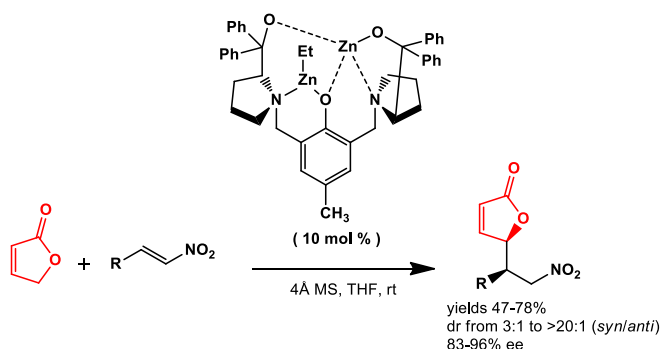
Scheme 3.4 Mukaiyama-Michael reaction of 2-trimethylsilyloxyfuran to (*E*)-3-crotonyl-1,3-oxazolidin-2-one

¹⁰⁴ S. P. Brown, N. C. Goodwin, D. W. C. MacMillan, *J. Am. Chem. Soc.*, **2003**, *125*, 1192-1194.

¹⁰⁵ For examples see: a) G. Desimoni, G. Faita, M. Guala, A. Laurenti, M. Mella, *Chem., Eur. J.*, **2005**, *11*, 3816-3824; b) G. Desimoni, G. Faita, S. Filippone, M. Mella, M. G. Zampori, M. Zema, *Tetrahedron*, **2001**, *57*, 10203-10212.

¹⁰⁶ For other examples of Michael addition to α,β -unsaturated oxazolidin-2-ones see: a) H. Kitajima, T. Katsuki, *Synlett*, **1997**, 568-569; b) H. Suga, T. Kitamura, A. Takehi, T. Baba, *Chem. Commun.*, **2004**, 1414-1415.

Trost and co-workers in 2009 developed the first direct asymmetric Michael addition of 2-trimethylsilyloxyfuran to nitroalkenes (scheme 3.5). The use of a dinuclear zinc complex allowed the synthesis of γ -butenolide nitro-derivatives with high enantiomeric excesses and diastereomeric ratios up to 20:1.¹⁰⁷



Scheme 3.5 Direct asymmetric Michael addition of 2-trimethylsilyloxyfuran to nitroalkenes

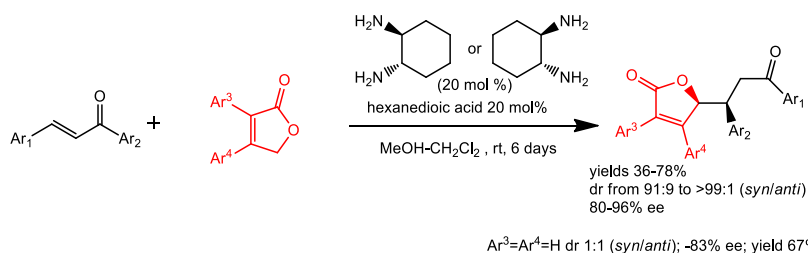
The asymmetric vinylogous Michael reaction of γ -butenolides to *trans*-chalcones has been extensively studied. This reaction has been described by Ge, Li and coworkers in the presence of chiral 1,2-diaminocyclohexane (scheme 3.6).¹⁰⁸ A wide variety of 3,4-diarylated 2-(5*H*)-furanones and chalcones reacted with high diastereo- and enantio- selectivities. An high enantioselectivity was obtained by using unsubstituted furan-2(5*H*)-one as well, although only a 1:1 *syn/anti* ratio was obtained in this case. An example of asymmetric vinylogous Mukaiyama-Michael reaction of 2-silyloxyfuran with *trans*-chalcones was conducted by Feng and co-workers (scheme 3.7). The use of Sc(OTf)₃ in the presence of a *N,N'*-dioxide chiral ligand containing L-proline residues has been particularly effective to obtain exclusively the *anti* adduct with high ee's.¹⁰⁹ However, from the atom economy point of view, the employment of commercially available unmodified γ -butenolides instead of 2-silyloxyfurans is more attractive. Ji, Wang and co-workers in 2010 obtained good diastereoselectivities and enantiomeric excesses in the Michael addition reaction between 2-(5*H*)-furanone and *trans*-chalcone derivatives

¹⁰⁷ B. M. Trost, J. Hitee, *J. Am. Chem. Soc.*, **2009**, *131*, 4572-4573.

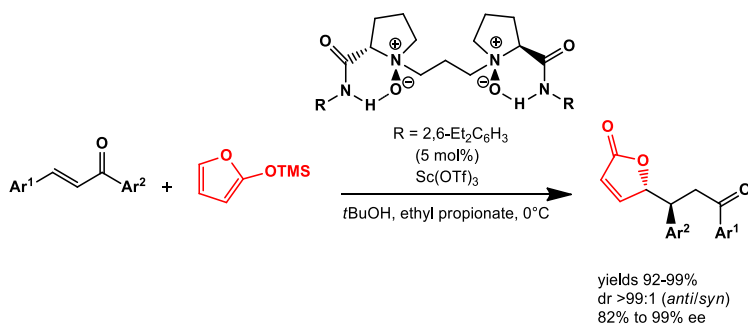
¹⁰⁸ J. Wang, C. Qi, Z. Ge, T. Cheng, R. Li, *Chem. Commun.*, **2010**, *46*, 2124-2126.

¹⁰⁹ Q. Zhang, X. Xiao, L. Lin, X. Liu, X. Feng, *Org. Biomol. Chem.*, **2011**, *9*, 5748-5754.

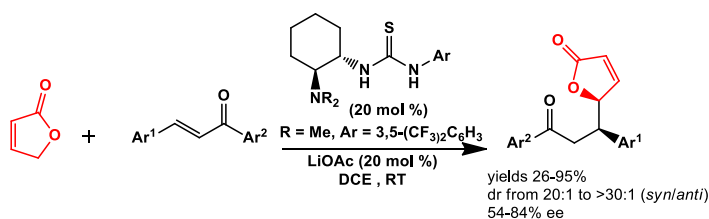
promoted by Takemoto catalyst (scheme 3.8).¹¹⁰ This catalytic approach proved to be ineffective with aliphatic enones. Liang, Ye and coworkers developed a triamine catalyst, characterized by a chiral spatial pocket, which afforded Michael adducts with excellent enantioselectivities (scheme 3.9).¹¹¹ However, the *anti* product was obtained with high diastereoselectivities only with methyl- α,β -unsaturated ketones ($R^2=Me$ in scheme 3.9); with more hindered Michael acceptor (*e.g.* $R^2=Ph$ or Bu) the *anti*-diastereoselectivities proved to be moderate.



Scheme 3.6 Direct asymmetric vinylogous Michael addition reactions of γ -butenolides to chalcones



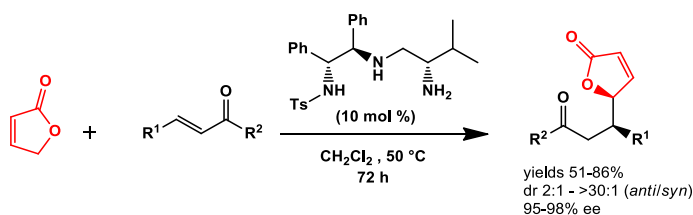
Scheme 3.7 Asymmetric vinylogous Michael addition of γ -butenolides to chalcone derivatives



Scheme 3.8 Organocatalytic direct conjugate addition of γ -Butenolide to chalcones

¹¹⁰ Y. Zhang, C. Yu, Y. Ji, W. Wang, *Chem. Asian J.*, **2010**, *5*, 1303-1306.

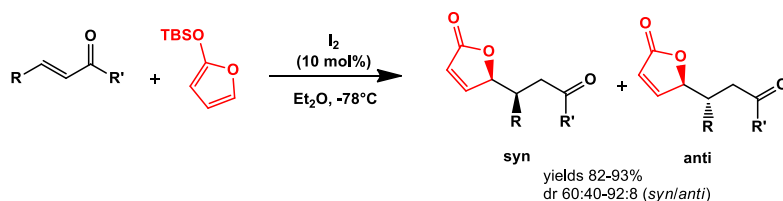
¹¹¹ H. Huang, F. Yu, Z. Jin, W. Li, W. Wu, X. Liang, J. Ye, *Chem. Commun.*, **2010**, *46*, 5957-5959.



Scheme 3.9 Organocatalytic asymmetric vinylogous Michael reaction

3.3 Diastereoselective vinylogous synthesis of γ -monosubstituted butenolides by Michael-type addition.

As previously seen, to date the research has been primarily aimed to the enantio- and diastereoselective vinylogous Michael addition of 2-silyloxyfuran or 2-(5*H*)-furanone promoted by chiral organocatalysts or transition metal complexes which are generally expensive or not commercially available. The latter may require a tedious laboratory synthesis starting from relatively expensive chiral building blocks. The use of chiral catalysts is unnecessary for the development of purely diastereoselective vinylogous Michael addition. This issue has recently encouraged the invention of novel methods based on simple and off-the-shelf catalysts. Yadav and co-workers reported in 2009 a metal-free synthesis of γ -substituted butenolides promoted by iodine, that is characterized by a mild Lewis acidity. The addition of 2-trimethylsilyloxyfuran to different α,β -unsaturated compounds at low temperatures afforded the *syn* diastereoisomer with moderate to high diastereoselectivity (scheme 3.10).¹¹²

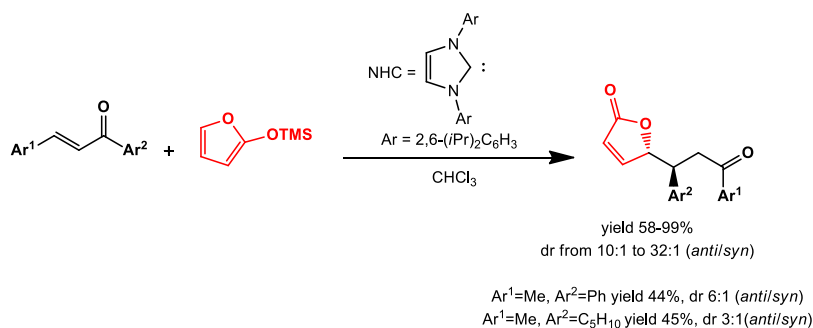


Scheme 3.10 Iodine-catalyzed synthesis of butenolides

¹¹² J. S. Yadav, S. B. V. Reddy, G. Narasimhulu, S. N. Reddy, J. P. Reddy, *Tetrahedron Lett.*, **2009**, *50*, 3760-3762.

In other studies the *syn/anti* diastereoselectivity in the Mukaiyama-Michael addition of 2-trimethylsilyloxyfuran to α,β -unsaturated ketones was disappointing or limited in scope.

Du, He and co-workers, in 2015, employed N-heterocyclic carbenes (NHCs) in a diastereoselective reaction of 2-trimethylsilyloxyfuran and enones. High *anti*-diastereoselectivities and excellent yields were achieved with various chalcone derivatives. This system was also applicable to aliphatic enones but moderate yields and moderate *anti*-diastereoselectivities were obtained (scheme 3.11).¹¹³



Scheme 3.11 N-Heterocyclic-Carbene-Catalysed Diastereoselective Vinylogous Mukaiyama/Michael Reaction of 2-(Trimethylsilyloxy)furan and Enones

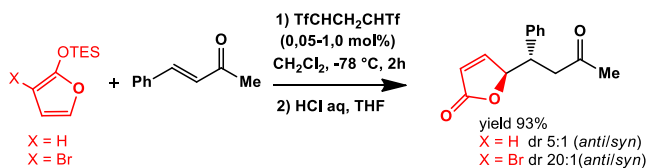
Taguchi and co-workers explored the effect of a Brønsted acid catalyst, 1,1,3,3-tetrakis(trifluoromethanesulfonyl)propane in this reaction (scheme 3.12).¹¹⁴ Although this proved to be an efficient regioselective method for the 1,4 addition, only moderate diastereoselectivities were obtained with 2-triethylsilyloxyfuran. Good *anti*-diastereoselectivities were achieved only with 3-bromo-derivative of 2-silyloxyfuran.

In 2012 Fraile and collaborators developed the Mukayama-Michael addition of 2-trimethylsilyloxyfuran to α,β unsaturated carbonyl derivatives, using a Lewis acid catalyst.¹¹⁵ They employed Cu(OTf)₂ as homogeneous catalyst or copper-exchanged laponite as heterogeneous catalyst. However low *anti*-diastereoselectivities were obtained with α,β -unsaturated ketones as Michael acceptors (scheme 3.13).

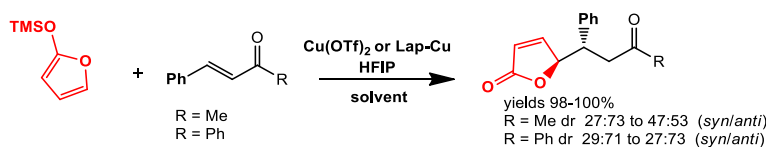
¹¹³ Y. Wang, G. Du, F. Xing, K. Huang, B. Dai, L. He, *Asian J. Org. Chem.*, **2015**, *4*, 1362–1365.

¹¹⁴ A. Takahashi, H. Yanai, M. Zhang, T. Sonoda, M. Mishima, T. Taguchi, *J. Org. Chem.*, **2010**, *75*, 1259–1265.

¹¹⁵ J. M. Fraile, N. Garcìa, C. I. Herrerías, M. Martín, J. A. Mayoral, *ACS Catal.*, **2012**, *2*, 56–64.



Scheme 3.12 Vinylogous Mukayama-Michael reaction catalyzed with 1,1,3,3-tetrakis(trifluoromethanesulfonyl) propane



Scheme 3.13 Vinylogous Mukayama-Michael reaction promoted by copper catalysts

3.4 Novel synthetic strategies for the synthesis of γ -butenolides using a diastereoselective Mukayama-Michael addition

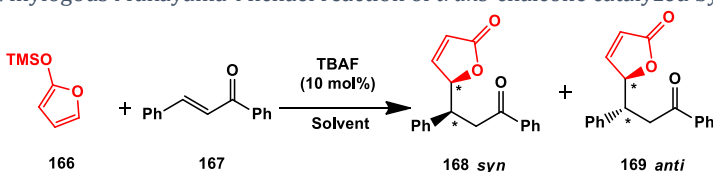
The interest in the developing convenient and stereoselective methodologies to obtain γ -butenolides, has been demonstrated by numerous studies reported in literature as discussed above. On the other hand, the diastereoselective vinylogous Mukayama-Michael addition of 2-silyloxyfuran catalyzed by achiral, cheap and easily available compounds, has been rarely reported. Furthermore, it would be intriguing to develop an efficient and convenient methodology that would afford both the *syn* and the *anti* diastereomer. Therefore, one of the aim of this PhD project was to test commercially available macrocyclic phase-transfer catalysts in fluoride-promoted Mukayama-Michael addition of silyloxyfurans to α,β -unsaturated ketones. While it is well-established the application of organic fluoride as promoters of Mukayama-Michael addition with silyl enol ethers, this strategy has never been applied to silyloxyfurans to date.¹¹⁶ To the best of our knowledge a unique example of vinylogous Michael addition of 2-trimethylsilyloxyfuran promoted by a fluoride, the tetra-*n*-butylammonium fluoride (TBAF), was reported as a step in the synthesis of mytomicins.^{91a} However, in this article the diastereoisomeric ratio obtained is not reported.

¹¹⁶ a) R. Noyori, K. Yokoyama, J. Sakata, *J. Am. Chem. Soc.*, **1977**, 1265-1266; b) T. V. RajanBabu, *J. Am. Chem. Soc.*, **1984**, 49, 2083-2089.

3.5 Mukayama-Michael addition of *trans*-chalcone with 2-trimethylsilyloxyfuran catalyzed by TBAF

Considering the few data reported in the literature, the use of organic fluoride, such as TBAF, was first investigated in the vinylogous Mukayama-Michael reaction of 2-trimethylsilyloxyfuran with *trans*-chalcone. The experiments were carried out using TBAF as catalyst in different solvents in order to evaluate differences between apolar solvent such as toluene, aprotic polar solvents (DMF and THF) and medium polar solvents (CHCl₃ and DCM). In all cases the adducts **168** and **169** were formed in mixture with their respective trimethylsilyl enol ethers. Therefore, once the reaction was complete, it followed a treatment with HCl in order to desilylate the adducts. The reaction in DMF and DCM led to a complex mixture of products (Table 3.1, entries 3,5), while in all the other solvents TBAF efficiently led to products with a preference for the *anti* diastereoselectivity. Interestingly in CHCl₃ a high diastereoisomeric ratio was achieved (98/2 *anti/syn*, Table 3.1, entry 2).

Table 3.1 Vinylogous Mukayama-Michael reaction of *trans*-chalcone catalyzed by TBAF^a



Entry	Solvent	T(°C)	Time(h)	<i>syn/anti</i> ^b	Yield ^{c,d} (%)
1	Toluene	-78	40	7/93	57
2	CHCl ₃	-55	4	2/98	84
3	DMF	-60	5	-	-
4	THF	-78	15	17/83	79
5	DCM	-78	24	-	-

^aAll reactions were carried out in liquid-liquid system at 0.218 mmol scale using **167** (1.0 eq.), 2-trimethylsilyloxyfuran (1.2 eq.) and catalyst TBAF (10 mol%) in the appropriate solvent (1.1 mL).

^b*syn/anti* ratio was determined by ¹H NMR spectroscopy of the crude products. ^cIsolated yields.

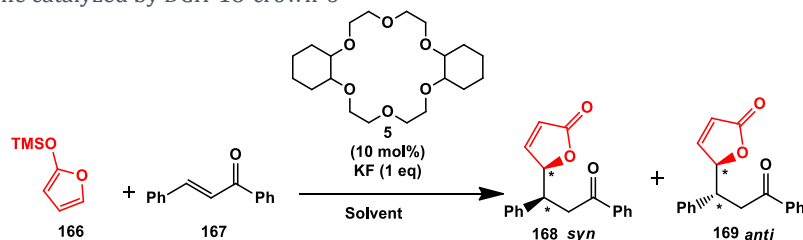
^dMixture of products.

3.6 Mukayama-Michael addition of trimethylsilyloxyfuran to *trans*-chalcone catalyzed by dicyclohexane-18-crown-6

Afterwards, the Mukayama-Michael reaction was carried out with inorganic fluoride, KF, in presence of dicyclohexane-18-crown-6 as a phase-transfer catalyst.

A screening of solvents was performed using toluene, halogenated solvents (DCE, CHCl_3 , DCM), aprotic polar solvents (THF, DMF, ACN). The temperature for each entry was chosen compatibly with the melting point of the solvent. Surprisingly, an extraordinary dependence of the diastereoselectivity on the solvent used, was observed. In toluene, differently from what observed with TBAF, a high *syn*-diastereoselectivity was achieved (93/7 *syn/anti*, Table 3.2, entry 1). However, when we move from toluene to CHCl_3 , DCM, DMF and ACN (Table 3.2, entries 5, 6, 7, 8) an inversion of diastereoselectivity was observed, and the *anti* product **169** prevailed again. This catalytic system showed a better solvent tolerability than TBAF. In addition, the same high *anti*-diastereoselectivity was obtained in CHCl_3 , DCM, DMF and ACN (98/2 *anti/syn*). This interesting result has led to further investigations on the combination of different commercially available macrocyclic phase transfer-catalysts with inorganic fluorides, as silyloxyfurans activating agents. In order to assess the effect of the inorganic salts in diastereoisomeric ratio, a screening study was conducted. In toluene, the *syn* product **168** was favoured with all the inorganic salts tested. However, the best result was achieved performing the reaction with KF (Table 3.3, entry 1).

Table 3.2 Vinylogous Mukayama-Michael reaction of 2-trimethylsilyloxyfuran and *trans*-chalcone catalyzed by DCH-18-crown-6^a



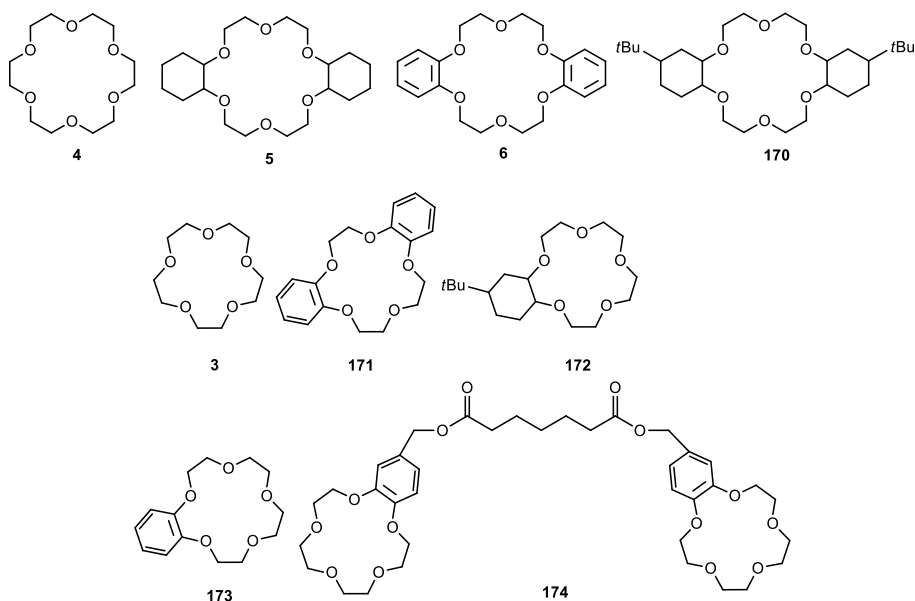
Entry	Solvent	T(°C)	Time(h)	<i>syn/anti</i> ^b	Yield ^c (%)
1	Toluene	-78	22	93/7	83
2	Et ₂ O	-78	21	57/43	32
3	THF	-78	23	12/88	12
4	DCE	-30	2	12/88	86
5	CHCl_3	-55	21	2/98	87
6	DCM	-78	4	2/98	98
7	DMF	-60	2	2/98	74
8	ACN	-40	21	2/98	72

^aAll reactions were carried out in liquid-liquid system at 0.218 mmol scale using **167** (1.0 eq.), 2-trimethylsilyloxyfuran (1.2 eq.), KF (1.0 eq.) and catalyst DCH-18-crown-6 (10 mol%) in the appropriate solvent (1.1 mL). ^b*syn/anti* ratio was determined by ¹H NMR spectroscopy of the crude products. ^cIsolated yields.

Table 3.3 Screening of inorganic salts in Mukayama-Michael reaction catalyzed by DCH-18-crown-6^{a,b}

Entry	Inorganic Salt	Time(h)	<i>syn/anti</i> ^b	Yield ^c (%)
1	KF	22	93/7	83
2	KOPh	43	83/17	63
3	KOAc	43	88/12	40
4	KOH	19	88/12	83
5	CsF	41	82/18	67

^aAll reactions were carried out in liquid-liquid system at 0.218 mmol scale using **167** (1.0 eq.), 2-trimethylsilyloxyfuran (1.2 eq.), KF (1.0 eq.) and catalyst DCH-18-crown-6 (10 mol%) in toluene (1.1 mL) at -78°C. ^b*syn/anti* ratio was determined by ¹H NMR spectroscopy of the crude products. ^cIsolated yields.

**Figure 3.6** 18-crown-6 and 15-crown-5 derivatives tested in the fluoride promoted Mukayama-Michael reaction

The effect of the catalyst's structure was then evaluated, using different crown ethers. 18-crown-6 derivatives and 15-crown-5 analogues were screened (figure 3.6, Table 3.4) in order to clarify the possible correlation between the cavity size of the macrocycle and the diastereoisomeric ratio. Most of the different catalytic systems showed good diastereoselectivities with the only exception of compound **172**. All the 18-crown-6 derivatives favored the *syn* isomer in toluene. Moreover with compound **5**, the presence of molecular sieves in the reaction medium and the use of different catalyst loadings showed negligible effect on the diastereomeric

ratio. Unexpectedly, 15-crown-5 analogues, even in toluene, favored the *anti* isomer, with the exception of compound **171** (Table 3.4, entry 6). In particular, compound **173** afford the *anti* product with a very high diastereoselectivity (97/3 *anti/syn*, entry 11).

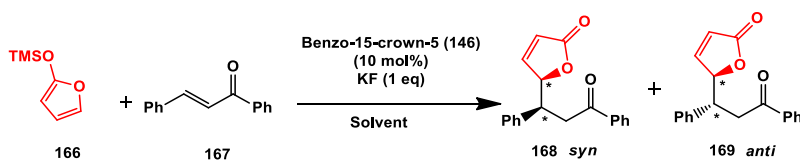
Taking into account that both 15-crown-5 ether derivatives and halogenated solvents promote mainly the *anti* products, we studied the performance of the best catalyst **173** in CHCl_3 and DCM (Table 3.5, entries 1 and 2). To our delight, the structure of the macrocycle and type of solvents exerted a synergistic effect, and the *anti* product was obtained exclusively.

Table 3.4 Screening of catalysts in Mukayama-Michael reaction of 2-trimethylsilyloxyfuran and *trans*-chalcone^a

Entry	Catalyst	Time(h)	<i>syn/anti</i> ^b	Yield ^c (%)
1	5	22	93/7	83
2	4	44	88/12	80
3	6	46	92/8	90
4	170	43	88/12	93
5 ^d	5	20	90/10	74
6 ^e	5	20	88/12	70
7 ^f	5	20	95/5	86
8	3	44	38/62	53
9	171	41	92/8	54
10	172	43	50/50	57
11	173	40	3/97	76
12	174	44	17/83	46

^aAll reactions were carried out in liquid-liquid system at 0.218 mmol scale using **167** (1.0 eq.), trimethylsilyloxyfuran (1.2 eq.), KF (1.0 eq.) and catalyst (10 mol%) in toluene (1.1 mL) at -78°C . ^b*syn/anti* ratio was determined by ^1H NMR spectroscopy of the crude products. ^cIsolated yields. ^dThe reaction was carried out with molecular sieves (4Å). ^eWith 2 mol% of **5**. ^fWith 1.0 eq. of **5**.

Table 3.5 Mukayama-Michael reaction catalyzed by benzo-15-crown-5 in halogenated solvents^a

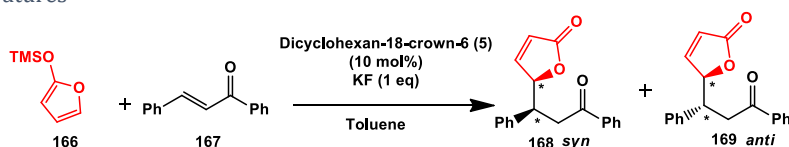


Entry	Catalyst	Solvent	T($^\circ\text{C}$)	Time(h)	<i>syn/anti</i> ^b	Yield ^c (%)
1	173	CHCl_3	-55	21	<1/99	94
2	173	DCM	-78	6	<1/99	99

^aAll reactions were carried out in liquid-liquid system at 0.218 mmol scale using **167** (1.0 eq.), trimethylsilyloxyfuran (1.2 eq.), KF (1.0 eq.) and catalyst **173** (10 mol%) in the appropriate solvent (1.1 mL). ^b*syn* and *anti* ratio was determined by ^1H NMR spectroscopy of the crude products. ^cIsolated yields.

Having optimized the *anti*-diastereoselective vinylogous addition, further efforts were made to improve the yield of the *syn* product **168** with the reaction catalyzed by dicyclohexane-18-crown-6 (**5**) in toluene, at different temperatures. The best result was observed at -50°C (94/6 *anti/syn*, Table 3.6, entry 3) while different values afforded a little decrease in diastereoselectivity. Finally, using the best solvents (toluene and DCM) the [2,2,2]-cryptand, known for his very good complexation ability for the potassium,¹ was used as catalyst (Table 3.7). In this case the behavior was very similar to TBAF, with a strong preference for the *anti* product both in toluene and DCM (*anti/syn* 98/2).

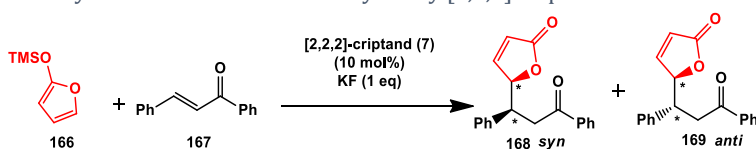
Table 3.6 Mukayama-Michael reaction catalyzed by dicyclohexane-18-crown-6 at different temperatures^a



Entry	T(°C)	Time(h)	<i>syn/anti</i> ^b	Yield ^c (%)
1	0	20	89/11	44
2	-20	2	91/9	79
3	-50	4	94/6	96
4	-78	22	93/7	83

^aAll reactions were carried out in liquid-liquid system at 0.218 mmol scale using **167** (1.0 eq.), 2-trimethylsilyloxyfuran (1.2 eq.), KF (1.0 eq.) and catalyst **5** (10 mol%) in toluene (1.1 mL). ^b*syn/anti* ratio was determined by ¹H NMR spectroscopy of the crude products. ^cIsolated yields.

Table 3.7 Mukayama-Michael reaction catalyzed by [2,2,2]-cryptand^a



Entry	Inorganic Salt	Solvent	T(°C)	Time(h)	<i>syn/anti</i> ^b	Yield ^c (%)
1	KF	Toluene	-78°C	40	2/98	82
2	KF	DCM	-78°C	5	2/98	83

^aAll reactions were carried out in liquid-liquid system at 0.218 mmol scale using **167** (1.0 eq.), trimethylsilyloxyfuran (1.2 eq.), KF (1.0 eq.) and catalyst **7** (10 mol%) in the appropriate solvent (1.1 mL). ^b*syn* and *anti* ratio was determined by ¹H NMR spectroscopy of the crude products. ^cIsolated yields.

In summary our preliminary results have shown that the vinylogous Mukayama-Michael addition of 2-trimethylsilyloxyfuran to *trans*-chalcone is promoted by TBAF or KF in presence of crown ethers of different sizes. TBAF promoted the formation of *anti* diastereoisomer with high selectivity. On the other hand, in apolar solvent such as toluene, KF/18-crown-6 ethers favour the *syn* product, while in aprotic polar or halogenated solvents, KF/15-crown-5 ethers afford exclusively to the *anti* diastereoisomer. KF/crown system definitely proved to be a more efficient and flexible promoter than TBAF, ensuring better yield and *anti*-diastereoselectivity, and giving the opportunity to switch the diastereoselectivity towards the *syn* diastereoisomer, by simply changing solvent or cavity size of macrocyclic catalyst (figure 3.7). The strenght of this work is represented by the possibility to control the diastereoselectivity. On the basis of these promising results we decided to investigate the reaction, in the optimized conditions, on different α,β -unsaturated carbonyl substrates.

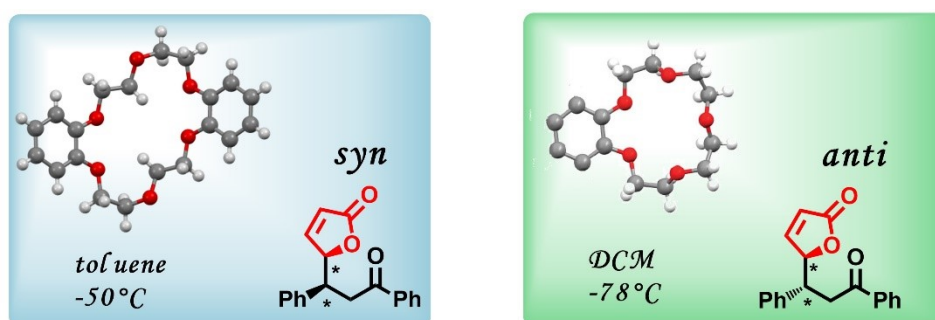


Figure 3.7 Switchable diastereoselectivity in the vinylogous Mukayama-Michael addition of 2-trimethylsilyloxyfuran by changing reaction conditions

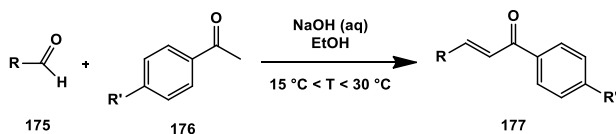
3.7 Synthesis of α,β -unsaturated carbonyl compounds

To extend the scope of conjugate addition of 2-trimethylsilyloxyfuran, different not commercially available α,β -unsaturated ketones were synthesized (compounds **177a**, **177e**, **177g-l**). For most of them the classical aldol condensation was used, as shown in Table 3.8, between aldehydes **175a-d** and ketones **176a-d**.¹¹⁷ The synthesis of *trans*-1-phenyl-2-octen-1-one (**180**) required a different strategy

¹¹⁷ E. P. Kohler, H. M. Chadwell, H. T. Clarke, R. P. Leavitt, *Organic Syntheses*, **1941**, *1*, 78.

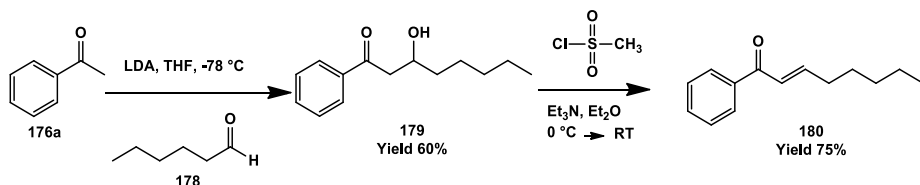
(scheme 3.14) which was realized by a modified literature procedure.¹¹⁸

Table 3.8 Synthesis of *trans*-chalcone derivatives by aldol condensations^a



Entry	Aldehyde	Ketone	Time(h)	Yield ^b (%)	Product
1			3	81	177a
2			3,5	75	177e
3			20	91	177g
4			5,5	57	177h
5			4	79	177i
6			4	50	177l

^aAll reactions were carried out at 4.2 mmol scale using the aldehydes **175** (1.0 eq.), ketones **176** (1.0 eq.), NaOH aq. (1.3 eq) in 1.25 ml of EtOH. ^bIsolated yields.



Scheme 3.14 Synthesis of *trans*-1-phenyl-2-octen-1-one (**180**)

¹¹⁸ C. Ni, L. Zhang, J. Hu, *J. Org. Chem.*, **2008**, *73*, 5699-5713.

3.8 Mukayama-Michael addition of 2-trimethylsilyloxyfuran to chalcones catalyzed by dicyclohexane-18-crown-6

With the new substrates in our hands the investigation started with dicyclohexane-18-crown-6 as catalyst, in toluene at -50°C . A correlation between the substitution on the aromatic ring of the chalcones and the diastereoisomeric ratio (Table 3.9) was observed.

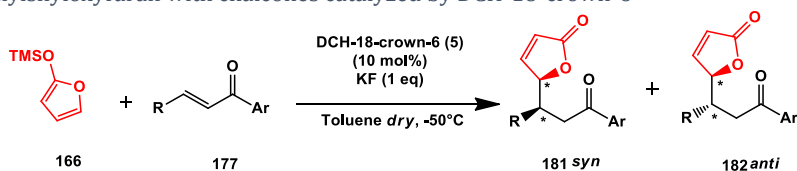
The presence of electron-withdrawing groups on the aromatic ring generally favoured the conjugate addition (Table 3.9, entries 3, 4, 5, 10) while electron-donating groups required longer reaction times (Table 3.9, entries 1, 2, 8, 9). As a consequence, moderate yields were obtained with electron-rich aromatic and heteroaromatic substrates **177b**, **177g** and **177i**. Indeed, the presence of an electron-poor β -aromatic ring probably increase the electrophile nature of C- β . Similarly, electron-poor aromatic groups attached to carbonyl group accelerate the reaction by polarizing the C=C bond and stabilizing the developing negative charge on C- α . As expected, the *syn* isomer, under those conditions, was the preferred product with all the chalcone derivatives, with *syn/anti* ranging from 80/20 to 94/6 in most cases. A lower diastereoisomeric ratio was just observed with the NO_2 -substituted Michael acceptor **177c** (73/27 *syn/anti*, entry 3). At any rate, at lower temperature, an even worse diastereoselectivity resulted.

3.9 Mukayama-Michael addition of 2-trimethylsilyloxyfuran to chalcones catalyzed by benzo-15-crown-5

The scope of conjugate addition was also studied using benzo-15-crown-5 as catalyst. The electron properties of substituents on the aromatic rings influenced the reaction rate, as well as before. In fact, longer reaction times were needed with electron-rich substrates (Table 3.10, entries 1-2 and 7-10). As expected, the *anti* isomer **182** could be obtained as a sole product with nearly all the substrates at -78°C . A small amount of *syn* byproduct was only observed with heteroaromatic substrate **177g** (*anti/syn* 97/3, entry 7). Under optimized conditions, yields were good with all the substrates. With methoxy-derivatives **177b** and **177i**, improved

yields were achieved by increasing the temperature up to -50°C , without affecting the *anti*-diastereoselectivity (Table 3.10, entries 2 and 10).

Table 3.9 *Syn*-diastereoselective vinylogous Mukayama-Michael reaction of 2-trimethylsilyloxyfuran with chalcones catalyzed by DCH-18-crown-6^a



Entry	Substrate	Time(h)	<i>syn/anti</i> ^b	Yield ^c (%)
1		85	92/8	72
2		110	85/15	50
3		20	73/27	90
4		20	87/13	81
5		65	80/20	75
6		20	88/12	80
7 ^d		40	95/5	50
8		110	94/6	72
9		85	84/16	58
10 ^e		20	89/11	99

^aAll reactions were carried out in liquid-liquid system at 0.218 mmol scale using **177** (1.0 eq.), trimethylsilyloxyfuran (1.2 eq.), KF (1.0 eq.) and catalyst **5** (10 mol%) in the appropriate solvent (1.1 mL). ^b*syn/anti* ratio was determined by ¹H NMR spectroscopy of the crude products.

^cIsolated yields. ^dReaction carried out at -78°C . ^eReaction carried out at -20°C .

Table 3.10 *Anti*-diastereoselective vinylogous Mukayama-Michael addition of 2-trimethylsilyloxyfuran to chalcones catalyzed by benzo-15-crown-5^a

Reaction scheme: 166 + 177 $\xrightarrow[\text{DCM dry, -78}^\circ\text{C}]{\text{Benzo-15-crown-5 (148) (10 mol\%), KF (1 eq)}}$ 181 *syn* + 182 *anti*

Entry	Substrate	Time(h)	<i>syn/anti</i> ^b	Yield ^c (%)
1		40	1/99	87
2 ^d		110	<1/99	75
3		20	<1/99	99
4		20	<1/99	88
5		20	<1/99	74
6		20	<1/99	90
7		40	3/97	78
8		40	<1/99	87
9 ^d		40	<1/99	70
10		20	<1/99	90

^aAll reactions were carried out in liquid-liquid system at 0.218 mmol scale using **177** (1.0 eq), trimethylsilyloxyfuran (1.2 eq), KF (1.0 eq) and catalyst **148** (10 mol%) in the appropriate solvent (1.1 mL) ^b*syn/anti* ratio was determined by ¹H NMR spectroscopy of the crude products. ^cIsolated yields. ^dReaction carried out at -50°C.

3.10 KF/crown ether promoted Mukayama-Michael addition of 2-trimethylsilyloxyfuran to different ketones.

In order to extend the scope of the methodology we decided to study the reaction with substrates different from chalcones. α,β -Unsaturated ketones **180**, **183**, **184**, with aliphatic substituents were first examined (figure 3.8).

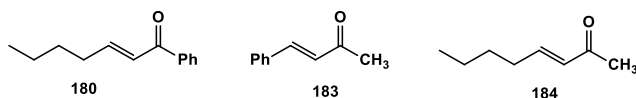
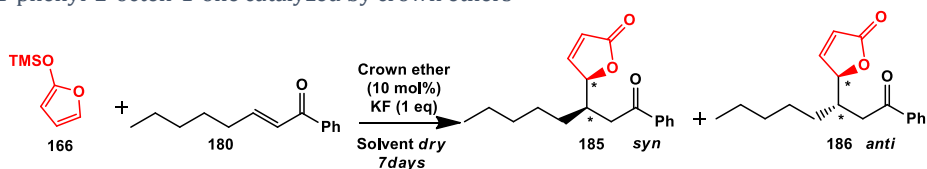


Figure 3.8 Structures of aliphatic enones

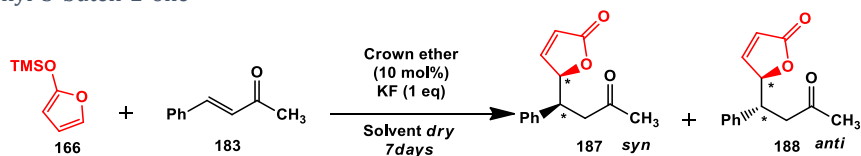
With compound **180** the reaction resulted slower in comparison with *trans*-chalcones but here again, the *anti* diastereoisomer was favoured with dicyclohexane-18-crown-6 in toluene (Table 3.11, entries 1-2) and the *syn* product with the benzo-15-crown-5 in CH_2Cl_2 (Table 3.11, entries 3-5). The best results were obtained at -20°C both with KF/dicyclohexane-18-crown-6 in toluene (*syn/anti* 84/16, 42% yield, Table 3.11, entry 2) and with with KF/benzo-15-crown-5 in CH_2Cl_2 (*anti/syn* 93/7, 62% yield, Table 3.11, entry 4). The latter catalyst, once again, has proved more efficient than TBAF (Table 3.11, entry 5). With substrate **183**, the yields were generally lower than the *trans*-chalcones, too.

Table 3.11 Vinylogous Mukayama-Michael reaction of 2-trimethylsilyloxyfuran with *trans*-1-phenyl-2-octen-1-one catalyzed by crown ethers^a



Entry	Catalyst	Solvent	T(°C)	<i>syn/anti</i> ^b	Yield ^c (%)
1	5	Toluene	-78	79/21	10
2	5	Toluene	-20	84/16	42
3	168	DCM	-78	43/57	23
4	168	DCM	-20	7/93	62
5	TBAF	DCM	-20	25/75	60

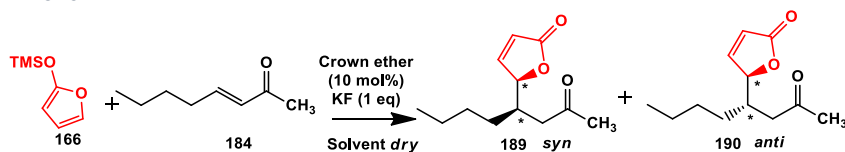
^aAll reactions were carried out in liquid-liquid system at 0.218 mmol scale using **180** (1.0 eq.), trimethylsilyloxyfuran (1.2 eq.), KF (1.0 eq.) and the appropriate catalyst (10 mol%) in the appropriate solvent (1.1 mL). ^b*syn/anti* ratio was determined by ¹H NMR spectroscopy of the crude products. ^cIsolated yields.

Table 3.12 Vinylogous Mukayama-Michael reaction of 2-trimethylsilyloxyfuran with (*E*)-4-phenyl-3-buten-2-one^a

Entry	Catalyst	Solvent	T(°C)	<i>syn/anti</i> ^b	Yield ^c (%)
1	5	Toluene	-78	93/7	17
2	5	Toluene	-30	96/4	46
3	5	Toluene	-20	95/5	60
4	5	Toluene	0	94/6	56
5	174	DCM	-78	19/81	16
6	174	DCM	-30	8/92	20
7	174	DCM	-20	16/84	37
8 ^d	174	DCM	-20	13/87	33
9 ^e	174	DCM	-20	12/88	34
10	174	DCM	0	21/79	35
11	174	CHCl ₃	0	17/83	37
12	174	Toluene	-20	81/19	21
13	5	DCM	-20	34/66	43
14	6	DCM	-20	87/13	51
15	6	CHCl ₃	-20	89/11	64
16	TBAF	DCM	-20	26/74	30

^aAll reactions were carried out in liquid-liquid system at 0.218 mmol scale using **183** (1.0 eq.), 2-trimethylsilyloxyfuran (1.2 eq.), KF (1.0 eq.) and the appropriate catalyst (10 mol%) in the appropriate solvent (1.1 mL). ^b*syn/anti* ratio was determined by ¹H NMR spectroscopy of the crude products. ^cIsolated yields. ^d3.0 eq. of KF were used. ^e2.0 eq. of 2-trimethylsilyloxyfuran were used.

However moderate yields and good diastereoselectivities were achieved, after an extensive screening of temperature, catalyst and solvent (Table 3.12): the best results were observed with KF/dicyclohexane-18-crown-6 in toluene at -30°C (*syn/anti* 96/4, 46% yield, Table 3.12, entry 2) for the *syn* isomer, and with KF/benzo-15-crown-5 in CH₂Cl₂ at -20°C (*anti/syn* 88/12, 34% yield, Table 3.12, entry 9) for the *anti* isomer. A slightly higher *anti*-diastereoselectivity was obtained at -30°C but the yield was disappointing (*anti/syn* 92/8, 20% yield, Table 3.12, entry 6). Finally, the aliphatic substrate (*E*)-3-octen-2-one **184** did not afford any product with different catalysts (Table 3.13, entries 1, 2, 3): this result demonstrates the crucial role of aromatic residues in the reactivity of the substrate.

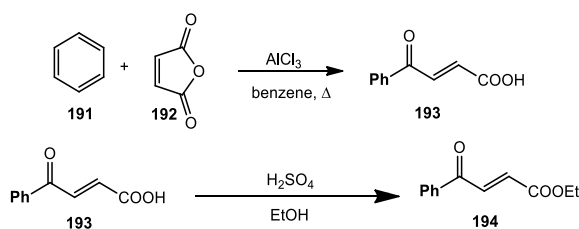
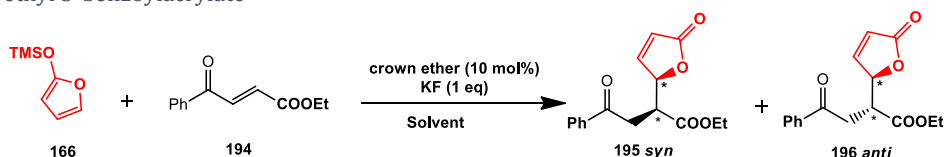
Table 3.13 Vinylogous Mukayama-Michael reaction of 2-trimethylsilyloxyfuran with (*E*)-3-octen-2-one^a

Entry	Catalyst	Solvent	T(°C)	Tempo(h)	<i>syn/anti</i> ^b	Yield ^c (%)
1	5	Toluene	-78	17	-	-
2	175	DCM	-78	17	-	-
3	175	DCM	-30	44	-	-

^aAll reactions were carried out in liquid-liquid system at 0.218 mmol scale using **175** (1.0 eq.), trimethylsilyloxyfuran (1.2 eq.), KF (1.0 eq.) and the appropriate catalyst (10 mol%) in the appropriate solvent (1.1 mL). ^b*syn* and *anti* ratio was determined by ¹H NMR spectroscopy of the crude products. ^cIsolated yields.

As mentioned before, the presence of an electron-withdrawing group attached to the β -carbon is expected to improve the reactivity of the Michael acceptor. With this in mind, we considered the ethyl ester of the β -benzoyl acrylic acid **194**, as a possible candidate for our Mukaiyama-Michael addition. The synthesis of β -benzoyl acrylic acid was performed, as reported in literature, by Friedel-Crafts acylation of benzene with maleic anhydride.¹¹⁹ Then, the esterification reaction with H₂SO₄ in presence of EtOH, led to **194** as reported in scheme 3.15. The substrate **194**, was used in the Mukayama-Michael reactions, under the usual conditions previously described. The reaction carried out with KF/DCH-18-crown-6, as expected, afforded preferentially the *syn* product with good yield, albeit with moderate diastereoselectivity (*syn/anti* 76/24, Table 3.14, entry 1). The reaction with benzo-15-crown-5 gave an high *anti*-diastereoselectivity with good yield (*anti/syn* 92/8, Table 3.14, entry 2). It should be noted that the *syn* and the *anti* products could be easily separated by column chromatography.

¹¹⁹ a) *Organic Syntheses*, Coll. Vol. 3, p.109 (1955); Vol. 29, p.11 (1949); b) B. J. Drakulić, T. P. Stanojković, Z. S. Žižak, M. M. Dabović, *European Journal of Medicinal Chemistry*, **2011**, 46, 3265-3273.

Scheme 3.15 Synthesis of ethyl 3-benzoylacrylate (**192**)Table 3.14 Vinylogous Mukayama-Michael reaction of 2-trimethylsilyloxyfuran with (*E*)-ethyl 3-benzoylacrylate^a

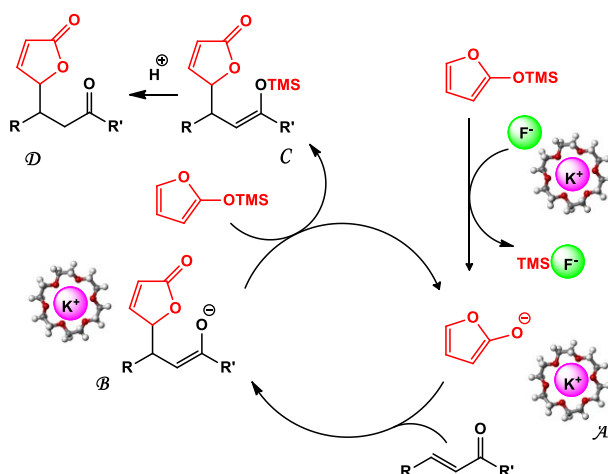
Entry	Catalyst	Solvent	T(°C)	Time(h)	<i>syn/anti</i> ^b	Yield ^c (%)
1	5	Toluene	-50	17	76/24	83
2	168	DCM	-78	15	8/92	86

^aAll reactions were carried out in liquid-liquid system at 0.218 mmol scale using **194** (1.0 eq.), trimethylsilyloxyfuran (1.2 eq.), KF (1.0 eq.) and the appropriate catalyst (10 mol%) in the appropriate solvent (1.1 mL). ^b*syn/anti* ratio was determined by ¹H NMR spectroscopy of the crude products. ^cIsolated yields.

3.11 Mechanistic hypothesis of fluoride-promoted Mukayama-Michael addition of 2-trimethylsilyloxyfuran to α,β -unsaturated carbonyl compounds catalyzed by crown ethers

Basing on the examples previously reported in literature,^{116^a} the fluoride promoted Mukayama-Michael addition of a silyl enol ether involves the formation of the corresponding enolate that after addition to the Michael acceptor, lead to an enolate adduct. The enolate adduct can desilylate the substrate and restart the catalytic cycle. From this point of view, the fluoride can be considered as an initiator. Analogously, in this case, a dienolate intermediate, generated by desilylation of 2-trimethylsilyloxyfuran can be supposed. The complexation of potassium cation with crown ethers, and formation of host-guest complex, with fluoride as counterion can be assumed. Then, through a phase-transfer process, the fluoride comes into contact with 2-trimethylsilyloxy furan, generating the ion pair dienolate/ K^+ -crown ether (Scheme 3.16, step A). This nucleophilic species reacts

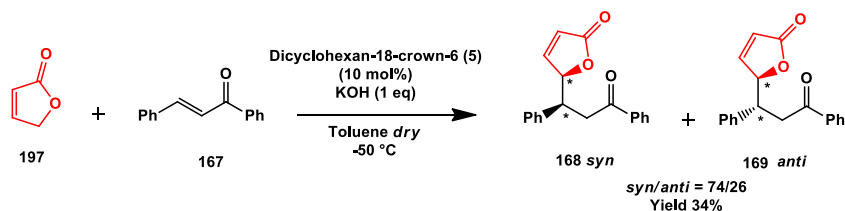
diastereoselectively with the α,β -unsaturated carbonyl compound (Scheme 3.16, step B). As a following step, the silylation of the product (Scheme 3.16, step C) with 2-trimethylsilyloxyfuran regenerate the dienolate. In support of this scenario, the product was recovered as a mixture of adduct and the corresponding silyl enol ether. The latter was usually cleaved in the following acidic work-up procedure (see the experimental section). In order to confirm the hypothetical involvement of a dienolate intermediate, some experiments were carried out. The reactions was performed with 2-(5*H*)-furanone in place of the 2-trimethylsilyloxyfuran and using KOH as a base in place of KF. In agreement with the results reported with KF/2-trimethylsilyloxyfuran, the conjugate addition with dicyclohexane-18-crown-6 led to the formation of the *syn* product (scheme 3.17) while the reaction with benzo-15-crown-5 afforded the *anti* product (scheme 3.18).



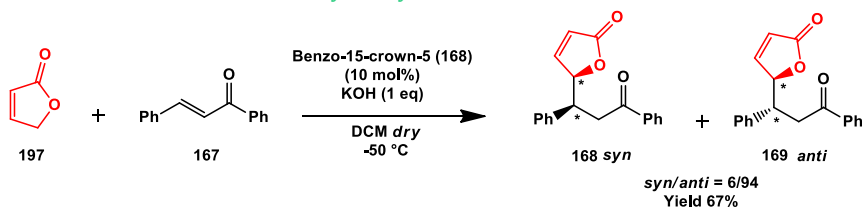
Scheme 3.16 Mechanistic hypothesis of Mukayama-Michael addition of 2-trimethylsilyloxyfuran catalyzed by crown ethers

Despite lower yields and diastereoisomeric ratios were obtained in comparison with the previously described protocol with KF and 2-trimethylsilyloxyfuran, these results support the involvement of a common dienolate intermediate. The *syn/anti* diastereoselectivity obtained under the different reaction conditions, proved to be under kinetic control. Some experiment indeed demonstrated that *syn* and *anti* adducts did not interconvert in presence of KF, dicyclohexane-18-crown-6, and 2-trimethylsilyloxyfuran. Diastereomerically enriched **169** (97/3 *anti*) was treated with KF and dicyclohexane-18-crown-6 in toluene for two days. After this time the

diastereoisomeric ratio was unchanged. The same experiment was also done in presence of 2-trimethylsilyloxyfuran with the same result. In a similar manner, diastereomerically enriched **168** (94/6 *syn*) was treated with benzo-15-crown-5 in CH_2Cl_2 for two days, in presence or not of 2-trimethylsilyloxyfuran. The diastereoisomeric ratio did not change in both cases. On the basis of these results a retro-Michael process should be ruled out.



Scheme 3.17 Mukayama-Michael addition of *trans*-chalcone with 2-(5H)-furanone catalyzed by DCH-18-crown-6



Scheme 3.18 Mukayama-Michael addition of *trans*-chalcone with 2-(5H)-furanone catalyzed by benzo-15-crown-5

3.12 Conclusions

In conclusion we have developed the first example of vinylogous Mukayama-Michael addition of 2-trimethylsilyloxyfuran, activated by potassium fluoride, catalyzed by crown ethers through a phase-transfer process. The system KF/crown ethers proved to be more efficient than TBAF with aromatic α,β -unsaturated ketones, affording γ -butenolides with good yields and high diastereoselectivity. The most intriguing aspect is the switchable *anti/syn*-diastereoselectivity controlled by the solvent polarity and the macrocycle catalyst's cavity size. To the best of our knowledge this is the first example reported in literature where the diastereoselectivity can be tuned in such an easy way. KF/dicyclohexane-18-crown-6 in toluene afforded *syn* products with good yields and good to high

diastereoselectivity, while *anti* products were obtained with good yields and excellent diastereoselectivity using KF/benzo-15-crown-5 in DCM (figure 3.9).

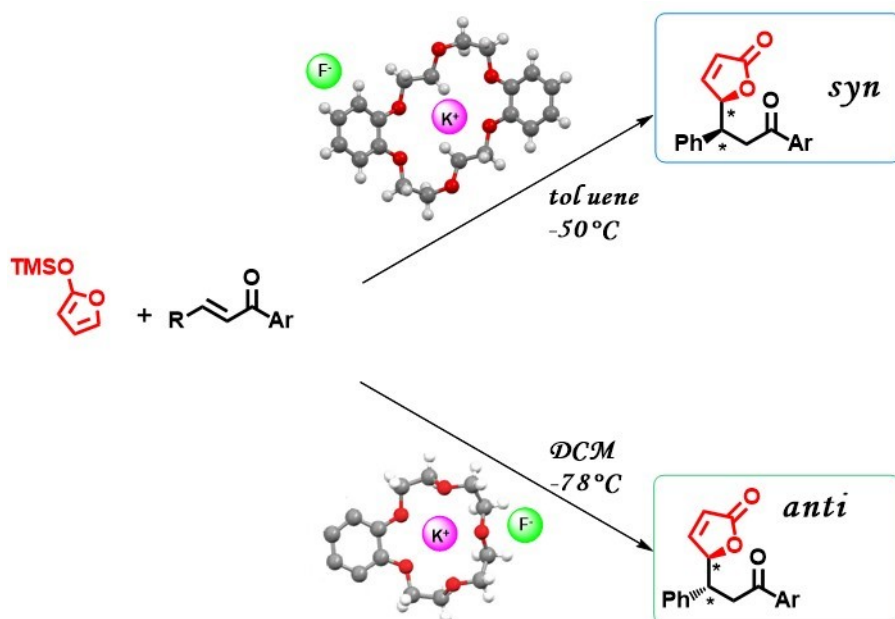


Figure 3.9 General scheme of the developed methodology

The figure 3.10 summarize the results obtained under these the two different reaction conditions. In general, for aromatic α,β -unsaturated ketones, the present methodology proved to be more efficient and flexible than the most diastereoselective procedures reported to date with achiral and commercially available catalysts.^{112,113}

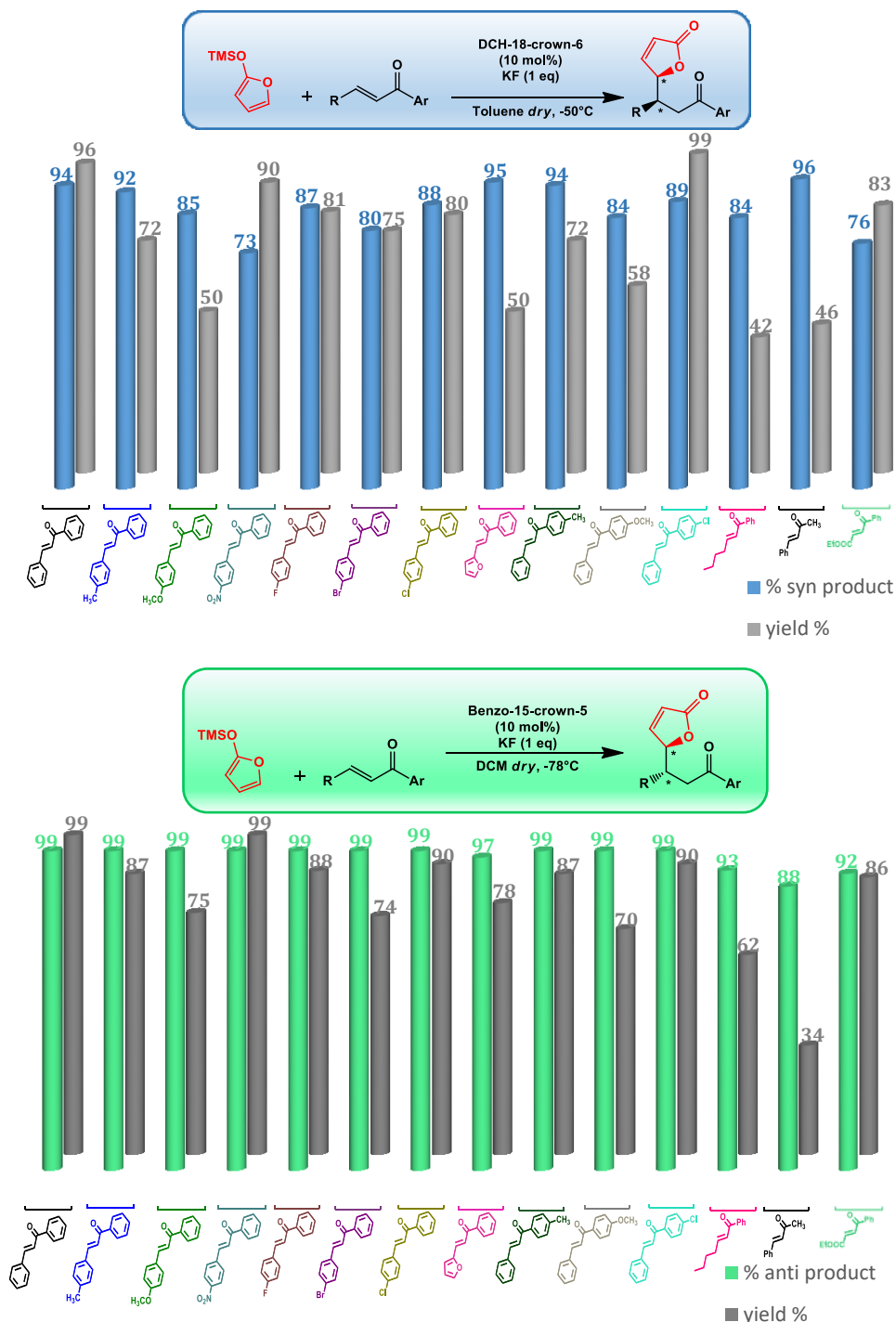


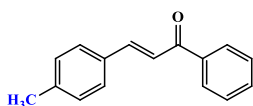
Figure 3.10 Best results obtained in Mukayama-Michael reaction of α,β -unsaturated carbonyl compounds with 2-trimethylsilyloxy furan, catalyzed by crown ethers

3.13 Experimental section

3.13.1 Synthesis of chalcone derivatives

The synthesis of compounds **177a**, **177e**, **177g**, **177h**, **177i**, **177l** were performed with a modified literature procedure.¹²⁰ To a solution of sodium hydroxide (0.2 g, 5.4 mmol) in water (2.5 mL) and ethanol (1.25 mL) ketone **176** (1.0 eq, 4.2 mmol) and aldehyde **175** (1.0 eq, 4.2 mmol) were added. The mixture was heated at 30°C for 4h. After that the stirring was removed and the mixture was left in an ice box for 12h. The white precipitate was filtered on a Büchner funnel, washed with water and cooled ethanol. Purification by silica gel chromatography (petroleum ether: Et₂O 95:5) afforded the desired products.

(E)-1-Phenyl-3-(p-tolyl)prop-2-en-1-one (177a)

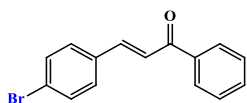


Prepared with acetophenone and *p*-methyl-benzaldehyde.

0.8 g, yield 81%, white solid; the spectroscopic data were in good agreement with the literature.¹²¹

¹H-NMR (400 MHz, CDCl₃): δ = 8.02 (dd, *J* = 8.2, 1.4 Hz, 2H), 7.80 (d, *J* = 15.7 Hz, 1H), 7.61-7.48 (m, 6H), 7.23 (d, *J* = 8.0 Hz, 2H), 2.4 (s, 3H).

(E)-3-(4-Bromophenyl)-1-phenylprop-2-en-1-one (177e)



Prepared with acetophenone and *p*-bromo-benzaldehyde.

0.9 g, yield 75%, yellow solid; the spectroscopic data were in good agreement with the literature.¹²²

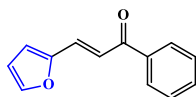
¹²⁰ E. P. Kohler, H. M. Chadwell, H. T. Clarke, R. P. Leavitt, *Organic Syntheses*, **1941**, *1*, 78.

¹²¹ G. Romanelli, G. Pasquale, A. Sathicq, H. Thomas, *Journal of Molecular Catalysis A*, **2011**, 24-32.

¹²² A. Stroba, F. Schaeffer, V. Hindie, L. Lopez-Garcia, I. Adrian, W. Fröhner, R. W. Hartmann, R. M. Biondi, M. Engel, *J. Med. Chem.* **2009**, *52*, 4683-4693.

$^1\text{H-NMR}$ (400 MHz, CDCl_3): δ = 8.01 (dd, J = 8.2, 1.1, 2H), 7.74 (d, J = 15.7 Hz, 1H), 7.62-7.50 (m, 8H).

(E)-3-(Furan-2-yl)-1-phenylprop-2-en-1-one (177g)

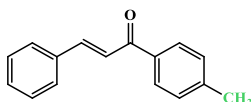


Prepared with acetophenone and furaldehyde.

0.9 g, yield 91%, white solid; the spectroscopic data were in good agreement with the literature.^{112,123}

$^1\text{H-NMR}$ (400 MHz, CDCl_3): δ = 8.03 (m, 2H), 7.54 (m, 6H), 6.73 (d, J = 3.4 Hz, 1H), 6.52 (dd, J = 3.4, 1.8 Hz, 1H).

(E)-3-Phenyl-1-(p-tolyl)prop-2-en-1-one (177h)

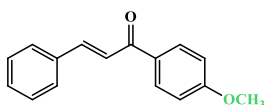


Prepared with *p*-methyl-acetophenone and benzaldehyde.

0.4 g, yield 50%, yellow solid; the spectroscopic data were in good agreement with the literature.¹²⁴

$^1\text{H-NMR}$ (400 MHz, CDCl_3): δ = 7.94 (d, J = 8.0 Hz, 2H), 7.81 (d, J = 15.7 Hz, 1H), 7.65 (m, 2H), 7.54 (d, J = 15.7 Hz, 1H), 7.42 (m, 3H), 7.31 (d, J = 8.0, 2H), 2.44 (s, 3H).

(E)-1-(4-Methoxyphenyl)-3-phenylprop-2-en-1-one (177i)



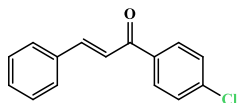
Prepared with *p*-methoxy-acetophenone and benzaldehyde.

0.4 g, yield 57%, yellow solid; the spectroscopic data were in good agreement with the literature.¹²⁴

$^1\text{H-NMR}$ (300 MHz, CDCl_3): δ = 8.05 (d, J = 8.7 Hz, 2H), 7.81 (d, J = 15.7 Hz, 1H), 7.65 (m, 2H), 7.55 (d, J = 15.7 Hz, 1H), 7.42 (m, 3H), 6.99 (d, J = 8.7, 2H), 3.90 (s, 3H).

¹²³ H. Lebel, M. Davi, *Adv. Synth. Catal.*, **2008**, *350*, 2352-2358.

¹²⁴ X. F. Wu, H. Neumann, A. Spennenberg, T. Schulz, H. Jiao, M. Beller, *J. Am. Chem. Soc.*, **2010**, *132*, 14596-14602.

(E)-1-(4-Chlorophenyl)-3-phenylprop-2-en-1-one (177I)

Prepared with *p*-chloro-acetophenone and benzaldehyde.

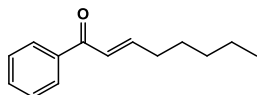
0.6 g, yield 79%, white solid; the spectroscopic data were in good agreement with the literature.¹²⁴

¹H-NMR (400 MHz, CDCl₃): δ = 7.96 (d, *J* = 8.6 Hz, 2H), 7.82 (d, *J* = 15.7 Hz, 1H), 7.64 (m, 2H), 7.49 (m, 3H), 7.43 (m, 3H).

3.13.2 Synthesis of *trans*-1-Phenyl-2-octen-1-one (180)

The synthesis of compound **180** was performed as previously described in literature.¹²⁵ To a solution of diisopropylamine (1.7 mL, 12.5 mmol) in 42 mL of *dry* THF at -78°C *n*-butyllithium (2.5 M in hexanes, 5.0 mL, 12.5 mmol) was added and the mixture was stirred for 30 min. The acetophenone (0.97 mL, 8.3 mmol) was added. After 30 min the hexanal (2.2 mL, 18.3 mmol) was added. After 120 min, the reaction was quenched with a solution of HOAc/H₂O (1:1 v/v) at -78°C. The flask was warmed to room temperature, and water (42 mL) was added. The aqueous layer was extracted with Et₂O (3 x 50 mL). The collected organic layers were washed with saturated solution of NaHCO₃ (50 mL) and brine (50 mL), dried over Na₂SO₄ and concentrated in vacuo. Purification by silica gel chromatography (petroleum ether : Et₂O 90:10 – 70:30) afforded the desired hydroxyl keton **179** (0.6 g, yield 60%). The aldol product was dissolved in 8.3 mL *dry* Et₃N at 0°C and methansulfonyl chloride (0.11 mL, 1.46 mmol) was added. The reaction was warmed to room temperature for 16h. Then water (6 mL) was added and the aqueous layer was extracted with Et₂O (3 x 9 mL). The combined organic layers were washed with 1M HCl aqueous solution (13 mL) and a saturated solution of NaHCO₃ (9 mL), dried over Na₂SO₄ and concentrated in vacuo. Purification by silica gel chromatography (petroleum ether : Et₂O 95:5 – 90:10) afforded the desired product **180**.

¹²⁵ R. Shintani, G. Fu, *Organic Letters*, **2002**, *4*, 3699-3702.

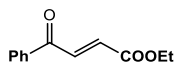
trans-1-Phenyl-2-octen-1-one (180)

170 mg, yield 75%, colorless liquid; the spectroscopic data were in good agreement with the literature.¹²⁶

¹H-NMR (400 MHz, CDCl₃): δ = 7.91 (d, J = 7.9 Hz, 2H), 7.50 (m, 3H), 7.06 (m, 1H), 6.87 (dd, J = 15.4, 1.3 Hz, 1H), 2.30 (m, 2H), 1.52 (m, 2H), 1.33 (m, 4H), 0.90 (t, J = 7.0 Hz, 3H).

3.13.3 Synthesis of ethyl 3-Benzoylacrylate (194).

The synthesis of compound **192** was performed as previously described in literature.¹⁰⁷ To a stirred solution of maleic anhydride (3.0 g, 30 mmol) in anhydrous benzene (18 mL), anhydrous AlCl₃ (8.8 g, 66 mmol) was added in portions in 30 minutes. The reaction mixture was warmed at reflux for 1 h, then cooled at 0°C and water (18 mL) was added. Concentrated HCl (5 mL) was added and the mixture was stirred for further 40 minutes, concentrated in vacuo. The residue was worked up with a solution of Na₂CO₃ until pH=8, warming at 40–50°C for 15 minutes, and washed with DCM (2 x 30mL). To the aqueous layer concentrated HCl was added dropwise until pH=2 and the resulting solid was filtered and crystallized from toluene. Finally the product was warmed at reflux in a solution of concentrated H₂SO₄ (8 μ L) and EtOH (50 μ L). The mixture was treated with water (0.3 mL) and extracted with EtOH (2 x 1 mL). The collected organic layers were washed with saturated solution of NaHCO₃ to pH=7 and then with water (2 mL), dried over Na₂SO₄ and concentrated in vacuo.

Ethyl 3-benzoylacrylate (194)

68.0 mg, yield 20%, colorless liquid. The spectroscopic data were in good agreement with the literature.

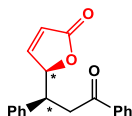
¹²⁶ R. Shintani, G. Fu, *Organic Letters*, **2002**, *4*, 3699-3702.

$^1\text{H-NMR}$ (400 MHz, CDCl_3): δ = 7.97 (m, 2H), 7.89 (d, J = 15.5 Hz, 1H), 7.60 (m, 1H), 7.49 (m, 2H), 6.86 (d, J = 15.5 Hz, 1H), 4.28 (q, J = 7.1 Hz, 2H), 1.33 (t, J = 7.2 Hz, 3H).

3.13.4 General procedure for diastereoselective vinylogous Mukayama-Michael addition with KF and 2-trimethylsilyloxyfuran catalyzed by crown ethers.

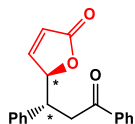
To a stirred solution of α,β -unsaturated carbonyl compound (1.0 eq, 0.218 mmol), KF (1.0 eq, 0.218 mmol), and catalyst (0.1 eq, 0.0218 mmol) in the appropriate solvent (1.1 mL) under inert atmosphere, the 2-trimethylsilyloxyfuran (1.2 eq, 0.262 mmol) was added after 15 min. The resulting reaction mixture was allowed to stir at the appropriate temperature for the required time. After complete conversion, estimate with TLC, the mixture was treated with 1M HCl aqueous solution (1 mL) and THF (3 mL). The resulting solution was stirred for 2h. The mixture was diluted with water (1.2 mL) and extracted with DCM (3 x 2 mL). The collected organic layers were washed with saturated solution of NaHCO_3 (1.5 mL), dried over Na_2SO_4 and concentrated in vacuo.

(R^*,S^*)-5-(3-Oxo-1,3-diphenylpropyl)furan-2(5H)-one (168)



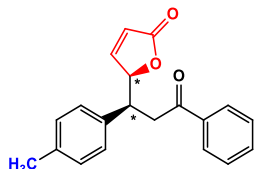
61 mg, yield 96%, white solid : mp = 97-100 °C.

$^1\text{H-NMR}$ (400 MHz, CDCl_3): δ = 7.97 (m, 2H), 7.58 (m, 1H), 7.46 (m, 2H), 7.36 (m, 1H), 7.30-7.16 (m, 5H), 5.85 (dd, J = 5.7, 1.9 Hz, 1H), 5.45 (m, 1H), 3.96 (m, 1H), 3.80 (dd, J = 18.0, 8.2 Hz, 1H), 3.46 (dd, J = 18.0, 5.5 Hz, 1H). $^{13}\text{C-NMR}$ (100 MHz, CDCl_3): δ = 197.7, 172.8, 155.3, 137.1, 136.4, 133.4, 128.6, 128.5, 128.3, 127.9, 127.5, 121.9, 84.3, 42.8, 40.0. HRMS (MALDI) $[\text{M} + \text{H}]^+$ calcd for $\text{C}_{19}\text{H}_{17}\text{O}_3$ 293.1172, found 293.1172. HRMS (MALDI) $[\text{M} + \text{Na}]^+$ calcd for $\text{C}_{19}\text{H}_{16}\text{NaO}_3$ 315.0992, found 315.0991.

(S*,S*)-5-(3-Oxo-1,3-diphenylpropyl)furan-2(5H)-one (169)

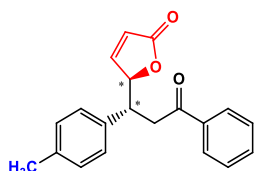
64.0 mg, yield 99%, white solid : mp = 83-85 °C.

¹H-NMR (400 MHz, CDCl₃): δ = 7.87 (m, 2H), 7.53 (m, 1H), 7.42 (m, 2H), 7.36-7.20 (m, 6H), 6.07 (dd, J = 5.7, 2.0 Hz, 1H), 5.25 (m, 1H), 3.69 (m, 1H), 3.56 (dd, J = 17.7, 5.0 Hz, 1H), 3.48 (dd, J = 17.7, 8.1 Hz, 1H). ¹³C-NMR (100 MHz, CDCl₃): δ = 197.2, 172.6, 155.6, 139.5, 136.4, 133.2, 128.8, 128.5, 128.0, 127.8, 127.5, 121.8, 85.7, 44.2, 40.0. HRMS (MALDI) [M + H]⁺ calcd for C₁₉H₁₇O₃ 293.1172, found 293.1170.

(R*,S*)-5-(3-Oxo-3-phenyl-1-(4-methylphenyl)propyl)furan-2(5H)-one**(181a)**

48.2 mg, yield 72%, white solid : mp = 129-131 °C.

¹H-NMR (400 MHz, CDCl₃): δ = 7.98 (m, 2H), 7.58 (m, 1H), 7.47 (m, 2H), 7.35 (m, 1H), 7.11-7.02 (m, 4H), 5.86 (m, 1H), 5.43 (m, 1H), 3.93 (m, 1H), 3.78 (dd, J = 18.0, 8.3 Hz, 1H), 3.43 (dd, J = 18.0, 5.7 Hz, 1H), 2.28 (s, 3H). ¹³C-NMR (100 MHz, CDCl₃): δ = 197.9, 172.9, 155.3, 137.3, 136.6, 134.1, 133.5, 129.3, 128.7, 128.2, 128.0, 122.1, 84.5, 42.5, 40.2, 21.0. HRMS (MALDI) [M + H]⁺ calcd for C₁₉H₁₉O₃ 307.1329, found 307.1327.

(S*,S*)-5-(3-Oxo-3-phenyl-1-(4-methylphenyl)propyl)furan-2(5H)-one**(182a)**

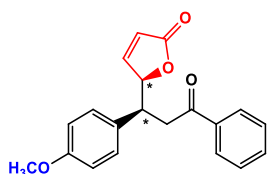
57.1 mg, yield 87%, white solid : mp = 95-98 °C.

¹H-NMR (400 MHz, CDCl₃): δ = 7.88 (m, 2H), 7.54 (m, 1H), 7.43 (m, 2H), 7.28 (m, 1H), 7.22 (d, J = 8.0 Hz, 2H), 7.13 (d, J = 8.0 Hz, 2H), 6.07 (dd, J = 5.8, 2.0 Hz, 1H),

5.24 (m, 1H), 3.64 (m, 1H), 3.57 (dd, $J = 17.5, 4.8$ Hz, 1H), 3.46 (dd, $J = 17.5, 8.3$ Hz, 1H), 2.31 (s, 3H). $^{13}\text{C-NMR}$ (100 MHz, CDCl_3): $\delta = 197.4, 172.7, 155.6, 137.3, 136.6, 136.5, 133.3, 129.6, 128.6, 127.9$ (2C), 121.9, 85.9, 44.1, 40.2, 21.0. HRMS (MALDI) $[\text{M} + \text{H}]^+$ calcd for $\text{C}_{19}\text{H}_{19}\text{O}_3$ 307.132, found 307.1329.

(R^*,S^*)-5-(3-Oxo-3-phenyl-1-(4-methoxyphenyl)propyl)furan-2(5H)-one

(181b)

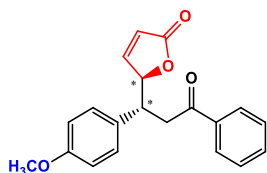


34.7 mg, yield 50%, yellow liquid.

$^1\text{H-NMR}$ (400 MHz, CDCl_3): $\delta = 7.97$ (m, 2H), 7.58 (m, 1H), 7.47 (m, 2H), 7.34 (m, 1H), 7.12 (d, $J = 8.4$ Hz, 2H), 6.79 (d, $J = 8.4$ Hz, 2H), 5.86 (m, 1H), 5.41 (m, 1H), 3.91 (m, 1H) 3.82-3.69 (m, 4H), 3.42 (dd, $J = 17.9$ Hz, 5.5 Hz, 1H). $^{13}\text{C-NMR}$ (100 MHz, CDCl_3): $\delta = 197.9, 172.9, 158.9, 155.4, 136.6, 133.5, 129.1, 129.4, 128.7, 128.0, 122.1, 113.9, 84.6, 55.2, 42.1, 40.4$. HRMS (MALDI) $[\text{M} + \text{H}]^+$ calcd for $\text{C}_{20}\text{H}_{19}\text{O}_4$ 323.1278, found 323.1277.

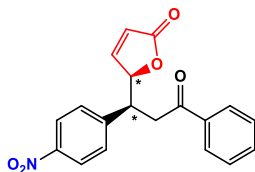
(S^*,S^*)-5-(3-Oxo-3-phenyl-1-(4-methoxyphenyl)propyl)furan-2(5H)-one

(182b)



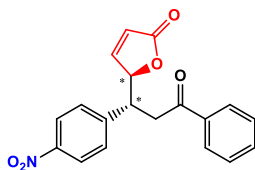
52.7 mg, yield 75%, yellow liquid.

$^1\text{H-NMR}$ (400 MHz, CDCl_3): $\delta = 7.87$ (m, 2H), 7.53 (m, 1H), 7.41 (m, 2H), 7.31-7.17 (m, 3H), 6.84 (d, $J = 8.6$ Hz, 2H), 6.06 (m, 1H), 5.22 (m, 1H), 3.76 (s, 3H), 3.62 (m, 1H), 3.53 (dd, $J = 17.5$ Hz, 5.0 Hz, 1H), 3.43 (dd, $J = 17.5, 8.3$ Hz, 1H). $^{13}\text{C-NMR}$ (100 MHz, CDCl_3): $\delta = 197.4, 172.7, 158.9, 155.6, 136.6, 133.3, 131.5, 129.1, 128.6, 127.9, 121.9, 114.2, 86.0, 55.2, 43.7, 40.3$. HRMS (MALDI) $[\text{M} + \text{H}]^+$ calcd for $\text{C}_{20}\text{H}_{19}\text{O}_4$ 323.1278, found 323.1277.

(*R,*S**)-5-(3-Oxo-3-phenyl-1-(4-nitrophenyl)propyl)furan-2(5H)-one (181c)**

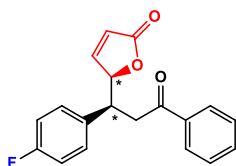
65.9 mg, yield 90%, colorless liquid.

$^1\text{H-NMR}$ (400 MHz, CDCl_3): δ = 8.14 (m, 2H), 7.97 (m, 2H), 7.61 (m, 1H), 7.49 (m, 2H), 7.42-7.36 (m, 3H), 5.90 (m, 1H), 5.47 (m, 1H), 4.08 (m, 1H), 3.84 (dd, J = 18.3, 7.7 Hz, 1H), 3.56 (dd, J = 18.3, 6.1 Hz, 1H). $^{13}\text{C-NMR}$ (100 MHz, CDCl_3): δ = 196.9, 172.1, 154.4, 147.4, 144.7, 136.2, 133.9, 129.5, 128.8, 128.0, 123.8, 122.8, 83.6, 42.9, 40.3. HRMS (MALDI) $[\text{M} + \text{H}]^+$ calcd for $\text{C}_{19}\text{H}_{16}\text{NO}_5$ 338.1023, found 338.1017.

(*S,*S**)-5-(3-Oxo-3-phenyl-1-(4-nitrophenyl)propyl)furan-2(5H)-one (182c)**

73.8 mg, yield 99%, white solid : mp = 163-165 °C.

$^1\text{H-NMR}$ (400 MHz, CDCl_3): δ = 8.18 (d, J = 8.3 Hz, 2H), 7.87 (d, J = 7.9 Hz, 2H), 7.63-7.52 (m, 3H), 7.44 (m, 2H), 7.34 (d, J = 5.6 Hz, 1H), 6.14 (m, 1H), 5.30 (m, 1H), 3.93 (m, 1H), 3.56-3.38 (m, 2H). $^{13}\text{C-NMR}$ (100 MHz, CDCl_3): δ = 196.5, 172.1, 154.6, 147.4, 147.3, 136.0, 133.7, 129.3, 128.7, 127.9, 124.0, 122.7, 84.7, 43.5, 38.8. HRMS (MALDI) $[\text{M} + \text{H}]^+$ calcd for $\text{C}_{19}\text{H}_{16}\text{NO}_5$ 338.1023, found 338.1024.

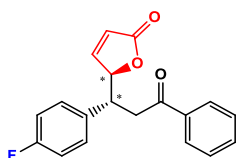
(*R,*S**)-5-(3-Oxo-3-phenyl-1-(4-fluorophenyl)propyl)furan-2(5H)-one (181d)**

54.8 mg, yield 81%, white solid : mp = 106-109 °C.

$^1\text{H-NMR}$ (400 MHz, CDCl_3): δ = 7.96 (m, 2H), 7.57 (m, 1H), 7.46 (m, 2H), 7.34 (m,

1H), 7.17 (m, 2H), 6.94 (m, 2H), 5.86 (m, 1H), 5.41 (m, 1H), 3.95 (m, 1H), 3.77 (dd, $J = 18.1, 8.0$ Hz, 1H), 3.45 (dd, $J = 18.1, 5.0$ Hz, 1H). $^{13}\text{C-NMR}$ (100 MHz, CDCl_3): $\delta = 197.5, 172.6, 162.0$ (d, $J = 246$ Hz), 155.1, 136.4, 133.5, 132.8, 129.9 (d, $J = 8$ Hz), 128.7, 127.9, 122.2, 115.4 (d, $J = 21$ Hz), 84.2, 42.1, 40.4. HRMS (MALDI) $[\text{M} + \text{H}]^+$ calcd for $\text{C}_{19}\text{H}_{16}\text{FO}_3$ 311.1078, found 311.1073.

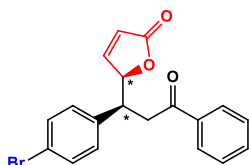
(S^*,S^*)-5-(3-Oxo-3-phenyl-1-(4-fluorophenyl)propyl)furan-2(5H)-one (182d)



58.8 mg, yield 88%, white solid : mp = 102-105 °C.

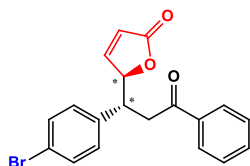
$^1\text{H-NMR}$ (CDCl_3 , 400 MHz): $\delta = 7.86$ (m, 2H), 7.54 (m, 1H), 7.42 (m, 2H), 7.36-7.25 (m, 3H), 7.0 (m, 2H), 6.08 (dd, $J = 5.7, 1.9$ Hz, 1H), 5.23 (m, 1H), 3.71 (m, 1H), 3.51 (dd, $J = 17.8, 5.0$ Hz, 1H), 3.42 (dd, $J = 17.8, 8.0$ Hz, 1H). $^{13}\text{C-NMR}$ (100 MHz, CDCl_3): $\delta = 197.1, 172.4, 161.9$ (d, $J = 246$ Hz), 155.2, 136.3, 135.3 (d, $J = 2$ Hz), 133.4, 129.7 (d, $J = 8$ Hz), 128.6, 127.8, 122.1, 115.7 (d, $J = 21$ Hz), 85.5, 43.3, 39.8. HRMS (MALDI) $[\text{M} + \text{H}]^+$ calcd for $\text{C}_{19}\text{H}_{16}\text{FO}_3$ 311.1078, found 311.1079.

(R^*,S^*)-5-(3-Oxo-3-phenyl-1-(4-bromophenyl)propyl)furan-2(5H)-one(181e)



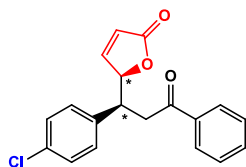
61.0 mg, yield 75%, colorless liquid.

$^1\text{H-NMR}$ (400 MHz, CDCl_3): $\delta = 7.95$ (m, 2H), 7.58 (m, 1H), 7.46 (m, 2H), 7.38 (m, 2H), 7.34 (m, 1H), 7.08 (d, $J = 8.3$ Hz, 2H), 5.87 (m, 1H), 5.41 (m, 1H), 3.92 (m, 1H), 3.76 (dd, $J = 18.0, 8.1$ Hz, 1H), 3.45 (dd, $J = 18.0, 5.8$ Hz, 1H). $^{13}\text{C-NMR}$ (100 MHz, CDCl_3): $\delta = 197.4, 172.6, 155.0, 136.4, 136.2, 133.6, 131.7, 130.1, 128.7, 128.0, 122.4, 121.6, 84.0, 42.4, 40.2$. HRMS (MALDI) $[\text{M} + \text{Na}]^+$ calcd for $\text{C}_{19}\text{H}_{15}\text{BrNaO}_3$ 393.0098, found 393.0096.

(S*,S*)-5-(3-Oxo-3-phenyl-1-(4-bromophenyl)propyl)furan-2(5H)-one**(182e)**

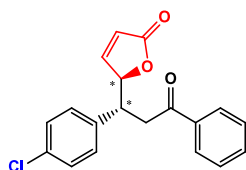
60.1 mg, yield 74%, white solid : mp = 138-141 °C.

¹H-NMR (400 MHz, CDCl₃): δ = 7.87 (m, 2H), 7.56 (m, 1H), 7.49-7.36 (m, 4H), 7.32-7.18 (m, 3H), 6.10 (dd, J = 5.8, 2.0 Hz, 1H), 5.24 (m, 1H), 3.70 (m, 1H), 3.51 (dd, J = 17.8, 5.1 Hz, 1H), 3.41 (dd, J = 17.7, 8.2 Hz, 1H). ¹³C-NMR (100 MHz, CDCl₃): δ = 197.0, 172.4, 155.1, 138.7, 136.3, 133.5, 132.0, 129.9, 128.7, 127.9, 122.3, 121.6, 85.3, 43.6, 39.6. HRMS (ESI) [M + Na]⁺ calcd for C₁₉H₁₅BrNaO₃ 393.0098, found 393.0096.

(R*,S*)-5-(3-Oxo-3-phenyl-1-(4-chlorophenyl)propyl)furan-2(5H)-one (181f)

57.3 mg, yield 80%, white solid : mp = 115-118 °C.

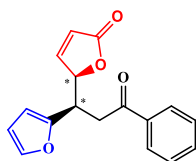
¹H-NMR (400 MHz, CDCl₃): δ = 7.97 (m, 2H), 7.59 (m, 1H), 7.48 (m, 2H), 7.34 (m, 1H), 7.24 (m, 2H), 7.15 (m, 2H), 5.88 (dd, J = 5.7, 1.9 Hz, 1H), 5.43 (m, 1H), 3.94 (m, 1H), 3.78 (dd, J = 18.0, 8.0 Hz, 1H), 3.46 (dd, J = 18.0, 5.7 Hz, 1H). ¹³C-NMR (100 MHz, CDCl₃): δ = 197.5, 172.6, 154.9, 136.4, 135.6, 133.6, 133.5, 129.7, 128.8, 128.7, 128.0, 122.4, 84.1, 42.3, 40.3. HRMS (MALDI) [M + H]⁺ calcd for C₁₉H₁₆ClO₃ 327.0783, found 327.0783.

(S*,S*)-5-(3-Oxo-3-phenyl-1-(4-chlorophenyl)propyl)furan-2(5H)-one (182f)

64.2 mg, yield 90%, white solid : mp = 111-113 °C.

$^1\text{H-NMR}$ (400 MHz, CDCl_3): δ = 7.86 (m, 2H), 7.54 (m, 1H), 7.42 (m, 2H), 7.34-7.24 (m, 5H), 6.08 (dd, J = 5.6, 1.5 Hz, 1H), 5.23 (d, J = 6.7 Hz, 1H), 3.71 (m, 1H), 3.51 (dd, J = 17.8, 5.0 Hz, 1H), 3.42 (dd, J = 17.8, 8.2 Hz, 1H). $^{13}\text{C-NMR}$ (100 MHz, CDCl_3): δ = 197.0, 172.4, 155.2, 138.2, 136.3, 133.5, 133.4, 129.5, 129.0, 128.7, 127.9, 122.2, 85.4, 43.5, 39.6. HRMS (MALDI) $[\text{M} + \text{H}]^+$ calcd for $\text{C}_{19}\text{H}_{16}\text{ClO}_3$ 327.0783, found 327.0782.

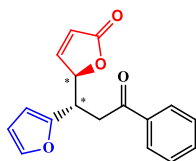
(R^*,S^*) -5-(3-Oxo-3-phenyl-1-(2-furanyl)propyl)furan-2(5H)-one (181g)



30.5 mg, yield 50%, yellow solid : mp = 91-93 °C.

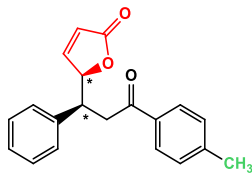
$^1\text{H-NMR}$ (400 MHz, CDCl_3): δ = 7.96 (m, 2H), 7.58 (m, 1H), 7.51-7.40 (m, 4H), 6.25 (m, 1H), 6.15 (d, J = 3.0 Hz, 1H), 5.99 (dd, J = 5.7, 1.9 Hz, 1H), 5.38 (m, 1H), 4.16 (m, 1H), 3.57 (dd, J = 18.0, 7.3 Hz, 1H), 3.41 (dd, J = 18.0, 6.6 Hz, 1H). $^{13}\text{C-NMR}$ (100 MHz, CDCl_3): δ = 197.1, 172.6, 154.8, 151.3, 141.8, 136.3, 133.5, 128.7, 128.0, 122.1, 110.4, 107.8, 83.3, 38.0, 36.8. HRMS (MALDI) $[\text{M} + \text{Na}]^+$ calcd for $\text{C}_{17}\text{H}_{14}\text{NaO}_4$ 305.0784, found 305.0784.

(S^*,S^*) -5-(3-Oxo-3-phenyl-1-(2-furanyl)propyl)furan-2(5H)-one (182g)



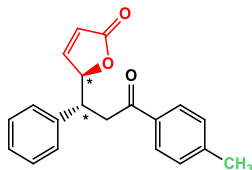
47.9 mg, yield 78%, yellow solid : mp = 80-83 °C.

$^1\text{H-NMR}$ (400 MHz, CDCl_3): δ = 7.92 (m, 2H), 7.56 (m, 1H), 7.44 (m, 2H), 7.40 (m, 1H), 7.32 (m, 1H), 6.29 (m, 1H), 6.21 (d, J = 3.3 Hz, 1H), 6.07 (dd, J = 5.7, 1.9 Hz, 1H), 5.34 (m, 1H), 3.88 (m, 1H), 3.54 (dd, J = 17.7, 7.8 Hz, 1H), 3.44 (dd, J = 17.7, 5.4 Hz, 1H). $^{13}\text{C-NMR}$ (100 MHz, CDCl_3): δ = 196.9, 172.4, 155.1, 152.2, 142.0, 136.4, 133.4, 128.7, 128.0, 122.0, 110.5, 107.6, 83.7, 38.0, 37.8. HRMS (MALDI) $[\text{M} + \text{H}]^+$ calcd for $\text{C}_{17}\text{H}_{15}\text{NaO}_4$ 283.0965, found 283.0965.

(*R,*S**)-5-(3-Oxo-3-(4-methylphenyl)1-phenylpropyl)furan-2(5H)-one****(181h)**

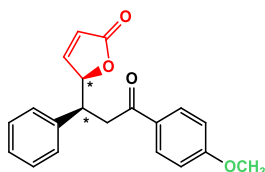
48.2 mg, yield 72%, white solid : mp = 110-113 °C.

¹H-NMR (400 MHz, CDCl₃): δ = 7.88 (*d*, *J* = 8.2 Hz, 2H), 7.36 (*m*, 1H), 7.30-7.13 (*m*, 7H), 5.85 (*dd*, *J* = 5.7, 2.0, 1H), 5.45 (*m*, 1H), 3.96 (*m*, 1H), 3.79 (*dd*, *J* = 18.0, 8.4 Hz, 1H), 3.43 (*dd*, *J* = 18.0, 5.5 Hz, 1H), 2.41 (*s*, 3H). ¹³C-NMR (100 MHz, CDCl₃): δ = 197.4, 172.9, 155.3, 144.4, 137.3, 134.1, 129.4, 128.6, 128.4, 128.2, 127.6, 122.0, 84.4, 43.0, 40.0, 21.6. HRMS (MALDI) [*M* + *H*]⁺ calcd for C₂₀H₁₉O₃ 307.1329, found 307.1329.

(*S,*S**)-5-(3-Oxo-3-(4-methylphenyl)1-phenylpropyl)furan-2(5H)-one (182h)**

57.1 mg, yield 87%, white solid : mp = 104-106 °C.

¹H-NMR (400 MHz, CDCl₃): δ = 7.78 (*d*, *J* = 8.1 Hz, 2H), 7.38-7.11 (*m*, 8 H), 6.06 (*m*, 1H), 5.26 (*d*, *J* = 7.1 Hz, 1H), 3.71 (*m*, 1H), 3.53 (*dd*, *J* = 17.6, 5.1 Hz, 1H), 3.43 (*dd*, *J* = 17.6, 8.0 Hz, 1H), 2.39 (*s*, 3H). ¹³C-NMR (100 MHz, CDCl₃): δ = 196.9, 172.7, 155.6, 144.2, 139.7, 134.1, 129.3, 128.9, 128.1, 128.0, 127.6, 121.9, 85.8, 44.3, 39.8, 21.6. HRMS (ESI) [*M* + *H*]⁺ calcd for C₂₀H₁₉O₃ 307.1329, found 307.1329.

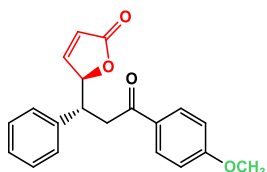
(*R,*S**)-5-(3-Oxo-3-(4-methoxyphenyl)1-phenylpropyl)furan-2(5H)-one****(181i)**

41.0 mg, yield 58%, white solid : mp = 149-152 °C.

$^1\text{H-NMR}$ (400 MHz, CDCl_3): δ = 7.97 (m, 2H), 7.35 (m, 1H), 7.27-7.17 (m, 5H), 6.94 (m, 2H), 5.84 (dd, J = 5.7, 2.0 Hz, 1H), 5.45 (m, 1H), 3.95 (m, 1H), 3.87 (s, 3H), 3.77 (dd, J = 17.7, 8.5 Hz, 1H), 3.39 (dd, J = 17.7, 5.3 Hz, 1H). $^{13}\text{C-NMR}$ (100 MHz, CDCl_3): δ = 196.3, 172.9, 163.8, 155.3, 137.3, 130.4, 129.7, 128.6, 128.4, 127.5, 122.0, 113.8, 84.4, 55.5, 43.0, 39.7. HRMS (MALDI) $[\text{M} + \text{H}]^+$ calcd for $\text{C}_{20}\text{H}_{19}\text{O}_4$ 323.1278, found 323.1278.

(S^*,S^*) -5-(3-Oxo-3-(4-methoxyphenyl)1-phenylpropyl)furan-2(5H)-one

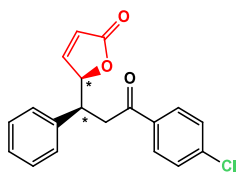
(182i)



49.0 mg, yield 70%, white solid : mp = 139-141 °C.

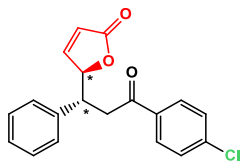
$^1\text{H-NMR}$ (400 MHz, CDCl_3): δ = 7.86 (d, J = 8,6 Hz, 2H), 7.37-7.20 (m, 6H), 6.89 (d, J = 8.6 Hz, 2H), 6.05 (m, 1H), 5.26 (d, J = 6.8 Hz, 2H), 3.84 (s, 3H) 3.70 (m, 1H), 3.50 (dd, J = 17.4, 5.1 Hz, 1H), 3.40 (dd, J = 17.4, 8.0 Hz, 1H). $^{13}\text{C-NMR}$ (100 MHz, CDCl_3): δ = 195.7, 172.7, 163.6, 155.6, 139.8, 130.2, 129.7, 128.8, 128.1, 127.6, 121.9, 113.7, 85.8, 55.4, 44.3, 39.5. HRMS (ESI) $[\text{M} + \text{H}]^+$ calcd for $\text{C}_{20}\text{H}_{19}\text{O}_4$ 323.1278, found 323.1278.

(R^*,S^*) -5-(3-Oxo-3-(4-chlorophenyl)1-phenylpropyl)furan-2(5H)-one (181j)



71.0 mg, yield 99%, white solid : mp = 100-102 °C.

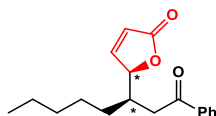
$^1\text{H-NMR}$ (400 MHz, CDCl_3): δ = 7.91 (m, 2H), 7.44 (m, 2H), 7.34 (m, 1H), 7.30-7.15 (m, 5H), 5.85 (dd, J = 5.7, 1.9 Hz, 1H), 5.44 (m, 1H), 3.95 (m, 1H), 3.76 (dd, J = 18.0, 8.3 Hz, 1H), 3.43 (dd, J = 18.0, 5.6 Hz, 1H). $^{13}\text{C-NMR}$ (100 MHz, CDCl_3): δ = 196.6, 172.7, 155.1, 140.0, 137.0, 134.8, 129.4, 129.0, 128.6, 128.3, 127.7, 122.1, 84.2, 42.9, 40.1. HRMS (MALDI) $[\text{M} + \text{Na}]^+$ calcd for $\text{C}_{19}\text{H}_{15}\text{ClNaO}_3$ 349.0602, found 349.0602.

(*S*,S)-5-(3-Oxo-3-(4-chlorophenyl)1-phenylpropyl)furan-2(5H)-one (182j)**

63.6 mg, yield 90%, white solid : mp = 102-105 °C.

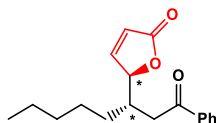
$^1\text{H-NMR}$ (400 MHz, CDCl_3): δ = 7.80 (m, 2H), 7.44-7.18 (m, 8H), 6.07 (m, 1H), 5.24 (m, 1H), 3.64 (m, 1H), 3.53 (dd, J = 17.6, 4.8 Hz, 1H), 3.44 (dd, J = 17.6, 8.3 Hz, 1H).

$^{13}\text{C-NMR}$ (100 MHz, CDCl_3): δ = 196.1, 172.6, 155.5, 139.7, 139.4, 134.9, 129.4, 128.9 (x 2), 128.0, 127.7, 122.0, 85.7, 44.5, 40.2. HRMS (ESI) $[\text{M} + \text{Na}]^+$ calcd for $\text{C}_{19}\text{H}_{15}\text{ClNaO}_3$ 349.0602, found 349.0603.

(*R*,S)-5-(3-Oxo-1-phenylhexyl)furan-2(5H)-one (185)**

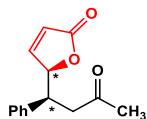
26.2 mg, yield 42%, yellow liquid.

$^1\text{H-NMR}$ (400 MHz, CDCl_3): δ = 7.96 (m, 2H), 7.58 (m, 1H), 7.52-7.39 (m, 3H), 6.15 (m, 1H), 5.25 (m, 1H), 3.24 (dd, J = 17.7, 7.9 Hz, 1H), 2.96 (dd, J = 17.7, 5.1 Hz, 1H), 2.65 (m, 1H), 1.42-1.11 (m, 8H), 0.85 (m, 3H). $^{13}\text{C-NMR}$ (100 MHz, CDCl_3): δ = 199.0, 173.1, 155.4, 136.7, 133.4, 128.7, 128.0, 122.2, 85.2, 39.1, 36.3, 31.7, 28.0, 27.0, 22.4, 13.9. HRMS (MALDI) $[\text{M} + \text{H}]^+$ calcd for $\text{C}_{18}\text{H}_{23}\text{O}_3$ 287.1642, found 287.1642.

(*S*,S)-5-(3-Oxo-1-phenylhexyl)furan-2(5H)-one (186)**

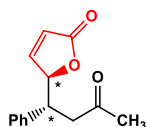
38.9 mg, yield 62%, white solid : mp = 56-59 °C.

$^1\text{H-NMR}$ (400 MHz, CDCl_3): δ = 7.89 (m, 2H), 7.55 (m, 1H), 7.50-7.37 (m, 3H), 6.01 (dd, J = 5.7, 1.6 Hz, 1H), 5.23 (m, 1H), 2.93-2.77 (m, 2H), 2.70 (m, 1H), 1.70-1.19 (m, 8H), 0.87 (m, 3H). $^{13}\text{C-NMR}$ (100 MHz, CDCl_3): δ = 198.7, 173.1, 156.2, 136.6, 133.3, 128.7, 127.9, 121.6, 84.8, 36.8, 36.2, 32.1, 31.7, 26.8, 22.5, 14.0. HRMS (MALDI) $[\text{M} + \text{H}]^+$ calcd for $\text{C}_{18}\text{H}_{23}\text{O}_3$ 287.1642, found 287.1642.

(*R*,S)-5-(3-Oxo-1-phenylbutyl)furan-2(5H)-one (187)**

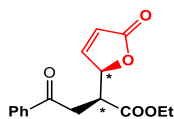
84.5 mg, yield 46%, colorless liquid.

$^1\text{H-NMR}$ (400 MHz, CDCl_3): δ = 7.36-7.18 (m, 4H), 7.12 (m, 2H), 5.84 (m, 1H), 5.34 (m, 1H), 3.74 (m, 1H), 3.24 (dd, J = 18.2, 8.3 Hz, 1H), 2.92 (dd, J = 18.2, 5.8 Hz, 1H), 2.17 (s, 3H). $^{13}\text{C-NMR}$ (100 MHz, CDCl_3): δ = 206.5, 172.8, 155.1, 137.0, 128.6, 128.2, 127.6, 122.0, 84.1, 44.7, 42.5, 30.5. HRMS (ESI) $[\text{M} + \text{Na}]^+$ calcd for $\text{C}_{14}\text{H}_{14}\text{NaO}_3$ 253.0835, found 253.0834.

(*S*,S)-5-(3-Oxo-1-phenylbutyl)furan-2(5H)-one (188)**

18.8 mg, yield 37%, white solid : mp = 77-78 °C.

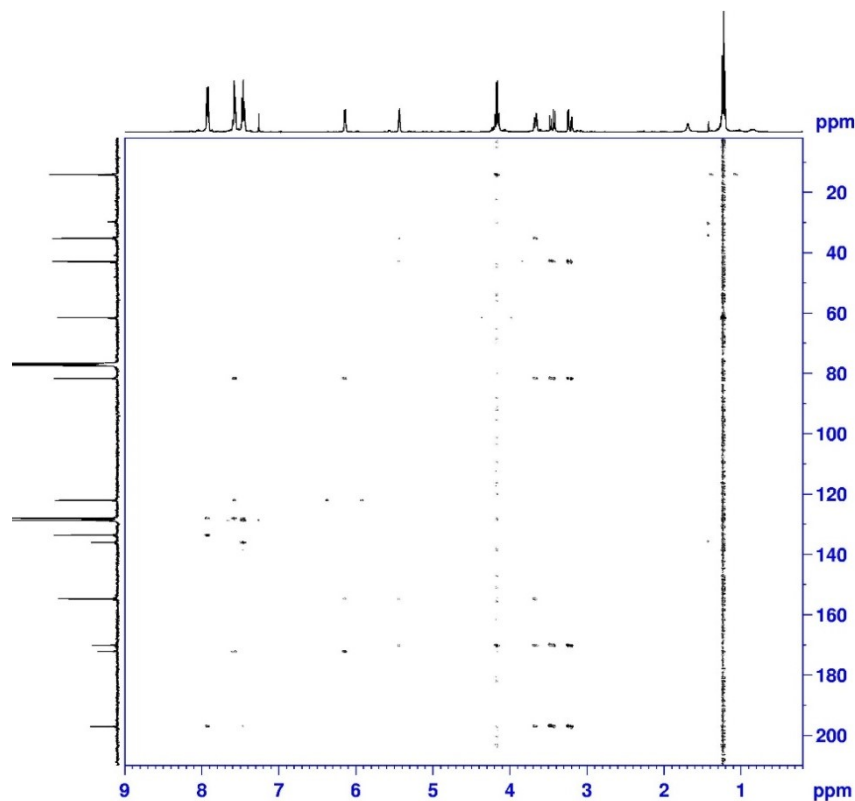
$^1\text{H-NMR}$ (400 MHz, CDCl_3): δ = 7.37-7.33 (m, 2H), 7.31-7.25 (m, 3H), 7.22 (m, 1H), 6.10 (m, 1H), 5.15 (m, 1H) 3.45 (m, 1H), 3.04 (dd, J = 17.6, 5.2 Hz, 1H), 2.91 (dd, J = 17.5, 8.2 Hz, 1H), 2.07 (s, 3H). $^{13}\text{C-NMR}$ (100 MHz, CDCl_3): δ = 205.9, 172.7, 155.5, 139.3, 129.0, 128.0, 127.8, 121.9, 85.7, 45.0, 44.2, 30.6 ppm. HRMS (MALDI) $[\text{M} + \text{Na}]^+$ calcd for $\text{C}_{14}\text{H}_{14}\text{NaO}_3$ 253.0835, found 253.0835.

(*R*,S)-5-(3-Oxo-3-ethylbutanoate-1-phenyl)furan-2(5H)-one (195)**

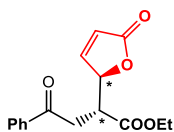
52.0 mg, yield 83%, colorless liquid.

$^1\text{H-NMR}$ (400 MHz, CDCl_3): δ = 7.92 (m, 2H), 7.61-7.54 (m, 2H), 7.46 (m, 2H), 6.14 (dd, J = 5.8, 2.0 Hz, 1H), 5.44 (m, 1H), 4.17 (q, J = 7.1 Hz, 2H), 3.67 (m, 1H), 3.44 (dd, J = 18.2 Hz, 7.7 Hz, 1H), 3.21 (dd, J = 18.2, 5.1 Hz, 1H), 1.22 (t, J = 7.1 Hz, 3H). $^{13}\text{C-NMR}$ (100 MHz, CDCl_3): δ = 197.0, 172.1, 170.2, 154.7, 136.0, 133.6, 128.7, 128.0, 122.0, 81.6, 61.5, 42.9, 35.2, 14.1. HRMS (MALDI) $[\text{M} + \text{H}]^+$ calcd for $\text{C}_{16}\text{H}_{17}\text{O}_5$ 289.1070, found 289.1070.

^1H - ^{13}C HMBC NMR of compound **195** (400 MHz, CDCl_3)



(*S^*,S^)-5-(3-Oxo-3-ethylbutanoate-1-phenyl)furan-2(5H)-one (196)**

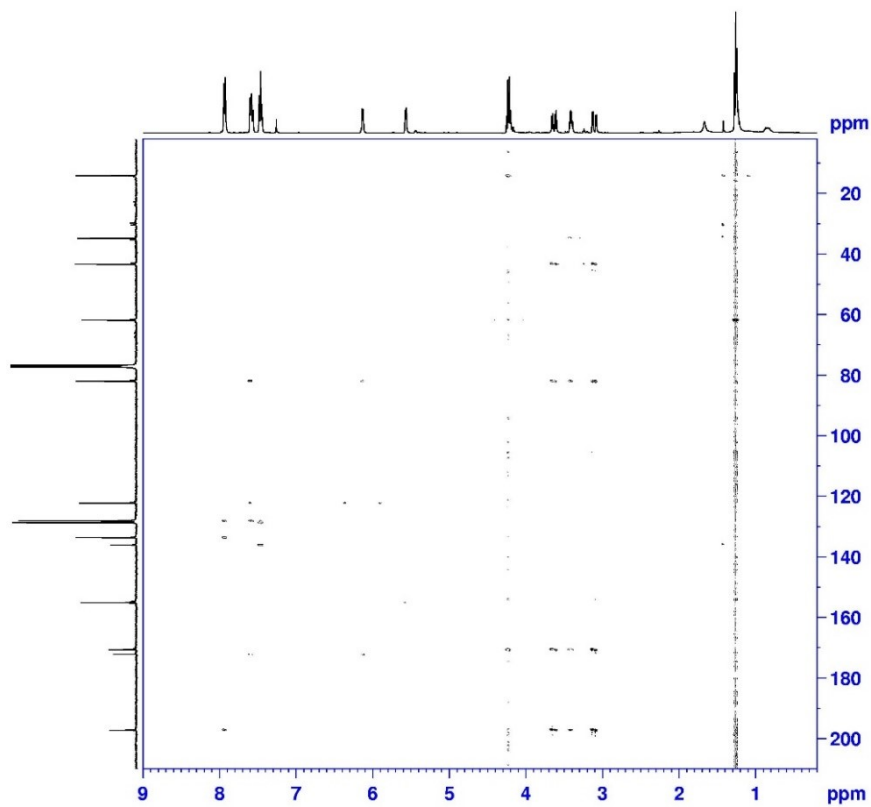


27.1 mg, yield 86%, colorless liquid.

^1H -NMR (400 MHz, CDCl_3): δ = 7.94 (m, 2H), 7.62-7.54 (m, 2H), 7.46 (m, 2H), 6.13 (m, 1H), 5.57 (m, 1H), 4.22 (q, J = 7.1 Hz, 2H), 3.63 (dd, J = 18.2 Hz, 6.8 Hz 1H), 3.41 (m, 1H), 3.10 (dd, J = 18.1, 4.9 Hz, 1H), 1.26 (t, J = 7.1 Hz, 3H). ^{13}C -NMR (100 MHz, CDCl_3): δ = 197.1, 172.1, 170.6, 155.1, 136.0, 133.6, 128.7, 128.0, 122.2, 81.9, 61.7,

43.2, 34.7, 14.0. HRMS (MALDI) $[M + Na]^+$ calcd for $C_{16}H_{17}NaO_5$ 311.0890, found 311.0889.

1H - ^{13}C HMBC NMR of compound **196** (400 MHz, $CDCl_3$)



Acknowledgments

During my PhD I did a research internship at the Universidad Autonoma de Madrid (from 11-02-2016 until 15-04-2016) under the supervision of Dr. José Alemán Lara.

I would like to thank first of all Dr. José Alemán Lara for accepting me in his labs and inside the team. I would like to thank him for my human and professional growth. It was a pleasure to appreciate his chemistry and learning from him. Thanks to all people that I met during my time abroad in Universidad Autonoma de Madrid.

Sono già trascorsi tre anni, come dico sempre! Sembra strano essere qui a scrivere i ringraziamenti della mia tesi di dottorato perché ho la sensazione che questo meraviglioso tempo sia volato. Sono lieta di poter ringraziare tutte le persone che hanno fatto parte di questo mio percorso, quelle che mi sono rimaste affianco ogni giorno, che hanno gioito o condiviso qualche lacrima tra le pareti del laboratorio, che mi hanno insegnato e ispirato con costanza nel tempo.

Innanzitutto, Irene e Giorgio, siete il mio esempio quotidiano e vi sono grata per tutti gli insegnamenti che ho ricevuto costantemente, per la gioia con cui nei nostri laboratori si porta avanti la ricerca, per la grinta nelle nuove idee e nei successi, ma anche e soprattutto per la forza che siete stati in grado di trasmettermi negli insuccessi; proprio grazie a questa forza ogni giorno ero pronta a ripartire con una spinta maggiore. Grazie del supporto umano che non mi è mai mancato e della fiducia riposta nel progetto di dottorato. Spero che il conseguimento del titolo sia anche per voi momento di gioia. Grazie per le varie opportunità di crescita professionale che mi avete concesso: l'esperienza in California e quella in Sud Africa per me rappresentano motivo di crescita e orgoglio. Grazie Francesco De Riccardis per l'entusiasmo di ogni singolo momento in laboratorio, per lo stimolo a fare sempre meglio e di più. Grazie Consiglia Tedesco per avermi introdotto nella cristallografia in Sud Africa: è un'esperienza che conservo nel cuore. Mamma, Papà, Catia e

Christian siete rimasti costantemente al mio fianco supportandomi e sopportandomi in questi tre anni, anche quando tante volte la chimica ha rubato un poco del nostro tempo. Mi avete sempre incoraggiato e siete rimasti orgogliosi dei miei piccoli traguardi. Fortemente mi preme ringraziare tutti i ragazzi che ho avuto la possibilità di seguire nei loro percorsi di tesi; hanno costituito per me motivo di crescita, soddisfazione e hanno contribuito alla realizzazione di questo progetto: Assunta, Emil, Luisa, Chloè, Julien, Marina, Antonella, Veronica, Valentina; grazie per ogni giorno trascorso fra le pareti del laboratorio, per le risate e le emozioni che mi avete regalato. Ai rapporti speciali oltre il laboratorio: Tiziana e le nostre serate, Chloè la mia "polpetta" francese sempre nel cuore, Luisa, e Marina alle risate e ai nostri momenti skype scolpiti nel cuore; grazie dei momenti indimenticabili trascorsi insieme che mi hanno rafforzato nei momenti difficili e che mi rendono lieta di condividere con voi tanti momenti gioiosi di vita. Con il cuore ringrazio Brunello ed Alessandra, persone speciali, con cui ho condiviso la parte iniziale del mio percorso e che a distanza continuano a sostenermi nelle scelte di vita; grazie ragazzi per tutte le gioie condivise e per gli insegnamenti che mi avete trasmesso, per esserci sempre anche a distanza. Grazie a Benedetta, Rosa, Silvia e Serena che ogni giorno hanno creduto in me. Un grazie speciale va a Stefania, Raffaele ed Arico per le risate e i momenti di spensieratezza che fa una reazione e l'altra abbiamo condiviso. Grazie di cuore a Carmen sempre pronta e disponibile in qualsiasi momento, per il sostegno in qualsiasi situazione, per l'appoggio umano e professionale. Grazie a Paolo, Mario, Stefano, Nicola, Chiara, Rita, Francesco, Eleonora, Maria Leda per tutti i momenti condivisi insieme e i tanti caffè.



Grazie di cuore ad ognuno di voi!

